A Holistic Approach to Evaluating the Performance of Consolidants on Sandstone

Richard Ivan Grove

St Cross College

University of Oxford

Supervisor: Professor Heather Viles

Thesis submitted for the degree of Doctor of Philosophy in Science and Engineering in Arts Heritage and Archaeology

Trinity Term 2021

Abstract

Sandstone, one of the most ubiquitous building materials around the globe and across time presents a complex range of characteristics and responses to environmental and physical erosion over time. The range of sandstone sub-types that have been used for structure and decorative carving through history was highly variable but is diminishing as a resource as more and more quarry sites are worked out or closed. This process has led to the use of 'replacement' stones in conservation work which are sourced from a small number of known sites and are similar to historic types in appearance if not age or internal characteristics. This project examines one of these replacement stones, Locharbriggs sandstone from Dumfries in Scotland, and couples it with two of the most commonly used silane consolidants in order to improve the understanding of the performance of both in lab and field conditions.

The project begins by taking observations on site at Kenilworth Castle (Warwickshire, UK) shaping the research through the identification of areas of concern for the conservation of historic sites, such as erosion driven by visitor footfall and the effects of prior treatment applications. These are used to formulate an experimental programme which combines lab and field experiments, and begins with the development of a method for artificially weathering the stone substrate using the controlled application of heat, in preparation for consolidation.

The field-based experimental work, hosted at the Wytham Woods research site near Oxford UK, examines the uses and limitations of two forms of field trial; the exposure of laboratory-prepared stone samples on a purpose-built exposure rack, and the incorporation of stone samples of variable size and treatment within a purpose-built test structure. Both experiments trial a range of assessment metrics for the detection and monitoring of consolidants applied to the samples, within the context of exposure to local weather conditions. In addition to these experiments, a further trial was hosted by SATRA Technologies (Kettering, UK) which utilises a mechanical prosthetic leg to simulate physical abrasion analogous to that observed on site, modelling the type of wear driven by footfall across exposed stone surfaces.

These experiments trial the use of a range of systems for the assessment of stone condition and consolidant performance, combining those which are understood in other heritage contexts with the novel combination of handheld optical and laser scanners for the detection of change on samples. These are formalised into a 'toolkit' of methods and instruments that can be applied to sandstone-consolidant experiments, including novel methods of visualising and analysing data.

The thesis concludes that the range of assessment techniques trialled here have a range of useful applications in the detection of consolidants in heritage sandstone and for the detection of change on site and in laboratory conditions, and that there is significant scope to employ them in a range of conservation applications.

“How will you go about looking for that thing, the nature of which is unknown to you?”

-Plato (Trans. Rebecca Solnit)

For Travis

Acknowledgements

My first thanks are given to my supervisor Professor Heather Viles for her unfailing support throughout this project. At times during the last four years that problems have seemed unsurmountable, and her patience and understanding have been vital in dealing with what life has thrown at me both personally and academically. This thesis would not exist without her support.

I am grateful for the support of my family, my wife Rebecca, father Ivan, and my much-missed grandparents Molly and Howard Byng who started this journey with me but unfortunately were not able to make it to the end. Thanks and biscuits are also due to Travis and Tilly, my dogs. They have kept me sane throughout, and our walks have provided time and space for vital reflection.

I also express my gratitude to Dr Mona Edwards and Hong Zhang at the School of Geography for their practical and academic support throughout, especially during the COVID pandemic where their quick thinking and professionalism helped to facilitate my research in extremely challenging circumstances. In addition to this, Dr Martin Coombes and Dr Jenny Richards and Dr Scott Orr of OxRBL have provided invaluable technical help and moral support throughout the project, as have Dr Jack Matthews of the Natural History Museum and Dr Patricia Sanmartin of the Universidad de Santiago de Compostela.

This project has been made possible by funding provided by the UK Engineering and Physical Sciences Research Council (EPSRC) and by the Getty Conservation Institute, and thanks go to both of these organisations for their support, enabling me to carry out this research and to attend a range of training and academic events throughout, allowing me to grow as a researcher and individual. In particular I would like to thank Tom Lerner, Alick Leslie, Beril Bicer-Simser, Davide Gulotta and Julie Desarnaud for their help and feedback.

This project has been hosted at the University of Oxford through the Science and Engineering in Arts Heritage and Archaeology Centre for Doctoral training, and thanks must be given to Dr Julie Eklund

and Dr Robyn Parker, as well as the academic and administrative support staff at both Oxford and UCL for their support throughout. Mention must me made also of Alex Black and Joe Milkovic of the School of Geography facilities management team for their continued assistance, often with extremely heavy bits of stone. Finally, I must thank Sophie López Welsch at the University Welfare office for her fantastic support.

The fieldwork undertaken for this project was made possible through the support of three organisations, and thanks are due to each. Firstly, to Nigel Fisher and Lucy Kilby at the Wytham Woods research station, who hosted the exposure rack trial and test wall experiments and were extremely helpful throughout. Also of note are the staff at the English Heritage Charitable Trust, who allowed me free and extensive access to Kenilworth Castle, and freely shared their insight and knowledge of the care of one of the most complex heritage sites in Europe. Thanks are due to Gus Nasser, Rebecca Crites, Laura Reynolds, and Jane Edwards for their enthusiasm throughout.

A special note of thanks must go to David Smith and Harriet Mason at SATRA Technologies Ltd, who made possible the Pedatron experiment, and worked extremely hard to make their facilities available through the COVID lockdown, without them this project would be much the poorer.

Last, and by no means least, I would like to thank the long line of academics who have raised me from tractor driver to post-graduate student in an academic career that started in 2002. Thomas Cavanagh & Dr Diane Whitehouse at Moreton Morrell College of Agriculture, Drs Jodie Lewis and Helen Loney at the University of Worcester, Harriet Devlin MBE at the University of Birmingham, and Dr Josep Grau Bove at UCL all deserve huge thanks here.

Table of Contents

CHAPTER ONE: INTRODUCTION AND LITERATURE REVIEW 12

1.1 Introduction 13
1.2 Overview of Project 14
1.2.1. Aim and Objectives. 15
1.2.2 Research Methodology 16
1.2.3 Case Study Site 18
1.2.4 Laboratory-based research 19
1.2.5 Field-based Research 19
1.2.6 Thesis Summary 20
1.3. Literature Review: Stone-Built Heritage Research 21
1.3.1 Sandstone and the Deterioration of Built Heritage 22
1.3.2 Overview of Consolidant Use in Heritage Conservation 26
Limes 28
Nanolimes 29
Siliceous Consolidants and Hydroxides 30
Polymers 31
Alkoxysilanes/ Silanes 32
1.3.3 Built Heritage Conservation Research 34
Studying Heritage Assets Using Laboratory Trials 35
Image Based Rendering for Conservation 37
Studying Heritage Assets Using Field Trials 39
1.4 Summary, the State of the Art 43

CHAPTER TWO: CASE STUDY OF KENILWORTH CASTLE 45

2.1 Introduction 46
2.2 Overview of Kenilworth Castle 46
2.2.1 Conservation of the Historic Structure 52
2.2.2 Past Consolidation Trials 57
2.2.3 Conservation of Floor Surfaces 59
2.3 Summary 62

CHAPTER 3: MATERIALS AND METHODS 64

3.1 Locharbriggs Stone 65
3.2 Consolidants 67
3.3 Preparation of Samples for Experiment 68
3.3.1 Stone Cutting and Preparation for Field Trials 68
3.3.2 Stone Cutting for and Preparation for Pedatron Simulation Experiment 70
3.4 Artificial Weathering of Stone for Sample Preparation 71
3.5 Application of Consolidants and Pre-exposure Preparation 72
3.6 Techniques for Field Experimentation 77
3.6.1 Ultrasonic Pulse Wave Velocity 78
3.6.2 Colorimetry 79
3.6.3 Microwave Moisture Meter 80
3.6.3.1 Gravimetric Calibration of Moisture Meter Data 80
3.6.4 Surface Roughness 83
3.6.5 Handheld Laser Scanning 83
3.7 Statistical Analyses 84
3.7.1 Exposure Rack Trial 84
3.7.2 Test Wall Trial 85

3.7.3 Pedatron Erosion Test *86*

CHAPTER FOUR: THE EXPOSURE RACK TRIAL **87**

4.1. Introduction *88*
4.1.1 Aim and Scope of Field Trial *89*
4.1.2 Links to Research Framework *90*
4.2 Methodology *91*
4.2.1 Preparation of Samples *91*
4.2.2 Consolidant Treatments for the Rack Trial *92*
4.2.3 Laboratory Pre-trial Measurements *93*
4.2.4 Laboratory Stone Weathering Methodology *93*
4.2.5 Application of Consolidants and Pre-exposure Preparation *93*
4.2.6 Exposure Trial Methodology *94*
4.2.6.1 Rack Samples *94*
4.2.6.2 Wall 'Embedded' Samples *95*
4.2.6.3 Laboratory Control Samples *96*
4.2.7 Data Collection Methodology *97*
4.2.7.1 Rack Samples *97*
4.2.7.2 Laboratory Control Samples *98*
4.2.7.3 Test Wall 'Embedded' Samples *98*
4.2.8.1 Mass *98*
4.2.8.2 Pulse Wave Velocity *99*
4.2.8.3 Colorimetry *99*
4.3. Results and Discussion *100*
4.3.1 Weather and Climate *100*
4.3.2 Field Trial Data *102*
4.3.2.1 Mass *102*
4.3.2.1.1 Statistical Analysis *106*
4.3.2.2 Colorimetry *107*
4.3.2.2.1 Statistical Analysis *117*
4.3.2.3. Ultrasonic Pulse Wave Velocity *119*
Wall Embedded Samples *124*
Statistical Analysis *126*
4.4.1 Discussion *128*
4.4.2 Conclusion *130*

CHAPTER FIVE: TEST WALL FIELD TRIAL **133**

5.1 Introduction *134*
5.1.1 Aim and Scope of Test Wall Trial *134*
5.2 Experimental Design and Construction of the Test Wall *135*
5.2.1. Design and Construction of the Test Wall Trial *135*
5.3 Methods *138*
5.3.1 Preparation of Sandstone for the Structure *138*
5.3.2 Construction of the Test Wall *139*
5.3.3 The Use of Non-Destructive Techniques for the Assessment of Variable Treatment Application and Performance on Sandstone *139*
5.3.4 Calibration Using Gravimetric Testing *140*
5.3.5 Data Collection Methodology *141*
5.4 Results *143*
5.4.1 Overview of Field Data *143*
Key to Visualisations *144*
5.4.2 Assessment by Dimension: WA Samples *147*
Statistical Analysis: WA Category *150*
5.4.3 Assessment by Dimension: WB Category *151*
Statistical Analysis, WB Category *154*

5.4.4 Assessment by Dimension: WC Samples *156*
Statistical Analysis for WC Blocks *159*
5.4.5 Control Samples (NF) *160*
5.5 Discussion *163*
5.6 Conclusion *165*

CHAPTER SIX: THE PEDATRON EROSION TRIAL **167**

6. Introduction *168*
6.1 Aims and Objectives. *168*
6.1.1 Links to DPhil Project Framework *168*
6.1.2 Overview of Experimental Design *169*
6.2. Methodology *169*
6.2.1 Selection and Preparation of Stone for the Pedatron Experiment *169*
6.2.2 Preparation of "Wear Platform" for the Pedatron Experiment *170*
6.2.4 Pedatron Experimental Methodology *172*
6.2.5 3D Scanning Equipment *175*
6.2.6 Pre- and Post- Experiment Measurement Methodology *175*
6.2.6.1 Ultrasonic Pulse Wave *176*
6.2.6.2 Colorimetry *177*
6.2.6.3 Surface Roughness *179*
6.2.6.4 3D Scanning and Rendering *179*
6.3 Results *182*
6.3.1 Observations During the Pedatron Test *182*
6.3.2 3D Scans and Visualisation *183*
Significant Change *187*
6.3.2 Surface Roughness *189*
6.3.3 Statistical Analysis *192*
6.4 Discussion *193*
6.5 Conclusion *196*

CHAPTER SEVEN: DISCUSSION AND CONCLUSIONS **199**

7.1 Introduction *200*
7.2 Conclusions *212*

8. BIBLIOGRAPHY **215**

List of Figures

1.1 Project Flow Chart Showing Structure of The Thesis…… 15
1.2 Location of field trials site at Wytham, Oxford, UK…… 18
1.3: Left. Kenilworth Castle, south elevation of 12Th Century Keep, Brethane treated area…… 31
1.4 "Asterixe" test pieces on site in Holzkirchen, Germany…… 40
2.1 Plan of Kenilworth Castle grounds with phasing of main structures…… 45
2.2 Leicester's building (left), the great Hall (centre) and the Norman Keep (Right) taken from the base courtyard…… 46
2.3 West elevation of Great Hall taken from King's Gate, with ruins of the Strong Tower (to left) and Saintlowe's Tower (right) …… 47
2.4 The Gatehouse from the south-west, showing later extensions and mullioned windows likely taken from Leicester's Building…… 47
2.5 "Kenilworth Castle" by Henry Eldridge, circa 1808, oil on canvas…… 48
2.6 Inner wall of Great Hall showing Alveolisation caused by wind driven rain…… 50
2.7 (left) Pooling rainwater in the north entrance to the Keep, and (right) the combined effects of water and footfall erosion on a doorway stone, State Apartments…… 51
2.8 (left) Grass and mosses colonising inaccessible floor surface in the Great Hall, and (right) Self-set Ash tree behind a permanent screen in the Swan Tower…… 52
2.9 Delamination of structural stone, located in the Great Hall…… 52
2.10 Looking south-west from the base court, Leicester's Building (left) and the State Apartments…… 53
2.11 Modern stabilisation and structural repairs, using brick and concrete mortar to infill lost stonework…… 54
2.12 section of the Keep wall used in the Brethane trial. Cores were taken areas highlighted in red…… 55
2.13 Left: Historic floor stone Type 1 with Type 4 infill, adjacent to the Norman Keep. Linear wear appears to be wheeled traffic derived. Actual age of stone is unknown…… 59
2.14 Left: Type 3 floor surface historically covered but now exposed to environmental erosion Right: Type 4, modern stone, concrete, and aggregate mix. This setting is adjacent to the earliest extant area of the castle complex (12Th Century) …… 59
3.1 Locharbriggs Sandstone at10x magnification, shown in thin section…… 63
3.2 Ternary Diagram, Locharbriggs Sandstone. Based on Q-F-L format, after Tucker 2001, fig. 2.50….. 64
3.3 Left: Stone for test wall during cutting, at Geolabs, Right: Sample blocks for exposure rack trial following experiment. Note darker shade of Weathered and Untreated samples (2nd from right)…… 67
3.4 Norton Clipper saw at Geolabs Facility, with Locharbriggs sample pre-cutting…… 67
3.5 Construction of the Pedatron Foot Erosion Platform…… 68
3.6 Applying TEOS consolidant to test wall samples using brushing. Excess consolidant is collected in the tray below…… 72
3.7 Samples in sealed consolidant bath stored in ventilated fume cupboard at Geolabs facility…… 74
3.8 Proceq Punditlab direct array configuration as used throughout tests…… 76
3.9 The interaction of the three axes of hue within CIELAB colour space…… 77
3.10 Results of gravimetric test, mean mass of sample groups plotted with MOIST 350B percentage values…… 80
4.1 Flowchart of sample use through trial…… 90
4.2 Samples on the exposure rack at Wytham…… 93
4.3 East Facing elevation of the test wall…… 94
4.4 Mask template used for colorimetry readings…… 98
4.5 Scatterplots with relative humidity on the day of sampling plotted against mean mass of each sample group…… 100
4.6 Scatterplots showing the mean mass of each sample group with cumulative rainfall 48 hours prior to data collection…… 102
4.7 Colorimetry data collected from each ten-stone sample set. …… 106
4.8 Mean of all sample groups L value, plotted against total rainfall in the 48 hours prior to data collection…… 107*
4.9 Mean a values of each group per month plotted against percentage ambient relative humidity at the time of sampling…… 111*

4.10 Mean a values of each group per month plotted against total rainfall in the 48 hours prior to data collection…… 113*
4.11 ΔE Values plotted with percentage ambient relative humidity at the time of sampling…… 114
4.12 Mean ΔE values of each group per month plotted against total rainfall in the 48 hours prior to data collection…… 115
4.13 Clusters of P Wave Velocity data throughout the trial…… 118
4.14 P Wave Monthly mean velocity plotted against total rainfall (mm) in 48 hours prior to collection 121
4.15 P Wave Monthly mean velocity plotted against percentage relative humidity at time of collection…… 122
4.16 Scatterplots showing relationship between P Wave Velocity of embedded wall samples and environmental conditions on site at Wytham Woods…… 123
5.1 Layout of wall components by block size…… 134
5.2 Images of wall under construction in July 2019, facing East…… 135
5.3 Placement of blocks with categories, see Table 6.1 for key to categories and treatment…… 135
*5.4 L*C*h* Colour Scale as applied to Test Wall visualisations…… 139*
5.5 MOIST 350B DM Sensor head in contact with a sample stone…… 140
5.6 Approximate location of each MOIST 305B sampling point (in blue), showing number of readings per block size. Sensor was positioned to avoid overlap with other sampling points and mortar joints… 141
5.7 Key to block treatment as denoted by sample border within all wall visualisations…… 142
5.8 Whole-Wall Moisture visualisations by month, excluding "F" blocks…… 143
5.9 Key to WA block placement…… 145
5.10 Size-delineated Groupings, No.1. WA Blocks…… 147
5.11 Key to WB block placement…… 150
5.12 Size-delineated Groupings, No.2. WB Blocks…… 151
5.13 Key to WC block placement…… 154
5.14 Size-delineated Groupings, No.3. WC Blocks…… 156
5.15 Key to control sample placement…… 158
5.16 Size-delineated Groupings, No.3. Control Blocks…… 160
*6.1 **LEFT**: plan of experimental platform with dimensions. (c) denotes consolidated with teos. **RIGHT**: The prepared walking platform, samples 1 (closest to camera) and 4 (farthest corner) are treated with TEOS consolidant…… 169*
6.2 Pedatron with platform, denoting movement of boot and rotation of base to simulate foot twist. Note: extent of individual twist is 15, smaller than indicated by arrow…… 170
6.3 Kenilworth Castle site plan, including exposed stone flooring and common visitor route through site. Base map © Edina Digimap 2021…… 171
6.4 Representative Exposed Stone Flooring At Kenilworth Castle…… 172
6.5 Diagram of Tile as laid within frame, showing bedding planes and direction of P Wave Propagation for pre-test assessment…… 174
6.6 Explanation of colorimetry and Surface Roughness templates as fitted to platform for measurement…… 175
6.7 Colorimetry ΔE (total change) for each Tile and sub-section (including error bars), before and after consolidation (Samples 1 and 4 only) …… 176
6.8 Test Platform with rectification points, image ©SATRA…… 178
6.9 Alignment of individual tiles (sample 1 shown). Before first test (a) is closely aligned with the post-test tile (b) and the difference determination is represented as a colour scale representation (c) 179
6.10 Walking Platform immediately post- first test, pre-cleaning. The 'doughnut' effect is clearly visible as a circle spanning the four tiles. Also clear is the movement of the tiles within the frame. Image © SATRA…… 181
6.11 Difference models showing change after first Pedatron test, created using CloudCompare. Grey areas denote no significant alteration between two models. Scales are mm (c) denotes Consolidated tile…… 182
6.12 Difference models showing change after second Pedatron test, created using CloudCompare. Grey areas denote no significant alteration between two models. Scales are mm (c) denotes Consolidated tile…… 184
6.13 Significant change as determined by M3C2 algorithm, test 1. Red areas denote change in excess of a minimum threshold of 0.6 mm…… 185

6.14 Significant change as determined by M3C2 algorithm, test 2. Red areas denote change in excess of a minimum threshold of 0.6 mm…….. 186
6.15 Graphical representation of surface hardness plot as generated by INNOWEP TRACEiT, showing axes of measurement. Scale within plot in mm, depth scale in µm…… 188
*6.16 Oblique scans of the test platform at each stage of test. **Left**: before first test, **Middle**: after first test. **Right**: after second test. Note pitch of tiles in middle image following loosening…….. 193*
7.1 The four toolkit compartments arising from the Sandstone Consolidant Project…… 207

List of Tables

1.1 Summary of Manifestations of Stone Decay. Source: ICOMOS 2008…….. 22
1.2 Summary of Consolidant types covered in this chapter…… 25
2.1 Visitor Numbers for Year 2019-20, Kenilworth Castle…… 49
2.2 Stonework categories on site at Kenilworth Castle…….. 58
2.3 Outline patterns of wear to floor surfaces ……. 58
3.1 Mass increase in grammes of Exposure Rack Samples following consolidant treatment…… 73
3.2 Mass Changes (Kg) In Test Wall Blocks Treated by Immersion…….. 75
3.3 Mass Changes (Kg) In Test Wall Blocks Treated by Brush Application…….. 75
3.4 Summary of Techniques used with links to Project Objectives. …….. 77
3.5 Methodology for Gravimetric Testing…….. 81
3.6 Mean results for all sample Groups for Gravimetric Testing…… 81
4.1 Breakdown of Locharbriggs Sandstone samples and labelling nomenclature…….. 89
4.2 Summary Weather Data for Oxford, period between March and September 2019- Phases 1 & 2…… 101
4.3 On-site Data Collection Time and conditions…….. 101
4.4 Mean mass readings for sample groups (10 replicates) throughout Exposure Trial…… 103
4.5 Range of Mass readings (g) across Exposure Trial…….. 103
4.6 Coefficient of Determination, Mean Mass of Groups with weather…… 107
4.7 Coefficient of Determination for R^2; L, a*, and ΔE Values determined by on site rainfall and percentage relative humidity…… 110*
4.8 Mean Colorimetry values for Test Rack Trial. #Controlled %RH in laboratory conditions, ++Laboratory readings mimic treatment stages for symmetry…… 112
4.9 Results of Pearson Correlation Coefficient test for colorimetry and on-site conditions…….. 118
4.10 Result of comparison T-Tests for a colorimetry values…… 119*
4.11 Summary of P Wave Velocity readings for all groups…….. 121
4.12 Wall Embedded Samples, Mean P Wave Velocity…… 124
4.13 Coefficient of Determination for P Wave Values collected on site with rainfall and percentage relative humidity…… 125
4.14 Pearson's Correlation Coefficient for P Wave Values collected on site with rainfall and percentage relative humidity…… 126
4.15 P Value Results of T Tests between P Wave Means and weather conditions…….. 127
4.16 Results of T Tests for P Wave Means Comparison between Wall embedded and Rack samples……. 128
5.1 Guide to structural components of test wall…….. 137
5.2 Radcliffe Met Station (Oxford) data for dates of data collection…….. 146
5.3 Values for WA sample set across duration of experiment…….. 148
5.4 Single Factor ANOVA, WA subsets month-on-month using an α value set to 0.01…….. 150
5.5 P Value of Two Sample T Test on WA subset groups 2, 3, and 4. using an α value set to 0.01…….. 150
5.6 Values for WB sample sets across duration of experiment…… 154
5.7 Single Factor ANOVA, WB subsets month-on-month, using an α value set to 0.01…….. 155
5.8 P Values of Multi Factor ANOVA analysis, based on an α value of 0.01…… 155
5.9 Values for WC Samples across duration of trial…… 156
5.10 Single Factor ANOVA, WC subsets month-on-month, using an α value of 0.01…… 159
5.11 P Value results for T Tests comparing WC1 and WC2 MOIST 350B results…….. 159
5.12 T Test P Values for Control sample pairings…….. 161
6.1 Water applied to surface of walking platform during Pedatron test…….. 175
6.2 Summary of measurements and their timing…….. 176
6.3 Mean P Wave Values Pre- and Post- Artificial Weathering. (c) denotes consolidated tiles…… 177
6.4 Consolidated Tiles, Mean P Wave Values Pre- and Post- Consolidation…….. 177
6.5 Surface Roughness measurements (Rz) and standard deviation (SD), taken pre- and post- first Pedatron Test, in µm. Green background denotes drop in Rz value…….. 190
6.6 Surface Roughness measurements (Rz) and standard deviation (SD), taken pre- and post- second Pedatron Test, in µm. Green background denotes a decrease in Rz value, red an increase…… 191
6.7 Difference in Surface Roughness (Rz) values before and after the Pedatron tests (µm)…… 192
6.8 Results of T Tests for Surface Roughness change…….. 193
7.1 The four toolkit compartments arising from the Sandstone Consolidant Project…….. 209

Chapter One: Introduction and Literature Review

1.1 Introduction

Conservation of historic stonework with consolidants presents a complex problem for the owners of buildings, curators of works of sculpture, archaeologists, architects, conservators and researchers alike. Whilst historic structures or pieces of art derived from natural stone carry a level of resilience related to their formation and natural setting, their working and subsequent placement within exposed environments frequently triggers a set of interactions that are ultimately deleterious. The practice of hindering, halting, or even repairing the subsequent decay is heavily debated in both theoretic and functional terms (Kennedy 2015, Forster 2010a, 2010b). This project represents an attempt to address some of the needs for successful conservation for stone-built heritage- in particular sandstone, offering practical solutions for the creation of material for testing in lab and field, and bridging the gap between science-based assessment and field observations.

Sandstone, one of the most ubiquitous sedimentary building materials across the globe, is not as uniform a material as one may imagine. The variation of principal materials, inclusions and binders means that the term 'sandstone' covers a broad spectrum of characteristics in appearance and use. In the British Isles on one end of the spectrum there are highly cemented and mature quartz-rich stones bound with high levels of indurated iron, making a durable building stone with characteristic pink to red tones (Hains *et al* 1987; Toghill 2000). At the other end of the spectrum are the marine greensand stones found in the south-east of England, immature and highly vulnerable to abrasion and air pollution alike but favoured for workability and blonde colour (see for instance Kentish Reigate stone, as found in the Royal palaces in London) (Tatton-Brown, 2001).

In general, the use of sandstone as a structural material is best viewed (in a modern context at least) as a trade-off of between its workability and those material vulnerabilities as exposed through use. Historically however, the selection of what may be interpreted as an inferior material in modern engineering terms came as a result of availability, transport infrastructure (of lack thereof), and

aesthetic considerations. Gilberto Artioli (2010; 223) describes sandstone as a group of "rather soft poly crystalline rocks… easily modelled, drilled, and polished", and it is these characteristics which have seen it favoured over time by masons and architects alike. Despite the accepted weaknesses of sandstone as a stone type, it should be noted that given the right setting and management it can be as durable as many of the alternative -tougher- building stones. Evidence of this longevity can be found at Bronze Age sites in the north of England such as Long Meg and her Daughters stone circle (Historic England 2021), and Ireland (Newgrange, 5300 years old) (O'Kelly 2004), not to mention the famous cityscapes of antiquity at Petra and Luxor, where the material has far outlived not only the perceived use and lifespan, but the cultures that created them.

Across the British Isles a wide range of stone typologies have been used throughout history, in varied contexts from low-status vernacular structures to royal palaces (Clifton-Taylor 1972, Brunskill 1987). However, many of the quarries which provided the stone have been lost; and those that remain face increased demand for their material for both their traditional markets and as replacement stone sources for historic buildings. Conservation of this vulnerable resource is therefore becoming increasingly important, leading to some conservators and site managers adopting the application of chemical treatments for material repair and for weather proofing, often with mixed results. This project is focused on the use of Locharbriggs Sandstone, quarried in Dumfries (Scotland), and employed at a range of sites both from construction and used as a repair material (where original source stone is not available.

1.2 Overview of Project

This DPhil project aims to address the need for improved understanding of the effects and performance of consolidant treatments as applied to sandstone, and in particular those as may be found on heritage sites in the British Isles. Much research has been done on consolidants, their formulation, means of application, and reaction to climate and traffic; but the majority of these

projects have used limestone as the substrate for testing, and where sandstone has been employed, materials from central and Europe or the Americas have commonly been used (Drdacky *et al* 2020, Remzova *et al* 2019, Wheeler *et al* 1992). Consequently, an opportunity exists to address the knowledge gap on the performance of consolidant treatments on British sandstones, by trialling a range of experimental frameworks and data collection techniques, some of which have provided useful data on a range of other stone types and treatment systems.

This project forms part of the wider Built Heritage Research (BHR) collaboration between the University of Oxford and the Getty Conservation Institute (Los Angeles, USA); and is undertaken as part of the ESPRC "Science and Engineering in Arts Heritage and Archaeology" Centre for Doctoral Training. The project has been hosted by the University of Oxford School of Geography and the Environment, with additional support and specialist advice from the Getty Conservation Institute science department.

1.2.1. Aim and Objectives.

The overall aim of the project is "**To improve the evaluation of consolidant performance on deteriorating sandstone through the combined use of laboratory and field experimentation".** This is achieved through addressing the following objectives:

Objective 1. To investigate the development of a novel methodology for the preparation and analysis of sandstone for consolidant assessment trials

Objective 2. To investigate the use of sample-based and structure-based experiments in field settings for the assessment of consolidant performance on sandstone

Objective 3. To investigate the use of simulated wear experiments for the assessment of consolidant performance on sandstone

Objective 4. To produce a 'Toolkit' of methods for the evaluation of consolidant performance on sandstone, arising from Objectives 1,2, and 3

1.2.2 Research Methodology

This project utilises a range of assessment techniques common to heritage science and built heritage conservation, combining novel laboratory and field-based experimental frameworks in a holistic way to answer previously unanswered questions on the effectiveness of consolidants on a chosen sandstone common to heritage conservation in the British Isles. Throughout the project, the selection of materials and methods has been driven by the need to provide a set of practical methods to assess consolidant performance which can be used in both the research and conservation sectors. In order to achieve this goal, the project undertakes a portion of its research and development within a laboratory setting, but wherever possible employs the simplest processes and methodologies possible to enable dissemination of results and understanding to this diverse community. Furthermore, the field experiments have been designed to make them readily replicable in other locations or using other components, using commercially available consolidant treatments and sandstone from a commercially active quarry which supplies material for repairs of sandstone monuments where the original source material is no longer available.

The structure of the thesis (figure 1.1) follows the research and experimental workflow, beginning with a review of relevant literature (Chapter one) and identifying and investigating a case study site- Kenilworth Castle (Chapter two) in Warwickshire- from which to make observations of stone in situ as it weathers and is eroded through use. Following a period of on-site observation and interviews with staff, the experimental phase of the project began with selection of stone for the project, followed by the development and refinement of a heat-based artificial weathering technique for preparing stone for consolidation which is explained in Chapter three. Chapter four develops these methods further and applies them to a field-based exposure trial using sets of blocks (consolidated and unconsolidated), trialling the use of Ultrasonic Pulse Wave, Colorimetry, and fluctuations of mass within the samples as metrics of change over a year of field exposure. Chapter five takes this basic model and increases the complexity of the exposure trial, using prepared samples to construct

a test wall which was monitored using a microwave moisture meter as it interacted with weather conditions, this time for a period of fifteen months (allowing for a three month hiatus during COVID-19 restrictions on movement).

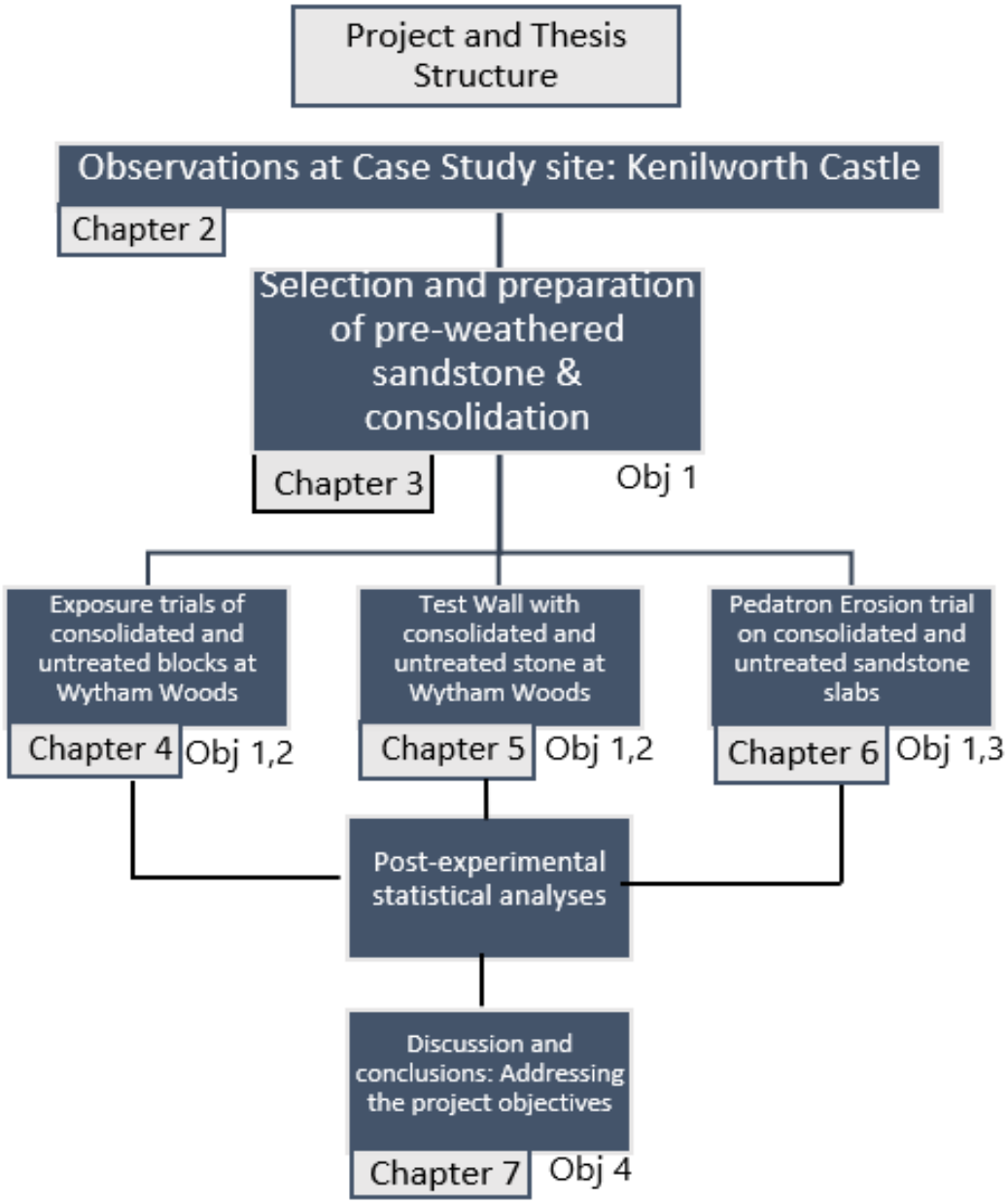

Figure 1.1 Project Flow Chart Showing Structure of The Thesis

The final experimental chapter (Chapter six) moves away from traditional exposure trials, and instead pioneers a novel erosion simulation experiment which utilises a mechanical 'walking foot' to create conditions analogous to extensive visitor footfall on a replica floor surface. These conditions

were monitored using a combination of laser scanning and surface roughness measurement. Chapter seven brings all the threads of the project together, linking findings from each of the experimental chapters, and addressing objective four. The conclusion in this chapter outlines how the work contained within this thesis is to be taken forward following the conclusion of the DPhil project. Figure 1.1 shows how the substantive chapters are organised in thesis, showing where each apply to the four research objectives stated in §1.2.1. Following the culmination of these experiments, the final objective of the project is the creation of a framework of methods that can be employed by researchers and conservationists on a sandstone substrates in order to better understand consolidant performance in situ. The key themes throughout this project are replicability and accessibility; all of the instruments used here are available commercially, and the methods can be undertaken with relative simplicity at the most basic of facilities. Where specialist operations have been used (such as during the mechanical erosion experiment) commercial laboratories have been employed, such as are available to any organisation seeking to undertake research on heritage materials.

1.2.3 Case Study Site

In order to ground this research in real-world context, Kenilworth Castle in Warwickshire (UK) has been used as a case study site (Chapter two), courtesy of the English Heritage Charitable Trust. The structure is made predominantly of sandstone and is the largest extant castle complex in western Europe, with construction and use phases spanning the 13th to 17th centuries CE, followed by several centuries of ruination and abandonment. Today, the site is a mixed-preservation tourist attraction with a restored gatehouse and stable block, ruinous Medieval and Tudor structures, and a range of partially buried and buried stonework. The castle has been used here to observe the physical effects of tourism on heritage sandstone, the range of measures taken to mitigate these effects, and to study the management of the site, both historically and contemporaneously. These observations, augmented by interviews with staff and estate custodians are used to inform the experimental design for the experimental phase of the project.

1.2.4 Laboratory-based research

Laboratory-based research in this project is based in two locations. Firstly, preparation and assessment of sandstone in sample form was done in the Geolabs, School of Geography and the Environment, University of Oxford). This work includes the development and testing of a heat-only based artificial weathering process designed to create sandstone samples that mimic naturally weathered stone in preparation for the application of consolidant treatments. Subsequently, also undertaken at the Geolabs facility were the heat-weathering of all samples used in the three experiments that follow in this thesis, and the following application of consolidants for these experiments.

In addition to this, a novel experiment was undertaken at the SATRA Technologies testing facility in Kettering, UK; which utilised a mechanically driven foot- "the Pedatron" to simulate the effects of foot traffic on sandstone paving. All preparation for this experiment was undertaken in the Geolabs, including the weathering and consolidation of samples, and the construction of the platform into which these were mounted prior to the experimental runs.

1.2.5 Field-based Research

Two of the key pieces of research within this project involve field-based experiments, and these were undertaken at the University of Oxford's field research station at Wytham Woods, near Oxford (UK national grid ref SP4723 0881) (figure 1.2, below). The location of the test area provided a fully exposed aspect for the weathering of sandstone samples once they had been prepared. The experiments included the monitored exposure of forty sample cubes (of which twenty were pre-consolidated) to weather conditions in order to test the performance of consolidants in ambient conditions (the rack exposure trial – see chapter 4). The second field experiment accommodated at this site was a test wall experiment, comprising the construction of a purpose-built sandstone wall for the testing of variables such as treatment method and block size on the establishment and performance of consolidants in situ (see chapter 5).

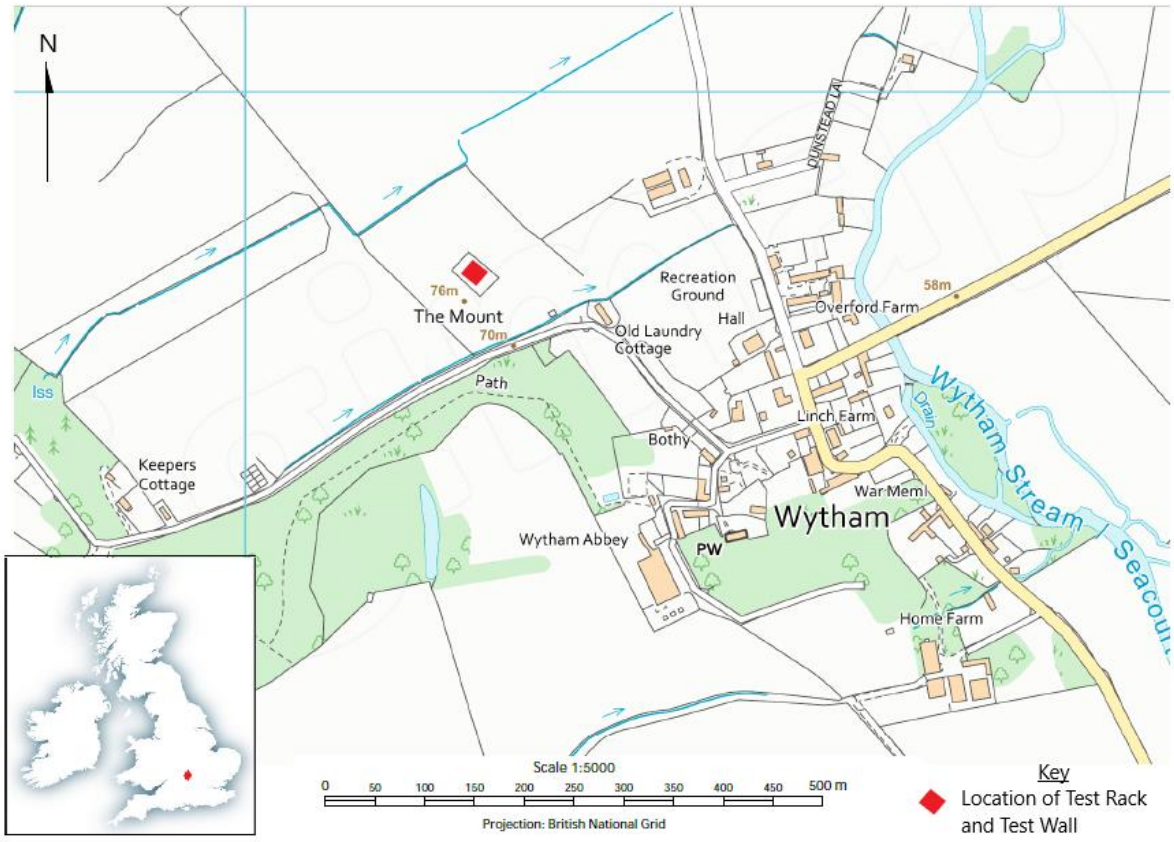

Figure 1.2 Location of field trials site at Wytham, Oxford, UK. Rack at Wall Trials are both located in the same field enclosure at grid ref SP4723 0881. Base Map Crown Copyright © Edina Digimap 2021

1.2.6 Thesis Summary

This thesis is written as a traditional long-form document, and its chapters are structured as follows. After this section, the remainder of chapter one forms a review of relevant literature, giving an overview of both consolidant use in stone conservation and a range of contemporary approaches to research in both field and laboratory settings.

Leading on from the literature review, **Chapter two** introduces the first fieldwork of the project in the form of observations taken at the case study site of Kenilworth Castle. Within this chapter the justification for the experiments in the following chapters is set out, based on a combination of field observation and interview. **Chapter three** presents the materials and methods that were selected for the experimental phase of the project, covering the selection of stone and the method used to

artificially weather it in preparation for consolidants, the selection and application of consolidants, and the preparation of stone for trials.

Chapter four outlines the first of the field experiments; an exposure rack trial set in the semi-rural Wytham Woods research centre. This trial consists of forty sample stones of varying treatment and runs for twelve months, testing the response of stone samples to local environmental changes. Following on from this, **Chapter five** builds on this field experiment by introducing more complexity to the research design. This second experiment takes the form of a test wall exposure trial, trialling different consolidant application methods and sample treatments in a fifteen-month experiment. **Chapter six**, the final experimental chapter, introduces a novel erosion simulation method, namely the 'Pedatron', a mechanical walking foot operated by SATRA Technologies Ltd which was developed to test the durability of safety and leisure footwear. The experiment simulated the equivalent of 200,000 visitor 'steps' on a replica sample of sandstone floor, and uses a combination of laser scanning and surface roughness measurement to assess the development of wear on the surface of the stone. Finally, **chapter seven** summarises the findings of the preparatory and experimental work from chapters three to six, and draws conclusions on the success of the trials in answering the aim and objectives of the project, offering some suggestions for further research.

1.3. Literature Review: Stone-Built Heritage Research

This section reviews published heritage science research as relevant to the theoretical and experimental development of this project. The review itself is not exhaustive in scope, but focuses on those areas that informed the three experiments as detailed in chapters four, five, and six of this thesis; setting out the scope and methodologies of much of modern heritage science as applied to the conservation of heritage sandstone. The following sections cover the overall nature of sandstone deterioration as observed on heritage structures, give an overview of consolidant use in the sector,

and set out a selection of recent lab and field trials which provide context for the experimental framework of this project.

1.3.1 Sandstone and the Deterioration of Built Heritage

Sandstone is a clastic sedimentary stone with a composition based on the conditions and location of bed formation. It can include "almost any pre-existing mineral or rock fragment" (Stow 2005, 139), but is generally defined by a volume of at least 50% quartz sand or sand-sized grains of other minerals or rock fragments (0.06-2mm) (Stow 2005). It is "among the most widespread of geological building materials" (Muir 2006: 191) and has an extended use-history. Formed by "the consolidation and cementation of sand or calcareous grains in slow geochemical processes" (Hall & Hoff 2012;1). Cementation is commonly achieved through the binding of elements such as hematite, calcite, silica, dolomite or feldspars (Muir 2006, Dutton and Willis 1998, Sibley 1978). In Dott's (1964) classification sandstones are categorised as arenites (more than 85% quartzite grain) and wackes (between 15-75% quartzite or mud matrix) with further sub-categorisation of stone into Quartz arenite (>95% quartz grains), lithic wacke (>5% lithic fragments, more lithic fragments than feldspars) and feldspathic or arkosic wackes (>5% feldspar, more feldspar than lithic fragments) (Dott 1964). See Figure 3.2 (§3.1, p64) for graphic representation of this categorisation. These categories are subject to further complexity when cementation and matrix materials are taken into consideration, as well as age of deposition and subsequent geological activity.

Formation of the stone occurs when minerals are compacted under increasing pressure at depth, following sedimentary deposition. The following diagenetic processes (also known as lithification) occur during this compaction phase where pressure-sorting and deformation of grains takes place together with chemical compaction and cementation. The final formation phase, telogenesis, occurs when the stone is quarried and exposed to climatic conditions and some of the less well bound minerals are lost, adding to the porosity of the stone (Choquette, P.W. & Pray, L.C. 1970, Muir Wheeler 1978).

Sandstone is therefore typified by great variability between stone sources and geological formations. However, wear and deterioration mechanisms are frequently common across the spectrum represented in this stone type (Halsey *et al* 1995). In summary, there are a number of common agents of change or deterioration that may affect a sandstone structure (natural formation or human-made), which can be defined as:

- Airborne pollutants
- Salts and waterborne minerals
- Material stress (including slippage and subsidence, structural failure, etc)
- Bio-colonisation (including micro and macro-organisms)
- Human erosion (e.g. use-wear or vandalism), and
- Disaster events (fire, flooding, etc)

Although this list is not exhaustive, these categories initiate many conservation interventions, and are therefore the focus of much of the research carried out either directly on heritage assets or on proxy materials. In addition to these drivers of change, it is also necessary to understand how deterioration manifests on the stone, patterns of which frequently allow for the determination of causality (ICOMOS 2008). The five decay groups summarised in table 2.1 cover the broad spectrum of change as observed on built heritage assets. In addition to these, an assessment of severity is commonly applied to the phenomenon in order to determine the extent of deterioration and the urgency for intervention.

Of these, material loss caused by the deposition and efflorescence/ subflorescence of water borne salts and minerals is one of the most deleterious, owing to its effect on stone of all compositions, and the tendency for it to exacerbate other existing processes of deterioration (Tümer 2003). Other forms of deterioration found on sandstone buildings are commonly derived from airborne pollutants (Adamson *et al* 2012, Mottershead *et al* ,2003, Slížková 2002).

Table 1.1 Summary of Manifestations of Stone Decay. Source: ICOMOS 2008

Cracking and Deformation	Detachment	Material loss	Discolouration and deposit	Biological Colonisation
Fracturing	Blistering	Coving/ dishing out	Crust formation	Algae
Star Cracking	Bursting	Erosion	Discolouration	Lichen
Hair Cracking	Delamination	Mechanical Damage	Efflorescence/ subflorescence	Mosses
"Craquele" (thin cracks)	Disintegration	Alveolisation/ Lacuna	Concretion	Mould
Splitting	Fragmentation	Gapping	Patina	Plant colonisation
	Peeling	Perforation	Graffiti	
	Scaling	Pitting	Film deposit	

Note: shaded areas denote phenomenon most likely to be treated by consolidation

Historically, these deposits often originated from the burning of fossil fuels for domestic, industrial, and transport use, and have been mitigated in many towns and cities by recent air quality legislation and the development of reduced sulphur fuels (La Russa *et al* 2018, Rao *et al* 2014). The historic deposition of these airborne acids is still a significant factor in the conservation of sandstone monuments however (Halsey *et al* 1995, Turkington *et al* 2003), with the long-term effects of build-up often compounded by inappropriate high-pressure water or chemical cleaning of spalled surfaces (Young *et al* 2003).

The geographical setting of the asset is a key determining factor here, with local environment and neighbouring activity frequently providing the catalyst for change (Elhaddad *et al* 2018, Turkington *et al* 2003, Wright 2002). Aspect also has been shown to have a defining influence on the type and speed of change likely to happen during the lifespan of heritage asset; with exposure to direct sunlight, prevailing wind and rain, and the variability of wetting/ drying and heating/cooling cycles as associated with these factors determining the conditions specific to change as observed over time

(Mottershead *et al* 2003). Turning to the mechanisms of change, the first to note are the formation and subsequent detachment of crusts, often the result of the transportation and deposition of minerals and waterborne particulates (Halsey *et al* 1995). The detachment of these build-ups frequently occurs either as a result of the breakdown of surface cohesion at the stone surface interface (driven by continuing cycling of minerals and environmental inputs) (Sabbioni 2003) or as a result of removal such as during cleaning (Young *et al* 2003).

Mass loss is not limited to that which is associated with the removal of deposits however, and sandstones which contain diverse and highly variable materials within their matrix present a range of patterns of breakdown associated with the dissolution and leaching of internal deposits, chemical interactions with the environment, and with physical abrasion through use. In short, these can be typified as the propagation of cracks and deformities, detachment and delamination, and alveolisation; as per Table 2.1 which summarises sub types of decay under these headings. Whilst conservation responses to these have been increasingly formalised over recent years, there is still a great deal of ambiguity available at the point of individual decision-making. Guidance is freely available In the United Kingdom from the national organisations in England (Historic England 2017; Odgers 2014; Odgers & Henry 2012) and Scotland (Andrew, Young & Tonge 1994; Young, Cordiner, and Murray 2018), as well as from independent organisations such as the Institute for Historic Building Conservation (IHBC) who publish and update guidance for planners and practitioners under the guide of the IHBC Toolkit, and the Society for the Protection of Ancient Buildings (SPAB) who maintain a free resource of technical guidance notes on their website.

These publications and resources all originate from and are guided by international-level charters. The ICOMOS Charter for The Conservation and Restoration of Monuments and Sites (the 'Venice Charter') for instance set out the principles of recourse to science for guidance in conservation practice (ICOMOS 1965, Article 2), and that modern materials must only be introduced after traditional approaches have been proven "inadequate" (ibid, Article 10). However, the link between

published research on the nature of the mechanisms as outlined above and the practical guidance as directed by these conservation institutions is not always self-evident. As stated above, decision making at the individual case level is still open to interpretation from individuals at both professional and stakeholder level, and the application of scientific knowledge in a conservation setting is still acknowledged as an area wherein collaboration and the diffusion of knowledge is sometimes impacted (Dillon *et al* 2014).

1.3.2 Overview of Consolidant Use in Heritage Conservation

Consolidation of decayed stone, or the constraint of deterioration through the application of binding agents is not a new development. In London's Westminster Abbey during the 19th Century for instance, waxes suspended in turpentine were applied to decayed stone in multiple instances (Clifton 2008, §4.4). Further back in history, the Roman architect Vitruvius also describes a wax treatment used on masonry in the later years of the Republic (Price 1975).

Today's array of treatments naturally encompasses a much wider range both of materials and application techniques, driven in part by the 20th Century expansion of oil and the plastics industry, though there remain common threads which may be recognised by those historic conservators. In practice, the process of consolidation is most commonly that of a solution applied by "brush, spray, pipette, or immersion" (Price & Doehne 2011; 36). Additions to these traditional techniques have been developed using poultices, contact "pockets" of solution, pressurised or vacuum injection, and containerised supply introduced through targeted dispersion points (Domaslowski 1969, Mirowski 1988, Pummer 2008). Scale is a major consideration in the selection process for these methods, with some of the more elaborate or complex methods being size-limited and therefore suitable only for objects such as sculptures (Price and Doehne 2011). Furthermore, the selection of consolidant type is crucial. There are a range of serious secondary effects associated with inappropriate consolidant

use, ranging from discolouration to accelerated delay (Wheeler 2005). The decision-making process

Table 1.2 Summary of Consolidant types covered in this chapter

Category	Characteristics	Comment	Useful References
Acrylics & Polymers	Historically poor performance in UV exposed settings	Huge variation in sub types and specialisation in final use	Wheeler 2005, Yang 2011, Zhang et al 2013
Lime	Traditional method, new developments and research have both informed and cast doubt on effectiveness of established methods	Commonly used in the UK for a variety of conditions. Use has been augmented by the reestablishment of reliable, industrially produced limes	Ashurst, 1998; Clarke, and Ashurst. 1972; Price et al. 1988; Historic England 2017
Nanolime	Nanoscale particles suspended in alcohols to enhance penetration	Promising developments in application using alcohols, greater penetration, curing which does not hinder air/moisture flow	Daniele and Taglieri. 2010; Giorgi et al. 2000; Howe, 2007
Barium (carbonate and hydroxide)	Characterised by the introduction of a solid phase within pores to mimic natural bonding Developments in nanotechnology are improving the performance of these treatments	Inorganic consolidants used on limestone and calcareous sandstone Much debate as to the effectiveness of these treatments in traditional form Nano-hydroxides offer the potential to have much greater penetration in aqueous solution	Hansen et al 2003; Clifton, 2008; Giorgi 2010; Ciliberto *et al* 2008
Siliceous/ Silicofluorides	Including magnesium, zinc, and aluminium	Limited penetration due to vigorous contact reactions leading to surface deposition of material	Clifton 2008; Fassina 1995
Alkoxysilanes (commonly referred to as silanes)	Complex chemical subtypes, long period of development and testing	“the most promising... for Sandstones” (Clifton, 2008). Brethane is included in this category. TEOS and variants are common	Franzoni et al 2015; Wheeler 2005

is further compounded by the increasing range of products available worldwide.

The text below sets out the most common industrial products and chemical combinations used currently and (where appropriate) historically- also summarised in table 1.2 above, outlining out their recognised strengths and limitations as published by practitioners and researchers alike.

Limes

One of the most traditional consolidant systems, calcium oxide or hydroxide has been used in an attempt to weatherproof, decorate, and bind a range of building materials since Late Iron Age and Roman era at least, across Europe and the Mediterranean (McKay 1975). It endured in the British Isles throughout the medieval and into the modern period, and today is seen by some as a typically British practice in a modern context (Clifton Taylor 1987; Price and Doehne 2011). That said, lime is not a 'dead' technique, and is evolving in both material and usage. With regard using lime in a consolidant capacity, there are two key areas to examine; variants on a traditional lime application, and modern 'nano-limes'.

Traditional limes, whether in the form of a limewash, a mortar, or as a poultice/ render, have been extensively used, and trialled as a repair material on a range of stone types, predominantly limestone but also calcareous sandstones (Historic England 2017). Their effectiveness as either a repair or protective application is subject to much discussion (see for instance Price and Doehne 2011, chapter 2; and Price et al, 1988).

One key issue is that calcium hydroxide, used in the mixing of limewater, is limited by its concentration of ≤1.6g of lime per litre of water, which translates to a need for multiple coatings for any meaningful quantity of material to be introduced to the stonework, of the many issues this may cause, in particular each application has its own penetration limited by the previous one (Historic England 2017). Time of curing and the effectiveness of aqueous solution as a means of introduction are also the subject of debate. Price et al (1988) for instance demonstrated that in repeated tests

the consolidating lime was deposited in a very narrow band at the near surface of the stone and did not penetrate more than a few millimetres.

Other lime techniques include the application of mortars either as a traditional sacrificial jointing medium or as a binding component in a poultice applied temporarily, or as a more permanent barrier to failing stone surfaces in the form of a render (used mainly on limestone structures). These applications are often recommended where structures have pathologies typified by salt efflorescence or biological colonisation; often resulting from an impedance of moisture flow from the internal structure to the surface (by excessive water entering the structure or by inappropriate application of non-porous paint or weather protective coating). In this respect, limes should most commonly not be employed as a consolidant in the long term, but as part of an intervention designed to return a structure, or part of a structure to an equilibrium state. Extensive work on the lime technique has been published by the late John Ashurst (1998, 2007) and by Ashurst & Ashurst (1988), as well as Ashurst and Dimes (1998). The use of lime is still widespread across the United Kingdom, and often a combination of the above methods are employed on a structure to effectively consolidate and conserve stonework, whilst simultaneously improving appearance.

Nanolimes

The first commercial nanolime treatment for the consolidation of limestones (CaLoSiL) became available in 2006 although their inception lay in the 1960's for the treatment of frescoes (Slížková and Frankeová 2012, Historic England 2017). In effect, nanolimes are liquid treatments containing calcium hydroxide particles less than 100 nanometres in length, suspended in an alcohol. These particles are typically plate-like in shape, and their diameter is often four or five times their thickness (Historic England 2017). A notable difference between nanolime solutions and more traditional limewashes is that the upper limit of strength in solution as noted above is lifted, with triple strength applications achievable in single applications (Otero 2017). Using synthesised calcium hydroxide with

alcohol, further improvements were made subsequently during trials, with a concentration of up to 50g per litre being achieved (Historic England 2017).

The key differentiation in performance between nanolimes and traditional limewashes is therefore a combination of greater concentration of calcium deposits and the improvements in mobility of solution, as the alcohol suspensions are capable of being drawn farther into the pore structure of the substrate stone, allowing for a much less surface-limited mass to be consolidated.

Nanolimes are most effective in treating a specific range of deterioration phenomena such as powdering and granular breakdown, but not more structural failings such as cracking or delamination. They are also affected significantly by the presence of biota or surface crusts, which act as a barrier to absorption and are liable to become detached, taking any treatment with them whilst simultaneously exposing new material to the atmosphere (ibid).

Siliceous Consolidants and Hydroxides

Analogous to Limes in application, siliceous consolidants use silica to fill pore spaces and bind loose materials within a failing stone (Fassina 1995, Clifton 1980). Sodium hydroxide for instance has been used to introduce Silica to stonework, although the Sodium needs to be subsequently removed from the stonework through washing to prevent future efflorescence and the associated damage caused by salt crystallisation (Clifton 2008). Silica can also be introduced through reaction between Sodium Silicate or potassium silicate, and hydrochloric or sulphuric acid. However, a biproduct from these solutions; calcium acetate, can damage stonework through crystalline growth, as with salts, and so must be removed during the curing process. Both of these formulations have been applied with varying degrees of effect to both limestone and sandstone, the former often deleterious and the latter ineffectual (ibid).

A magnesium silicoflouride solution (for example SURFHARD®, developed for use on concrete) has been used to consolidate limestone, though also with limited penetration and unwanted biproducts such as a hardened crust or secondary deposits such as insoluble salts (Lehmann 1970).

Aside from calcium hydroxide, other hydroxide solutions in use for cultural heritage conservation include Strontium and Barium. Barium reacts in a similar manner to calcium hydroxide, depositing carbonates near to the surface of treated stone. However, unlike calcium, barium sulphates are insoluble which allow for more effective consolidation, in the short term at least. Opinion and experiences of researchers and practitioners vary however, with some dismissing the material as ineffective in all of its applications (Schaffer 2016, Schnabel 1992, Toniolo *et al* 2001). In other fields, a barium hydroxide nanoparticle application similar to the Nanolime approach outlined above has been trialled on wall paintings and plaster (Giorgi 2010), and when used in tandem with the lime treatment has shown an improved performance of the consolidant through symbiotic cross reactions (ibid).

strontium hydroxide has a similar history of use to both above hydroxides, with parallel limitations in use. Ciliberto et al (2008), outlines once again a dispersion of the material into a solution (this time aqueous rather than alcohol), on a nanoparticle scale for the effective introduction into heritage materials (not limited to stone, but also for use on "wall paintings (frescoes), paper, stone, wood and other artistic artefacts" (Ciliberto *et al* 2008; 137). Maurizio Licchelli (*et al* 2014) argues that strontium nanoparticle solutions applied by brush penetrate as effectively as both Nanolimes and TEOS (see below) control samples in laboratory tests (Licchelli *et al* 2014; 681).

Polymers

Resins, including non-structural polymers such as styrenes and acrylics, as well as structural materials including epoxies, polyesters, and polyurethanes, have a long established and often problematic relationship with conservation (King 1988). Uses differ, and the outcome of the application is often dependant on the matching of product to problem, something that in the past has been overlooked by decision makers (ibid). As adhesives, the structural polymers often perform their designated role effectively, although for conservators their appearance, and the changes they effect upon the stone are problematic, especially in the long term where UV exposure can discolour

the treated areas -notably with regards polyurethane (Wheeler 2005, Yang 2011). Other colour changes are recorded immediately following treatment where samples are exposed to salts, resulting in a noticeable darkening of the surface (Zhang *et al* 2013; 1128).

Where more success with these materials has been found is in the application of them in resinous mortars or grouts, though where their inclusion in render and mortar mixes has been to replace lime it has been proven that they do not provide the same tolerance for movement, or to 'self-heal' as would the traditional lime (King 1988).

Alkoxysilanes/ Silanes

James Clifton (1980) asserts that silanes as a group are the most "promising" treatments for the conservation of heritage stone; and they are certainly some of the most prominent, as an industrial product. This is not a universally shared viewpoint however, as Yang *et al* (2011) point out, the drawbacks of these materials are almost as numerous and varied as there are products available.

A varied group of chemical subtypes, silanes (or alkoxysilanes) are often designated a key tool in the conservation of stone, and in particular siliceous sandstone. Prominent variants include MTMOS (methyltrimethoxysiilane), MTEOS (methyltrieothoxylsilane), trialkoxysilane, and TEOS (tetraethylorthosilicate)- the latter also known as ethyl silicate. These have been developed, refined, and produced widely across the industrial complex. In use the liquid solution is applied to the surface and percolates through the open pore structure and between any delaminated or separated stone, depositing a layer of silica upon stone surfaces without blocking the flow of air or moisture. This silanisation- the industry term for the process- is the said to form a durable "heterogeneous bond between inorganic and organic materials" creating a uniform composite (Gelest 2014; 4). As with other materials and processes outlined here, one of the main problems identified with silane application on stonework however, is that of limited penetration and deposition of consolidant material (Price 1975, Wheeler 2005); typically 25-40 mm from the surface, advertised as 100 mm by manufacturers (Wacker 2014), with Brethane a trialkoxysilane developed by the Buildings Research

Establishment in the 1970s but phased out in 1997 due to Lead content, being notable for penetrating up to 50mm during tests (Wheeler 2005). Another issue, which is contested by some manufacturers (e.g. Wacker 2014), is the curing time of these materials. Whilst advertised as being cured to "full hardness" after 2 weeks (Wacker 2014, 1), trials of TEOS consolidants (of which Wacker OH is a variety) were shown during tests to take several months to achieve full consolidation (Franzoni *et al* 2015, 399). In favour of this class of treatment however is the relative low viscosity of the solution, and the capacity for curing without depositing deleterious substances in or on the surface of the stone (ibid).

Despite it being withdrawn as a commercial product over 20 years ago, it is worth mentioning Brethane again at this point, as it has been subject to some long-term performance evaluation and can still be seen in situ at a range of sites in the UK (see figure 1.3, below). Studies carried out by Butlin *et al* (1995), and Martin *et al* (2002) documented the performance of this treatment over a 20-year period, over ten sites encompassing a range of limestone and sandstone structures. Results from these surveys are conflicting, but the overall conclusions are that the treatment had a more pronounced effect on limestone, but that over the elongated timeframe of the process, none of the treated surfaces weathered favourably over neighbouring untreated areas (Wheeler 2005).

Figure 1.3: Left. Kenilworth Castle, south elevation of 12Th Century Keep, Brethane treated area. Taken 1997, © English Heritage Photo Archive, after Fidler 2002.Right. Same area, image taken 2018, © Author

In more general terms, silanes are also affected by the composition of the stone substrate. The presence of clays within the stone in particular has a limiting effect on both short- and long-term performance (Sattler & Snethlage 1988), as does the environmental setting of the structure to be treated (Wacker 2014). Evidence of this latter factor- the inability of silanes to repel environmental extremes can be found in Oliver's (2002) study of sandstone monuments in U.S. National Parks, where abnormally high temperature and rainfall proved an effective block to the treatment's establishment within the substrate (Oliver 2002, Franzoni et al 2015).

1.3.3 Built Heritage Conservation Research

Experimental work on historic structural materials commonly falls into two broad categories: sample-based trials (both lab and field), and testing carried out on heritage structures themselves, which includes the taking of samples, images, scans, and the collection of proxy data. Both of these approaches, though well-grounded with regard to methodology and scope, have common limitations. For the latter, the direct sampling of heritage assets presents ethical and practical issues, not least in the form of legislation. In the England and Wales for instance the Ancient Monuments and Archaeological Areas Act (1979) and Town and Country Planning Act (1990) codifies the status of monuments and buildings respectively (the latter often placed on the National Heritage List as 'listed buildings'). As a result, any intervention that causes visible or traceable change to any area of a designated asset subject to the prior permission of consent; a step that can take several years for those categorised as most valuable (for instance Scheduled Monuments or Grade I listed buildings). As a consequence, much of the research carried out in the name of heritage science will (either by choice or obligation) use a proxy for the monument or building in the form of representative samples. In these circumstances the requirement for holding the experiment on the site of the heritage asset itself can be less critical, and this introduces the option of hosting at analogous sites, or even conducting the experimental work entirely within a laboratory setting. Critical to the decision-making process in this respect are the specific research questions to be addressed,

proximity to a given site may be essential if contemporary atmospheric conditions are to be studied, whereas removal of aged samples make this less critical if this is an option. Conversely, placing a range of new samples in the context of a monument allows for the study of contemporary conditions without directly interacting with the historic material itself. There are many instances where the research design is a compromise based on similar considerations. The following sections will outline a range of contemporary heritage research projects which provide examples of the variant styles of sampling and trial frameworks commonly used by scientists and conservators today.

Studying Heritage Assets Using Laboratory Trials

Sample based trials in the laboratory are most effective where they are able to utilise materials taken directly from heritage structures. These provide the opportunity for direct assessment of the material itself, and any chemical changes or accumulated deposits over extended lengths of time. The process of removing these samples is not without issue however, and in situations where removal is not possible, the relationship between proxy samples and historic structures must be garnered by extrapolation. Destructive tests on proxy materials can produce important data however, and often it is preferrable not to use historic fabrics for these trials. Characterisations and durability tests are conducted on stone to determine their susceptibility to wear or erosion stemming from a range of stimuli. Salt crystallisation resistance and acid immersion tests for instance measure the capacity of building stones to withstand some of the more common environmentally derived factors (Benavente 2020, Halsey *et al* 1995). As the results of such tests are not reversible, in the main it is not appropriate for historic building fabric to be used. The development of proxy samples which behave in analogous ways to those which have been weathered in situ is therefore an important avenue of heritage science research. This artificial weathering of sample stones falls into that which is driven by chemical or physical processes. Of the former, the application of salts and acids have been extensively trialled, often with only partially successful results (Ban *et al* 2016). Other physical weathering trials often use heat or freeze-thaw as

a catalyst for change, of the former, Franzoni *et al* (2013), and Hajpál & Török (2004) successfully altered the characteristics of sandstones under laboratory heating. Conversely, Ruedrich (*et al* 2011) concluded that freeze-thaw was often an energy- and time- consuming mechanism for driving change in sandstone, with samples needed up to fifty cycles to register any measurable difference.

Where trials include sampling of heritage assets, limits are commonly placed on both access to structures and the type of sampling permitted. Often these are limited to non- or minimally-destructive procedures, under the 'principle of minimal intervention' (BSI 2013;10).

A hybrid approach to sampling historic fabrics was adopted by a study of the Charles Bridge in Prague (Drdacky *et al* 2020) which took otherwise unwanted material left after repairs to the monument and used them as sample material for a range of laboratory-based trials on the effectiveness of consolidant treatment, facilitated in the laboratory.

Other destructive simulations carried out in controlled laboratory conditions include those which simulate disaster events. The benefits of carrying out these tests in laboratory conditions are clear, with the need to closely monitor processes such as extreme heating in a safe and controlled environment coupled with the ability to bring about the early conclusion of test runs a major consideration. Whilst these tests often have some element of compromise involved, for example the replacement of fire exposure with furnace heating, much is been done to quantify how these experiments can be redesigned or adapted to more accurately mimic real-world conditions. A good example of this are the fire simulation experiments carried out by Nadine Freudenburg *et al* (2020) at the Institute of Geotechnics (Freiburg) which compared oven heating with real fire heating to imitate the fire storms experienced during the Dresden bombing raids of the second world war, highlighting the limitations of the former approach as a methodology.

Moving away from the study of stone and definition of its characteristics as a principal aim, there is a significant body of work on the range of consolidant applications set out in §2.2; encompassing their uses, limitations, and application methods. The array of instruments and techniques that have been

applied to this research is now vast and is ever increasing; and ranges from the most basic (in terms of equipment and methodology) such as the Karsten/ RILEM Tube and contact sponge (Gulotta *et al* 2020), to the highly specialised application of Neutron radiography and tomography to create high resolution visualisations (Ban *et al* 2019, Hameed *et al* 2009). Studies frequently include the characterisation of treated stone through a combination of non-destructive and destructive means. For the characterisation of internal structure and integrity, Ultrasonic Pulse Wave Velocity is commonly used as a non-destructive method (Ban *et al* 2016, Benavente 2020, El-Goharty 2013, McAllister 2013, Wilhelm *et al* 2021), whereas in tests where the samples are sacrificial, the Drilling Resistance Measurement System (DRMS) can be employed to good effect to test for the presence and depth of consolidant within samples (Bracci *et al* 2004, Ludovico- Marques & Chastre 2014). These techniques are commonly used in concert with other analyses of change, especially pertaining to the surface condition of stone and consolidant alike. For these, colorimetry is a reliable and well understood non-destructive means of detecting minute changes to a sample, and it can be used to test not only for the condition of stone and any treatment but to test for biological colonisation of materials as an indicator of conditions (Bergamonti *et al* 2018, Sanmartin *et al* 2020).

In recent years, studies that focus purely on the chemistry of consolidants and how they interact with the substrate have made use of the increasing array of complex high tech visualisation techniques including X-Ray Diffraction (XRD) (De Ferri *et al* 2011), Scanning Electron Microscopy (SEM) (Bergamonti *et al* 2018), Raman Spectroscopy (ibid), and Neutron Radiography and Tomography (Ban *et al* 2019, Hameed *et al* 2009). Whilst these approaches offer a valuable and often unique insight into the conditions within treated stone, the cost of equipment and limited access to host facilities can render them unavailable for many research projects.

Image Based Rendering for Conservation

The use of digital rendering for heritage management purposes is long established. From the earliest iterations of computer vision in the 1960s (Huang 1996), where digital models of classical period

architecture were created using the features of monuments for monitoring of large-scale changes (particularly with regard to major events such as earthquakes), the value of virtual-space rendering has been apparent. The development of technology from these early processes into the range of applications available to heritage professionals today is a complex story that falls outside of the remit of this work (but see for instance Gomes *et al* 2014, Guidi et al 2004, Scopigno, *et al* 2017, and Vilbrandt *et al* 2004). However, it is important to pick up on one thread within this section of technological development that is directly relevant to this project. The use of reflected light laser scanning (commonly referred to as LiDAR) represents one of the most significant technological advances because of its potential for highly accurate rendering of objects at a variety of scales and in almost real time (Bewley et al 2005). Initially developed as an aerial technique used for landscape scale interrogation of topography and near-surface geological formations (Bewley *et al* 2005), continual refinement of both sensors and processors have reduced the size and cost of the instruments, whilst increasing their resolution and accuracy. At the time of writing there are a range of commercially available scanners (both handheld and tripod mounted) that are capable of feature identification and reconstruction at millimetre and sub-millimetre scales (Creaform 2021, Leica 2016).

The use of digital 3D modelling on heritage structures and surfaces has developed into one of the most promising and valuable avenues or non-destructive testing in modern conservation (see for example Dellepiane *et al* 2011, Guidi et al 2004, and Stefani *et al* 2014). The continual development of both hardware and software capabilities means that year-on-year the computing power required to construct models becomes more affordable, as the level of detail possible increases. Whilst image-based rendering (IBR) approaches such as traditional photogrammetry or Structure from Motion (SfM) continue to have technical limitations that constrain the resolution of reconstructions (Remondino & El-Hakim 2006), advances in laser and structured light scanning -particularly regarding handheld scanners- have revolutionised both the process of data capture and the post-processing of point-clouds into usable datasets (Sansoni et al 2009; Zlot *et al* 2014). Furthermore, the end-use for

these models is now more widely recognised in a range of sectors with the growth of Building Information Models (BIM)- and specifically in this context Heritage BIM (HBIM), which provide a platform for the integration of repeated models over time (Lopez *et al* 2018), as well as the curation and dissemination of digitised artefacts in a museum and learning context (Younan & Treadaway 2015). The possible benefits of this are numerous, but crucially they allow for the high-level monitoring of wear and decline over time, in an accurate and transferrable format (Lopez *et al* 2018). At the artefact or sample scale, outputs for the interrogation of these models include a range of opensource software projects that allow for the combination and comparison of datasets at the sub-millimetre scale, for instance within packages such as CloudCompare and Meshmixer, both of which are capable of handling complex data topographies for the measurement of change, and which the former benefits from the addition of a range of functions which streamline the calculation of change detection and provide for the interrogation of detail at high resolution (Lague *et al* 2013).

Studying Heritage Assets Using Field Trials

Away from the laboratory, field-based studies commonly fall into the category of research *in-situ* or at a remote location, and often include an element of each. As a rule, the study of built heritage assets *in situ* offers the most direct means of improving understanding of the processes of decay, and by extension the effectiveness of conservation strategies. Traditional approaches to the study of sites, structures, and monuments often required the removal of samples for testing in laboratory settings (Andre *et al* 2011). This kind of sampling, though often referred to as destructive, ranges in scope and intrusiveness from the removal of micro-scale deposits such as atmospheric particulates (e.g. Halsey *et al* 1995), to the removal of cores or large pieces of masonry. This latter is most appropriate where repairs are already scheduled, for example the study of seven Sandstone types carried out by Drdacky et al (2020), which took advantage of the need to replace damaged areas of the historic Charles Bridge in Prague (Czech Republic), a site which presented as a 'palimpsest' of stone following many years of damage and ad hoc repair. This particular project may be viewed as

an example of 'rescue science' whereby the material that was selected for replacement was taken by the research team and used in the laboratory, as opposed to physically sampling from extant materials. In a similar vein, field investigations at Kathmandu, Nepal, utilised already ruinous parts of the site to source material for laboratory tests (Parajuli 2012). This last example combined an on-site study of historic Kathmandu, a settlement historically at high risk of earthquake damage, with remote test experiments wherein test structures (small composite 'brick wallets') were made from previously ruined building material taken from site. This approach allowed for the direct comparison of test results with those taken on historic structures, whilst allowing destructive testing (core sampling, load testing) to be carried out on authentic and aged materials, without further damaging already vulnerable structures.

Other field-based approaches utilise samples placed in a range of external situations in the capacity of stone as 'sensor' for the study of decay (Bidner *et al* 2002, Slížková 2002). This includes the placement of sample stone on-site in a range of formats, ranging from individual samples placed on exposure racks at laboratory facilities (Bracci *et al* 2004), to situating them across a range of environments which allow for comparison of the effect of local conditions. One of the benefits of these type of trials is that they allow for the examination of many interacting factors in a single experiment in a way that studying a single site or monument may not. In one EPSRC-funded project of this type, sandstone samples were placed on exposure racks were placed at nine locations around Northern Ireland, encompassing urban, suburban, and rural environments. In addition to these factors, racks were positioned at each site with both north- and south- facing aspects at each, allowing for the assessment of both environment and position relative to sun exposure (Adamson *et al* 2012). An alternative to this approach was undertaken by Susanna Bracci, Maria Jao Melo and Piero Tiano at the CNR laboratory in Florence (Italy), where an exposure rack situated on the laboratory roof was populated with Pietra Forte sandstone treated with five commercially available consolidant treatments, and their response to UV exposure and the urban atmosphere was observed over a five-year period (Bracci *et al* 2004).

The third format for field-based research involves the use of test walls, or testing at 'model scale' as it is sometimes referred (Egermann et al 1991). This approach is well established in construction, engineering, and materials testing, and has significant precedence in heritage research. Large, complex projects have been carried out to determine both component and system performance characteristics of model-scale structures (for instance Messali *et al* 2017), as well as reproduction facsimilies at full-scale (Griffith *et al* 2007) notably in the field of disaster management (earthquakes, flooding, etc) and engineering sciences. The discipline of experimental archaeology has a strong tradition in this regard, with over thirty full size reconstructions of 'Iron Age' type roundhouses across the UK today (used for research as well as public engagement) (Mytum & Meek 2020, Townsend 2007); as well as a range of projects which utilise partial, scaled-down, or performative reconstruction activities to inform understanding of a range of objects and structures (Benjamin & Sivilarkitekt 2009, Bischoff *et al* 2014, Timberlake 2007). As the Venice Charter (1965) prescribes the use of scientific methodologies in researching the nature and characteristics of heritage structures (followed in 2003 by the Charter Principles for the Analysis, Conservation and Structural Restoration of Architectural Heritage, (ICOMOS, 2003), alternative approaches needed to be sought, especially where systems-scale data are required.

To this end, a particularly effective way of collecting reliable data without causing undue damage is to mimic conditions on heritage buildings, and many projects have utilised purpose-built structures for research in this manner, or the placing of proxy samples on or near to the heritage assets themselves. In Scotland, a series of earthen test walls have been constructed across the country to determine the extent to which changes in climate affect the material over extended periods of time (Walker, McGregor & Little 1996). In Derrygonnally (Northern Ireland) a "field laboratory" was constructed using Peakmoor sandstone, which included embedded sensors for the monitoring of the effects of a temperate climate on stonework (McAllister *et al* 2013). This test comprised a cabin which had sandstone cladding fitted on all sides, with a complex set of angled faces and overhangs designed to mimic a range of architectural features observed on buildings, for the purpose of

determining how aspect, shading, and run-off characteristics effect the rate of change. Further examples of this approach can be found in Granite (Fusade *et al* 2019, Orr *et al* 2020), and rammed earth/ adobe (Parajuli 2012).

One of the more innovative examples of this subcategory of research was the Stone Deterioration and Stone Conservation Project, run by the Ministry for Research and Technology in Germany between 1986 and 1996 and re-examined by the University of Oxford and Getty Conservation Institute (Wilhelm *et al* 2021). This project utilised a series of intricate and complex pre-cast concrete test pieces known colloquially as ”Asterixes” because of their similarity with Goscinny and Uderzo’s cartoon character (Figure 1.3). These were originally used in an exposure trial across two sites in northern Germany, and their complex geometries allowed for the interrogation of a number of variables over an extended period. The project, which officially ended twenty-five years ago, is again providing valuable insights into weathering over extended periods thanks to a collaboration between researchers at the Getty Conservation Institute, University of Oxford, and the Fraunhofer Institute (Wilhelm *et al* 2021).

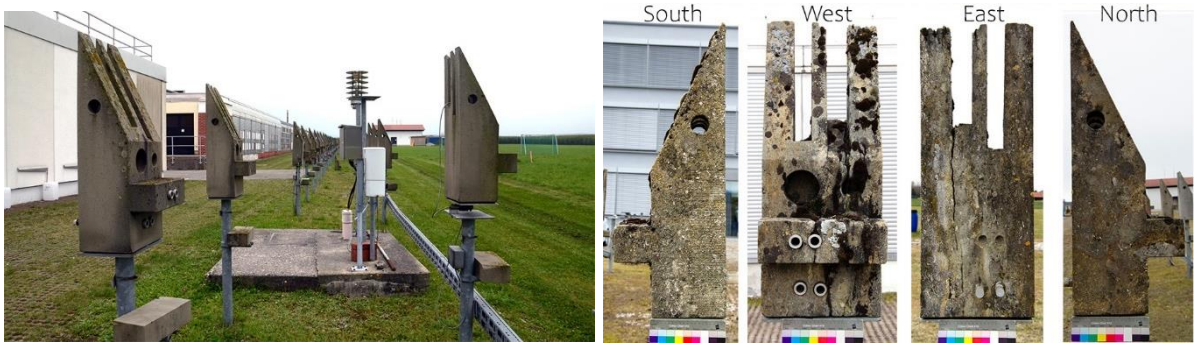

Figure 1.4 “Asterixe” test pieces on site in Holzkirchen, Germany. Images ©K Wilhelm

Finally, Historic Scotland have made good use of the test wall approach at their Conservation Centre in Edinburgh (Kennedy 2015; Young, Cordiner, & Murray, 2018). There are many factors in favour of this approach; not least that it removes the aforementioned limitations on destructive sampling, and by association the need for reversibility (Kennedy 2015). Furthermore, with the correct preparatory research into the materials and processes used, an understanding of historical performance can be

gained, thus informing future management practice. Where this field trial experiment varies from these examples is that commonly these experiments are focused on a single or dual research question; Fusade *et al* 2019 for instance measured the performance of mortars under variable simulated conditions, whereas Richards *et al* (2020) sought to measure the rate of erosion on the mass of a test wall. The key difference with this experiment is that the wall itself is designed to accommodate multiple variables and produce multiple data outputs, also allowing for the physical expansion of the structure with regards both size and complexity at a later date.

1.4 Summary, the State of the Art

In summarising the state of the art in built heritage science research relevant to this thesis, a complex picture emerges across a variety of materials and settings. In the last fifteen years some of the most important developments in the sector have arisen from the adaptation of highly complex processes, such as the application of neutron radiography and tomography, the refinement of Scanning Electron Microscopy; and the further development of digitisation techniques and equipment into more user-friendly products. Specialised laboratories in many locations across the world now have experience in hosting scientific heritage research, providing access to complex instruments and expertise. In addition to these technologies, the further development and testing of methodologically simple but highly robust applications such as the Karsten Tube and Contact Sponge have given researchers a range of techniques that are equally applicable in both lab and field conditions. Whilst some instruments and software systems remain highly-priced and out of the reach of many conservators and stakeholders, the range of field applications using those more modest instruments and techniques are providing the basis for a range of fast and cost-effective alternatives. Also of note here is the growing number of opensource applications for the digital heritage research sector. Until recently, the capture and processing of three dimensional datasets for samples and structures alike were the preserve of those who had access to specialist CAD suites, however, today there are several examples of free-to-use programmes (donation supported)

capable of handling multi-million point data clouds, and with the ever-improving consumer computer market making high spec processors and storage cheaper year on year, it is now possible to collect and manage these datasets at a reasonable cost. Coupled to this, developments in the capabilities of consumer mobile phones and tablets have created a parallel research space in which data can be collected using the technology many of us carry around on a daily basis, including extremely high-quality image collection (in both visual and non-visual parts of the spectrum), temperature, moisture, and position data.

Away from the forefront of technological development are the equally important efforts to improve access to prior knowledge. Since the inception of heritage science as a discipline within cultural heritage and conservation sector in 2006 (Kennedy 2015), concerted effort has been made to signal boost the work of heritage scientists and make access to these new technologies and findings more universal. A key element of this has been the move to Open Access publication for scientific papers, a move that removes a significant barrier to dissemination. However, this must be coupled with a greater focus on differentiated language; one of the biggest barriers remaining to the application of the wealth of applied scientific learning. In summary, the potential for research to directly influence conservation strategies in a positive and informed manner has possibly never been greater. The dissemination of technology into consumer markets coupled with increased access to reference material has created a situation where conservators are perfectly placed to apply scientific methodologies to the preservation of cultural heritage.

Chapter Two: Case Study of Kenilworth Castle

2.1 Introduction

In seeking to anchor the research and experimental work contained within this thesis in a 'real world' context, it was necessary to first look for examples of the conditions encountered in sandstone site management and conservation. Historic structures are increasingly being used as visitor attractions in an attempt to fund their ongoing preservation, and this phenomenon has created a situation where sites are vulnerable to different patterns and rates of wear. Observation of these patterns therefore provides an import resource to inform how conservation strategies are developed and applied. Kenilworth Castle is a prime example of this; a site with an extensive history and complex conservation needs and one which has seen increasing visitor pressure in recent years. A study of Kenilworth Castle therefore provides a unique insight into the challenges of managing a complex multi-phase heritage asset, balancing the needs of conservation with the necessity of accommodating visitors and generating revenue. Through the study of both historic and contemporary activities on site (including research, structural interventions, and visitor management) it is possible to build a picture of the range of issues that are faced by managers of many historic estates; and thereby identify the areas in which work carried out in this project can be applied by both researchers and custodians. In this contextual study, the rationale for the experimental work that follows is introduced, using examples from this internationally important heritage site.

2.2 Overview of Kenilworth Castle

The historic town of Kenilworth sits at a height of approximately 85 metres AMSL (Above Mean Sea Level) in a traditionally woodland and farm landscape in central Warwickshire, UK (lat. 52.347127, long -1.594488). Close to the modern conurbations of Coventry and Birmingham, as well as the historic towns of Warwick and Stratford on Avon, much of the medieval town of Kenilworth, including the ruined abbey and castle are built of the Helsby Sandstone which is found in outcrops to

the west of the castle site and was historically worked at Grounds Farm. The castle itself is a multi-phase ruin set in a semi rural location at the western edge of the town (see Figure 2.1)

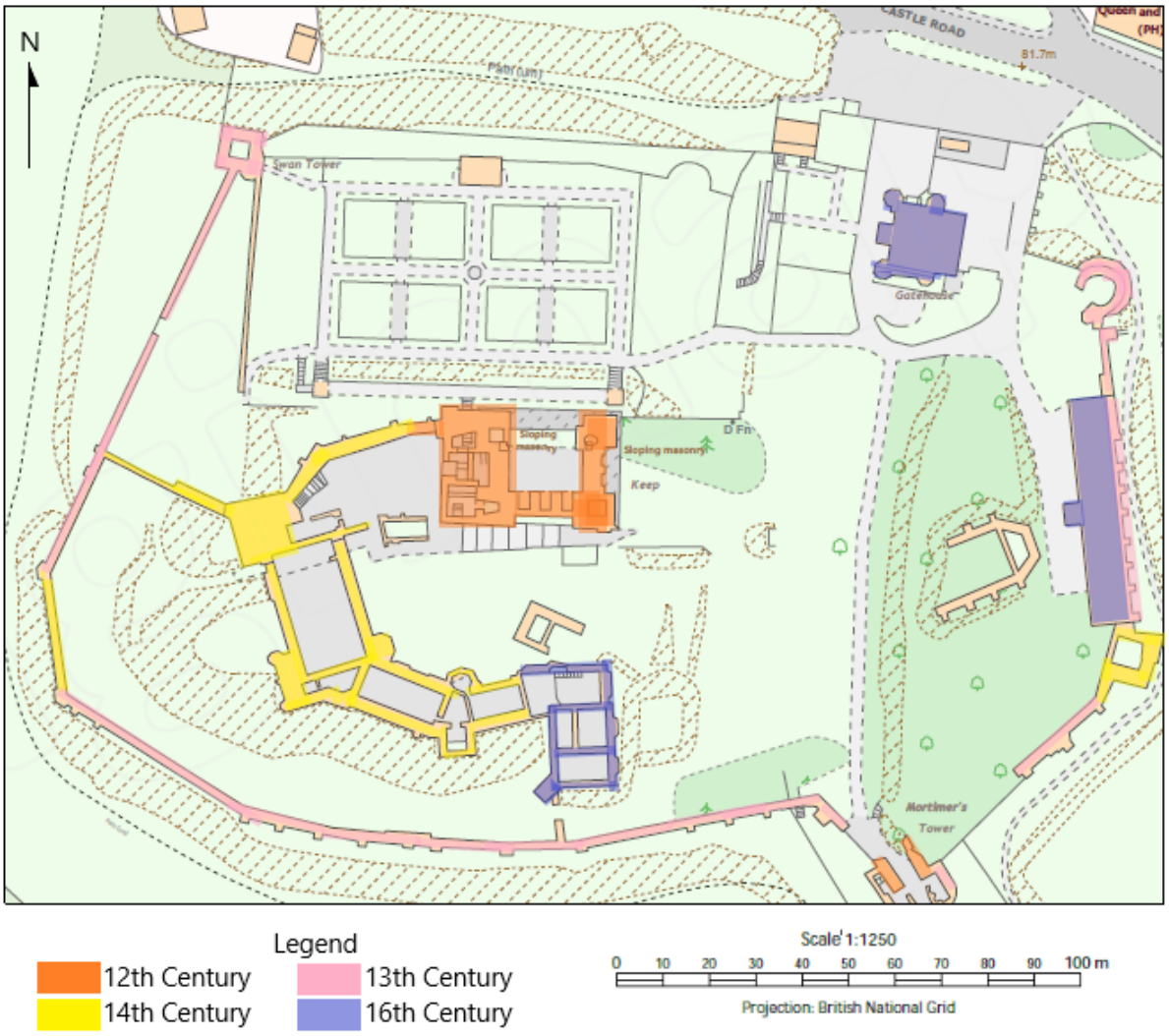

Figure 2.1 Plan of Kenilworth Castle grounds, with phasing of main structures. Base map (C) Crown Copyright Ordnance Survey, number 100025252

The local sandstone of which most of the structure is built is, part of the Sherwood Sandstone Group; a fine-to-medium grained sandstone of Triassic Age (251- 201 MYA) (Wills, 1970). This reddish-brown stone is typified by mixed cross- and flat- bedding and localised mica inclusions, and variants of the formation are common across the area, extending north to Cheshire and south west to Somerset (BGS, 2020). The local quarry which supplied the town ceased producing material during the twentieth century, meaning that all contemporary repair works requiring new stone must make

use of imported colour-matched stone from other sites, one of which is Locharbriggs sandstone from Dumfries in south-west Scotland (Historic England 2017a;5). The castle itself is a multi-phased ruin which began life in the 12th Century CE first as a motte and bailey enclosure and then an imposing stone-built keep of the Romanesque (Norman) style, with later Perpendicular style windows in the upper floors (figure 2.2).

Figure 2.2 Leicester's building (left), the great Hall (centre) and the Norman Keep (Right) taken from the base courtyard. Image © Author

The central structure was added to extensively in the following two centuries, with a chapel and tower to the south of the inner court, and substantially enlarged curtain walls. Also constructed during this period were the state apartments and Great Hall with architecture of the Romanesque and Perpendicular styles, notably the finely carved stonework in the ruined great hall building (Figure 2.3). Later buildings include the 16th Century stables with upper-level timber framing and tile floor, and Leicester's Gatehouse, which boasts fine sandstone mullioned windows and decorated stonework around doorways. This gatehouse is notable in the context of this project for having Locharbriggs sandstone inserts during recent repairs. Following extensive repairs to the internal fixtures and structure of the gatehouse, this now represents the most historically preserved structure within the castle complex, followed by the 16th Century stable block to the east of the site, which has been converted to a café and exhibition area following the removal of the inner partitions.

Figure 2.3 West elevation of Great Hall taken from King's Gate, with ruins of the Strong Tower (to left) and Saintlowe's Tower (right). Image © Author

Elsewhere on site, the curtain wall, reinforced and extended in several phases of works circles the courtyard and buildings, extending to around 690 metres in length, and to a height of four metres in places. From the 13th Century the castle was surrounded to the east, south, and west by an artificial lake known as the Great Mere, which covered over a hundred acres extending mainly to the west. This body of water was created by damming a natural stream to the south of the castle, a structure which was ultimately built into the tiltyard, and is today the pedestrian walkway into the site. The

Figure 2.4 The Gatehouse from the south-west, showing later extensions and mullioned windows likely taken from Leicester's Building. Image © Author

mere itself was drained in 1649 as part of the act of slighting, where the curtain wall was

simultaneously breached and the north elevation of the keep partially demolished (Salzman 1951). At this time the north gatehouse was converted a residence by Colonel Joseph Hawkesworth (Figure 2.5), who purchased the castle from the government under the condition that it was put beyond military service. The alterations to the gatehouse at this time created an interesting palimpsest of features removed from other parts of the castle that subsequently became ruinous (notably from the Earl of Leicester's 16th Century building (ibid).

In the ensuing three hundred years, the castle complex fell into increasing disrepair, and large quantities of the fallen masonry were taken away for use across the town. By the 18th Century the

Figure 2.5 "Kenilworth Castle" by Henry Eldridge, circa 1808, oil on canvas Image ©Wikigallery.org

ruins had become famous enough to warrant the publication of guidebooks (Morris, 2015), and there is suggestion that the castle buildings were further 'depleted for aesthetic effect' (Keay, N.D.) as was fashionable during the Romantic period. This decline, combined with continued robbing out of building material continued until 1937 when the castle site was purchased and the first remedial works undertaken following a grant from the new owner, the local industrialist Sir John Siddeley.

Following this, the site has been managed as a visitor attraction since it was granted to Kenilworth town council in 1956. In the years since, Kenilworth has seen a variety of research projects and conservation interventions, before large capital investment resulted in the development of the 'Elizabethan Garden' in 2009, and the installation of access platforms to the previously inaccessibly Leicester's Building in 2014 (Keay N.D). Today the castle is one of English Heritage's flagship attractions, mean visitor numbers for the years 2012-2018 were 109,220 (Visit Britain, 2018) and in the year 2019-20 total numbers were 114,972 (see Table 2.1). Whilst this represents a significant level of public engagement with heritage, the castle and associated buildings were never intended to accommodate such high footfall. Whilst the most vulnerable areas of the site are routinely restricted for access, such high numbers of people walking across the accessible areas of site create erosion issues that can be exacerbated by wet weather in a part of the country that sees an average of 700 mm rain per year (Met Office 2021). The following sections will outline some of the areas of change and the mechanisms of erosion associated with them.

Table 2.1 Visitor Numbers for Year 2019-20, Kenilworth Castle

Visitor Month	Total Visitor Number
March 2019	6196
April	14,704
May	14,726
June	11,876
July	13,919
August	17,954
September	9,836
October	11,831
November	2351
December	4937
January 2020	2356
February	4286
Total	**114,972**

Source: English Heritage MERAC System; Crites, R. Personal Communication March 18th 2020

2.2.1 Conservation of the Historic Structure

A site as complex as Kenilworth Castle presents a wide range of categories and patterns of erosion to study and to mitigate for in the management of the site. From localised surface breakdown of weathered and abraded stone, through colonisation of unused areas by plants and animals, to large scale mechanical erosion caused by movement of people, the care of a heritage asset such as this represents a significant challenge; and one with conflicting priorities. This being so, the site does also represent an almost unique

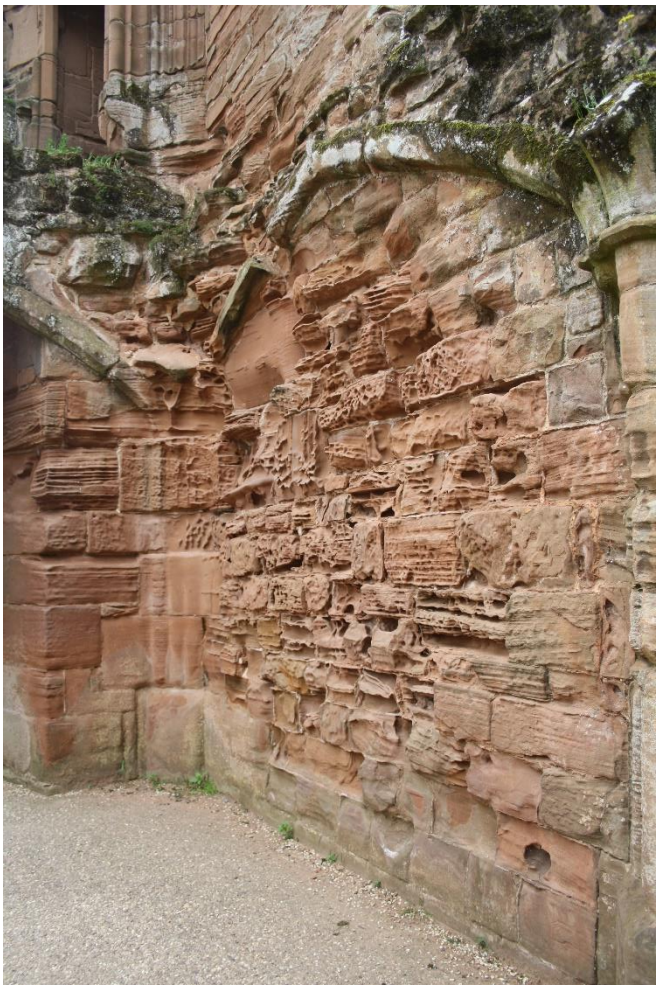

Figure 2.6 Inner wall of Great Hall showing Alveolisation caused by wind driven rain Image © Author

opportunity to study stone deterioration *in-situ* for a range of variables including surface types, common use, and durations of exposure.

Turning first to the structures of the castle site, the size and complexity of the buildings offer the opportunity to study a range of interactions and decay phenomena *in situ*. As the castle sits atop a mound which is surrounded to the south and west by low lying ground, the main structures of the Great Hall, Strong Tower, Saintlowe's Tower, and Leicester's Building are exposed to prevailing winds coming from the west, often bearing rain. The effects of this on the most exposed areas can be significant, with combined wind and rain scouring the softer materials within the stone (see figure 2.5). These patterns are repeated across the west-facing elevations of the structure but are much less significant in areas not directly exposed to the incoming weather fronts. Away from these areas, erosion of the structural fabric is driven by a mix of stimuli, including falling and pooling rainwater (Figure 2.7, left) often mixed with contact abrasion (Figure 2.7, right image).

Figure 2.7 (left) Pooling rainwater in the north entrance to the Keep, and (right) the combined effects of water and footfall erosion on a doorway stone, State Apartments. Images © Author

In addition to this, the combination of poor accessibility, pioneer plant species, and biological growth, where public access or direct sunlight are restricted are problematic (for example Figure 2.8). These areas are often either impractical to access or completely

inaccessible without specialist equipment, and consequently do not appear to be part of regular cleaning or maintenance schedules.

Figure 2.8 (left) Grass and mosses colonising inaccessible floor surface in the Great Hall, and (right) Self-set Ash tree behind a permanent screen in the Swan Tower. Images © Author

Figure 2.9 Delamination of structural stone, located in the Great Hall Image © Author

Whilst much of the non-rooting plant coverage may be benign or occasionally offer some protection from frost damage (Coombes *et al* 2018), other pioneer plants such as broadleaf

trees (*Fraxinus excelsior* and *Quercus robur*), herbaceous shrubs (*Rubus sp*), and grasses (*Agrostis sp*) have all been observed in inaccessible areas of the site. The former can cause significant damage to heritage structures through the action of rooting into mortar joints and breaking out exposed stonework. Other natural phenomena are observable across the castle as one would expect in a temperate maritime climate, such as the delamination of blocks exposed to weather and temperature cycling (Figure 2.9).

Of course, one of the main drivers of change at the castle was the English Civil War, or at least ramifications arising from its conclusion. By order of the Commonwealth Government the castle was slighted (partially destroyed) using explosives to bring down large sections of the curtain wall, the keep, and state apartments with adjoining towers (Best 1860). At this point the mere was also permanently drained. Not only did this event trigger a 288-year period of decline and neglect, it introduced huge structural weaknesses into almost every building on site.

Figure 2.10 Looking south-west from the base court, Leicester's Building (left) and the State Apartments. Image ©Author

Figure 2.10 shows the extent of this destruction, depicting Leicester's building on the left, and the remains of the state apartments in the centre of the image. All of these structures have suffered significant damage either at the time of the slighting or in the years afterwards as a consequence of their disrepair and neglect. The process initiated by the demolition was continued by a combination of natural decay and robbing out, with the result that none of the structures left standing (with the exception of the gatehouse which was converted into a residence) retained roof or floors, exposing the interiors and in many cases the core of the standing walls of the buildings to the weather; a condition that remains to this day.

Figure 2.11 Modern stabilisation and structural repairs, using brick and concrete mortar to infill lost stonework. Image © Author

Additionally, repairs and damage mitigation decisions taken over the eighty-four years of active management have added another dimension not only to the history of the site, but to the need for ongoing localised monitoring. Figure 2.11 provides a not uncommon example of this, where eroded sandstone has been patched with broken brickwork and coarse

cement mortar. Repairs of this kind ultimately encourage localised decay, through the processes of trapped water and minerals associated with the application of modern materials to traditional structures.

2.2.2 Past Consolidation Trials

In the past it was possible to study the fabric of the structure in ways that are no longer seen as appropriate, and Kenilworth has indeed hosted research on the use of consolidants on historic sandstone that would not be practical or ethical today. A key example of this was the Building Research Establishment (herein BRE) Brethane™ research project of 1976-83, which examined the efficacy of a consolidant application on a total of fifty-four sites, including the sandstone castles at Kenilworth and Goodrich in Herefordshire.

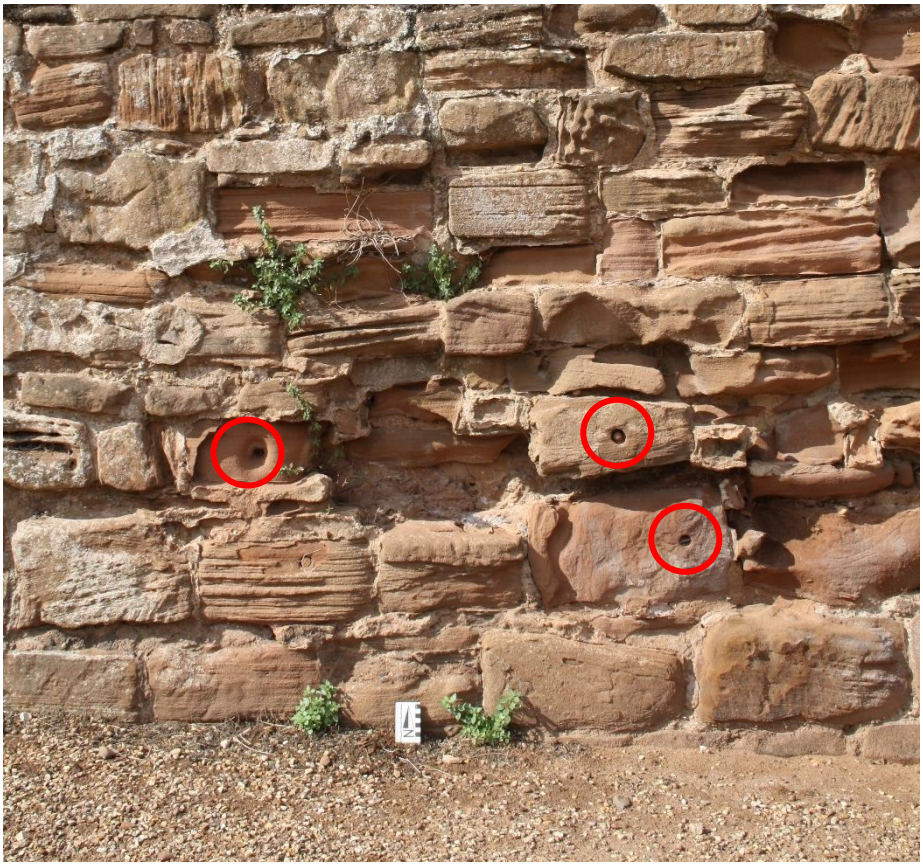

Figure 2.12 section of the Keep wall used in the Brethane trial. Cores were taken from areas highlighted in red. Image © Author

In this trial, three consolidants were applied to historic stonework- Brethane , Wacker OH100 (TEOS), and Belzona Clear Cladding (Fidler, 2002,11). It has only been possible to locate the place of the Brethane trial (see figure 2.12 above), which is located on the south elevation of the Keep structure. For this trial, consolidant was applied to the wall in liquid form, and core samples were taken at intervals across the structure in order to quantify the depth of establishment achieved by the treatment. This was, and remains today, a key limitation in the effectiveness of brush treatment on-site (Martin *et al* 2002), and this type of field trial was typical of the traditional approach to building research prior to the development and refinement of non-destructive techniques utilised today. The trial was subsequently followed up by an English Heritage-run study between 1983 and 1998, this latter phase reviewed in the English Heritage Research Transactions Volume 2- Stone, edited by John Fidler (2002). Unfortunately, methodology and data held by the Building Research Establishment for the earlier phase of work could not be obtained for review here. The tests carried out by English Heritage summarised a varying level of benefit from the application of the consolidants reviewed, and noted that limestone was more successfully treated, possibly as a result of increased porosity, although all samples showed a definite decline in the condition of all stone after extended periods of study. It would be highly beneficial if the complete dataset could be obtained, as a full review of this study would provide valuable long-term data of a kind not readily obtained elsewhere. Furthermore, the kind of sampling strategy used in this trial would not be possible on a scheduled monument today in all but the most exceptional circumstances, especially one as important as Kenilworth Castle. Accordingly, and importantly in the context of this project, the importance of proxy substrates for the accomplishment of such research now becomes apparent. The value of test walls and sample-based exposure trials as a contrast to the application of treatments to

historic structures is clear; they have no legislative constraints placed on sampling or access; nor is there a need for remedial measures following the conclusion of research. In addition to this, there is no ethical conflict in sacrificing test structures in the pursuit of knowledge acquisition. Even small-scale research on sites as large as Kenilworth have the potential to leave undesirable residues or scarring, as the Brethane™ project shows. Not only are the missing sample cores clearly visible on site today, the MTMOS-based consolidant has discoloured in areas, leaving a white tone on areas of the 11th Century structure.

2.2.3 Conservation of Floor Surfaces

One often neglected aspect of the deterioration and erosion of historic stonework is their impacts on floors and walkways. The castle site has an approximate ground surface area of 2.69 Ha (26,993 m^2) of which around 2328 m^2 is exposed historic stonework, which for the purposes of this project will be categorised into four 'types' (see Table 2.2). No specific data exists for average distance or route walked around the site by visitors, though observations taken during the course of fieldwork and anecdotal information gathered from site staff suggests a common circuit which is set out in Chapter seven (see Figure 7.5). In this scenario a journey around the main areas of the castle consists of a route between 900-1005 metres in length (excluding the interior of the Gatehouse and stables café, which comprise a variety of floor types and are managed using coverings and restrictions to access), of which approximately 550 linear metres are across exposed historic stone surfaces. With an average male gait step length of 54.2cm, and female length of 48.9cm (Öberg et al 1993; 221) a total of approximately 1070 steps fall on vulnerable stone surfaces for each visitor, based on the assumption that each individual crosses the floors without circling or doubling back.

Table 2.2 Stonework categories on site at Kenilworth Castle

Type 1	Historic stonework, external. Mixed group of flag and paving sandstone
Type 2	Historic stonework, internal. A mixed group of flag and paving stone with tiles, with clay tiles in later phases
Type 3	Historic stonework of type 2, formerly internal now exposed to weather
Type 4	Modern stone, mix of loose aggregates (sandstone and limestone) often adjacent to, and mixing with, types 1-3

In practice, deterioration as observed on-site manifests in four forms; aside from incidental damage there is footfall wear, environmental (weather and climate), historic (including traffic), and management-derived (for example aggregates placed adjacent to historic paving materials). Each of these situations present different patterns of wear, which develop at different rates as determined by their specific drivers. Taking these in turn, the indicative wear patterns can be summarised as follows (table 2.3).

Table 2.3 Outline patterns of wear to floor surfaces

Stonework Type *(from Table 2.2)*	**Main driver of erosion**	**Pattern of Wear**
Type 1	Environmental, traffic-derived, historic	Rounding of edges, loss of softer material/ inclusions within stone, some dishing out
Type 2	Traffic-derived, historic, some inappropriate setting	Dishing out, loss of leading edges, mass loss from inappropriate setting
Type 3	Mix of historic traffic-derived and environmental	Dishing out, surface wear, rounding and loss of leading edges
Type 4	Traffic-derived, some inappropriate setting	Spreading of aggregate, enhanced surface loss from adjacent stone

These patterns are not exclusively found on the individual category stone, but typologically these descriptors form a useful subdivision. Figures 2.13 and 2.14 illustrate the main differences as encountered on site, which can be summarised as a combination of exposure-driven and traffic-driven wear.

In terms of management, none of these areas have any explicit mitigation for reduction of wear, apart from during exceptional weather events (e.g. snow or severe frost) when the castle will commonly be closed to the public on safety grounds.

Figure 2.13 Left: Historic floor stone Type 1 with Type 4 infill, adjacent to the Norman Keep. Linear wear appears to be wheeled traffic derived. Actual age of stone is unknown. Scale 0.5m.
Right: Type 2 stone. Dishing out of stone centres (note pooled water) exacerbated by inappropriate resetting of stone in high strength modern mortar. Scale 0.3m. Images © Author

Figure 2.14 Left: Type 3 floor surface historically covered but now exposed to environmental erosion.
Right: Type 4, modern stone, concrete, and aggregate mix. This setting is adjacent to the earliest extant area of the castle complex (12Th Century). Scale 0.3m. Images ©Author

Each of these vulnerable flooring zones contains historic building fabric, frequently adjacent to or mixed in with modern or loose materials such as gravel, crushed limestone, or soil. Presently there is no measurement of change in any of these zones, and each of them, including the areas of modern or loose material, is covered by the Scheduled Monument status that covers the castle, meaning many of the survey and assessment surveying techniques would require either a Section 42 or Scheduled Monument Consent application and grant in order to carry out any analysis.

2.3 Summary

Kenilworth Castle presents an interesting and informative case study for the conservation of heritage sandstone in the UK. Not only is the site under significant (and increasing) pressure from visitor numbers, but the process of investigating and recording change is made more difficult by the complexity of the legislative protection specific to the monument.

Currently, the key tool used for monitoring change on site is quinquennial walkover surveys of the type carried out on heritage assets from Churches to Palaces. Any defects or areas of concern detected by these surveys are tendered out to a group of pre-approved conservation architects and masons, and work is undertaken as a standalone project. Other, day-to-day monitoring is carried out by site staff in regular walk-over surveys, detecting and reporting significant change on an ad hoc basis (Reynolds, 2020 pers comm).

The size and complexity of the monument as it stands today, including the many additions and alterations made in the interests of public safety presents researchers with a palimpsest of relationships to study; some symbiotic, others pernicious. The castle makes an interesting case study in this respect, as it offers a valuable perspective on not only the physical

differentiation found on site, but the constraints that are placed upon custodians and potential researchers. Whilst many of these considerations fall well outside of the scope of a single DPhil project, two elements that are particularly pertinent to the study of stone wear and consolidants stand out; and both provide useful a contextual basis for the experiments that follow. In the first instance, the need to develop the use of proxy materials to test applications such as chemical consolidants without the need for using the fabric of historic sites as a source of samples, as demonstrated by the Brethane™ research carried out on the wall of the Keep. Secondly, the necessity for heritage managers to better understand how stone flooring wears under the pressure of high footfall, a need echoed by English Heritage's own staff (Reynolds 2020, pers comm). That knowledge gaps remain in these areas is understandable; the constraints placed upon working on scheduled monuments such as this are significant, even when permission to work is obtainable- something that cannot always be guaranteed. Projects such as this are therefore well placed to bridge that gap, with access to non-destructive analytical equipment that is not freely available to many of the organisations invested in the care of these monuments, as well as the time and flexibility to design and test simulation experiments such as will be introduced in the chapters to follow. Observations on site have been invaluable in helping to shape those experiments, and the results from them will feed back into the knowledge which improves the conservation of these vulnerable sites.

Chapter 3: Materials and Methods

This chapter sets out the materials, processes and equipment used in the experimental phase of the project. Leading on from the introduction to consolidant use and an overview of recent field and laboratory trials found in chapter one, this chapter begins by outlining the choice of stone selection, and then covers the assessment methods and instruments chosen for the project, summarising how each fits into the programme of work. Finally, a rationale for the selection of statistical tests as employed in each of the experimental chapters concludes this chapter.

3.1 Locharbriggs Stone

Locharbriggs is a New Red Sandstone of the Permian Age (298-252 MYA) consisting wind-blown sand deposited at a time when the land mass which makes up modern Scotland was situated near to the equator (BGS 2021a). Visually, Locharbriggs is typified by its deep red to pink colour with distinct aeolian dune bedding between 0.5 and 2.0 metres thick, typically interspersed with dark strata (Orr *et al* 2019). It is a quartz-rich deposit bonded by haematite (Fe_2O_3) which gives the stone its characteristic colour, together with a small amount of silica cementation. In addition, the stone

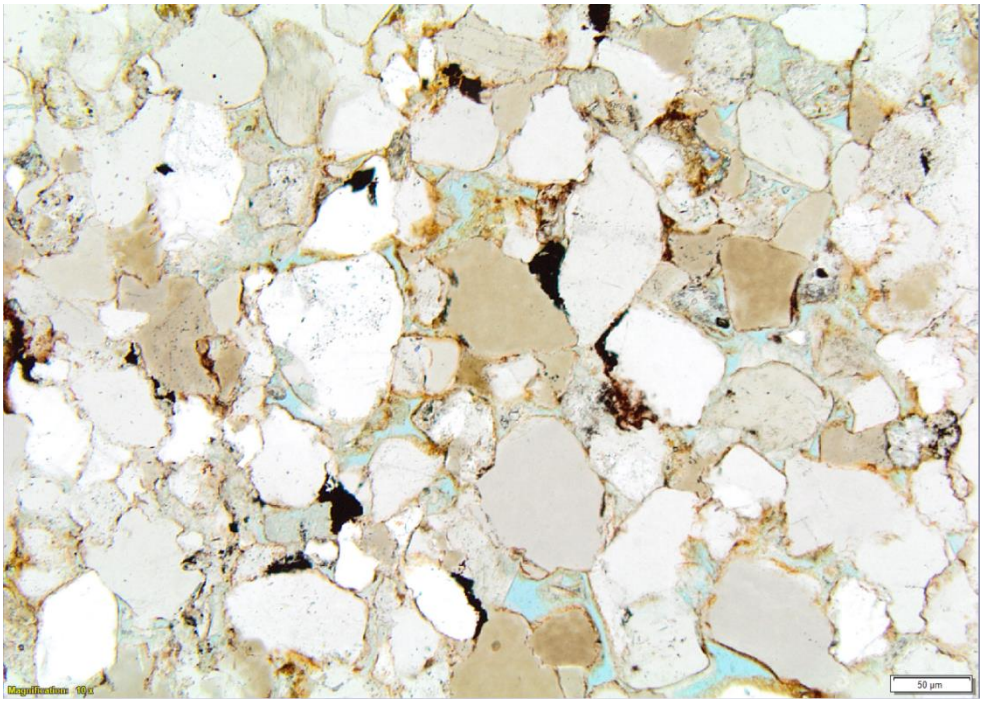

Figure 3.1 Locharbriggs Sandstone at10x magnification, shown in thin section.

matrix includes feldspars and swelling clays (Baraka-Lokmane *et al* 2009) with kaolinite the most dominant of the three (Pandey *et al* 2014). In a study undertaken by Baraka-Lokmane *et al* (2009), the mean mineral composition of Locharbriggs samples was 78.9% quartz, 12.6% feldspar, 6% hematite and clays (including smectite, illite, and kaolinite). The remaining components include 1% rock fragments and quartz/ feldspar overgrowths (<1%) (ibid 2009; Table 2, p48). Elements are plotted here on a Quartz-Feldspar-Lithic Fragment ternary diagram (after normalisation) (Figure 3.2) (Dott 1964, Tucker 2001 §2.6.1, Fig 2.50), plotting the compositional data from Baraka-Lokmane *et al* (2009) Locharbriggs can be characterised as a subarkose type sandstone (Tucker 2001).

Figure 3.2 Ternary Diagram, Locharbriggs Sandstone. Based on Q-F-L format, after Tucker 2001, fig. 2.50

The presence of the weathering-sensitive materials smectite, illite, and kaolinite within the composition is a key factor here in selecting the stone for heat weathering experiments (Hajpal and Torok 2004, Sirdesai et al 2017). The stone has a medium grain size ranging from 0.04- 0.4 mm (NBSD 2015) of sub-rounded and sub-angular grain shape (Adams *et al* 1984). The grains are well sorted and strongly cohesive (BGS 2021b). Open porosity is 24-26% (EN1936,1999; Stancliffe Stone ND) with a "high" water absorption of 9.3% by weight (57.2g/m^2/s by capillarity) (BGS 2021b, Stancliffe Stone ND), and a compressive strength of 44-57.4 MPa (EN1926,2006; Hutton Stone ND, Stancliffe Stone ND). The apparent density of the stone is 1960 kg/m^3 (EN 1936:199) (Stancliffe Stone ND). It has a slip resistance rating of between 94 and 104 and is suitable for moderately trafficked zones as a paving material (EN1341).

Locharbriggs sandstone is commonly used in Scottish buildings such as the Edinburgh College of Art and Caledonian Hotel (also Edinburgh), the People's Palace and Garden in Glasgow, and in northern England, with examples of use as far reaching as the United States of America where it makes up the 354 steps to the Statue of Liberty in New York (Scottish Places 2021). It is also a material of interest owing to its identification as a suitable replacement stone in heritage buildings where original quarries are no longer productive (Historic England 2017a), a factor that will likely see its inclusion in a greater number of British sandstone sites in need of repairs as time goes on.

In addition to its exploitation in historic sites, Locharbriggs is in contemporary use across the United Kingdom today Manchester's recent Convention Centre and Magistrate's Courthouse (Stancliffe 2007, Stone Specialist 2004), and as a result will be an increasingly significant stone type for study into the future.

3.2 Consolidants

For this study, two consolidants have been chosen for the experimental work. The first is tetraethyl orthosilicate (TEOS), a silane with the formula $Si(OC_2H_5)_4$ which is used extensively across the United States and Europe and is one of a small number employed in conservation work in the United Kingdom. TEOS is a widely available commercial product, sold under a range of trade names, for example WACKER OH 100 and SILANOL, the former being the product used here.

TEOS consolidants have a significant use-history in cultural heritage conservation and research on a range of building materials including adobe (Salazar-Hernández *et al* 2021) concrete (Barberena-Fernández *et al* 2015), Limestones (Briffa et al 2012), as well as a range of Sandstone types (Molina *et al* 2018, Sassoni *et al* 2013). Commercial TEOS consolidant (Wacker OH100) is supplied as a colourless liquid with a faint aroma and a flashpoint of 45°C. It is an irritant for eyes, skin, and respiratory exposure. In experimental use for this project TEOS was used in ventilated and temperature-controlled areas only.

The second consolidant selected for use in the experimental phase of this project is methyltrimethoxySilane (MTMOS) (alternatively trimethoxymethylsilane), with the formula $CH_3Si(OCH_3)_3$. MTMOS is another silane with a significant history in sandstone consolidation. MTMOS for this project was obtained in the form of a chemical preparation as opposed to a commercial product, supplied by Sygma Aldrich at 98% concentration. Variants of MTMOS have been extensively trialled on sandstone in the past, notably in the form of the Brethane product tested on site at Kenilworth Castle (see chapter one). It has a range of characteristics that set it apart from TEOS, such as stated hydrophobicity of material following treatment- as observed on a range of materials such as Marble, Limestone, Wood, and Sandstone (Cappelletti & Fermo 2016, Hochmańska 2014, Wheeler 2005). MTMOS consolidant is a colourless liquid with a faint aroma and a flash point of 9°C. It is an irritant to eyes, skin and the respiratory system and for the experimental work in this project was used in the temperature-controlled and ventilated environment of the Oxford Geolabs facility.

3.3 Preparation of Samples for Experiment

3.3.1 Stone Cutting and Preparation for Field Trials

Stone for the experimental areas of the project was purchased from source at Locharbriggs Quarry in Dumfries, Scotland. The stone arrived in two batches, one large bulk batch from a single source block covered all the stone requirements for both the exposure rack and test wall trials, and a separate order of flooring slab provided the material for the Pedatron wear simulation.

Figure 3.3 Left: Stone for test wall during cutting, at Geolabs, Right: Sample blocks for exposure rack trial following experiment. Note darker shade of Weathered and Untreated samples (2nd from right). Images © Author

The bulk ordered stone arrived pre-cut into 300 x 300 x 150 mm blocks, which dictated the maximum size of the blocks for the test wall. As a result, the two largest blocks within the subsequent structure remained uncut from arrival ("WC blocks", see Chapter five). Further to this, stone samples for the test wall trial were cut into three other sample sizes using a Norton Clipper 501 diamond tipped saw by the author (refer to chapter five, section 6.3 for sample sizes used).

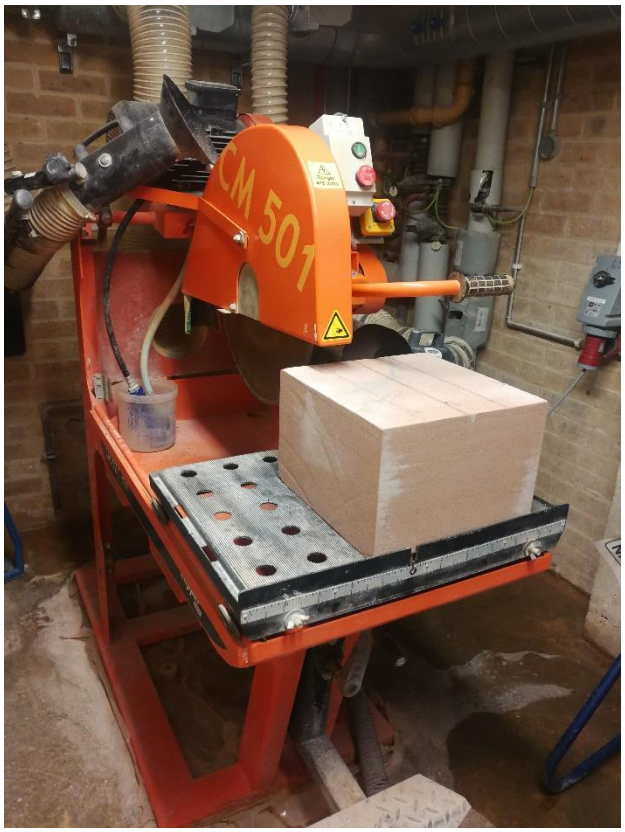

Figure 3.4 Norton Clipper saw at Geolabs Facility, with Locharbriggs sample pre-cutting, image © Author

For the exposure rack trial, all samples were cut to a uniform 70 x 70 x 70 mm using the diamond tipped saw and finished on a Battipav Jolly Max 300 tile saw for accuracy. All cutting for both trials took place before any heat weathering or consolidation took place.

3.3.2 Stone Cutting for and Preparation for Pedatron Simulation Experiment

Samples for the Pedatron foot erosion test differed from the other stone used in this project as the donor stone was pre-cut into a paving slab at the quarry and as such came from a separate batch of stone to that which formed the material for the exposure rack and test wall experiments (chapters four and five respectively). The slab was machined to a thickness of 40 mm and was originally 350 mm square. The slab was pre-cut with the bedding planes virtually parallel to the bedding direction, so that these would be in compression in use. Upon delivery the slab was further subdivided into four equal 170 x 170 mm tiles by the author using the Diamond tipped saw at Oxford Geolabs. These formed the component pieces of the Pedatron foot erosion trial, which were then given a numerical identifier and heat weathered as per section 3.3. Following this, two of the tiles (numbers one and four) were treated with TEOS consolidant using the capillary absorption method outlined in section 3.5, and the tiles were then set into an airtight container for a period of 28 days in laboratory conditions to allow for the uninterrupted establishment of consolidants. Following these treatment steps, the four tiles were set into a plywood holding frame using a 4:1 ratio sand- cement mortar (Figure 3.4), with approx. 15 mm of base bedding and a total bedding depth of 30 mm between tiles and around the outer border of the frame.

Figure 3.5 Construction of the Pedatron Foot Erosion Platform, Image © Author

Following setting, the platform was stored in laboratory conditions for fourteen days to allow for the cement to bond throughout before being moved to the test laboratory at SATRA Technologies in Kettering UK.

3.4 Artificial Weathering of Stone for Sample Preparation

The artificial weathering of building stone using the manipulation of temperature is not a new development. Franzoni *et al* (2013) Rao *et al* (2007), Zhang (2009), and Logan (2004) amongst others, have tested methodologies based on this in the past, recording differentiated changes on a range of lithotypes, for both engineering and cultural heritage conservation research objectives.

A decision was made to adapt one of these existing methods as a means of increasing the receptivity of sandstone for consolidants based on the ability for non-specialist laboratories or commercial companies to replicate the method in the future. A central tenet of this research project has been a desire to make the work here as 'democratised' as possible, enabling researchers at all levels to apply the methods to their own substrate stone as required. To this end, the project took as its starting point the work carried out by Elisa Franzoni and her team at the Universities of Bologna and Princeton which subjected a series of Pietra Serena sandstone samples to alternating heat and cooling cycles in a bid to "induce controllable microstructural, physical and mechanical alterations" (Franzoni *et al* 2013).

In the original methodology, stone sample cubes were artificially weathered following the following protocol:

> *1."Achieve dry weight; record dimensions and mass (±0.1mm, ±0.01g)*
>
> *2. Heat stone to 100°C, 200°C, 300°C, and 400°C maintaining each for one hour, allowing stone to return to ambient temperature (in desiccator) between heating.*
>
> *3. Immerse stone in deionised water for 24 hours then heat to 200°C and maintain for one hour.*
>
> *4. Allow stone to return to ambient temperature (in desiccator)*

5. Heat stone to 400°C, maintain for one hour.

6. Return to desiccator, process complete."

Franzoni et al 2013 §2.3

In the first iteration of this work this process was retained in its entirety, including successful use in the Master of Research project that preceded this project (Grove 2017). However, preparatory trials indicated that the process could be simplified on Locharbriggs stone, shortening the timeframe and energy required to achieve the desired results. In conclusion to the trialling of several variants on the original process, the following heat weathering process was selected as preparatory step for sample stones as used in this project:

1. *Achieve dry weight; record dimensions and mass (±0.1mm, ±0.01g)*
2. *Heat stone to 100°C and 200°C in fan assisted oven maintaining each for one hour and allowing stone to return to ambient temperature in desiccator between heating*
3. *Heat stone to 300°C and 400°C in electric furnace, maintaining each temperature for one hour and allowing stone to return to ambient temperature in desiccator between heating.*
4. *Return to desiccator (process complete).*

This weathering process was cycled only once for the samples used in experimental trials, following trials in which multiple cycles often resulted in significant fractures appearing in the stone. Prior to, and following this process, sample stones were tested for mass and colour change, and Pulse Wave Velocity, following which the samples were all re-heated until dry mass was achieved at 65°C in fan oven, prior to storage or further treatment.

3.5 Application of Consolidants and Pre-exposure Preparation

Consolidant treatments for the exposure rack trial, the Pedatron erosion test, and part of the Test Wall trial were applied using the full immersion method described below, after Liu *et al* (2013). For

treatment, samples treated with TEOS and MTMOS consolidants were subject to the heat weathering method as described in section 3.4 before being placed in a bath of liquid consolidant in sealable containers. Samples were placed on plastic straws in order to expose the maximum surface area to liquid whilst supporting the samples away from the plastic of the container, and lids were locked in place to prevent evaporation of consolidant into the atmosphere. Temperature and relative humidity were maintained at 23°C ±3°C and 55% ±5% (laboratory conditions) within a fume cabinet. Samples were removed from the consolidant at 8-hour intervals for visual inspection and mass measurement. Samples were returned to the consolidant bath until two consecutive stable mass measurements were recorded. This concludes the immersion stage of treatment.

Table 3.1 Mass increase in grammes of Exposure Rack Samples following consolidant treatment

Sample No.	**TEOS Samples, Pre-treatment**	**TEOS Samples after Consolidant**	**MTMOS Samples Pre-treatment**	**MTMOS Samples Post-treatment**
1	723.49	775.74	710.82	753.22
2	681.98	733.6	759.95	801.83
3	690.77	743.35	741.32	783.73
4	696.7	748.43	712.76	755.1
5	698.43	754.1	707.57	750.93
6	728.33	781.22	740.17	782.53
7	705.67	754.53	716.96	757.09
8	712.1	765.61	710.02	750.86
9	714.79	768.66	743.36	785.64
10	696.25	749.72	724.7	765.01

For the test wall experiment, a second additional application method is used for consolidating sample stones prior to their use in the construction. The purpose of this addition is to enable comparisons to be drawn for the performance of consolidants on Locharbriggs stone resulting from their application method (forming part of Project Objective 1). For this additional sample set (the #2 suffix samples within the test wall) the brush application technique (the most common on-site technique) was used. Samples were pre-weathered using heat as per the other consolidated samples, and then stored in a desiccator until treatment. For the application, samples were placed on plastic tubes within a plastic tray, to allow excess consolidant to run off the sample and prevent

the base of the sample from absorbing this excess liquid through capillary action. Following this, consolidant was applied to two faces of the treated sample, representing those faces that will be 'exposed' on the elevation face of the completed structure (thus imitating the application of consolidants in situ) (Figure 3.6). During the treatment process, consolidant is applied to the sample by horizontal brushing repeated until the stone 'refuses' (Sassoni *et al* 2013 §2.4) to take up further liquid and excess runs off to the collection tray. At this point a short delay allows the pore-bound liquid to be absorbed into the stone, and brushing is recommenced. This process is repeated until the stone does not begin to

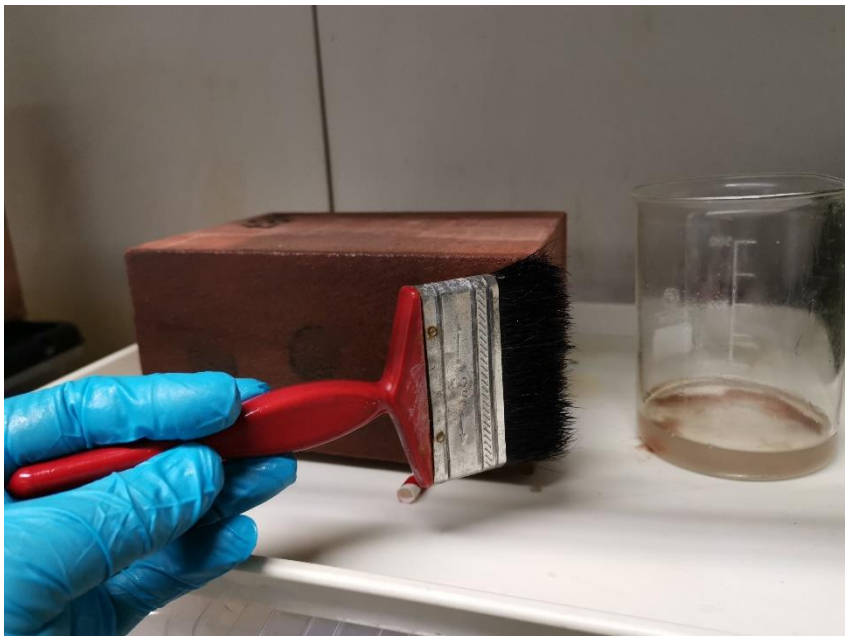

Figure 3.6 Applying TEOS consolidant to test wall samples using brushing. Excess consolidant is collected in the tray below. Image © Author

allow liquid to be taken up following a pause in brushing. The process is then repeated on the opposite face of the sample. The procedure is then repeated after 24 hours, with the samples being stored in a sealed container in the interim period. Consolidant uptake was measured by taking the mass of samples pre- and post- treatment, and by the comparison of this with the mass of liquid taken from the containers during treatment.

Table 3.2 Mass Changes (Kg) In Test Wall Blocks Treated by Immersion

SAMPLE NO.	200 x 100 x 150 mm blocks before treatment	200 x 100 x 150 mm blocks after treatment	300 x 300 x 150 mm before treatment	300 x 300 x 150 mm after treatment
1	6.189	6.623	26.631	28.928
2	6.025	6.447		
3	5.837	6.305		
4	5.787	6.121		
5	6.201	6.631		

Table 3.3 Mass Changes (Kg) In Test Wall Blocks Treated by Brush Application

Sample No.	200 x 100 x 150 mm blocks before treatment	200 x 100 x 150 mm blocks after treatment	300 x 100 x 150 mm before treatment	300 x 100 x 150 mm after treatment	300 x 300 x 150 mm before treatment	300 x 300 x 150 mm after treatment
1	6.123	6.203	9.211	9.276		
2	5.826	5.89	9.088	9.154	28.102	28.945
3	5.944	6.015	9.184	9.236		
4	6.179	6.248				
5	5.871	5.943				

The second stage of the consolidation process for both application methods consisted of samples being sealed in the containers with liquid consolidant removed, again on plastic straws to isolate them from the container, and with an open 100ml pot of consolidant liquid placed in each container alongside the samples. The open pot of liquid is added as a buffer to increase the level of consolidant in the sealed atmosphere of the container and reduce any evaporation from the stone samples. The containers were then sealed with the samples and open pot within for a period of 14 days. This period reflects the typical length of time for initial sol-gel process to take place as commonly advised by manufacturers (e.g. SILRES 2014), and so is the minimum time that treated stone should be protected against atmospheric fluctuations. During this period the temperature and relative humidity were maintained at 23°C ±3°C and 55% ±5% respectively (ambient laboratory conditions).

Figure 3.7 Samples in sealed consolidant bath stored in ventilated fume cupboard at Geolabs facility. Image © Author

Finally, the samples were removed from the container and their mass recorded again. Stable mass was recorded throughout the establishment process, indicating minimal loss of consolidant from the time of immersion to the end of the laboratory phase.

The final step for pre-trial preparation was an atmosphere-limited exposure whereby sample sets A,B,C, and D were placed on the exposure rack at Wytham Woods test site and covered in a weatherproof sheeting for a period of 14 days, preventing exposure to rainfall and UV light, but allowing for the ambient temperature and relative humidity fluctuations of the climate to reach the samples. This last step was designated as additional protection for the consolidant in case of heavy rainfall and was taken after consulting research (for example Franzoni *et al* 2015, Scherer and Wheeler 2009), wherein initial curing was observed as taking far longer than the manufacturers guidance. Following the final 14-day covered exposure, the protective sheeting was removed, and phase one of the exposure trial began.

3.6 Techniques for Field Experimentation

Arising from a review of the experimental produced in chapter one (section 2.2), a range of assessment techniques and associated instruments were selected to measure condition and change throughout the experiments; summarised here in Table 3.4 and described in more detail below.

Table 3.4 Summary of Techniques used with links to Project Objectives.

Project Objective	Project Activities	Instrument/ Techniques
Objective 1. To investigate the development of a novel methodology for the preparation and analysis of sandstone for consolidant assessment trials	Laboratory Preparation Exposure Rack Trial Test Wall Trial Pedatron Trial	• Heat Weathering treatment • Ultrasonic Pulse Wave Velocity (PunditLab) • Colorimetry (Konica Minolta CM700D) • Mass (Oxford Labs field balance) • Capillarity (ASTM standard test) • Karsten Tube Test (EN Standard test) • Observations and interviews taken at Kenilworth Castle
Objective 2. To investigate the use of sample-based and structure-based experiments in field settings for the assessment of consolidant performance on sandstone	Exposure Rack Trial Test Wall Trial	• Colorimetry (Konica Minolta 700) • Ultrasonic Pulse Wave Velocity (PunditLab) • Mass (Oxford Labs field balance) • Moisture measurement (MOIST 350B)
Objective 3. To investigate the use of simulated wear experiments for the assessment of consolidant performance on sandstone	Pedatron Erosion Test	• Pedatron Mechanical Walking Foot • 3D Laser Scanning (Creaform HandyScan) • Surface Roughness measurement (INNOWEP TRACE-iT)
Objective 4. To produce a 'Toolkit' of methods for the evaluation of consolidant performance on sandstone, arising from Objectives 1,2, and 3	Review of experimental results and assessment of the framework	

3.6.1 Ultrasonic Pulse Wave Velocity

Ultrasonic Pulse Wave Velocity, a non-destructive method of assessing the internal cohesion of stone samples through the propagation of an electrically generated 'primary wave'; a simulation of the seismic wave as observed in geophysical studies of the earth's formation and tectonic activity (Rahmouni *et al* 2013). The primary wave travels directly through solid material such as stone, and its velocity is measured in relationship to the size and density of the material (Gaviglio 1989, Vasconcelos 2007). Fluctuations in samples measured over time offer insight into the state of internal cohesion of the sample, and by extension any changes therein resulting from natural or induced processes. The technique is well understood in the context of material characterisation (Assefa *et al* 2003, Kahraman & Yeken 2008), and as such is chosen as a reliable and robust technique for assessment.

P Wave Velocity is measured here using the Proceq Punditlab, a portable instrument which utilises a pair of flat-faced cylindrical transducers to propagate and receive the pulse wave in a direct alignment, with the stone sample placed between the two transducers (see Figure 3.8).

Figure 3.8 Proceq Punditlab direct array configuration as used throughout tests. Image: author

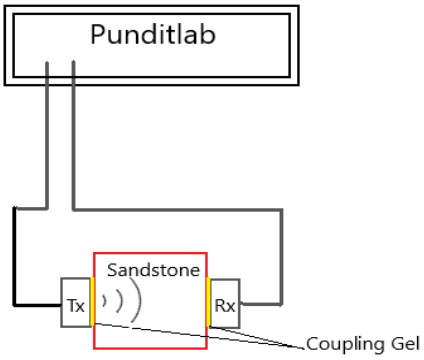

Transducers used here have a contact surface diameter of 30 mm (Proceq part 325 40 141) and use a small amount of water-based ultrasonic coupling gel to create a uniform surface for the transfer of propagated waves into and out of the stone without loss to air attenuation. For all experimental work in this thesis using P Wave Velocity, wave frequency is set at 150 kHz, and calibration of the equipment took place prior to each recording event using a 25.4 µs calibration rod (Proceq part 710 10 028).

3.6.2 Colorimetry

For the examination and quantification of visual characteristics in these trials colour spectra have been measured with a Konica Minolta CM700D Spectrophotometer using the CIELAB colour space, using the D65 illuminant. Data presented within this thesis are SCI (Specular Component Included) which includes specular and reflected components of the data, reducing the impact of surface conditions on the data collected (Konica Minolta ND). The axes of colour within this system are represented in Figure 3.9, and for the Locharbriggs sandstone used in these experiments the metrics used for the measurement of change are the L* and a* axes, which represent light-dark (black-white) and red-green changes respectively, together with ΔE (Delta E),

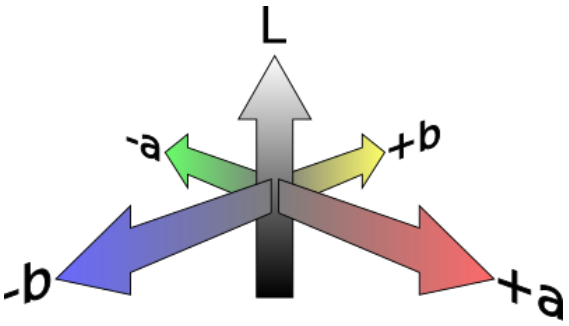

L* 0= black; 100= diffuse white

a* "-*x*" values= green hue, "+*x*" values= red hue

b* "-x" values= blue hue, "+x" values= yellow hue

Figure 3.9 The interaction of the three axes of hue within CIELAB colour space. Image © FREESVG.ORG

a calculation of 3-dimensional distance between spaces on all three-axis colour space (including the b*, yellow-blue axis), which is calculated using the following equation:

$$\Delta E = \sqrt{[(L_2-L_1)^2+(a_2-a_1)^2+(b_2-b_1)^2]}$$

As this final metric takes in change on all axes it is a measure of potential total change and provides an accurate summary of the differences of colour at any given stage of the experiment. For this method, data was collected using a Spectrophotometer fitted with a 6mm diameter sampling aperture and set to SAV (small aperture) sampling. In addition, target templates were prepared with pre-drilled holes which allow for set spaces on each sample to be repeatedly sampled for direct comparison over time.

3.6.3 Microwave Moisture Meter

Measurement of stone-bound moisture is key to assessing the performance of consolidants in this project For this set of trials the *hf Sensor GMBH* MOIST 350B Microwave Moisture meter has been selected. This portable system works by propagating a small electromagnetic wave (~1mW) within the microwave spectrum, which is transmitted into the sample material via a small contact sensor which simultaneously measures the strength of the reflected wave in the same sampling head (Göller 2006). The strength of this reflected wave is then used to calculate the level of moisture within the sample, presented as either a percentage value or in the format of the Moisture Index, a relative scale generated by the meter (hf Sensor ND, Orr *et al* 2019). The MOIST 350B has a selection of interchangeable sensor heads which penetrate to different depth/field sizes ranging from $3cm^3$ to $20cm^3$, for the work in this project, the DM sensor (~$10cm^3$ penetration field) is used. During the Test Wall experiment outlined in chapter five of this thesis, the percentage value output has been used to assess the moisture content of treated and untreated stone within the structure. In order to assess the accuracy of these percentage readings, and to quantify the precise amount of moisture present for each reading, a novel gravimetric calibration procedure was developed in the laboratory as a precursor to the collection of field data, and is outlined below.

3.6.3.1 Gravimetric Calibration of Moisture Meter Data

For the purposes of this trial, it is desirable to pre-calibrate the readings from the MOIST 350B using an independent metric which directly measures liquid water content within the stone against a

known quantity. For this process, a gravimetric test has been developed to quantify the strength of the correlation between moisture-driven changes in mass (g) and outputs of the MOIST 350B in moisture percentage mode. The test is based on processes set out in Hall and Hoff (2012, p38) and Eklund *et al* (2011) and is applied to samples of all pre-treatment categories. The methodology below sets out the steps taken:

Table 3.5 Methodology for Gravimetric Testing

	N.B. All steps take place in laboratory conditions
1	Cut and weigh samples
2	Heat in a ventilated fan oven at 65°C until dry mass is achieved (defined as stable mass reading with <1% variation across two or more readings)
3	Record dry mass
4	Place samples in water bath (normally ventilated), placed on cylindrical rods which allow the maximum surface area of the base of each sample to be exposed to liquid
5	Fill water bath with distilled water until the level covers the base and sides of the samples to a minimum of 10 mm. Maintain this minimum level throughout test
6	Record mass every 12 hours until saturation of stone is achieved (defined as stable mass reading with <1% variation across two or more readings).
7	Remove sample from water bath, remove surface water with cloth.
8	Record mass of sample and MOIST350B reading
9	Place samples in dry tray (normally ventilated). Repeat measurements from step 8 at 24-hour intervals for seven days (or until atmospheric equilibrium is achieved (defined as stable mass readings with <1% variation across two or more readings)

Results from this gravimetric test are summarised in Table 6.5. Each value represented in the table is the mean of five individual samples, cycled through the test three times. Included with these readings are scatterplots for each variant group (Figure 3.9), based on the mass at data collection points throughout the trial.

Table 3.6 Mean results for all sample Groups for Gravimetric Testing.

	Ambient	Dried	Saturated	Day 1	Day 2	Day 3	Day 4	Day 5	Day 7
TEOS Treated Group									
Mass (g)	737.78	734.30	773.90	759.79	747.38	742.86	741.41	740.23	738.85
MOIST 350B	1.3	0.5	9.5	6.5	0.5	2.3	0.1	0.9	1.5
Weathered Only Group									
Mass (g)	737.81	736.27	792.69	785.95	779.22	768.79	759.38	744.37	738.99
MOIST 350B	1.1	1.0	9.2	9.0	8.9	8.3	3.3	1.0	0.7
Unweathered Untreated Group									
Mass (g)	723.04	721.35	767.67	759.14	749.79	741.10	735.38	726.47	724.03
MOIST 350B	1.1	0.9	9.2	8.0	4.9	2.7	1.5	1.0	0.9

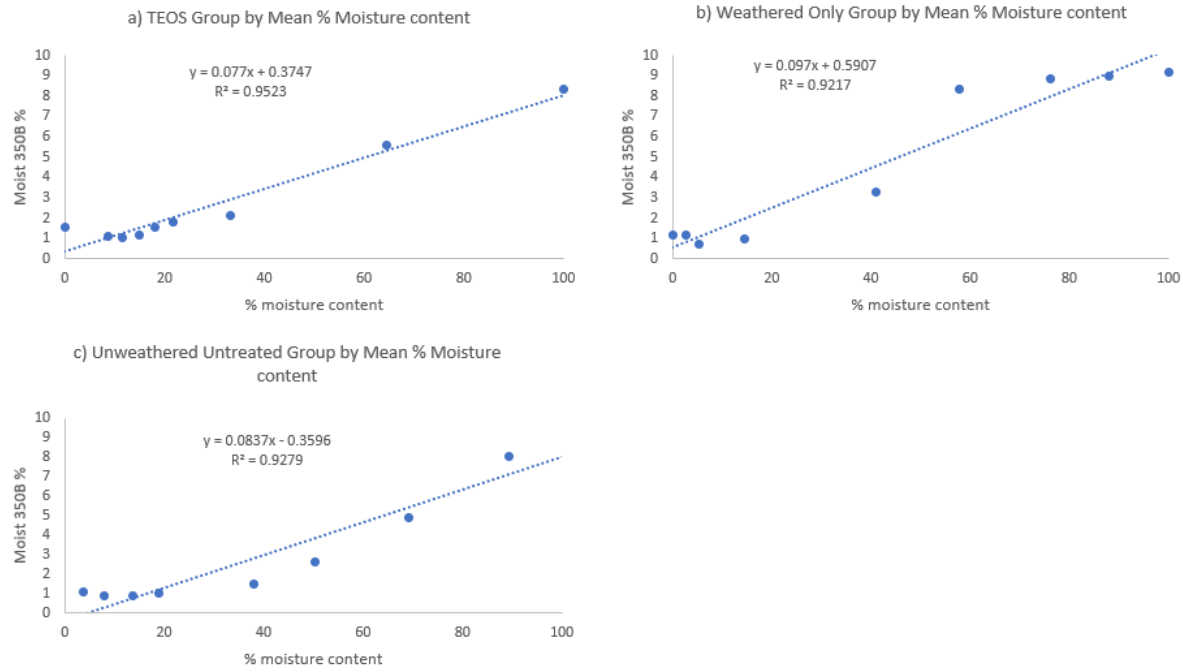

Figure 3.10 Results of gravimetric test, mean mass of sample groups plotted with MOIST 350B percentage values

The data shown in figure 6.4 (p172) shows a strong correlation and linear relationship between the MOIST 350B percentage measurement and moisture in the liquid state within the sample stone. Across the treatment groups the high coefficient of determination values (R^2) ranged between 0.92 (TEOS by Capillarity), and 0.95 (Weathered Only and Unweathered) indicate a strong correlation between pore-bound liquid (measured gravimetrically) and the percentage readings on the MOIST 350B meter. From this it has been possible to calibrate the moisture meter data and represent the values visually using a standardised CIE colour differential scale. This scale assigns the moisture 'percentage' values output by the MOIST350B to a colour on an arbitrary scale which runs from khaki (representing dry conditions) to deep blue (representing fully saturated stone). This scale is presented in figure 5.4 (chapter 5) and is used to plot values in subsequent test wall visualisations (figures 5.8, 5.10, 5.12, 5.14, and 5.16, Pp 143-160).

3.6.4 Surface Roughness

In addition to the measurement of internal stone cohesion (Ultrasonic P Wave), moisture content (Microwave Moisture Meter), and surface colour and hue (Colorimetry), further assessment of surface condition and change has been undertaken with two non-destructive techniques; the first of which is the measurement of surface roughness at micron (µm) scale, in association with a simulated erosion experiment (chapter six, the Pedatron Trial).

For this work the INNOWEP TRACE-iT surface roughness sensor was utilised, used with its native software. Described by the manufacturer as the 'fastest mobile optical profiler' (INNOWEP 2021), the instrument uses a sensor head with three triangulated white light optical sensors coupled to a high resolution camera, it samples a 5 mm x 5 mm target zone with 1500 measurements in both x- and y- axes (ibid) and creates a topographic representation of the sample area to a resolution of 0-187 µm in real time, with exportable meta-data including roughness in Rz format with standard deviation. The unit is entirely portable, comprising a small handheld sensor which is coupled to a laptop, and this factor allows it to be trialled as a possible *in-situ* assessment method, as per project objectives two and three.

3.6.5 Handheld Laser Scanning

The final technique applied to the assessment of sandstone and consolidants within this trial is the portable Creaform Handyscan 700 laser scanner. Utilised in the Pedatron erosion trial, this scanner is trialled here in its capacity to detect sub-millimetre change in the surface of eroded sandstone tiles and can therefore be used in principle to detect differences in physical change between consolidated and unconsolidated stone. In this trial, the scanning was undertaken at the SATRA Technologies laboratory in Kettering (UK), but the method is developed in a manner that can be replicated on site wherever stone erosion is a concern. Scanning of samples is taken using a handheld sensor head

connected to a laptop, and 3D point clouds are generated almost in real time within the native "VX" software. The scanner itself is portable, comprising a small sensor head which is coupled to a laptop, As with the TRACE-iT Surface Roughness profilometer, this allows the unit to be assessed for on site or *in situ* analysis, as per project objectives two and three. The scanner is accurate to 0.025 mm (Creaform 2021) and allows for real time assessment of point cloud quality, making it a suitable instrument for use in difficult to access areas. During the Pedatron erosion trial, scans were taken before erosion, after 100,000 'steps' of mechanically simulated wear, and then finally at the conclusion of the test following 200,000 'steps' (refer to Chapter six for erosion test methodology).

For visualisation and analysis of point clouds generated during this scan, the data was exported into a separate data processing package, CloudCompare. This allowed for the data to be aligned and for the production of digital surface topography overlays for inspection and assessment of change.

3.7 Statistical Analyses

Throughout the project, a combination of statistical methods have been used to test for significance within datasets. The following section outlines the varying methods used in each field trial, together with the rationale for their selection.

As a prerequisite for testing, all sample sets were tested for normality using a Shapiro-Wilk test, with an α value of 0.1. As no outliers were detected during the preparation of datasets, data was then subject to the following analyses within each experiment. For all statistical tests, following the normality test, an F test was carried out to test for variances and the results of these tests determine which T test (assumed/ not assumed variances) would then be applied to each pairing.

3.7.1 Exposure Rack Trial

For the exposure rack trial, sixty-eight samples were prepared. Eighteen of these samples were stored in laboratory conditions for use as control samples. Ten samples were amalgamated into the test wall structure, leaving forty samples in ten-sample groups for study in the exposure trial itself. As a result of the symmetry in replicate numbers, it was possible test the groups for significant change across the duration of the trial using an Analysis of Variance (ANOVA). Where significance is detected by the ANOVA, a limited number of parametric T Tests (maximum of four) were then carried out on selected pairs of data, based on weather conditions at time of data collection, using an α value of 0.01, in order to establish which pairs of data contain the significant changes within the trial.

3.7.2 Test Wall Trial

The test wall structure is made from a variety of sample stone sizes, with each set containing different numbers of replicates. Three sample sets contain an even number of samples: the “WA” set (300x100x150 mm) includes 18 samples (nine samples each of (i) brush treated and (ii) weathered stones), secondly the “WB” set (200x100x150mm) includes 30 samples (ten samples each of (i) brush treated (ii) capillary treated, and (iii) weathered stones). Finally, the “WC” set includes 2 samples (one each of (i) brush treated and (ii) capillary treated stones). In addition to these are a range of control samples comprising unweathered and untreated samples of both the “WA” and ”WB” sizes, as well as two further control “WD” samples of 150x100x150 mm (totalling nine control samples). Consequently, for the purposes of data analysis a combination of four statistical tests have been employed to cover all comparisons. Single- and multi- factor ANOVA have been used where symmetrical numbers of replicates allowed, followed by non-parametric two sample T Tests to identify which pairs contain significant differences, as within the exposure rack trial. Where asymmetrical replicates are compared, ANOVA cannot be effectively employed, so non-parametric T tests have been applied to selected pairs of data based on weather events at time of data collection (as drivers of condition change in stone), in order to identify which conditions direct significant

change. For all tests outlined here, α values are set to 0.01 to reduce the possibility of type I errors arising from the multiple tests carried out across datasets.

3.7.3 Pedatron Erosion Test

For the Pedatron test, selection and use of statistical analyses is handled entirely by the algorithm embedded within the CloudCompare software that is used to handle the digital 'point clouds' as exported from the laser scanner used to measure the surface shape of the test pieces. Significance in this experiment is measured as part of the process of aligning digital 'point clouds' created from repeated laser scans in the experiment. Within the automated fine registration process (which forms the last step of accurate model creation), a threshold of change analogous to an alpha value of 0.05 is applied, so all change above the correlating measurement of 0.6 mm is classed significant and is marked in the visualisations as such.

Chapter Four: The Exposure Rack Trial

4.1. Introduction

A key stage in the development of a consolidant assessment toolkit is the transfer of monitoring and assessment methods from the controlled environment of the laboratory to the more variable settings encountered when working on stonework in-situ. However, as obtaining access to materials on site for the purposes of research is a complex and often time-consuming process, it remains a matter of necessity that a workable compromise is available. The purpose of the work set out in this chapter is twofold; firstly, to test the workability of sample-based testing in real world conditions, and secondly to 'road test' a range of techniques more commonly employed in laboratory settings for the purposes of detecting change within consolidated stone.

The experiment comprises two main parts. Firstly, the laboratory preparation of samples, together with consolidation with two treatments (TEOS and MTMOS) and a controlled establishment phase of fourteen days; and second the exposure trial proper which comprises monthly and bi-monthly readings over a year with the samples on a wooden frame in a field site. This second part is separated into two data collection phases, with different collection intervals representing initial and secondary consolidation phases, based upon the study of hydrolysis-condensation stage by George Wheeler (2005). Within the trial, the effectiveness of three assessment techniques is tested. Each of the instruments and techniques used here are understood in both a material testing and cultural heritage conservation capacity. Taking each in turn, the processes can be divided into measures of sample surface condition (Colorimetry); and of bulk or internal condition (ultrasonic Pulse Wave Velocity, Mass). Each of these has some pedigree in either field or laboratory use in relevant context. Pulse Wave Velocity is used to measure the internal cohesion of samples removed from monuments or structures (see for example Wilhelm *et al* 2021, Park & Shin 2009), though it operates most effectively in controlled environments, where relative humidity and temperature can be controlled. This trial offers an opportunity to test its use on samples in two different settings, and to draw conclusions on how these variables may influence data collection and reliability.

To assist in the quantification of how these variables may influence P Wave readings, mass of samples is recorded at all stages of preparation and exposure, to allow these data to be plotted together and therefore interpreted accurately. It is understood that both rainfall and relative humidity have a dynamic relationship with exposed stonework, and therefore it was expected that trends associated with weather and climate through this test would be detected as fluctuations in this data (Franzen & Mirwald, 2004). Whilst mass is commonly employed in laboratory settings, its use in concert with P Wave and colour data in a field setting is less well established, and so this represents a timely exercise in testing its use as a field technique, where it is more commonly used in longer term studies. Further information on the characteristics of the stone will be collected using a Spectrophotometer, which collects data on the colour and reflectance of the surface (and treatments applied to the stone), plotting colour responses on a three-axis colour 'space'. Again, this metric is well understood in many conservation contexts, including cultural and built heritage studies (for example Grossi et al 2015; Lorusso et al 2007, Sanmartin *et al* 2020), though its use in field trials for the testing of Silane consolidants is limited. It is envisaged that the combination of these instruments and their complementary datasets allows for the development of a unique picture on the development and performance of treatments on sandstone in a field trial setting.

4.1.1 Aim and Scope of Field Trial

The trial has dual aims; in line with the project research objectives which it addresses.

Experimental Objective 1 is to prepare and apply treatment to stone samples in an effective and appropriate way in the laboratory for use in a field setting. This comprises the preparation and treatment of the sample sets in controlled laboratory conditions, allowing for the application of consolidant treatments with confidence for their successful establishment.

Once these steps have been taken, the samples are introduced to the exposure site in a controlled manner, introducing climate variables at the appropriate time in the curing process.

Experimental Objective 2 of the trial is to test a range of monitoring techniques and equipment, drawing comparisons between their function and the results obtained within both laboratory and field-based settings. This is a central aim of the trial, as the project is focused on finding the most appropriate means of monitoring the performance of consolidants on sandstone.

In this instance, the performance is indicated by tracking the consolidant as it completes its establishment phase (typically within the first six months of application (Wheeler 2005), when it is expected that the internal structure of the stone will continue to undergo detectable material changes.

4.1.2 Links to Research Framework

The experiment addresses the following elements of the research framework:

> **Objective 1. To investigate the development of a novel methodology for the preparation and analysis of sandstone for consolidant assessment trials**
>
> **Objective 2. To investigate the use of sample-based and structure-based experiments in field settings for the assessment of consolidant performance on sandstone**
>
> **Objective 4. To produce a 'Toolkit' of methods for the evaluation of consolidant performance on sandstone, arising from Objectives 1,2, and 3**

Drawn from the four main project Research Objectives, this part of the experimental programme addresses Research Questions 1 and 2 in full and forms the first part of the answer to Research Objective 4, an element that will also be addressed in the final chapter of the thesis.

4.2 Methodology

4.2.1 Preparation of Samples

Selection of stone and pre-preparation is outlined in section 3.3. For this experiment total 68 cubes were cut, separated into six categories, and labelled as follows:

Table 4.1. Breakdown of Locharbriggs Sandstone samples and labelling nomenclature

"A Series"	Numbers 1-10 for laboratory weathering, treatment with TEOS (consolidant "A") and exposure during trial Numbers 11-12 for laboratory weathering treatment with TEOS (consolidant "A") and storage as control
"B Series"	Numbers 1-10 for laboratory weathering treatment with MTMOS (consolidant "B") and exposure during trial Numbers 11-12 for laboratory weathering treatment with MTMOS (consolidant "B") and storage as control
"C Series"	Numbers 1-10 for laboratory weathering and exposure during trial with no consolidant treatment Numbers 11-12 for laboratory weathering and storage as control with no consolidant treatment
"D Series"	Numbers 1-10 for exposure during trial with no laboratory weathering or consolidant treatment Numbers 11-12 for storage as control with no laboratory weathering or consolidant treatment
"E Series"	Numbers 1-10 for storage as control, in controlled environment with no exposure to ambient relative humidity and UV light
"F Series"	Numbers 1-5 for laboratory weathering, treatment with consolidant A and inclusion in a separate "test wall" experiment Numbers 6-10 for laboratory weathering, no consolidant treatment and inclusion in a separate "test wall" experiment

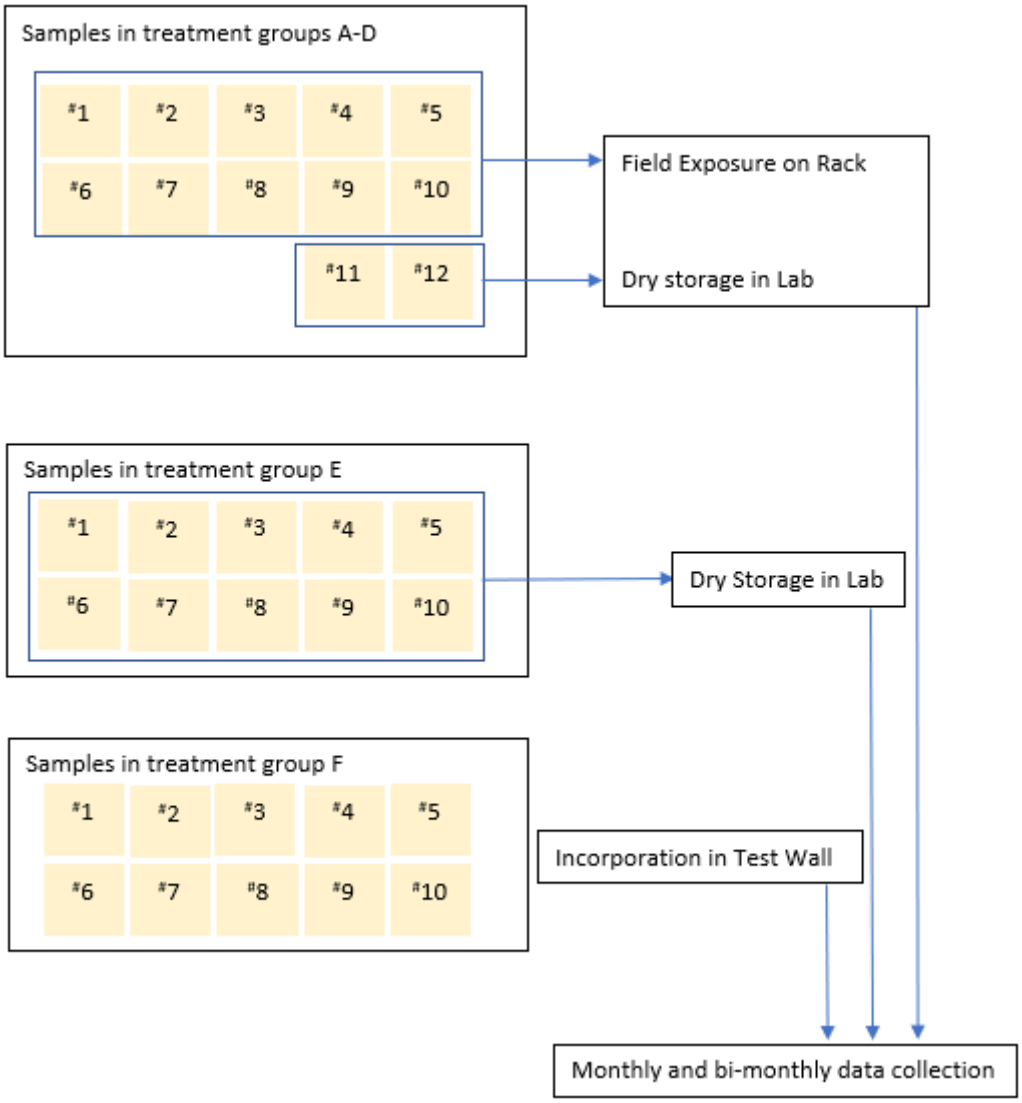

Figure 4.1 Flowchart of sample use through trial

4.2.2 Consolidant Treatments for the Rack Trial

Two consolidants were selected for the experiment, both with a long record of use in heritage conservation: Consolidant A: tetraethyl orthosilicate (TEOS); an ethyl ester with the compound $Si(OC_2H_5)_4$. It is commonly used as a binder and surface consolidant on historic stone and is used widely under the commercial name “Wacker OH100” distributed by ACS Ltd.

The second (Consolidant B): methyltrimethoxysilane (MTMOS) is a variant Silane mixture with the formula $CH_3Si(OCH_3)_3$ and was supplied by Sigma Aldrich. Further details of these treatments are available in section 3.2 (p62), together with reference to associated literature.

4.2.3 Laboratory Pre-trial Measurements

Following sample selection and cutting, each sample was marked with a group letter and sample number, using temperature resistant ink. The stone was then dried in a vented fan-assisted oven at 65°C until dry mass was achieved. From this point forward the stone was stored in a desiccator in stable laboratory conditions, and mass was taken before and after each set of measurements. The stone was again dried at 65°C until recorded mass was again achieved.

Measurements taken focused on surface condition and internal cohesion, and used the Konica Minolta CM700D to collect colorimetry data, Proceq Punditlab for Ultrasonic Pulse Wave Velocity, and an Oxford Instruments Research+ Balance for collecting mass data.

4.2.4 Laboratory Stone Weathering Methodology

Stone sample cubes were artificially weathered using the heat-only method as set out in Chapter three (sections 3.3-3.5 inclusive). Following this cycle of preparation, sample stones were measured for mass, colour, and P Wave velocity (see Table 4.2 for equipment used), following which the samples were all re-heated at 65°C in fan oven until dry mass was achieved prior to further treatment.

4.2.5 Application of Consolidants and Pre-exposure Preparation

Consolidant treatments were applied using the full immersion method described in §3.5, above.

Following the completion of the application process, samples were removed from the container and their mass recorded. Stable mass was recorded throughout the establishment process (see § 4.3.1, below), indicating minimal loss of consolidant from the time of immersion to the end of the laboratory phase.

4.2.6 Exposure Trial Methodology

4.2.6.1 Rack Samples

The Exposure trial consisted of 40 stone samples placed on a purpose-built wooden trial 'rack', positioned facing north-east in a fenced enclosure at Wytham Woods Test Site near Oxford, UK (Lat:51.7758569415398 Long:-1.3167971; 76m AOD). The rack consists of a series of open backed 'shelves' in a frame set at an incline of 45°, facing east and fixed to a semi-permanent base. The rack frame is made of treated softwood and is set within a fenced area on an exposed slope, where it is unshaded from wind, rainfall, and direct sunlight (see figure 4.2).

During the trial, sample numbers 1-10 of series prefix A, B, C, and D were set on the frame. The trial began on 28th March 2019 and concluded in March 2020 and comprised data collection intervals at 28-day intervals for six months up to September 2019, followed by 56-day intervals from November 2019 until March 2020). During the trial the following measurements were taken throughout:

- Mass
- Spectrophotometry
- Pulse Wave Velocity

Figure 4.2 Samples on the exposure rack at Wytham. Image © Author

Samples arranged in rows per treatment:
Top: TEOS treated, Second Row: MTMOS treated,
Third row: Weathered and Untreated, Bottom Row:
Natural condition

Between each data collection day, samples were left on the exposure rack at Wytham and left exposed to the weather. For the data capture, field equipment was taken to the site, and a mobile station set up for the collection of data. Samples remained on site throughout the process.

4.2.6.2 Wall 'Embedded' Samples

Further to the rack trial, the 'F' category of samples cut and prepared, and five treated with TEOS consolidant by capillary action before being incorporated into an east-west orientated 'test wall' construction, also at Wytham Woods close to the exposure rack (Lat:51.7758569415398 Long:-1.3167971, 76m AOD) (see Figure 4.3). In part the purpose of this structure is to test the extent to which exposure of individual samples to weather is a factor in measured consolidant performance.

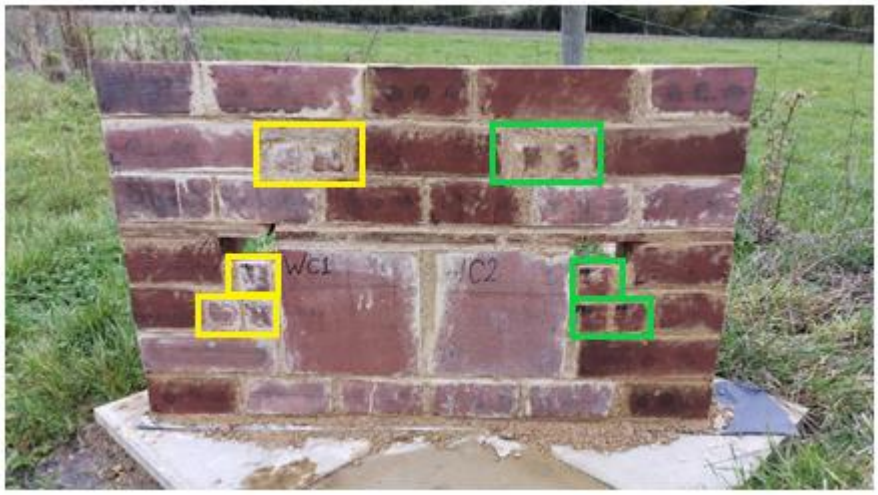

Figure 4.3 East Facing elevation of the test wall highlighting F Samples. Image © Author
Yellow: TEOS Treated F blocks, Green: Untreated F Blocks

This is achieved by incorporating comparable samples into a larger structure (constructed of Locharbriggs Sandstone and bonded with hydraulic lime mortar) and drawing comparisons between those samples fully exposed on the rack and those buffered by incorporation into a larger mass. The ten 70 mm^3 samples were prepared at the same time as the sample sets used in the exposure rack trial, and once the test wall was constructed were tested once a month, coinciding with data collection dates on the wall samples, and coinciding with phase two of the rack sample collection. For this comparative test P Wave Velocity data were collected from the wall samples, and means were compared with the TEOS treated and Weathered Only sample sets here to test for significance.

4.2.6.3 Laboratory Control Samples

The performance of all equipment used in this trial is tested against the E category control samples (no.s 1-10) throughout. The characteristics of these samples are expected to remain constant in normal operation, and deviation from this suggests either a fault in the equipment, the need for service/ calibration, or perhaps user error. In this trial control sets of two types were created; those understood as full controls, i.e. samples cut from the same source material and placed into

controlled storage throughout the experiment; and those which were subject to the same artificial weathering and consolidation as the exposed samples. This latter group were placed in desiccators for the duration of the trial and were used to check and verify the results collected in the field on each data collection day, in order to identify changes driven by environment and those resulting from the establishment of the treatments.

4.2.7 Data Collection Methodology

4.2.7.1 Rack Samples

All samples associated with the exposure trial were tested using the same methodology. As outlined above, samples were first tested in laboratory conditions (23°C ±5°C, 55%RH ±5%) at equilibrium with the atmosphere (i.e. undried). Following this, the samples were re-tested after dry mass was achieved. They were again tested following the artificial weathering process (samples at room temperature, dry mass), prior to application of consolidant.

Following application of consolidant treatment, samples were retested after 14 days of initial consolidant establishment (referred to hereafter as the 'post-treatment' data point) and then again 28 days after consolidant application- at the point the protective cover was removed on site at Wytham (hereafter March 2019 data point). From this point, data collection intervals were divided into two phases:

- Experimental Phase 1: 28-day intervals for an initial trial period of 168 days (six calendar months).
- Experimental Phase 2: 56-day intervals for a further 168 days, following the final recording of Phase 1.

There was no removal of samples from site during data collection, all readings were taken close to the test rack in a field shelter which protected equipment from wind and rain. Mass readings of 'F'

samples were not possible during the test wall trial as the samples were a fixed component of the wall structure.

4.2.7.2 Laboratory Control Samples

Control samples were tested within the laboratory at the time of each field data collection and were then re-dried at 65°C in a fan oven and immediately returned to the desiccator with silica gel pellets each also re-dried at time of data collection. The 'true' control samples ("E Series") were further stored separately in a desiccator in the basement to remove from exposure to sunlight for the duration of the experiment.

4.2.7.3 Test Wall 'Embedded' Samples

Pre-weathering, pre-treatment, and on-site readings were taken as per the Exposure Trial samples. Timescales varied in the construction and exposure phases of the test wall experiment (see Chapter five) whereby samples were treated and retained in the fume cupboard for a period of 28 days prior to construction of the wall by the author. On construction of the Test Wall, samples were recorded prior to construction and then at 28-day intervals in line with phase one of the exposure rack, and coinciding with data collection for the test wall experiment. Results from the embedded wall samples are detailed in §4.3.2.3 below.

4.2.8.1 Mass

Mass has been used here as an indication of potential fluctuations of moisture within the stone samples both before and during the rack trial, and not in the expectation that material will be lost through deterioration during the trial (excepting for handling/ accidental damage). These data can also be compared with weather trends to detect correlations between the two. This information was collected using an Oxford Instruments "Research+" balance, accurate to 0.01g. During field

collection this instrument was insulated from the disruptive effects of wind by being set up on a level workstation within a field shelter. Measurements were taken only when the balance was settled and acclimatised to the conditions. The balance and any other equipment were powered from a remote inverter connected to a vehicle.

4.2.8.2 Pulse Wave Velocity

Ultrasonic Pulse Wave Velocity measurement forms a central part of this study. The data, which is relatively straightforward to collect in the field, provides a range of possible information on the internal properties of the stone, including structural cohesion, density, and elastic modulus (Kassab & Weller 2014,1). As the method is understood as a measure of structural integrity, it has the potential to trace the changes to internal pore space that consolidation presents, particularly during the hydrolysis-condensation phase, where the mass of the consolidant within the sample undergoes significant change over time (Wheeler 2005; 18).

For samples within the Test Wall, the sampling methodology employed for the Rack trial was repeated, with three readings taken parallel to bedding planes (which are in compression within the wall construction). Sampling took place without removing samples from the structure. Mean values are taken from these with all raw data retained, in addition to on-site environmental data, for data analyses.

4.2.8.3 Colorimetry

Colorimetry data was collected in the field using a Konica Minolta CM700D portable Spectrophotometer, coupled to a Panasonic Toughbook laptop and processed using SpectraMagicNX software. A 6 mm diameter sampling aperture was employed, with the Spectrophotometer set to SAV sampling. Data in the L*a*b* (D65) colourspace was recorded for analysis, and details of the methodology can be found in section 3.6.2 (p74).

For accuracy, an Aluminium template was created at the outset of the project, which fitted to the face of the sample stone and ensured all readings were taken over the same region throughout. The template was treated with matte paint prior to use, to prevent interference with results from the material, and to help create a full seal for the exclusion of any ambient light.

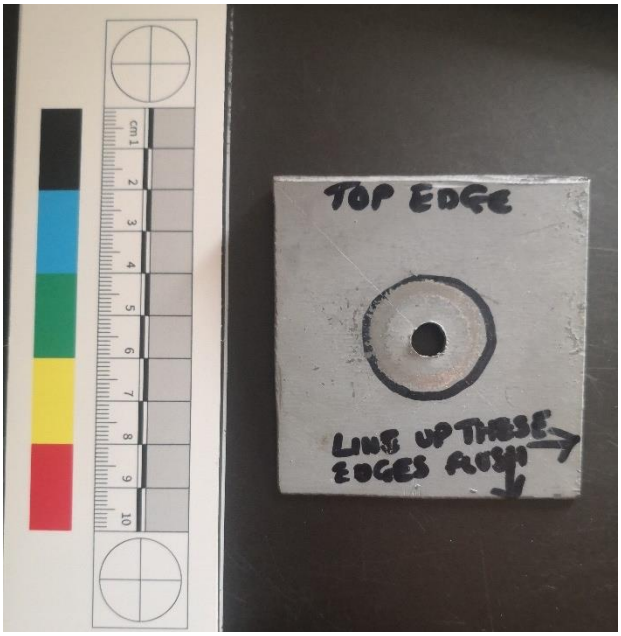

Figure 4.4 Mask template used for colorimetry readings. Image © Author

The Spectrophotometer was black-white calibrated prior to use on each occasion and had been calibrated by the manufacturer before the start of the project.

4.3. Results and Discussion

4.3.1 Weather and Climate

The following table (4.2) summarises daily weather data collected by the Radcliffe Meteorological Station (RMS). The meteorological station is located within the University at Green Templeton College in Oxford and is 2.1 miles east-south-east of the test site. Table 4.3 is a record of observations taken by the author during data collection.

Table 4.2 Summary Weather Data for Oxford, period between March 2019 and September 2020, Phases 1 & 2

Weather Data by Month	Experimental Phase 1						
	March	**April**	**May**	**June**	**July**	**August**	**September**
Max Temp °C	15.5	16.1	24.2	20.2	23.6	21.6	25.1
Min Temp °C	4	8.2	7.9	10.1	14.7	13.4	12
Mean Temp (collection day)°C	9.8	12.2	16.1	15.2	19.2	17.5	18.6
Rainfall (mm)	0	1.6	0	0.2	1.7	6.7	0
Total Sunshine (hr)	8.6	8.8	12.1	9.5	9.7	9.7	6.8
% Relative Humidity	66	67	54.1	65.9	75.5	63	80.8

	Experimental Phase 2		
	November	**January**	**March**
Max Temp °C	8	3	9.1
Min Temp °C	5.4	5.2	3.1
Mean Temp (collection day) °C	4.3	7.6	6.1
Rainfall (mm)	0.5	7.3	3
Total Sunshine (hr)	1.3	4	5.7
% Relative Humidity	92.5	78.2	91.8

Table 4.3 On-site Data Collection Timetable and conditions

Month	Time	Weather conditions
March 2019	28th 12pm-1pm	Cool, dry, light breeze with cloud
April 2019	25th 12pm-1pm	Cool, dry, sunny
May 2019	23rd12pm-1pm	Warm, dry, sunny with sparse cloud
June 2019	20th12pm-1pm	Warm, dry, sunny
July 2019	18th12pm-1pm	Warm, dry, with cloud cover
August 2019	15th12pm-1pm	Warm, damp, cloud cover
September 2019	12th12pm-1pm	Warm, dry, cloud cover
November 2019	8th 12pm-1pm	Slight drizzle, cold, damp
January 2020	3rd 12pm-1pm	Overcast, cold, damp
March 2020	2nd 12pm-1pm	Overcast, cold, damp

4.3.2 Field Trial Data

4.3.2.1 Mass

Figure 4.5 shows the mean mass of each sample group (ten samples) plotted against ambient Relative Humidity. Relative Humidity plotted here represents the conditions at midday on the day of sampling at each interval, coinciding with collection time. Each scatterplot includes two groups of results, phase 1 covering monthly readings March- September 2019, and phase 2 covering bi-monthly readings November 2019- March 2020.

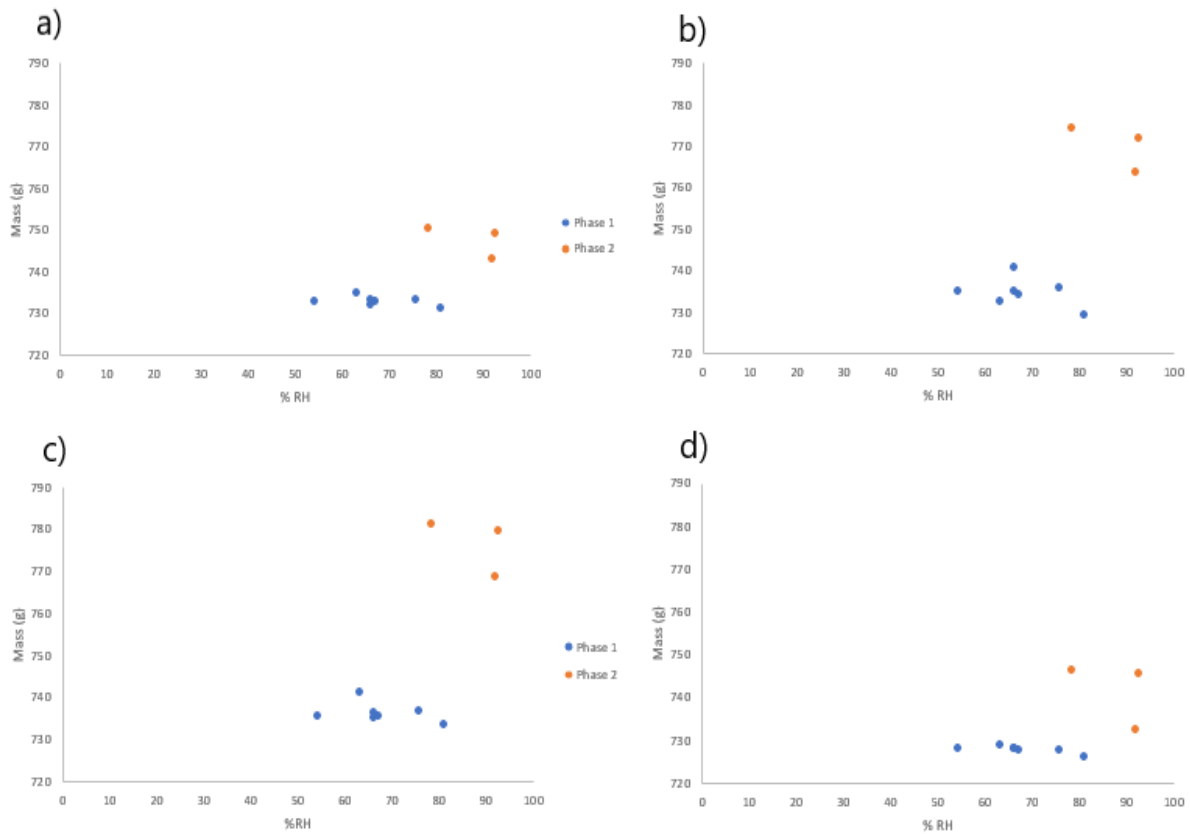

Figure 4.5 Scatterplots of mean mass of each sample group plotted against relative humidity on the day of sampling. a) TEOS Group samples, b) MTMOS Group samples, c) Weathered Only Group Samples, d) Natural Group Samples

Looking first at the two groups of consolidated samples (fig 4.4, plots a and b), the TEOS treated group has a much tighter range of readings for the period of phase 1 (3.92g, with 11.38g for MTMOS, see also Table 4.5), with no outliers associated with upper or lower relative humidity values, and the R^2 figure associated with both (TEOS 0.188 and MTMOS at 0.142) suggest that correlation between the increased relative humidity and an increase in mass is weak. Phase two

generally includes higher values and a greater spread of readings, with only one data point overlapping the phase 1 cluster (January 2020). This point in particular relates to an uncharacteristically high rainfall and above average relative humidity reading, and so further affirms the lack of correlation borne out from these datasets. The two unconsolidated sample sets (plot b- Weathered Only, and plot d- Unweathered and Untreated) are also grouped more tightly during the spring and summer months, with the Weathered Only group registering the largest range of readings over the whole trial (46.196), and the highest mass readings of the whole set- 779.83g and 778.01g, in November 2019 and January 2020 respectively.

Table 4.4 Mean mass readings for sample groups (10 replicates) throughout Exposure Trial

(Standard Dev in brackets)	**TEOS Group**	**MTMOS Group**	**Weathered Only Group**	**Unweathered Untreated Group**
Pre-Weathering	706.46*(14.00)*	728.46*(17.31)*	734.82*(14.91)*	726.03*(13.28)*
Post- Weathering	704.85*(13.98)*	726.76*(17.23)*	732.85*(14.85)*	725.68*(13.31)*
March	733.35*(14.43)*	740.83*(17.79)*	735.54*(14.61)*	728.30*(13.53)*
Apr	732.95*(14.48)*	734.57*(18.1)*	735.73*(14.22)*	727.98*(14.15)*
May	732.96*(14.16)*	735.07*(18.02)*	735.83*(14.37)*	728.15*(14.24)*
June	732.27*(14.21)*	735.28*(17.3)*	736.60*(14.7)*	728.34*(14.45)*
July	733.52*(14.82)*	735.85*(17.32)*	737.02*(13.81)*	728.01*(13.98)*
Aug	735.24*(14.51)*	732.76*(17.15)*	741.44*(14.39)*	728.99*(13.54)*
Sept	731.32*(14.45)*	729.45*(17.54)*	733.63*(14.98)*	726.41*(13.33)*
Nov	749.27*(15.01)*	772.08*(17.99)*	779.83*(14.58)*	745.88*(13.34)*
Jan	750.55*(15.57)*	774.5*(16.9)*	781.41*(15.11)*	746.54*(14.23)*
Mar	743.15*(15.46)*	763.77*(17.72)*	768.90*(18.26)*	732.70*(14.56)*
Standard Deviation	14.05	17.26	18.78	7.28
Variance	197.55	298.05	352.87	53.11
Max	750.55	774.50	781.41	746.54
Min	704.85	726.76	732.85	725.68
Range	45.70	47.74	48.56	20.86

Table 4.5 Range of Mass readings (g) across Exposure Trial

	TEOS Group	**MTMOS Group**	**Weathered Only Group**	**Unweathered Untreated Group**
Phase 1 Range	3.92	11.38	7.80	2.57
Phase 2 Range	7.40	10.72	12.51	13.83
Combined Phases	19.23	41.73	47.77	20.12

With regards rainfall as a possible influencing variable, figure 4.6 plots the mean mass of sample groups with total rainfall in the 48 hours leading up to data collection (the sum of rainfall recorded at midday on the day of collection and the previous day). Of these readings, only April (1.6 mm), July (1.7 mm), and August (6.7 mm) registered more than 1 mm of rain in the 48 hours preceding data collection in phase one, whilst only January 2020 (7.3 mm) passed the same threshold in phase two of the trial.

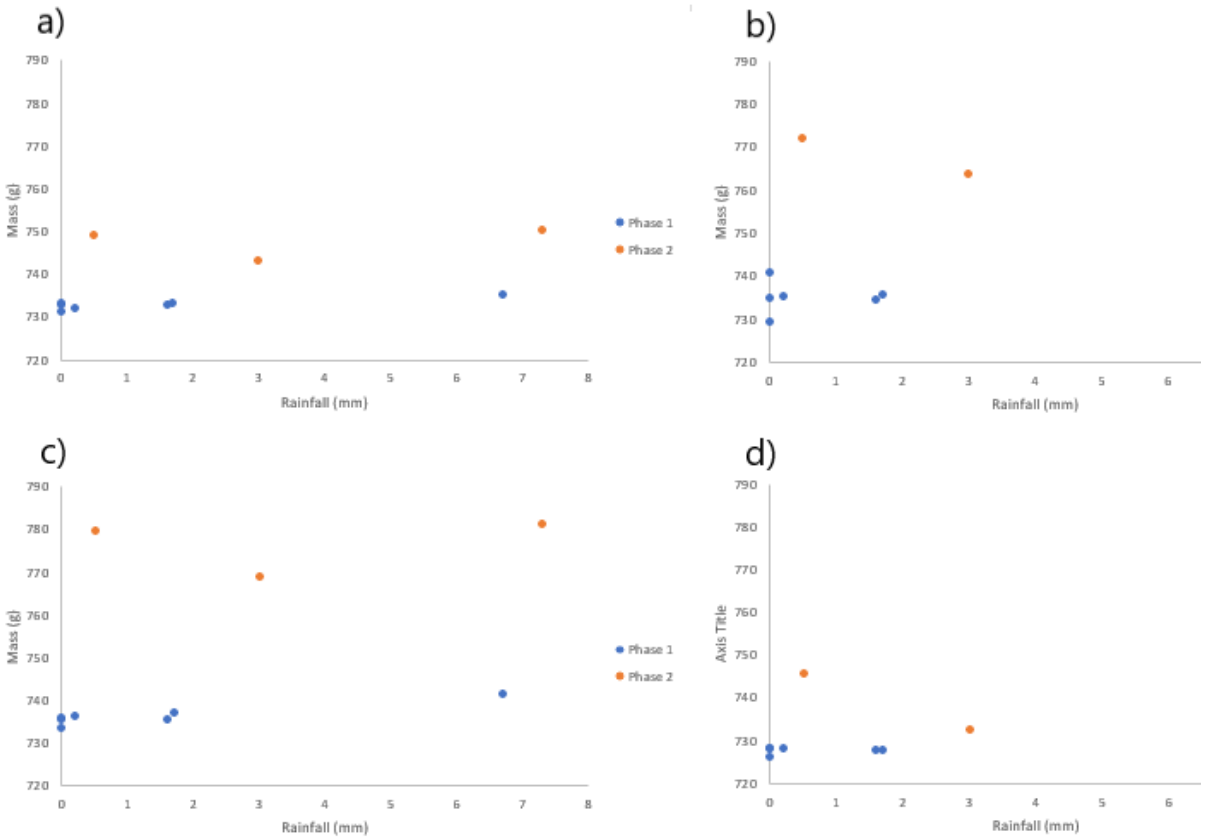

Figure 4.6 Scatterplots showing the mean mass of each sample group with cumulative rainfall 48 hours prior to data collection. a) TEOS Group samples, b) MTMOS Group samples, c) Weathered Only Group Samples, d) Natural Group Samples

Looking at each sample set in turn, the TEOS group all show a slight increase in mass in the August reading (735.27g, see Table 4.5), suggesting a possible uptake of water as a response to the increased rainfall in this period (6.7mm in the 48 hours prior to collection). When this increase is compared to the two untreated stone sets -both Weathered Only and Unweathered- Untreated it is

possible to see a similar response in both. Taken together, these appear to bear out the claim that Ethyl Silicate treatments such as TEOS may allow evaporation from the stone in analogous ways to stone in its natural state; a key selling trait for the product (Wacker 2021). Otherwise, no clear trend can be readily seen from the mass data for TEOS treated stone. Most importantly it does not seem possible to use this method to identify and follow the hydrolysis- condensation process as Ethyl Silicate (TEOS) consolidants become established within the stone. In the case of TEOS treated stone, the consolidant is understood to lose mass equivalent to around 40% in the months following application (Wheeler 2005). As treatment increased mass of the group by a mean of 29 g, this would represent mass loss of between 12 and 14 g in the early stages of the exposure trial. It is unclear from this dataset if this is a limitation of the technique, or if this process had completed in between data collection points following lab treatment and prior to the first data collection of the exposure trial.

In contrast, the MTMOS group as a whole shows a uniform loss of mass in the first month of exposure (with the exception of sample no.7) of between 5 and 10 g, representing approximately 40-50% of the mass increase following treatment, and in line with expected changes during early establishment (Wheeler 2005). Sample 7 diverges slightly from the group trend, but still loses 3.3 g of mass across the first month. This is only a small variation from the mean and represents a loss of 33% of the mass increase at time of treatment, an outlier percentage wise, but not one that presents a significant contraindication.

Otherwise, the MTMOS treated group shows no clear trend; with 3 of the group showing a slight increase, one a marginal increase, and the rest registering a loss of mass between July and August, where both relative humidity and rainfall increased. As mentioned above, MTMOS functions as a weather repellent as well as a surface consolidant, so these readings are to be expected. Looking at the unconsolidated groups, the Weathered Only group shows a greater spread of values, with both Variance and Range being the largest of all the stone groups (see Table 4.6) possibly indicating a

more open near surface pore network resulting from the heat weathering treatment. By comparison, the Unweathered- Untreated group are the tightest grouped results, with by far the lowest Variance and Range.

4.3.2.1.1 Statistical Analysis

A total of 40 sample stones were tested for normality using a Shapiro Wilk test, each consisting of ten replicates. All of the data passed the threshold for normality using an α value of 0.01. This value has been used throughout the experimental process to reduce the potential for Type I errors in the statistical output, owing to the number of tests required to fully examine the dataset.

An Analysis of Variance was carried out for each treatment group using an α value of 0.01. The result of the test for the TEOS treated group was P= 0.06, indicating that the effect of relative humidity on the mass of the samples was not statistically significant. Similarly, the effect of relative humidity on the MTMOS group (p = 0.05) was not significant at the conservative α value of 0.01.

In addition to these, the two unconsolidated groups; Weathered Only and Unweathered-Unconsolidated both returned P Values > α; (0.055 and 0.025 respectively). This confirms that in none of the sample groups is there sufficient evidence to claim that fluctuations in ambient relative humidity influence samples sufficiently to indicate the presence or absence of consolidants, at least using an α of 0.01. Similarly, rainfall was found to have an effect on the samples (p = 0.017), although this was not statistically significant at the conservative α level.

For the MTMOS sample set, the result of the ANOVA is clearer with a resulting P value of 0.08 confirming that there is no statistically significant relationship between recent rainfall (i.e. 48 hours prior to collection) and fluctuations in sample mass. Significantly for the Weathered Only set, and by extension for the validity of the heat weathering treatment, there is clearer evidence of a positive relationship between the exposure of the weathered blocks to rainfall and the fluctuation of mass (p=0.003). Confirmation that this is an effect of the heat weathering and not the absence of

consolidant comes from examination of the Unweathered-Untreated set, which return a P value of 0.015, again not passing the statistical threshold for significance.

Furthermore, the Coefficient of Determination (R^2) (Table 4.6) values for the pairings also bear out the limited correlation between rainfall, percentage relative humidity, and the mass of the sample groups as taken on site at Wytham Woods. The largest R^2 value from these calculations indicates only 50% of the data fit the regression model (Weathered Only-%RH), with the rest of the relative humidity pairings spread between 31% and 47%. The correlation results for the rainfall-mass pairings were lower again, with a spread of values from 13% to 23%, which when taken with the results of the ANOVA tests bears out the lack of statistically significant relationships between the mass of samples and the on-site conditions tested.

Table 4.6 Coefficient of Determination, Mean Mass of Groups with weather

	TEOS Group	MTMOS Group	Weathered Only	Unweathered-Untreated
%RH	0.435	0.473	0.502	0.317
Rainfall (mm)	0.235	0.135	0.210	0.171

4.3.2.2 Colorimetry

As with other measurements, these were taken on site at Wytham Woods, following initial measurements in laboratory conditions. Following the pre-treatment and consolidation of samples, colorimetry data were collected in the same two phases, with data points every 28 days between March and September 2019, and every 56 days thereafter to March 2020.

All data represented are SCI (Specular Component Included) which includes specular and reflected components of the data, reducing the impact of surface conditions on the data collected. The scatterplots below plot the mean L* value from each stone sample set against the percentage ambient relative humidity (Figure 4.7) at time of sampling and rainfall (mm) in 48 hours prior to collection (Figure 4.8). Each point is the mean of ten readings taken at a single collection point (monthly or bi-monthly depending on experimental phase).

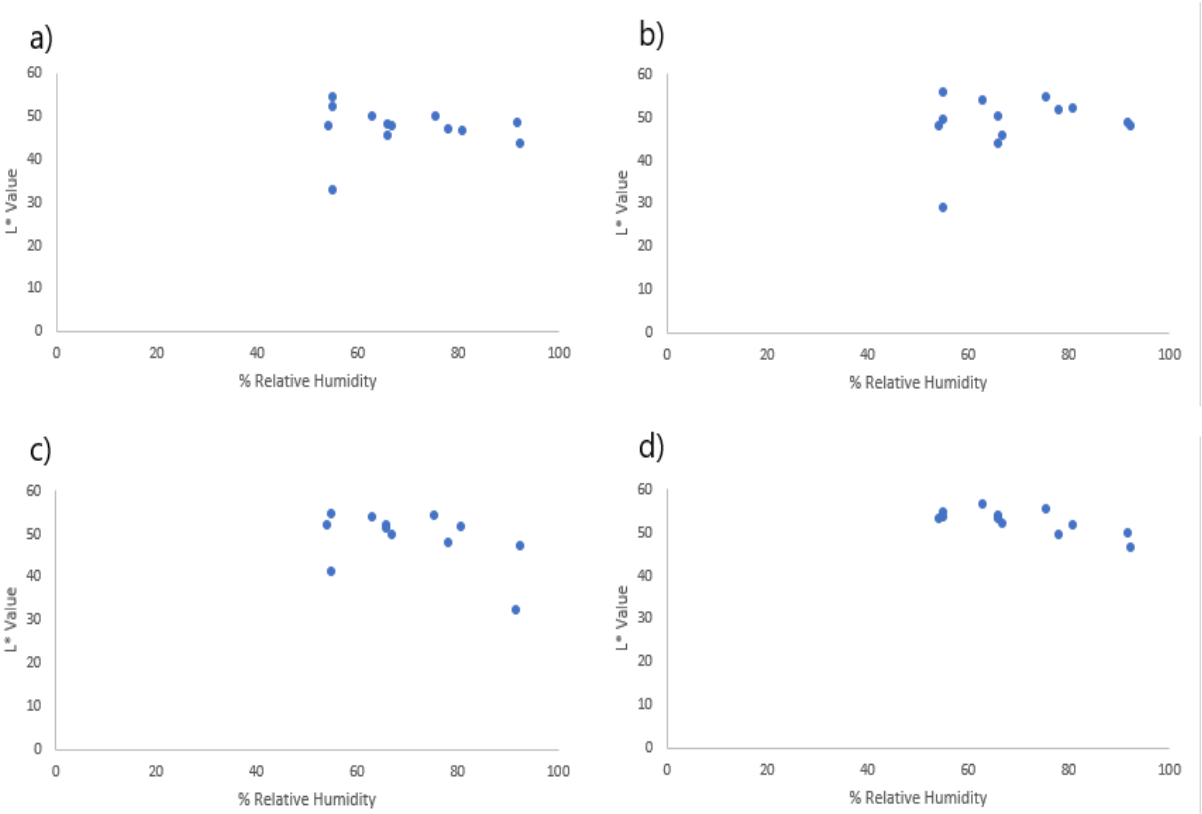

Figure 4.7 Colorimetry data collected from each ten-stone sample set. a) TEOS Group samples, b) MTMOS Group samples, c) Weathered Only Group Samples, d) Natural Group Samples

The L* axis of the CIE colour space represents the light-dark element of the hue, where 0 is completely black and 100 a completely reflective surface (or 'pure white' as it is generally understood). A significant change to L* value was recorded after the consolidation of both TEOS and MTMOS samples; a mean drop of 39.75% and 48.32% respectively (values of 21.3 (TEOS), and 26.9 (MTMOS) from pre-weathering to post-treatment). This is to be expected where liquids are applied to the substrate as wetting typically darkens surfaces, and the enduring nature of this effect suggests deposition of consolidant at the surface of the samples.

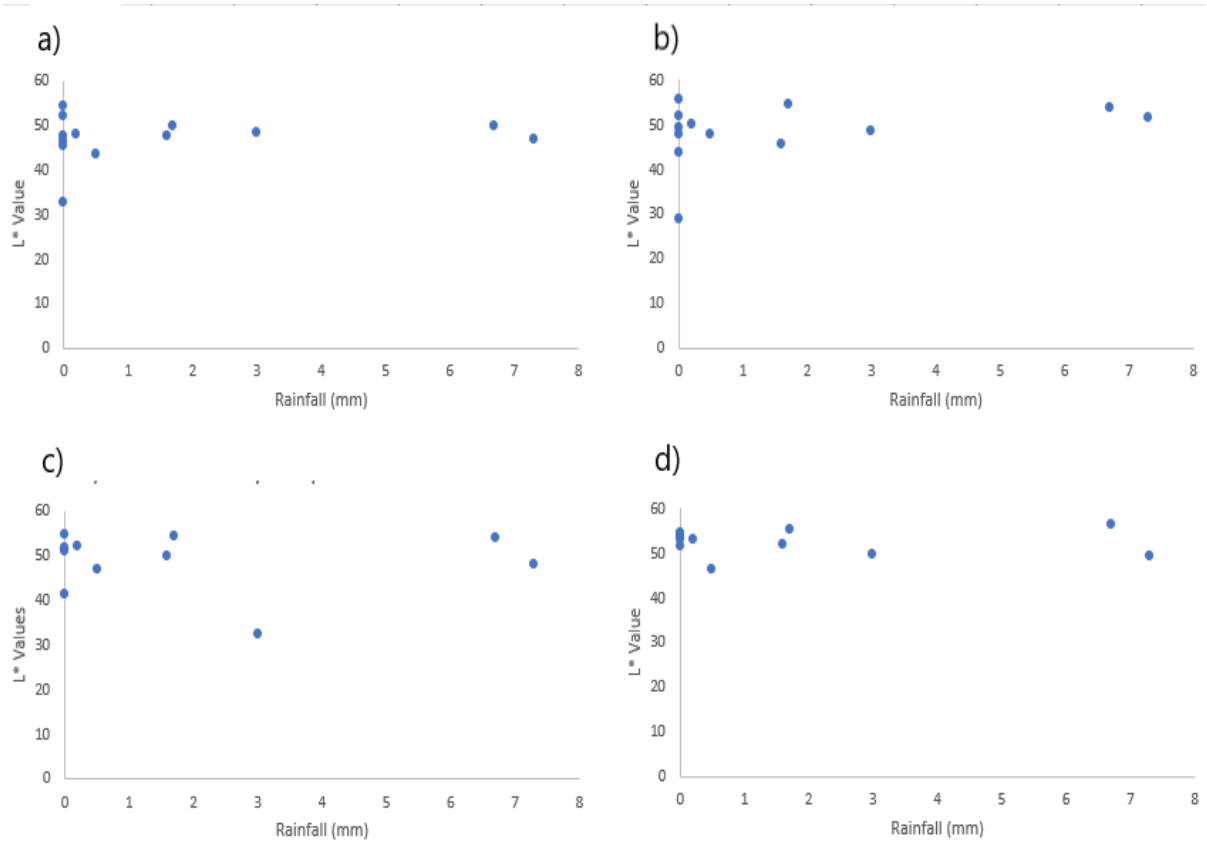

Figure 4.8 Mean of all sample groups L value, plotted against total rainfall in the 48 hours prior to data collection.* a) TEOS Group samples, b) MTMOS Group samples, c) Weathered Only Group Samples, d) Natural Group Samples

This functions as a useful pre-cursor test to how L* values may be prone to influence by ambient moisture (in the form of diffuse water vapour or direct rainfall). Fig 4.7 therefore plots mean L* values against percentage relative humidity, and Fig 4.8 against rainfall in the immediate 48 hours prior to collection for the purpose of comparison with ambient conditions on site at Wytham Woods With regards establishment of treatment, both TEOS and MTMOS groups record a significant drop in L* value as a response to the consolidation phase of the treatment phase, and these values do not return to pre-treatment L* values once the initial curing phase has completed- typically after 28 days (Rong *et al* 2013), demonstrating a residual effect from the consolidants on surface appearance.

It should therefore be possible to detect changes in the hue of these deposits as a function of the condition of the consolidant going forward, either as an assessment of the consolidant as a whole or as a surface-specific indicator of early change.

What the two sets of data plotted in figures 4.6 and 4.7 express is that there is no clear correlation between change to L* values as a direct response to increased humidity or rainfall - the two main drivers of 'damp conditions' on site. One might expect to see a fall in L* values (a darkening of stone surface) in these conditions, in a response analogous to the consolidation process. Only during September (TEOS group), November (All groups), and January, February and March 2020 (Unweathered untreated group) does the L* value drop below the median value, correlating between this and high relative humidity, a total of eight mean readings from a total of fifty-five across the trial.

Table 4.7 Coefficient of Determination for R^2; L, a*, and ΔE Values determined by on site rainfall and percentage relative humidity*

	TEOS Group	MTMOS Group	Weathered Only	Unweathered-Untreated
L* Value with %RH	0.001	0.005	0.206	0.547
L* Value with rainfall (mm)	0.002	0.097	0.057	0.001
a* Value with %RH	0.215	0.06	0.002	0.252
a* Value with rainfall (mm)	0.009	0.082	0.312	0.033
ΔE Value with %RH	0.017	0.132	0.158	0.657
ΔE Value with rainfall (mm)	0.074	0.087	0.000	0.053

When pairing changes with rain events (see Tables 4.7 and 4.8), both the TEOS and MTMOS groups record no values that would indicate a significant link between expected darkening of surface hues (L*) and incidents of high rainfall. TEOS samples, the lowest L* value on-site corresponds with a rainfall total of just 0.5 mm (November). For the MTMOS set, the lowest value (43.84) corresponds with March 2019 and so is most likely associated with the consolidation process as opposed to rainfall, which on the day totalled only 0.2 mm. Of the rest of the trial, April 2019 records an L* of

45.7 (1.7 mm of rainfall) and May 47.84 (6.7 mm of rainfall). Inversely, the two wettest months August 2019 and January 2020 (both 7.3 mm of rain) both correlate with high L* values (53.9 and 51.63 respectively), suggesting again that there is no definite link.

Coefficient of determination (Table 4.7) ranges from 0.001 and 0.132 for these combinations, affirming that the link between these variables is weak. Both untreated groups (Fig 4.8 (c) and (d) above) again indicate at most a weak correlation with relative humidity changes across the exposure trial period, the coefficient of determination being between 0 and 0.657 across all combinations of L* and ΔE values with rainfall and percentage relative humidity (summarised in table 4.9). Notably June to July, and August to September where distinct changes occur in the relative humidity percentage on site, for both groups. In general terms however, the L* values of both the untreated groups remain far closer to their pre-trial readings, with the unweathered and untreated group performing as one would expect in relation to the weathered group; with less variation and a tighter spread of values across the group itself.

The Weathered Only group register an interesting reaction to the weathering process (table 4.8), with a sharp drop of the whole-group value range following furnace exposure. This group of values returns to within 5 L* units of their original state by the March reading, excepting for one sample stone which returns to this margin by May. There may be several drivers for this change, but a return to pre-weathering values indicate that those changes were reversible and therefore not a structural/ chemical change in the stone as has been detected in other heat ageing tests (see for example Hajpál & Török 2004). Taking both L* and a* values for this interval into account, the L* shows an increase upon introduction to the atmosphere whereby the lightness value of the samples returns to a similar range to pre-weathering, though does not reach a truly pre-weathering cluster of values until July.

	TEOS GROUP			MTMOS GROUP			WEATHERED ONLY GROUP			UWEATHERED/ UNTREATED GROUP			ON-SITE CONDITIONS	
	L* Mean	a* Mean	ΔE Mean	L* Mean	a* Mean	ΔE Mean	L* Mean	a* Mean	ΔE Mean	L* Mean	a* Mean	ΔE Mean	%RH	Rain (mm)
Pre 'heat treatment'	54.14	13.98	N/A	55.71	12.15	N/A	54.59	12.28	N/A	N/A	11.62	N/A	55#	N/A
Post 'heat treatment'	51.91	13.39	3.40	49.49	7.05	9.72	41.34	9.36	14.38	54.72 ++	11.34	N/A	55#	N/A
Post Consolidation	32.62	13.9	22.17	28.79	6.874	28.90	N/A	N/A	N/A	53.34 ++	N/A	2.03 ++	55#	N/A
March 2019	45.17	14.86	9.25	43.84	10.98	2.45	51.11	9.56	5.79	53.79	11.83	1.96	66	0.2
April	47.47	13.7	7.10	45.70	11.72	10.23	49.81	10.45	5.72	51.83	11.41	3.22	67	1.7
May	47.73	13.23	7.02	47.84	11.98	8.09	51.78	10.41	4.50	53.01	11.36	2.50	54.1	6.7
June	47.86	13.48	6.74	49.99	11.79	6.03	52.05	10.5	4.15	53.25	11.16	2.32	65.9	0
July	49.73	13.3	5.54	54.64	12.65	2.76	54.33	10.9	3.02	55.21	10.83	2.91	75.5	0.5
August	49.83	13.21	5.68	53.90	12.3	3.03	53.90	11.14	3.35	56.27	10.71	3.32	63	7.3
September	46.33	11.4	9.17	52.15	11.93	4.05	51.48	9.95	5.24	51.57	10.05	4.23	80.8	3
November	43.67	12.68	10.73	47.86	10.14	8.08	46.98	8.45	9.19	46.49	8.632	9.65	92.5	0.5
January 2020	46.95	13.54	7.36	51.63	11.43	5.17	47.99	11.13	7.10	49.28	11.43	5.98	78.2	7.3
March	48.43	13.26	6.26	48.59	10.92	7.66	32.41	12.23	22.36	49.66	11.58	5.34	91.8	3

Table 4.8 Mean Colorimetry values for Test Rack Trial. #Controlled %RH in laboratory conditions, ++Laboratory readings mimic treatment stages for symmetry

The a* values for this group are also interesting, as one might expect desiccated stone to display a return to pre-weathered a* values when introduced to the natural conditions of the test site (resulting from relative humidity and rainfall acting upon the samples), but 5 samples do not return to this value at all during the test, and 3 of the 5 that do take until July or August before they reach this value.

Whilst this set of values is unusual it is entirely possible to see them as an artefact of the inherent variability that Locharbriggs stone is known to contain, wherein some areas of the stone display more evident variations in the bedding planes.

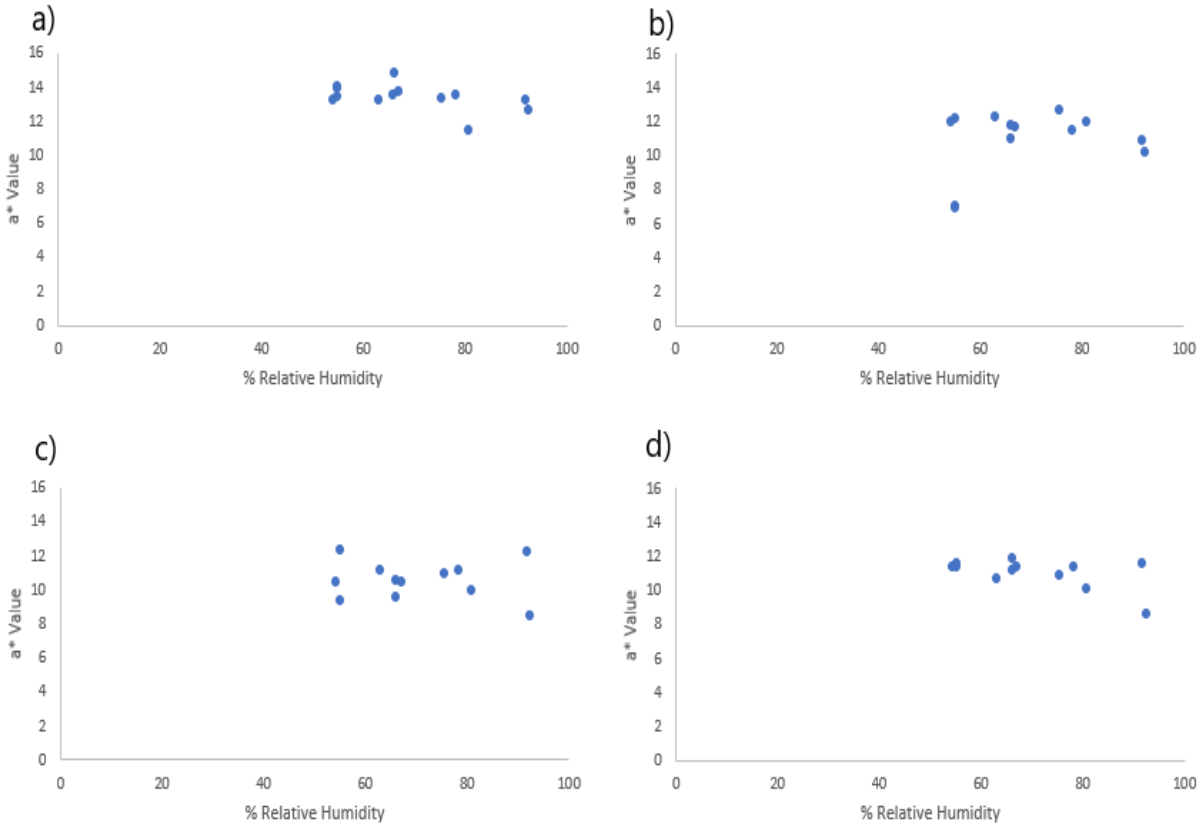

Figure 4.9 Mean a values of each group per month plotted against percentage ambient relative humidity at the time of sampling* a) TEOS Group samples, b) MTMOS Group samples, c) Weathered Only Group Samples, d) Natural Group Samples

Moving on from L* readings, the next metric recorded are the a* CIE space values, which represent the green (-) to red (+) spectrum of the colour space. As Locharbriggs Sandstone is naturally red- pink this is the axis on which change is most likely to appear (as opposed to the b* axis which plots yellow

(+) to blue (-) colour range). Figure 4.9 shows the four treatment groups plotted against percentage relative humidity and again demonstrates little correlation between relative humidity and a* readings. Of each of the four groups, the Unweathered- Untreated group has the highest coefficient of determination, at 0.252.

In general terms, a* values of TEOS and MTMOS treated stone stayed relatively stable through all recorded fluctuations of relative humidity, though notably there was a recorded drop coinciding with higher-than-average relative humidity percentages in both September and November of 2019; followed by an increase in March 2020 (this latter effect on TEOS samples only). These indicate that there is not a simple direct relationship between the prominence of this hue and airborne moisture, where consolidated stones are concerned.

Moving on to the unconsolidated groups, the range of a* values recorded for both sets are similar to the consolidated samples, showing that the consolidation process has little significant effect on the a* axis, unlike the L* values which were significantly suppressed in the immediate post-treatment phase (see Table 4.8). In response to the on-site relative humidity conditions, both sets performed similarly, with a noted dip in the a* values recorded in November 2019, corresponding with the highest relative humidity reading (92.5%).

With regards the effects of direct rainfall on the sample groups, the data tell a similar story to that of ambient relative humidity. Across all four groups the coefficient of determination ranges from 0.009 (TEOS), and 0.312 (Weathered Only) (Table 4.8). Looking at the spread of means on table 4.9 it is clear to see that values of all treatment groups are clustered around a central mean and values do not deviate significantly, regardless of weather conditions at the time of data collection.

The combined story these data tell is that as with L* axis readings, there is little or no evidence of significant causal relationships between moisture (in the form of rainfall or ambient relative humidity) and a* values, at least with regard those that are observable in the temperate climate of the south of England.

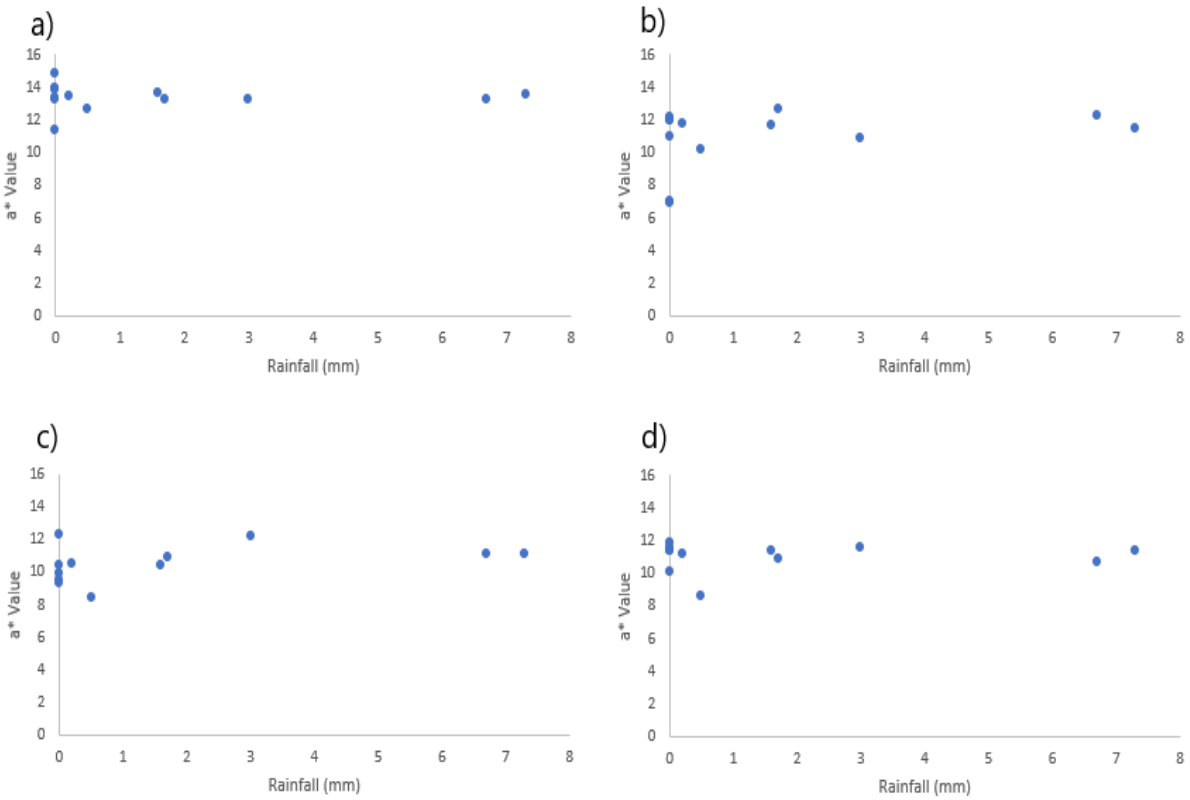

Figure 4.10 Mean a values of each group per month plotted against total rainfall in the 48 hours prior to data collection.* a) TEOS Group samples, b) MTMOS Group samples, c) Weathered Only Group Samples, d) Natural Group Samples

The final variant observed in the colorimetry category is the ΔE or total change of each sample group across the exposure trial intervals. ΔE can be thought of as a calculation of 3-dimensional distance between space on the three-axis colour space and is calculated using the following equation:

$$\Delta E = \sqrt{[(L_2-L_1)^2+(a_2-a_1)^2+(b_2-b_1)^2]}$$

As expected, the greatest movement from natural (Pre-Weathering/ Treatment) characteristics comes during the heat treatment and early consolidant establishment phase. Following pronounced changes in the MTMOS group after heat weathering in the lab, and subsequent consolidation, the general month-on-month trend from initial exposure in March 2019 to August sees a progressive reduction in the size of change for the stone group; after which change increases again in line with more unsettled conditions in phase two of the trial. The TEOS group records a similar story, although this stone group responded less to the heat weathering stage; possibly resulting from variability

within in the stone group. However, ΔE values following consolidation are more analogous to the MTMOS treated samples, with a large initial change followed by a steadily decreasing amount of subsequent change in the following months.

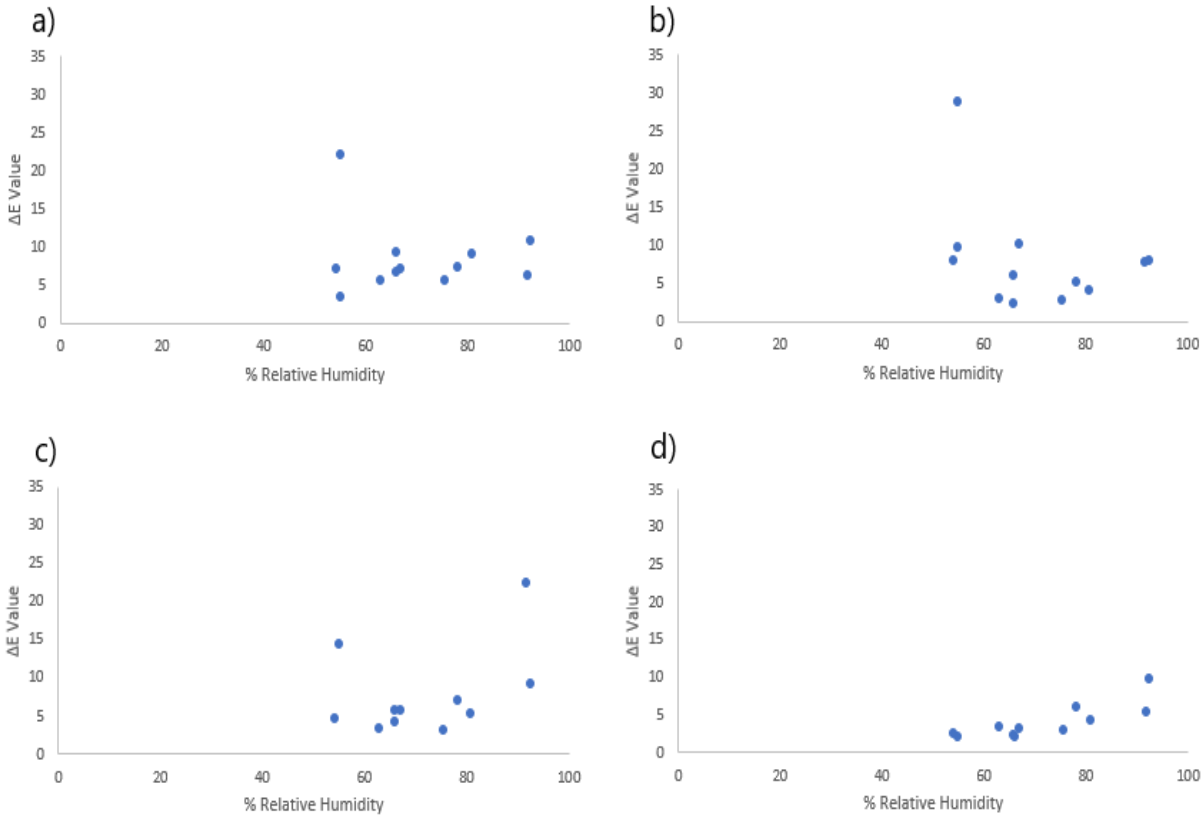

Figure 4.11 ΔE Values plotted with percentage ambient relative humidity at the time of sampling. a) TEOS Group samples, b) MTMOS Group samples, c) Weathered Only Group Samples, d) Natural Group Samples

In contrast, the Weathered Only Group registered the largest response to the heat weathering process but then (in the absence of consolidation) remained constant throughout the trial, increasing only in regard ΔE value into phase two of the trial, where humidity and rainfall are more variable. The Unweathered- Untreated Group records the smallest changes on each of the plotted months of phase one excepting September where it changes marginally more than the Weathered untreated group, but less than both the treated groups. From September, and in line with the other three sample sets, the ΔE value increases, possibly as a response to the more variable weather during collection.

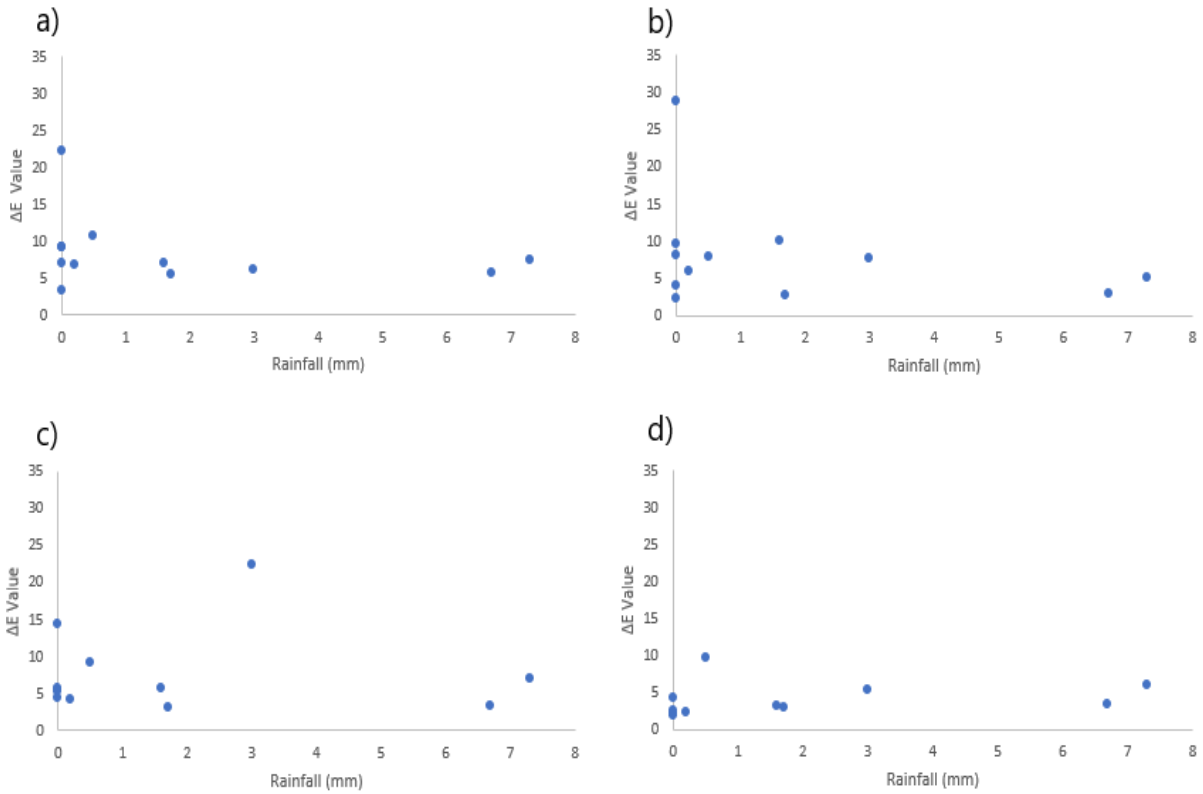

Figure 4.12 Mean ΔE values of each group per month plotted against total rainfall in the 48 hours prior to data collection. a) TEOS Group samples, b) MTMOS Group samples, c) Weathered Only Group Samples, d) Natural Group Samples

4.3.2.2.1 Statistical Analysis

All colour data were tested for normality using the Shapiro Wilk test, which was passed in all cases. The Pearson correlation coefficient was calculated for each set of grouped data, pairing each colour space element in turn with percentage relative humidity and total rainfall (mm) at time of data collection. The results are listed in table 4.9, and as with Coefficient of Determination (Table 4.8), results generally point to only a weak correlation between the two factors in the majority of results. Notably within these results, the only "strong positive" indicators of correlation come within the Weathered Only (L* with %RH and ΔE with %RH), and Unweathered-Untreated groups (L* with %RH, and ΔE with %RH). These observations use Evans (1996) measures of correlation to determine the level of significance, with the threshold set at ±0.632.

Table 4.9 Results of Pearson Correlation Coefficient test for colorimetry and on-site conditions

Correlation	L* with %RH	L* with Rainfall (mm)	a* with %RH	a* with Rainfall (mm)	ΔE with %RH	ΔE with Rainfall (mm)
TEOS Group	-0.353	0.423	-0.396	0.098	0.365	-0.451
MTMOS Group	0.104	0.48	-0.584	0.165	0.114	-0.202
Weathered Only	-0.653	-0.115	-0.044	0.559	0.667	0.093
Unweathered-Untreated	0.732	0.049	-0.502	0.181	0.797	0.177

Following on from correlation between variables, ANOVA was carried out using the monthly mean of each sample set and an α value of 0.01, to determine if colorimetry is recording significant variability within sample sets across the time period of the trial. For the L* colour space, the ANOVA produced a P Value of 0.091, thus not passing the threshold for significant variance across the four datasets. Similarly, using the ΔE measure of change there is a P Value of 0.149, again indicating that the sample groups do not vary to a significant level. In the a* colour space however, the ANOVA returned a P Value of 0.000, indicating that the sample group contained significant variance throughout the test. Post hoc multiple comparisons were then carried out using t-tests to further identify the source of this variation by comparison the following data:

Test 1: Months of highest and lowest percentage relative humidity (May and November 2019)

Test 2: Months of the two closest percentage relative humidity (May and June 2019)

Test 3: Months with highest and lowest rainfall (May and August 2019); and

Test 4: Months of the closest high rainfall (August 2019 and January 2020).

These four tests were carried out independently on each of the four treatment groups, and the results are summarised in Table 4.10, below.

Table 4.10 Result of comparison T-Tests for a colorimetry values*

	TEOS Group			MTMOS Group			Weathered Only Group			Unweathered-Untreated Group		
	T-Stat	T-Crit	P-Value	T-Stat	T-Crit	P-Value	T-Stat	T-Crit	P-Value	T-Stat	T-Crit	P-Value
Test 1	-1.187	2.898	0.251	1.519	3.169	0.159	-5.339	2.552	0.000	-4.937	2.898	0.000
Test 2	0.551	2.552	0.587	2.681	3.169	0.023	0.315	2.878	0.755	-0.45	2.898	0.657
Test 3	-0.032	3.012	0.974	3.131	3.249	0.012	2.967	2.602	0.009	-1.342	2.787	0.196
Test 4	-0.542	3.105	0.059	1.58	3.054	0.139	6.793	3.012	0.000	-1.239	2.92	0.232

Null Hypothesis: there is no significant difference between groups.
Alternative Hypothesis: there is a significant difference between groups.

None of the TEOS groups passed the threshold for significance. This was also the case for the MTMOS groups, although the p-value of one test (Test 3: high/low rainfall) was very close to significance (Table 4.10). For the Weathered Only group, one comparison (Test 3) was statistically significant, and similarly for the Unweathered-Untreated Group, one comparison (Test 1: months of highest/lowest relative humidity) was significant (Table 4.10).

These results indicate that with more polarised weather events it may be possible to effectively identify and track the response of consolidated stone to environmental conditions using the a* axis of the CIELAB colour space. With the unconsolidated stone groups, the stone recorded more pronounced reactions to rainfall, which is to be expected when seen in parallel to the consolidated stone results.

4.3.2.3. Ultrasonic Pulse Wave Velocity

Because application of ultrasonic coupling gel used with the Punditlab presents a possible source of error introduction for mass and colorimetry, the Punditlab measurements were done last at each measurement period. Readings were taken in triplicate on each stone, and a mean recorded for each sample. Each test was taken with the transducers in contact with the same predetermined stone faces, positioned at the same place on the face for each data capture, to ensure repeatability between tests. As noted, a small film of water-based coupling gel was applied to the transducers prior to each set of sample readings being taken.

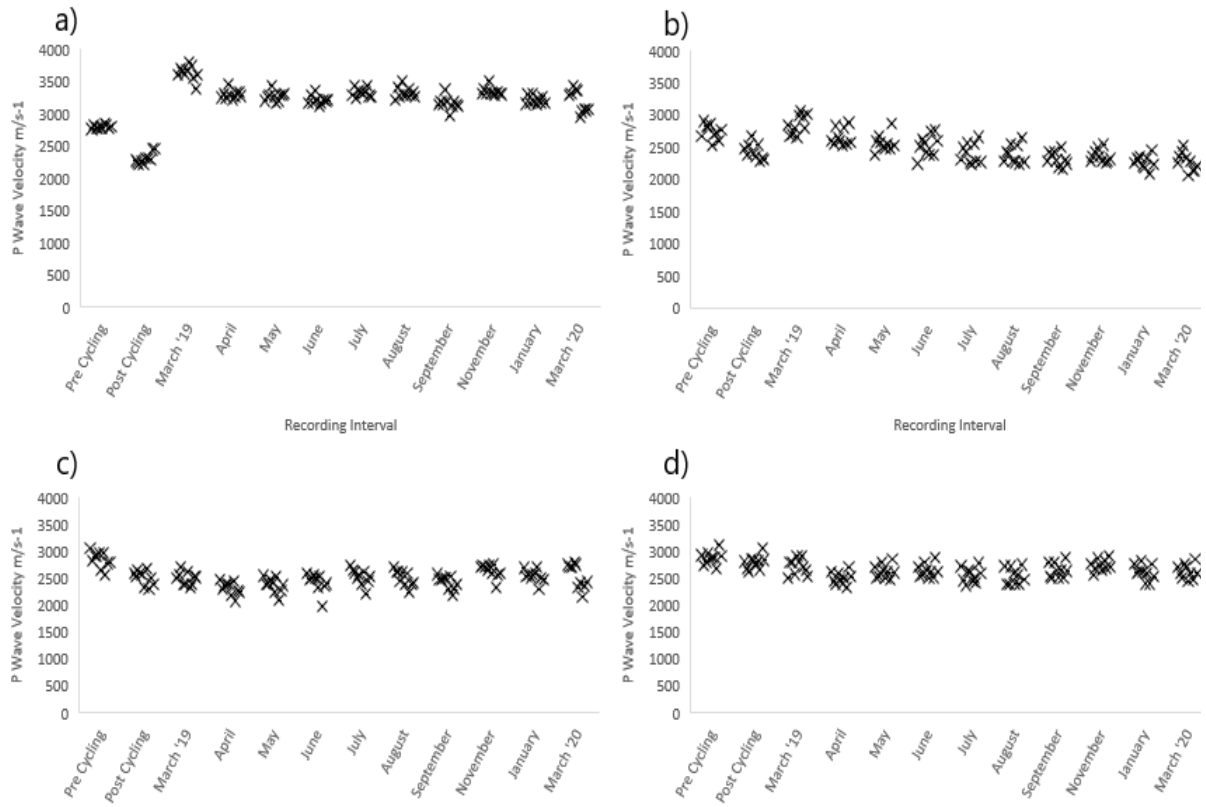

Figure 4.13 Clusters of P Wave Velocity data throughout the trial. Pre and Post Cycling readings were taken in the University of Oxford Geolabs facility, on-site readings March 2019- March 2020 were taken at Wytham Woods test facility. a) TEOS Group samples, b) MTMOS Group samples, c) Weathered Only Group Samples, d) Natural Group Samples

As with the other elements of this trial, the data were collected in two phases; first separated by a 28-day interval between March and September 2019, followed by a second phase of 56-day interval readings from November to March 2020. The first collection phase has more frequent data points in an attempt to plot any variability in performance during the consolidant establishment phase, understood to take approximately six months (Wheeler 2005). Subsequently, bi-monthly collection captures the winter months of the trial, where typically increased rainfall and higher relative humidity contrast the warmer and drier summer months of the early trial phase.

Table 4.11 Summary of P Wave Velocity readings for all groups

TEOS Group	Mean	St Deviation of Group	**Weathered Untreated Group**	Mean	St Deviation of Group
Pre-Weathering	2793	63	**Pre-Weathering**	2842	147
Post-Weathering	2302	92	**Post-Weathering**	2517	133
March	3634	122	**March**	2498	121
April	3299	68	**April**	2315	125
May	3272	74	**May**	2373	133
June	3211	70	**June**	2427	170
July	3327	80	**July**	2522	144
August	3323	93	**August**	2504	142
September	3159	99	**September**	2422	123
November	3341	65	**November**	2434	125
January 2020	3206	75	**January 2020**	2637	129
March	3192	173	**March**	2544	115
MTMOS Group	**Mean**	**St Deviation of Group**	**Unweathered-Untreated Group**	**Mean**	**St Deviation of Group**
Pre-Weathering	2742	127	**Lab Reading 1**	2876	124
Post-Weathering	2432	144	**Lab Reading 2**	2789	124
March	2852	167	**March**	2723	144
April	2656	132	**April**	2497	113
May	2564	137	**May**	2626	119
June	2527	158	**June**	2639	119
July	2407	148	**July**	2557	129
August	2396	141	**August**	2541	152
September	2327	105	**September**	2646	129
November	2360	96	**November**	2645	130
January 2020	2227	101	**January 2020**	2739	109
March	2277	139	**March**	2641	142

Figure 4.13 plots the readings of each group as clusters, at each measurement point. Of note, the TEOS group (plot a) registers a significantly higher P Wave velocity following consolidant treatment, the biggest increase in mean values of all four stone groups. This initial peak then follows a pattern of stabilisation from March to April, following which the group cluster around a total mean 3253 m/s^{-1} (±91 m/s^{-1}).

The MTMOS group (Fig 4.13, plot b) does not register such a high post-treatment peak as TEOS for P-Wave (mean of 2852 ms^{-1}), which may possibly be a attributed to the significantly higher viscosity of MTMOS, and its consequential characteristic lack of penetration (Wheeler 2005). Further to this, the MTMOS sample set follows a more differential pattern of P-Wave speed loss throughout the trial when compared to the TEOS samples; reflected in its spread of readings in plot b of Fig 4.13. Overall, the means are spread out more in the MTMOS group, the central mean of all readings being 2464 m/s^{-1}, ±287m/s^{-1}.

With regards P Wave Velocity, the heat weathering process caused only minor (and not statistically significant) changes to the characteristics of the stone. The group subsequently treated with TEOS showed a mean velocity drop of 214m/s^{-1} following the heat process, and the MTMOS group 310 m/s^{-1} for the same. The final group heat treated, the 'Weathered Only' group recorded a mean drop of 326 $m/s^{-1;}$ the largest variation, though still not statistically significant on that metric alone.

Following treatment, consolidation and placement on the exposure rack prior to the March 2019 readings, the 'Weathered Only' samples and the two consolidated groups (TEOS and MTMOS groups) diverged noticeably. Whilst both the TEOS and MTMOS groups registered a significant increase as a response to the consolidation process, the Weathered Only group did not diverge from the readings taken in laboratory conditions following heat treatment; results that were echoed by the Unweathered- Untreated Group.

From April to July the Weathered Only group uniformly increases P Wave speeds, before declining again from August to September, and remaining constant from November to March 2020; three data points which include fluctuating and significant measures of rainfall and percentage relative humidity.

The 'Unweathered- Untreated' group (Figure 4.13, plot d) behaves as one may expect when compared to the other sample sets. After an initial adjustment to the outside conditions (March to April, whereby many samples registered the biggest single month change of the trial), the sample set fluctuated little, without following deviating significantly in any of the high rainfall or high humidity events. In this manner, the sample set performs entirely as unweathered and undamaged stone would be expected to in a temperate climate. As noted, the most interesting change in the 'Unweathered and untreated' group was the in the first month of exposure. However, this was not a uniform change of P-Wave speed, with four samples out of the ten increasing their speed, whilst six registered a significant drop. As there was no major weather event in the days prior to collection, the nature of the changes cannot be assigned to any weather event. As the plotted changes following this month appear to smooth out and become more consistent, the most likely explanation is that samples were undergoing natural acclimatisation. From this point forward the set reacted in a logical manner to increases in rainfall and relative humidity, best typified by its increase between August and September.

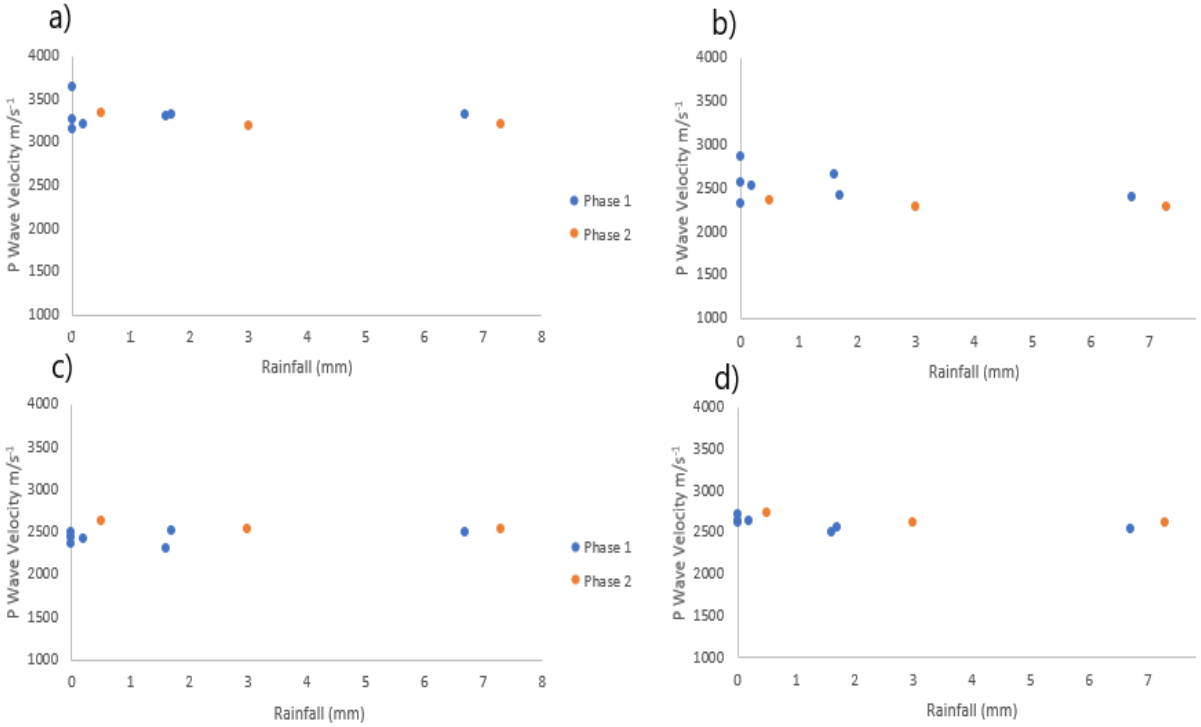

Figure 4.14 P Wave Monthly mean velocity plotted against total rainfall (mm) in 48 hours prior to collection. a) TEOS Group samples, b) MTMOS Group samples, c) Weathered Only Group Samples, d) Natural Group Samples

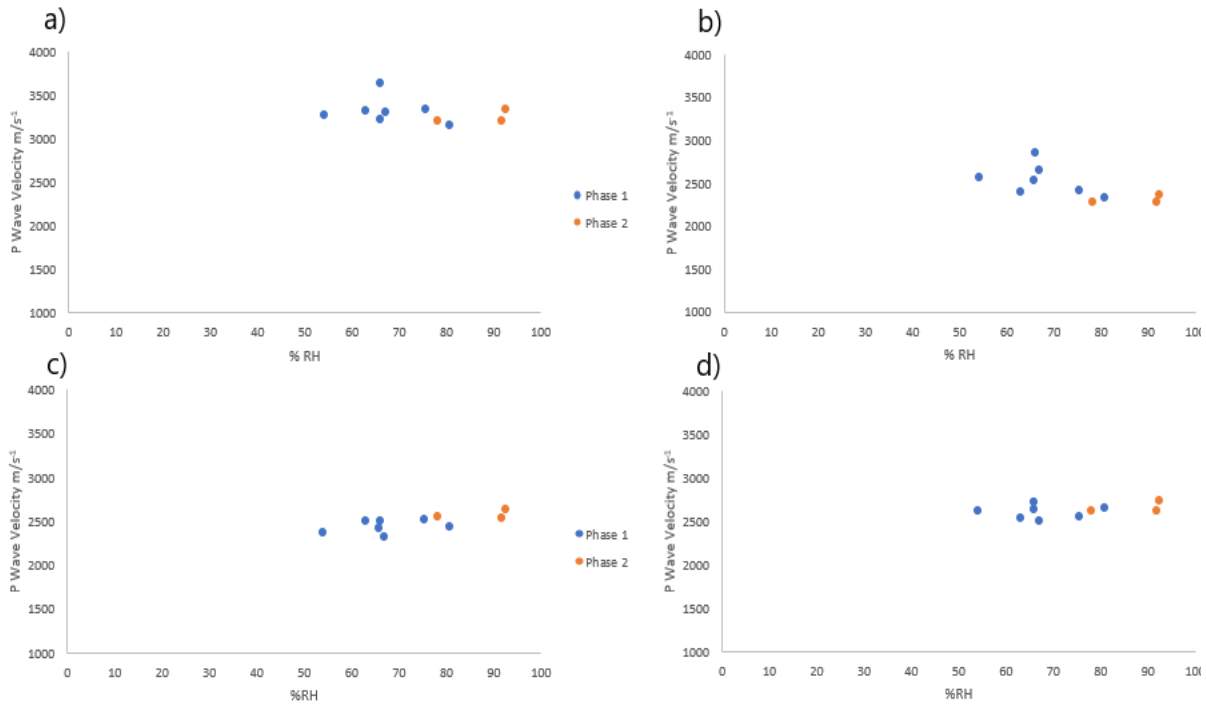

Figure 4.15 P Wave Monthly mean velocity plotted against percentage relative humidity at time of collection. a) TEOS Group samples, b) MTMOS Group samples, c) Weathered Only Group Samples, d) Natural Group Samples

Wall Embedded Samples

Samples embedded into the test wall were tested monthly for a period of seven months from October 2019 to March 2020, until the COVID-19 lockdown stopped fieldwork, curtailing the final months of planned data collection. Within this timeframe, there were four occasions where wall and test rack sampling overlapped (in phase two of the rack trial), allowing for direct comparison of performance between the sample sets within the wall and on the rack (see Table 4.12).

Table 4.12 Wall Embedded Samples, Mean P Wave Velocity

			TEOS Consolidated				
	September	**October**	**November**	**December**	**January**	**February**	**March**
Mean	3197	3353	3365	3340	3376	3414	3213
St Dev	204	153	176	122	114	104	277
			Weathered Only				
Mean	2514	2600	2788	2624	2574	2715	2665
St Dev	127	189	274	307	196	259	275

Table 4.13 Coefficient of Determination for P Wave Values collected on site with rainfall and percentage relative humidity

	TEOS Group	MTMOS Group	Weathered Only	Unweathered-Untreated
P Wave Value with %RH	0.072	0.400	0.478	0.124
P Wave Value with rainfall (mm)	0.047	0.231	0.089	0.186

In general terms, the wall samples behaved in directly analogous ways to those on the rack when comparing Pulse Wave Velocity. Mean velocity for TEOS consolidated samples grouped between 3000-3500 m/s^{-1} throughout, which compares to TEOS consolidated samples on the rack for similar or directly comparable weather conditions.

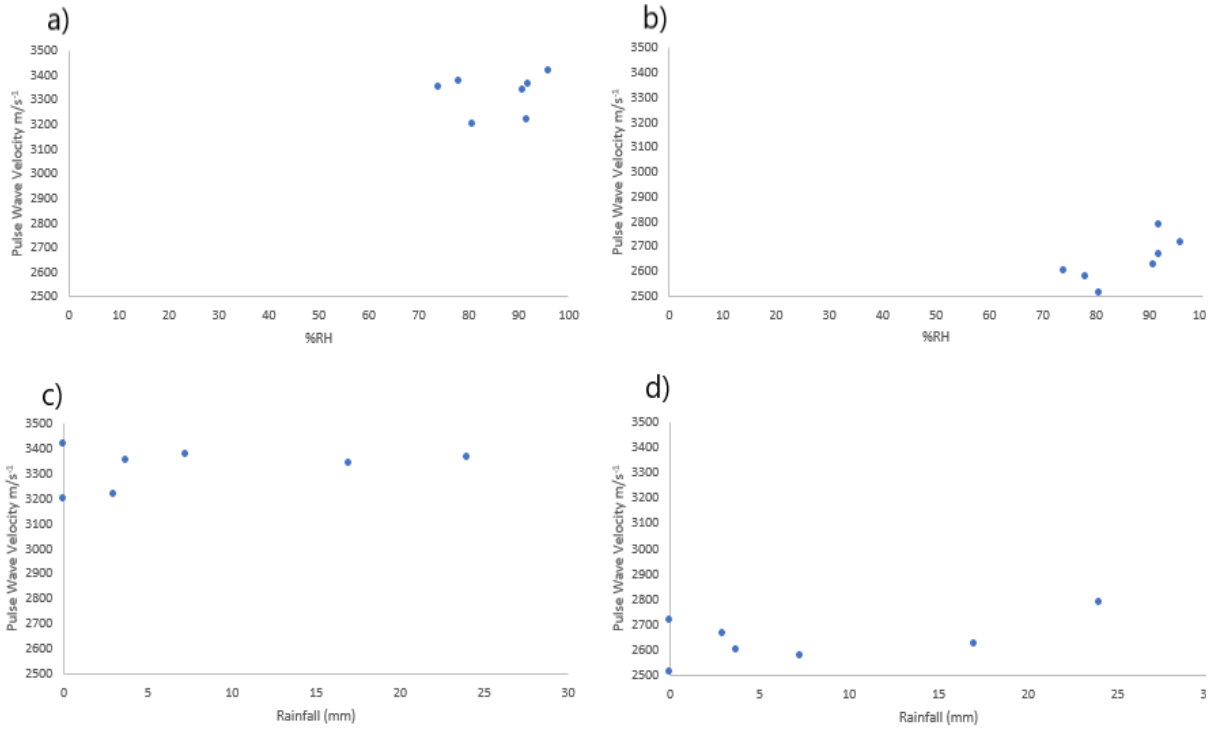

Figure 4.16 Scatterplots showing relationship between P Wave Velocity of embedded wall samples and environmental conditions on site at Wytham Woods. a) TEOS Group samples with %RH, b) Weathered Only Group samples with %RH c) TEOS Group Samples with Rainfall (mm) d) Weathered Only Group Samples with Rainfall (mm)

Weathered Only samples are clustered at a lower velocity, between 2500-2900 m/s^{-1} as is the case with those on the rack. Although replicate numbers and sampling durations vary between the wall and rack groups, there is no early indication that there is a significant difference between the samples in the two situations.

Statistical Analysis

Looking at further possible correlation between P Wave velocity and environmental inputs, particularly percentage Relative Humidity and total rainfall immediately preceding the collection of data, the coefficient of determination (R^2) value associated with figures 4.15 and 4.16 are represented in table 4.13. As with other metrics assessed during this trial, there is only a weak correlation indicated across the four groups and two factors. When comparing these with the results of Pearson's Correlation Coefficient calculation, the two measures are approximately analogous. In comparison, the Weathered Only group recorded the strongest positive relationship of all the combinations. This is a trait borne out in the other datasets, where the trend is repeated (see for instance table 4.9, a* colour space). Of the other tests, the MTMOS group records the next highest values in both, with a strong negative value for the Pearson's Correlation, and a weak positive R^2 value. None of the other pairings demonstrated any significant correlation between the P Wave Velocity and the environmental variable.

Table 4.14 Pearson's Correlation Coefficient for P Wave Values collected on site with rainfall and percentage relative humidity

	TEOS Group	**MTMOS Group**	**Weathered Only**	**Unweathered-Untreated**
P Wave Value with %RH	-0.269	-0.632	0.692	0.352
P Wave Value with rainfall (mm)	-0.217	-0.480	0.299	-0.431

Further to testing for correlation, a series of ANOVA were carried out on the means of each group across the time of the test to see if the method detected any significant variance in between the monthly datasets. Normality was confirmed using the Shapiro Wilk test for the TEOS, Weathered Only, and Unweathered-Untreated groups; the MTMOS initially failed the normality test but passed when an outlier (sample B10) was excluded.

Analysis of Variance was subsequently carried out on each treatment group, comparing month-on - month results for each group from the pre-treatment tests through to the end of the field trial in

March 2020. As with the other test methods in this trial, the α value for the ANOVA has been set to 0.01; as a precautionary measure to avoid type I error following a range of tests. The P value resulting from each ANOVA is a 0.000 indicating significant variation within each of the four groups. Following this, T Test comparisons were conducted on the following pairs of data: highest rainfall against the lowest, highest and next highest rainfall, the highest against lowest relative humidity values, and the two closest relative humidity values, for which a conservative α value of 0.01 was adopted. The results of these tests are summarised in Table 4.15.

For the TEOS treated group, only highest/ next highest rainfall comparison produced a statistically significant difference between the groups. As the highest/lowest comparison was not significant, this suggests that in the case of TEOS treated stone, the level of rainfall is more important than its presence/ absence. For the MTMOS Group it was the high/low percentage relative humidity comparison that produced a significant result, with the two rainfall related tests coming close to significance on the more common 0.05 alpha value, but not passing the threshold with our 0.01 value, indicating some effect but not at a significant level. For the Weathered Only group again the high/ low percentage relative humidity test produced the only significant result. In the final set of tests, none of the Unweathered Untreated Group recorded a statistically significant variation in P Wave Velocity as a response to the weather conditions. This last group of samples generally responded less markedly than the other groups, so the lack of significant variation borne out from these tests is unsurprising.

Table 4.15 P Value Results of T Tests between P Wave Means and weather conditions

α= 0.01	**TEOS Group**	**MTMOS Group**	**Weathered Only Group**	**Unweathered Untreated Group**
High/Low Rainfall	0.171	0.033	0.056	0.187
High/High Rainfall	0.003	0.051	0.508	0.284
High/Low %RH	0.040	0.003	0.000	0.045
Closest %RH	0.077	0.519	0.466	0.807

Table 4.16 P Value results of T Tests for P Wave Means Comparison between Wall embedded and Rack samples

α= 0.01	**TEOS Treated**	**Weathered Only**
September 2019	0.704	0.221
November	0.787	0.294
January 2020	0.000	0.764
March	0.879	0.413

Table 4.16 outlines the relationship between samples embedded into the test wall and those on the exposure rack, as tested using a T Test (unequal variance). In only one of the eight comparative tests did the difference between the rack and wall samples pass the statistical threshold: the TEOS treated samples when compared in January 2020, coinciding with one of the highest rainfall events at time of collection.

4.4.1 Discussion

Appraisal of the data shows a varying success rate for detection of physical changes in sample stones across the three main assessment techniques. It is important to draw a distinction between the ability of the assessment methods to detect change in the stone, and in the ability of these methods to assign these changes to external factors, such as rainfall. In the former capacity, the three techniques both demonstrate some capacity for success; whereas in the latter, there remains some uncertainty.

Taking each of the methods individually, the output of the trial is summarised as follows. As a technique, mass performed extremely well in the laboratory, where samples were fluctuating as a result of treatment processes; but once introduced to the field the technique provided limited data in its own right, though it provided a useful comparison for weather data. There was very little evident variation within the dataset during normal weather events (including rainfall, and high- low relative humidity variations for instance) and only registered a significant change during the unusually wet August and January data collection periods. That this is the case may be a function of block size as much as a limitation of the technique; it is entirely possible that wet-dry cycles change

too quickly to be detected by the collection methodology; and further tests should be carried out to determine if this is indeed the case. There is evidence that in-extremis the introduction of rain water can make a significant change to the mass, and so it may be possible to simulate rain events in the laboratory for instance; to gauge the success of more intense or focused collection intervals. Where the August rainfall registers, it is more prominent in the TEOS than MTMOS dataset, which correlates with the understanding that this treatment allows for natural wet-dry cycling through the pore network of the stone, the latter being equally well known as a water repellent than a consolidant (Wheeler, 2005).

Moving on to colour, the technique again provided a variable set of results. It was hoped that the consolidants deposited at the surface of samples would have reacted to introduction to the environment early in the trial, but there was little evidence of this in practice. What is apparent from the individual plots for both L* and a* axes however, is that in none of the stone sample sets is there a clear and definite trend. As with Mass however, this is possibly an artefact of arising from the combined effects of the data collection programme with the small sample sizes, and not a direct result of the process. Again, further, more targeted trials would resolve this uncertainty. Perhaps the most informative data is the ΔE metric (Figures 3.8 and 3.9). This metric neatly conveys the trends as observed both in the laboratory and field trial setting, including large deviations in colour during treatment and consolidation, followed by much smaller fluctuations later in the trial when consolidants are fully cured and conditions on-site are relatively stable.

Turning finally to the P Wave measurements, this technique has shown the most promise throughout the trial, particularly when used in parallel with weather data on site. During the initial phase of the trial, where heat and consolidants were moving the samples away from a point of equilibrium, P Wave detected the changes effectively. P Wave Velocity increased following consolidation and these increases were followed by a steady reduction in velocity to near to pre-consolidated state in both cases following introduction to the field site. These observations were

complemented by the untreated and unweathered stone sets, both of which yielded readings much closer to the pre-treated (or initial) state. As with mass and colorimetry, P Wave was not able to effectively detect any variability within the sample sets as related to rainfall or relative humidity. It should be stated however, that it is not definite that this correlation exists, and more tests would be needed to specifically ascertain the causal effect of moisture on stone. Of note are the two phases of data collection, the monthly and bi-monthly timings were originally decided upon based on the observations of George Wheeler (2005, pp20-22) that complete establishment of silane consolidants took in excess of 120 days (four months). With this in mind, initial consolidant application in laboratory conditions was followed by five months of monthly data collection, after which it was understood that both TEOS and MTMOS consolidants would have completed their establishment phase, and therefore less likely to yield evidence of change each month. From this point forward the sampling changed to bi-monthly, and readings taken throughout this phase bear out the strategy, with stabilisation of readings across all sample sets.

4.4.2 Conclusion

In order to assess the success of this trial, it is necessary to return to the original objectives and examine them in turn. Firstly, the preparatory treatment and consolidation phase. Experimental objective one of the trial was to “prepare and apply treatment to stone samples in an effective and appropriate way in the laboratory for use in a field setting”. This comprises both the heat weathering and subsequent consolidation, and critically the detection and monitoring of these steps using the chosen methods. The artificial weathering successfully prepared samples for consolidation by immersion, by increasing the rate at which liquids were drawn into the pore network of the stone (see chapter three), and subsequently both of the consolidants chosen for this trial were successfully established within the stone. Each of the test metrics applied confirmed this, with mass, colour, and pulse wave velocity recording significant alterations from pre-consolidated condition. A central

hypothesis of this trial was that if these metrics were successful in detecting the establishment of consolidants in the lab, then they may be adapted to monitor these same consolidants in the later stages of their lifespan, when their physical effect on the stone begin to decline in the field. This latter forms the second experimental objective of the trial; “to test a range of monitoring techniques and equipment, drawing comparisons between their function and the results obtained within both laboratory and field-based settings”. On this basis, this part of the trial can be said to have been a success, as there are obvious differences between the characteristics of the consolidated and unconsolidated stones at the outset of the test. That all of the data derived from the field did not pass statistical thresholds across all of the data points thereafter should not be viewed as evidence that the concept is not workable, merely that further development of the methodology is needed. Perhaps this may take the form of more intense data collection (points taken ‘within’ a storm for instance) or the addition of simulated extreme weather events in order to quantify the response of sample stones in a controlled manner. Alternatively, extending the trial for a period of three to five years would increase the potential for more complete data on the performance of consolidants, which may take several years to alter significantly, a time span beyond the scope of most DPhil-type projects.

In several of the statistical tests there is an indication that the processes acting upon samples (such as rainfall) may be having an effect, but that the quantity, duration, or timing may have to be altered to maximise the potential of the data to tell a complete story. On the subject of the assessment methods and equipment, the data tells a similar story. Mass in particular performed well as a metric within the lab setting but did not yield the desired results in the field. As above, this may be a result of the timing of data acquisition, or of the particular nature of the events as recorded. Colorimetry was more successful in the field, though most prominently immediately after the consolidation process, where surface deposits were more apparent after treatment. Of the three colour space variants, a* (red-green hue) recorded the most critical changes; with both MTMOS and Weathered Only groups passing the threshold for significance during periods of high rainfall.

Finally, Pulse Wave Velocity again performed well in the early phase of the trial, notably with the addition of TEOS consolidant to stone samples. In this trial across all sample groups there were incidences where readings varied to a statistically significant level. Of all the assessment methods examined in this trial, this is therefore the most encouraging. The next suggested step for this trial is therefore to look further into the possibilities of Pulse Wave Velocity as an assessment tool. This is likely to include an assessment of more than one instrument and transducer combinations, as well as introducing different sandstone types and simulated weather conditions as a means to quantify the boundaries of reliable data collection.

Chapter Five: Test Wall Field Trial

5.1 Introduction

This chapter explores the use of purpose-built structures for research in heritage. Following on from the use of sample stones in both laboratory and field environments, this chapter tests a methodology for the incorporation of sample stones into larger structures (including the possible effects of the structure on the samples), as well as developing a method of creating dedicated structures for conducting field-based research. For the purposes of assessing the performance of consolidants within the trial, work here is focused on the use of the HF Sensor 350B Microwave Moisture Meter.

5.1.1 Aim and Scope of Test Wall Trial

The trial has dual aims, both of which inform separate sections of the research programme, addressing the following objectives:

Experimental Objective 2 investigates the use of sample-based and structure-based experiments in field settings for the assessment of consolidant performance on sandstone. This trial addresses this element of the research framework fully, utilising both sample blocks (cut and prepared in the laboratory to the methodology laid out in chapter three), and sandstone cut as for use in construction, in larger dimensions than the samples. In particular, this trial will examine how these size differences may influence uptake of consolidants and the performance of the treatment in situ.

Experimental Objective 4 aims to produce a 'Toolkit' of methods for the evaluation of consolidant performance on sandstone, arising from the results of objectives 1,2, and 3, as set out in this thesis. This chapter and trial addresses this aim by introducing and evaluating a different non-destructive technique- the *Hf Sensor GmbH* MOIST 350B Microwave Moisture Meter, which offers a range of sensors to suit a range of sample dimensions. This instrument and approach have been trialled in similar heritage contexts by (Fusade 2019) and (Orr *et al* 2019) but it has had little direct evaluation

either on Locharbriggs sandstone substrates or in the context of ethyl silicate consolidant performance.

5.2 Experimental Design and Construction of the Test Wall

5.2.1. Design and Construction of the Test Wall Trial

The test wall experiment has been designed to allow for the investigation of several questions, summarised as follows:

1. Is it possible to identify differences in the performance of treated stone samples based on their dimensions or position within the structure?
2. Do Locharbriggs sandstone samples in the test wall structure perform in different ways as a result of method of consolidant application method (brush or capillarity absorption)?
3. Does artificial weathering of Locharbriggs sandstone affect its response to weather and climate variables when compared to control samples in a natural state?
4. How can time-series data be used to assess performance of treated and untreated Locharbriggs sandstone samples within a test wall structure?
5. To what extent can the MOIST350B be used to gather and interpret useful *in situ* data on the performance of consolidants on complex structures?

To address these aims and answer the questions above, a test wall was constructed using the a range of bocks of different sizes, laboratory pre-treatment (heat weathering or not), and laboratory pre-consolidation (brush and capillary absorption of TEOS consolidant or unconsolidated).

Structurally, the wall is made up of six block size categories (see figure 5.1).

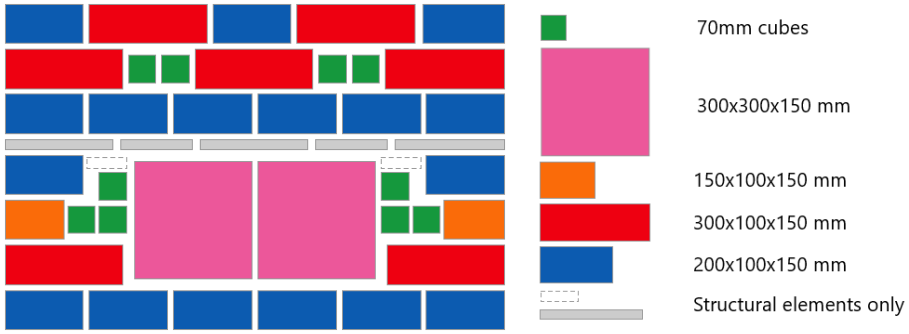

Figure 5.1 Layout of wall components by block size

The wall was built at the Wytham Woods research station near Oxford (UK) in July 2019. Following a period of two months for curing of hydraulic lime mortar, the experiment ran from October 2019 to December 2020 with data collected monthly throughout, excepting March, April, and May 2020 due to COVID-19 restrictions. Aesthetically, the test wall has been constructed in such a way that it mimics the part-randomised appearance of a range of traditional stone walls found commonly across the UK, Europe, and the USA from the medieval period to the present day (see figure 5.2). Faithfulness to this style is confined to the appearance of the wall however, as the need to control variables mean that the wall is limited to a single face, what may be interpreted as the outer 'face' of this style of wall- which traditionally supports a rubble or soil fill (with the exception of some boundary walls which can be narrow).

Individual stones are placed within the structure to allow for performance assessment across categories as these relate to environmental inputs. Examples of this are surface area exposed to rainfall, and/or wicking of moisture by wind. The wall is therefore designed in a way that places sample blocks from each size? category in each of the three exposure categories available: exposed on three sides (top and sides of the wall), exposed on two sides (within the mass of the structure but excluding outer courses), and in contact with ground (see Table 6.3 and Figure 6.1).

Figure 5.2 Images of wall under construction in July 2019, facing East ©Author

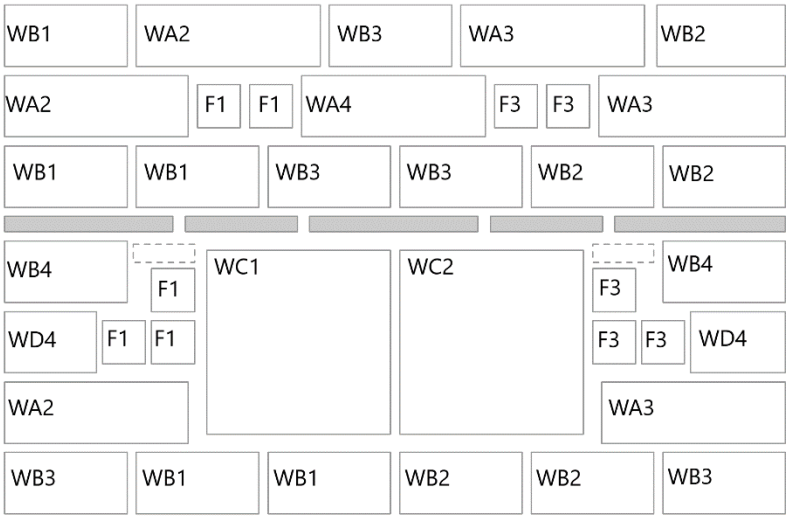

Figure 5.3 Placement of blocks with categories, see Table 6.1 for key to categories and treatment

Table 5.1 Guide to structural components of test wall

Category prefix	Category suffix	Treatment, sample size	Dimensions (mm)
"WA"	**2**	Artificially weathered, treated with TEOS by brush (three blocks)	300x100x150
	3	Artificially weathered, no consolidant (three blocks)	
	4	Controls, no weathering, no consolidant (one block)	

"WB"	**1**	Artificially weathered, treated with TEOS by capillarity (five blocks)	200x100x150
	2	Artificially weathered, treated with TEOS by brush (five blocks)	
	3	Artificially weathered, no consolidant (five blocks)	
	4	Controls, no weathering, no consolidant (two blocks)	
"WC"	**1**	Not artificially weathered, treated with TEOS by capillarity (one block)	300x300x150
	2	Not artificially weathered, treated with TEOS by brush (one block)	
"WD"	**N/A**	Controls, no weathering, no consolidant (two blocks)	150x100x150
"Control"	**N/A**	Samples of "WD" category plus all "4" suffixes (five blocks)	As above
"F"	**1**	Artificially weathered and TEOS treated by capillarity (five samples)	70x70x70
	3	Artificially weathered and not consolidated (five samples)	

5.3 Methods

5.3.1 Preparation of Sandstone for the Structure

As per the methodology for trials in this project, a single source batch of Locharbriggs stone has been used for this experiment. Different preparatory steps were taken to vary the characteristics of stone within the structure. As with the rack trial (Chapter four), these are:

i. heat weathered in the laboratory (See chapter 3 for heat weathering process),

ii. heat weathered and treated with TEOS consolidant by capillary absorption (in lab conditions),

iii. heat weathered and treated with TEOS consolidant by brush application (in lab conditions)

iv. stone in natural condition (no treatment or consolidant application).

To further differentiate the stone samples within the wall structure, there is a variation in block size both within and across treatment groups. This allows for comparative studies between areas of the wall, whereby mass of individual pieces can be quantified as a potential influence on consolidant performance and behaviour in response to environmental conditions.

5.3.2 Construction of the Test Wall

Stone for the wall came directly from the Locharbriggs Quarry in Dumfries, Scotland, and was delivered as a single batch cut on request from one large piece of quarried material. Locharbriggs stone is extracted from a variety of beds within the site, and materials of mixed origin within this site are characterised by inherent differences in the appearance and performance of the material. By cutting all samples from one parent block, the risk of unintended variability is therefore limited.

Upon delivery to Oxford Geolabs, the stone was then cut into the four different sizes used in the trial (see table 5.1). Additionally, ten 70 mm^3 samples cubes (the "F" group) were included in this structure as part of the Test Rack Trial as discussed in Chapter four (see Figure 5.1), and tested using the Pulse Wave Velocity technique. In addition to the sample stones, there are five thin 'string course' pieces of sandstone which act as a binding element near the centre of the structure. These are not part of the main test wall experiment but are included as a structural stabiliser to break up a large vertical joint line in the centre of the structure; and to prevent moisture vectoring down the central vertical mortar joint to the centre of the structure.

5.3.3 The Use of Non-Destructive Techniques for the Assessment of Variable Treatment Application and Performance on Sandstone

This experiment makes use of non-destructive methods, which provide a means to interpret conditions without damage or loss. Although the use of non-destructive testing has many

advantages over sample removal, the processes are not without drawbacks, one of which is the inherent relativity within the datasets: they do not always relate to absolute measurements without some form of transformation or processing.

Within this trial the main assessment is carried out using the MOIST 350B microwave moisture meter fitted with a DM sensor head with maximum depth penetration of ~100 mm (as described in chapter 3). This instrument generates a small (~1 mW) microwave pulse which passes through a coil in the sensor head. This pulse is attenuated in direct proportion to the quantity of water present within the measurement field, and the extent of this attenuation is used to calculate the quantity of water within the mass of the stone within a three-dimensional field, the size of which is dependent on the sensor head (Orr *et al* 2019, hf Sensor ND).

5.3.4 Calibration Using Gravimetric Testing

Non-destructive testing utilises proxy measurements to express real-world conditions, so the reading and interpretation of this data carries a risk of sampling error (Orr 2019, Raj *et al* 2002). In order to mitigate for this risk, a gravimetric calibration procedure was used for microwave moisture data collected in this trial. Using mean values from three sample group tests (see Section 3.6.3.1, p75), values generated from these tests were potted against an arbitrary colour plot (Figure 5.4, below)- the CIE L*C*h* (“Lightness, Colour, hue”) default colour palette was chosen due to the simplicity of each component element and its ability to ‘accurately represent underlying data’ (Simmon, 2013). The use of this allows for at-a-glance assessment of the conditions within the test wall in a standardised colour plot, following the charting of these values onto a pre-defined base model (see for example Figure 5.8). On this scale, dry mass (no moisture) relates to a value between 0.5 and 1.0 on the moisture meter, which has a beige to low blue value in the colour scale, and samples fully saturated with water register a maximum of 9.5 equating to a deep blue hue.

*Figure 5.4 L*C*h* Colour Scale as applied to Test Wall visualisations*

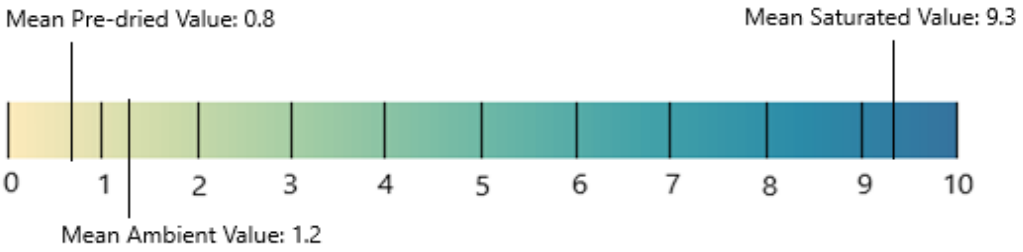

The visualisation of the wall and its component pieces, together with their moisture meter percentages is plotted onto a 'base model' created using the open source "R" software package (see figure 5.6) which allows for the easy representation of on-site data into static or animated models. The utilisation of the "R" suite also facilitates straightforward and rapid sharing between users; a small number of lines of code can be copied alongside a .csv file with field data in, and researchers can see on site conditions in a matter of minutes.

5.3.5 Data Collection Methodology

Data collection for this field trial followed the protocol set out by the instrument manufacturer *HF Sensor Gmbh*. The instrument is pre-loaded with material-specific settings, including those for sandstone. These are based on a known average material density, in this case 1.92 kg/dm³ (hf Sensor n.d). The Locharbriggs sample stone used throughout this trial was tested in the laboratory prior construction of wall, with samples ranging from 1.89-2.05 kg/dm³, with a mean of 1.99 kg/dm³ (calculated by dividing dry mass of each sample by its volume), in line with the parameters for sandstone pre-set on the instrument.

The instrument collects data in triplicate, displaying a value either in a relative scale (the "Moisture Index"), or as used in this experiment, a moisture percentage value. To ensure the sensor recorded a settled value for each position, these triplicate readings were then recorded again in triplicate (totalling 9 readings for each position), and the mean of these nine recorded for analysis. For the trial, the instrument was fitted with the DM sensor head, which has a stated penetrative depth of approximately 100 mm. However, the precise geometry of the field varies with penetration and values are more skewed towards the surface in contact with the sensor head (Göller 2006, Orr 2019). As this does not penetrate the full depth of the wall, the shortfall reduces the risk of atmospheric influence within the data, as per the manufacturer's guidance (hf Sensor n.d.; 27). For the "F" samples, the RM1 sensor head was fitted. The data is collected with the face of the sensor head placed flat against the face of the stone (see figure 5.5) in the absence of surface water or debris, which is brushed away if present. Once contact is settled, the monitor button is pressed three times to generate a mean percentage sum.

Figure 5.5 MOIST 350B DM Sensor head in contact with a sample stone

As not all of the sample stones are the same dimension, the number of reading points varies according to size. Referring to Figure 5.6, the readings are taken at 100 mm intervals horizontally across the structure and centred vertically on each stone to ensure that readings are taken from to the stone and not adjoining mortar. In the case of the WC stones, the readings are equidistantly spaced both horizontally and vertically, ensuring the readings to not overlap in any significant way.

5.4 Results

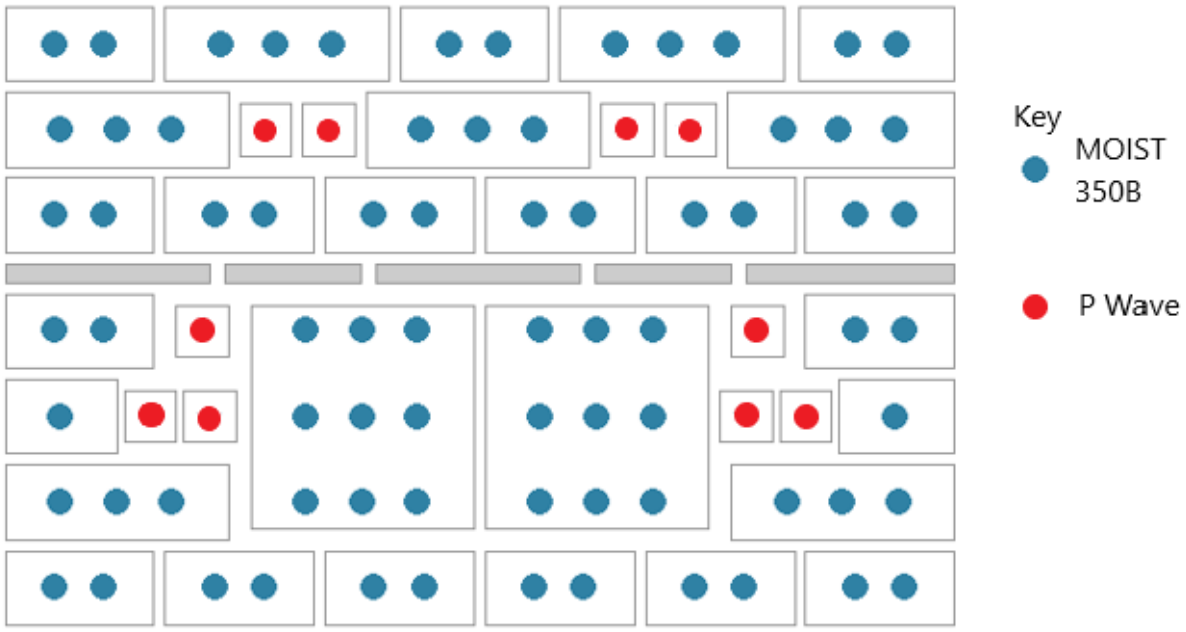

Figure 5.6 Approximate location of each MOIST 305B sampling point (in blue), showing number of readings per block size. Sensor was positioned to avoid overlap with other sampling points and mortar joints.

The following sections contain the results of the trial data separated by sample size, examining each size-based group in turn. Within these groups the samples are subject to cross comparison based on pre-treatment, to determine if treatment is the significant differentiating factor between them. Following this breakdown, the samples are then examined by cross-comparison of treatment across size categories. By grouping samples for application method, heat treatment, and lack of either, the samples are tested for the influence of variables such as block size and position in the structure, to determine if either of these are the key differentiating factor instead.

5.4.1 Overview of Field Data

Data presented in the following section is organised according to the research questions set out in section 5.2.1. Each subsection hereafter is organised by sample block size as per question 1, and

associated visualisations are reproduced within each subsection. Within this framework, questions 1-4 are addressed in turn; and cross-comparisons conducted thereafter. Each of the tests is then subject to a series of statistical tests for significance.

Key to Visualisations

Each of the wall visualisations in the following section denote percentage values as per the colour scale introduced in §5.3.4. Within the plots, the pre-treatment of each block is denoted by a differentiated border on the samples, as shown here in figure 5.7.

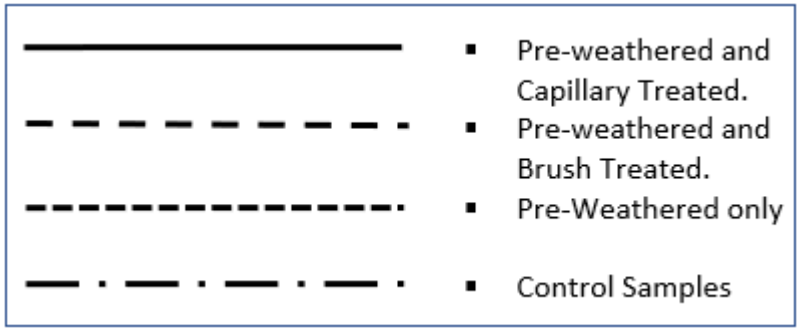

Figure 5.7 Key to block treatment as denoted by sample border within all wall visualisations

Figure 5.8 Whole-Wall Moisture visualisations by month, excluding "F" blocks

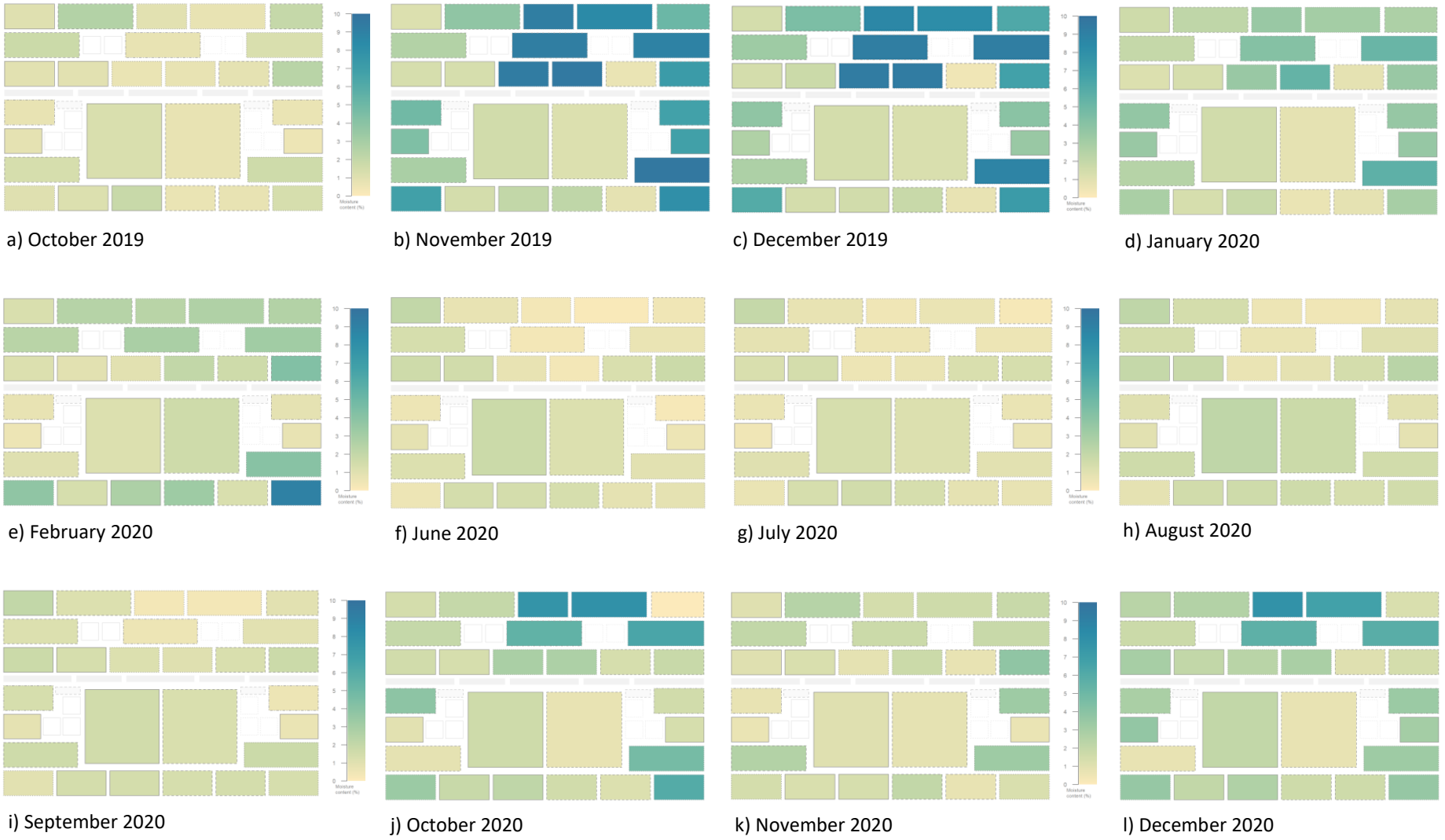

a) October 2019 b) November 2019 c) December 2019 d) January 2020

e) February 2020 f) June 2020 g) July 2020 h) August 2020

i) September 2020 j) October 2020 k) November 2020 l) December 2020

Initial comparisons between figure 5.8 and weather data summarised in table 5.2 suggest a link between rainfall and high readings in the upper part of the wall, though this association is not entirely linear using this metric alone. Figure 5.8 illustrates that December 2019, January 2020, and December 2020 have the highest moisture meter readings on the plot; especially looking at the upper and right side areas of the wall where weathered and untreated samples are situated. Conversely, the hottest and driest months, June to September 2020 (inclusive), coincide with the lowest readings across all treatment groups. Viewing the wall as a complete system in this way it is possible to pinpoint where consolidated stones are situated within the structure merely by looking at these renderings; a process that becomes easier in more variable weather conditions.

Table 5.2 Radcliffe Met Station (Oxford) data for dates of data collection

	Temperature °C			Rainfall (mm)				
Date	Max	Min	Mean	Previous 24hr	On day	Total	Sunshine (hours)	RH %
10/10/19	16.2	8	12.1	tr	3.7	3.7	3.5	74.7
13/11/19	7.9	3.6	5.8	0.2	23.9	24.1	1.5	73.9
19/12/19	12.3	3.5	7.9	5.7	12.2	17.9	0.6	91.2
3/1/20	8.7	6.5	7.6	7.2	0.1	7.3	4	78.2
5/2/20	9.4	2.2	5.8	0	0	0	4	96.7
2/6/20	25.5	10	17.8	0	tr	0	14.2	43.7
14/7/20	20	14.6	17.3	1.9	tr	1.9	0.7	77.9
10/8/20	33.1	15.4	24.3	0	0	0	8.5	73.9
15/9/20	27	12.7	19.9	0	0	0	5.8	71.3
23/10/20	14.6	10.4	12.5	1.3	tr	1.3	2.4	89.4
26/11/20	6.6	-0.5	3.1	0.2	0.2	0.4	3.1	100
3/12/20	6.5	3.7	5.1	4.2	6	10.2	0	95.2

*%RH is collected at time of sampling. Temperature is recorded repeatedly, and values calculated across 24-hour period centred on sampling time. Rainfall Total is total recorded in 48hrs up to time of each data sampling

For measurements where rainfall exceeding a trace (>0 mm) has been recorded in the 48 hours preceding the data capture (figure 5.7; plots a, b, c, d, & j), there is a tendency toward higher readings where weathered and untreated stone are located (seen as darker blue hues). Differentiation between brush and capillary treatment is less readily detected in these plots, as is the

different size of block across treatment types. For these differences, a more detailed appraisal of the readings themselves is required, and this is carried out in the following subsections.

These initial insights do in general terms demonstrate the usefulness of the plots and the collection methodology. For a more detailed analysis however, it is necessary to examine the responses of individual treatment groups to the environmental variation. In the following pages each of these groups are examined with a view to assessing the effectiveness of the method for analysing consolidant performance *in situ*.

5.4.2 Assessment by Dimension: WA Samples

WA Blocks are 300 mm in horizontal length, 100 mm high, and have a wall depth of 150 mm. There are seven WA blocks in the structure, separated into three sub-groups: Weathered and TEOS treated by brush, Weathered Only, and Unweathered- Untreated (figure 5.8).

Figure 5.9 Key to WA block placement

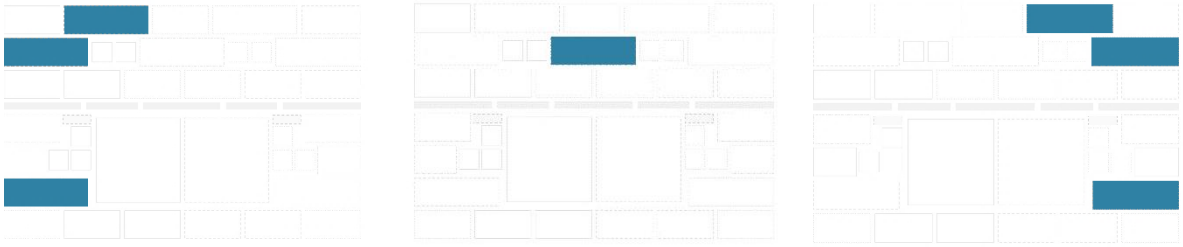

a) WA2, Pre-weathered and Brush Treated with TEOS Consolidant

b) WA4, Unweathered and untreated 'control' block

c) WA3, Pre-weathered and not treated with consolidant

Figure 5.9 shows the placement of the WA sample blocks in the structure. To the left (plot a) are the "WA2" blocks: pre-weathered in the laboratory and brush treated. These are mirrored by those on the right of the wall (plot c) which are the pre-weathered and unconsolidated blocks. Centrally (plot b) is the single untreated control block of this size. Referring to Figure 5.10 below, it is clear by the colour rendering of moisture values that brush treated consolidated blocks present consistently lower values across the whole 12 months of the experiment, reflecting changes in weather but

fluctuating between narrower upper and lower limits. These trends are summarised in table 5.3, where the difference in values between the groups is clear.

In addition to the consolidant-influenced performance variability, figure 5.10 shows seasonal variation linked to general trends in local climate. The three summer months (June-July-August) correlate visually with the driest overall conditions, including highest temperatures, joint lowest relative humidity, and lowest overall rainfall per month (refer to Table 5.2 for summary). Conversely two of the darkest coloured plots (November and December 2019) correlate with highest recorded rainfall preceding the collection of data (November 2019 recorded the highest rainfall at point of data collection, and cumulatively saw 42.9mm of rain in the seven days prior to reading).

Furthermore, the Weathered Only group (WA3) and Unweathered- Untreated sample (WA4) both respond to rainfall fluctuations in extremely similar ways. Consequently, using this metric alone it is not possible to detect any significant difference caused by the heat weathering of the samples in this group.

Table 5.3 Values for WA sample set across duration of experiment

	Maximum	Minimum	Mean	Median	Variance
WA2	4.5	0.5	1.7	1.6	0.6
WA3	9.6	0.1	3.4	2.7	8.4
WA4	9.2	0.3	3.1	1.8	9.4

Of the other available climate data, relative humidity has no discernible direct influence on the WA stone samples, in the absence of other inputs such as rainfall. A good example of this is November 2020, where at the time of data collection relative humidity was 100%, but in the absence of rainfall the moisture meter records lower values than in either adjoining month where there had been rain preceding the data collection. In the other months with high non-rainfall related relative humidity (February and December 2020), the WA3 samples did register a higher percentage value than the WA2, although not in a uniform manner. If it worth noting that they were all higher than the WA4 control sample in these instances, however.

Figure 5.10 Size-delineated Groupings, No.1. WA Blocks

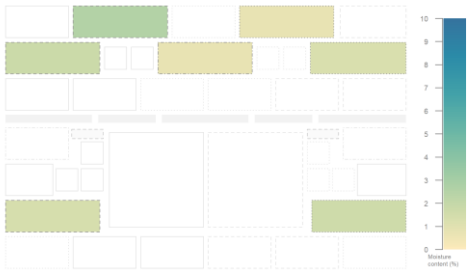

a) October 2019

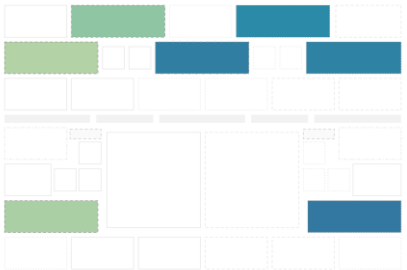

b) November 2019

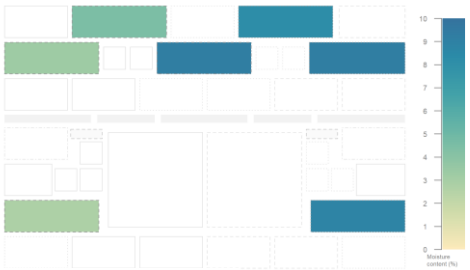

c) December 2019

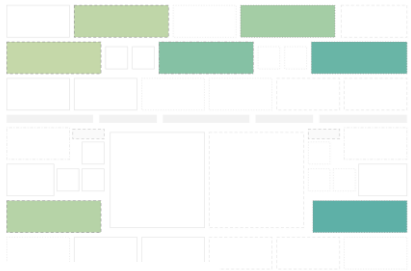

d) January 2020

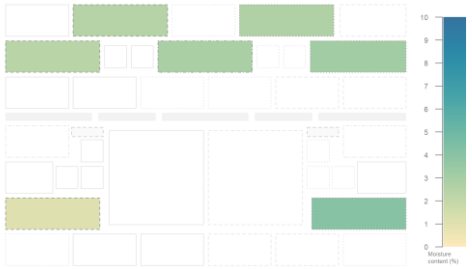

e) February 2020

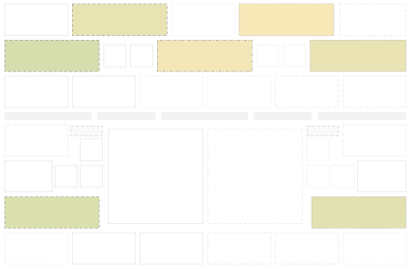

f) June 2020

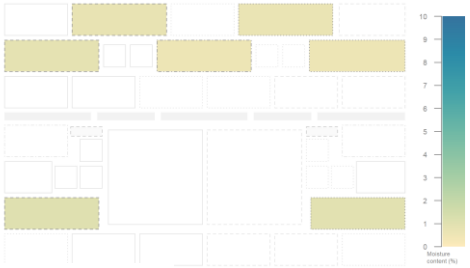

g) July 2020

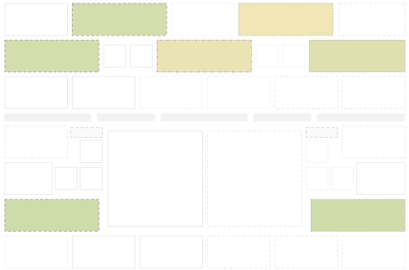

h) August 2020

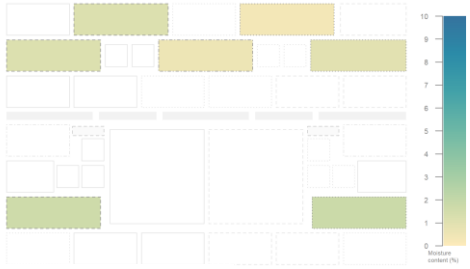

i) September 2020

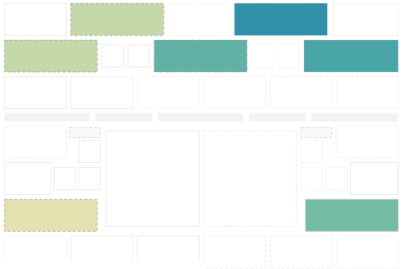

j) October 2020

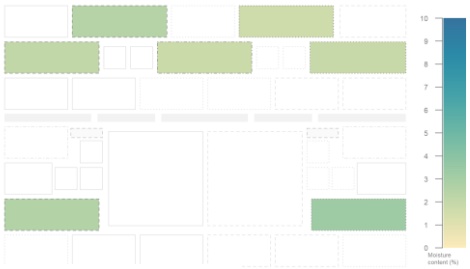

k) November 2020

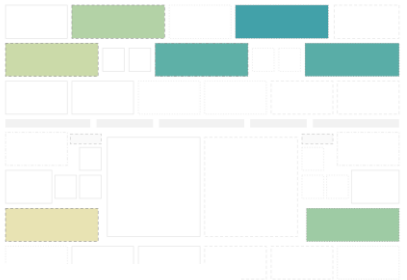

l) December 2020

Statistical Analysis: WA Category

Sample stone in the WA category was assessed using a combination of Single Factor ANOVA and Two Sample T Tests where required. Firstly, the three subsets of this size category- WA2, WA3, and WA4, were subject to an individual month-on-month ANOVA. Results from this set of analyses were universal in rejecting the null hypothesis (see Table 5.4), meaning that across all three groups there were significant variations in readings as collected via microwave moisture meter across the field trial.

Table 5.4 Single Factor ANOVA, WA subsets month-on-month, using an α value of 0.01

	F Stat	F Crit	P Value
WA2	11.93	2.43	0.000
WA3	103.92	2.43	0.000
WA4	77.35	3.09	0.000

Following this, a two sample T Test was carried out for each set of the WA samples, this time comparing the results across the three categories for each month of the trial. This approach is necessary due to the unequal numbers of samples across the three groups.

Table. 5.5 P Value of Two Sample T Test on WA subset groups 2, 3, and 4. α value set to 0.01

October 2019	Brush vs Weathered	0.069	**July 2020**	Brush vs Weathered	0.133
	Brush vs Control	0.001		Brush vs Control	0.023
	Weathered vs Control	0.009		Weathered vs Control	0.099
November 2019	Brush vs Weathered	0.000	**August 2020**	Brush vs Weathered	0.010
	Brush vs Control	0.000		Brush vs Control	0.000
	Weathered vs Control	0.056		Weathered vs Control	0.111
December 2019	Brush vs Weathered	0.000	**September 2020**	Brush vs Weathered	0.311
	Brush vs Control	0.000		Brush vs Control	0.000
	Weathered vs Control	0.308		Weathered vs Control	0.038
January 2020	Brush vs Weathered	0.000	**October 2020**	Brush vs Weathered	0.000
	Brush vs Control	0.008		Brush vs Control	0.000
	Weathered vs Control	0.371		Weathered vs Control	0.206
February 2020	Brush vs Weathered	0.002	**November 2020**	Brush vs Weathered	1
	Brush vs Control	0.128		Brush vs Control	0.146
	Weathered vs Control	0.215		Weathered vs Control	0.249
June 2020	Brush vs Weathered	0.007	**December 2020**	Brush vs Weathered	0.000
	Brush vs Control	0.000		Brush vs Control	0.381
	Weathered vs Control	0.195		Weathered vs Control	0.207

Looking first at the comparison between Brush Treated and Weathered Only samples, eight of the twelve pairings passed the statistical threshold for significant differences. Of these, five relate to

'wet months' (where rainfall > trace fell on the wall in the 48 hours preceding sampling). Of the three relating to dry sampling conditions, the spread of relative humidity values is 43.7%, 73.9%, and 96.7%. Four of the pairings failed to pass the threshold, meaning there is no statistically significant difference across the data groups. These four also include a spread of values in both weather metrics, with rainfall ranging from zero to 3.7 mm, and relative humidity from 71.3 to 100%.

Moving on to the Brush Treated and Control sample comparison, again eight of the twelve pairings passed the threshold for significant difference. Of these, six correlated with the Brush Treated and Weathered Only comparisons (November and December 2019, January, June, August, and October 2020). Again, there is no striking trend in either those which pass or fail the test, with a mix of wet and dry conditions, and relative humidity values ranging from 43.7 to 100%.

Finally, with the Weathered Only and Control comparison, the significant finding is that eleven of the twelve pairs failed to pass the threshold for significance. The only month where this is not the case is October 2019, a wet month with 3.7 mm of rain and 74.7% relative humidity, not exceptional in either metric.

5.4.3 Assessment by Dimension: WB Category

WB Blocks are 200 mm in horizontal length, 100 mm high, and have a wall depth of 150 mm. They are the most numerous of the block categories in the structure, with seventeen individual samples. Being the most numerous sample group, the WB samples are subdivided into four groups (see Figure 5.10). "WB1" samples (plot a) are heat-weathered and consolidated by capillarity, "WB2" are heat-weathered and consolidated by brush (plot b), "WB3" are heat-weathered only (plot c), and "WB4" (plot d) are untreated control blocks. Each block yields two readings per sampling (one per each 100 mm of horizontal length).

Figure 5.11 Key to WB block placement

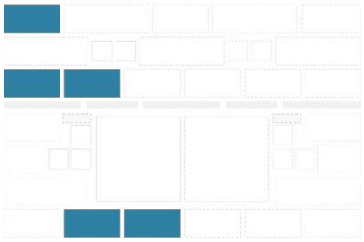

a) WB1, Weathered and Capillary Treated

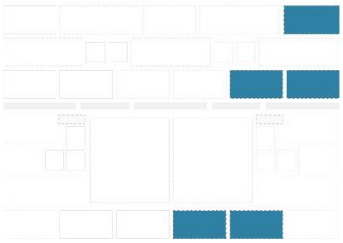

b) WB2, Weathered and Brush Treated (above)

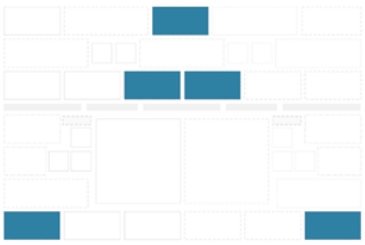

c) WB3, Weathered and untreated

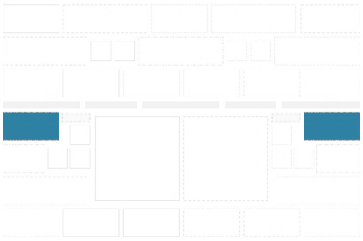

d) WB4, Control samples

Referring to figure 5.12 and looking first at the weathered and consolidated blocks (WB1 and WB2), there is a similar but not identical response to environmental fluctuation between the two application methods. The differences are not statistically significant however (see below) and may be a result of inherent variability within the stone. The WB1 group, artificially weathered and treated by capillarity, perform closest to the natural stone, though often register lower percentage values than the natural stone. This is a useful trend, as it presents an opportunity to differentiate between consolidated and natural stone as a baseline for assessing microwave moisture as a technique.

Figure 5.12 Size-delineated Groupings, No.2. WB Blocks

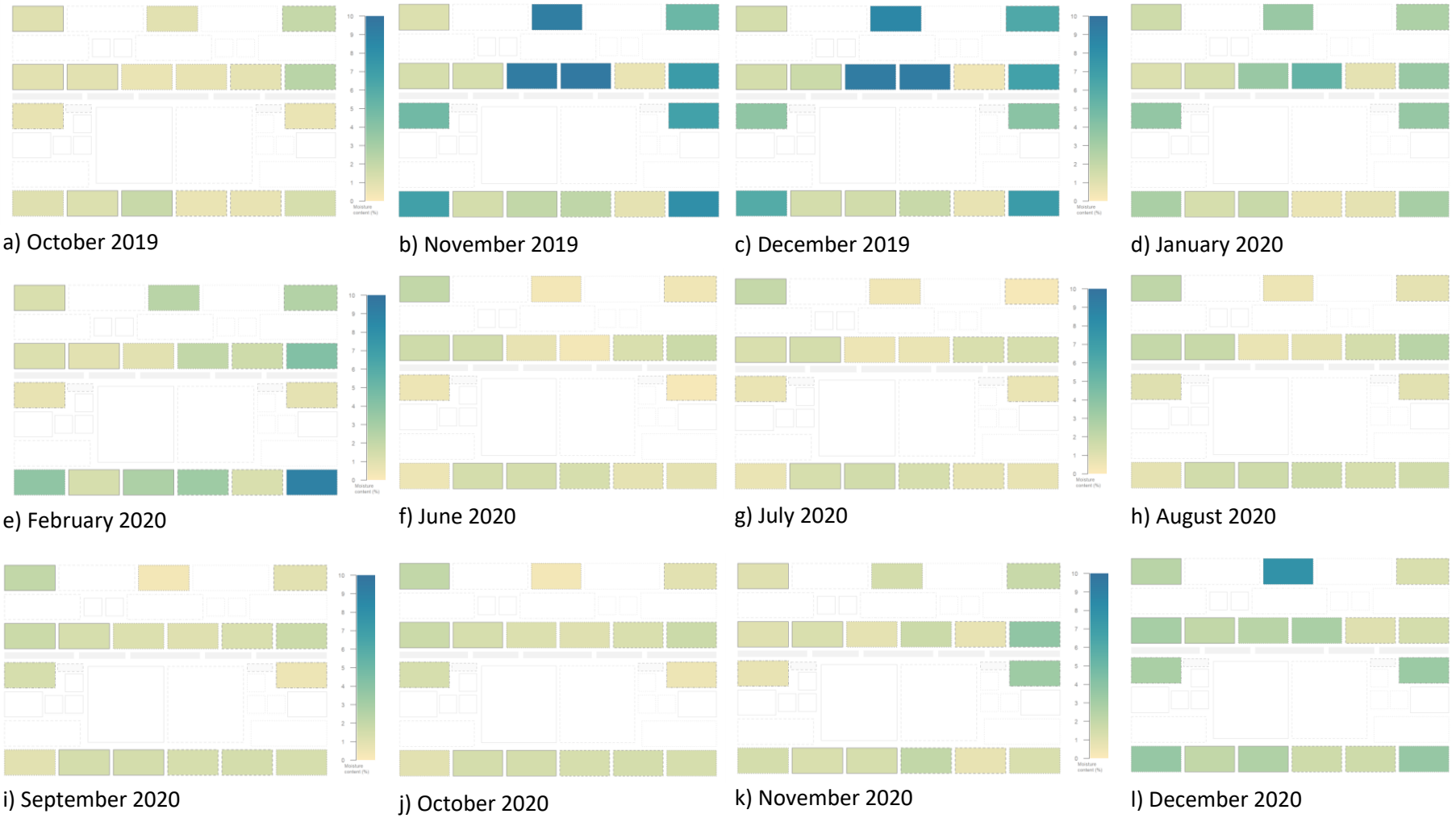

a) October 2019 b) November 2019 c) December 2019 d) January 2020

e) February 2020 f) June 2020 g) July 2020 h) August 2020

i) September 2020 j) October 2020 k) November 2020 l) December 2020

Of equal importance here is the difference between the consolidated samples of WB1/2 and the Weathered Only group (WB3). Looking at the plots for this latter group (figure 5.12, see figure 5.11 for key), it is apparent from the behaviour of the WB3 samples which months coincide with incidences of high rainfall (November and December 2019), wherein each plot shows a marked

Table 5.6 Values for WB sample sets across duration of experiment

	Maximum	Minimum	Mean	Median	Variance
WB1	3	0.7	1.5	1.4	0.2
WB2	7.2	0.1	1.7	1.4	1.9
WB3	9.5	0.2	3	1.6	8.4
WB4	6.7	0.2	2.1	1.2	2.9

increase in the values plotted (depth of blue hue), especially in the upper courses of stonework. In addition to the high rainfall response in the WA3 samples, the four driest months (June- September 2020 inclusive) are plotted as expected in the region of low ambient values, a pale khaki on the colour scale (corresponding to around 1.2-1.6 on the MOIST 350 percentage scale). For the three months with the highest non-rainfall related relative humidity (February, November, and December 2020), the Weathered Only (WA3) and some of the Weathered and Brush Treated (WA2) samples, notably those on the northern end of the structure (right side of each plot) registered higher values than Weathered and Capillarity Treated, and Control samples.

Statistical Analysis, WB Category

Assessing each category individually first, month-on-month comparison using single factor ANOVA, each of the four subsets showed significant changes across the twelve months of the trial. This demonstrates that regardless of pre-treatment and consolidant application, the microwave moisture meter can detect changes associated with fluctuations in weather conditions (see table 5.7). Following this, a Single Factor ANOVA was then applied to each month, comparing the results of WB1, WB2, and WB3 subsets against each other. In nine of the twelve monthly datasets there was a statistically significant difference between the three groups (see table 5.7).

Table 5.7 Single Factor ANOVA, WB subsets month-on-month, using an α value set to 0.01

	F Stat	F Crit	P Value
WB1	8.58	2.41	0.000
WB2	3.05	2.41	0.001
WB3	45.68	2.41	0.000
WB4	24.31	2.78	0.000

This set of tests show that the MOIST350B detected significant differences in the condition of variably treated stone across a range of weather conditions, with the exception of October 2019, and February and November 2020, during which months no significant differences were observed. Further inspection of these groups using individual two sample T-Tests show that in October 2019 none of the WB subsets showed any significant differences between categories one, two, and three. When tested against the control group (WB4) only the TEOS treated-by-capillarity samples (WB1) registered a significant difference. Furthermore, the same combination of T tests were carried out on the data from February 2020; in this case, no significance was found. This month coincided with dry weather and high sunshine for the season, although the relative humidity was one of the higher readings for the trial at 96.7%. Finally, for November 2020 no significant difference was detected between the three treatment subsets. Furthermore, the tests carried out against WB4 control samples showed that there was no significant difference across any of the pairings. On this occasion there was again low rainfall but high relative humidity, suggesting that absence of rainfall may be the defining factor across the sample subsets.

Table 5.8 P Values of Multi Factor ANOVA analysis, based on an α value of 0.01

Month	Variable	P Values	Month	Variable	P Values
October 2019	Block Size	0.050	**July 2020**	Block Size	0.558
	Treatment	0.013		Treatment	0.002
November 2019	Block Size	0.778	**August 2020**	Block Size	0.673
	Treatment	0.000		Treatment	0.000
December 2019	Block Size	0.984	**September 2020**	Block Size	0.965
	Treatment	0.000		Treatment	0.019
January 2020	Block Size	0.151	**October 2020**	Block Size	0.041
	Treatment	0.000		Treatment	0.000

February 2020	Block Size	0.619	**November 2020**	Block Size	0.065
	Treatment	0.047		Treatment	0.337
June 2020	Block Size	1	**December 2020**	Block Size	0.281
	Treatment	0.000		Treatment	0.000

5.4.4 Assessment by Dimension: WC Samples

WC Blocks are 300 mm in horizontal length, 300 mm high, and have a wall depth of 150 mm. As these are the largest stone samples in the structure, they each contain the highest number of readings per stone (9 in each).

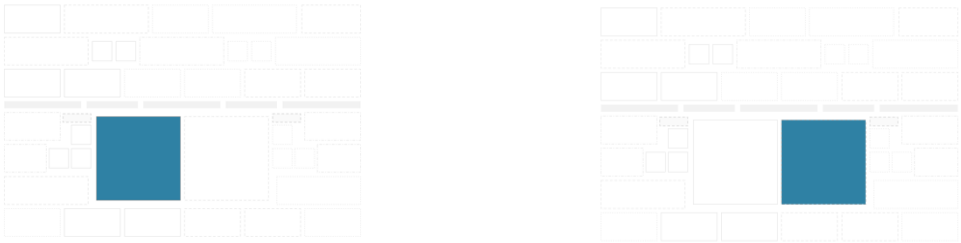

a) WC1 not weathered, and capillarity treated

b) WC2 not weathered, and brush treated

Figure 5.13 Key to WC block placement

As stated in the methods section above, the WC samples have not been artificially weathered by heat owing to their size. They have both been treated with TEOS consolidant: WC1 block by capillarity, WC2 by brush.

Of note in looking at this category is that it is the only one of the four sample sets that does not have any samples that are exposed directly to weather on three sides, placed centrally in the lower portion of the structure. These are also the samples with the largest mass, by a multiple of 2.6 against the WA samples- the next largest size group.

Table 5.9 Values for WC Samples across duration of trial

	Maximum	Minimum	Mean	Median	Variance
WC1	2.2	0.6	1.24	1.2	0.10
WC2	1.8	0.1	0.73	0.7	0.14

The visual difference in the plots for WC samples (Figure 5.14) in contrast to the WB samples (Figure 5.12) is stark. Caution must be taken when making a direct comparison however, as there are no 'Weathered Only' samples in the WC category, and the treated samples are not weathered before treatment due to their size.

As a result, comparison can only be sought between the condition of an individual sample over time at this scale, and secondly comparison of the two WC samples against each other to test any significant differences resulting from their application method. Finally, a comparison between the two treated samples and their treatment counterparts in the other categories will be made, but one that is caveated by several limiting factors including the lack of pre-treatment by heat, and the small number of samples in this category.

Figure 5.14 Size-delineated Groupings, No.3. WC Blocks

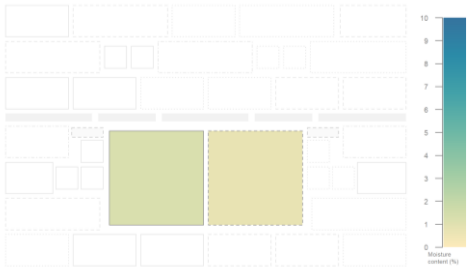

a) October 2019

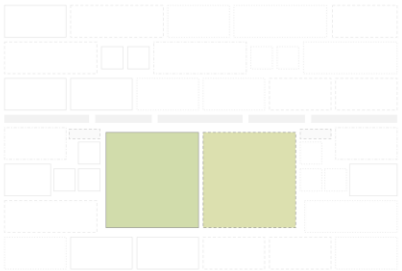

b) November 2019

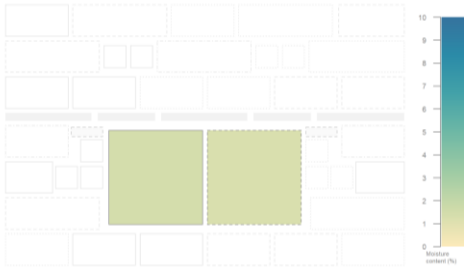

c) December 2019

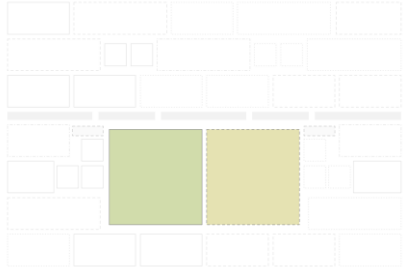

d) January 2020

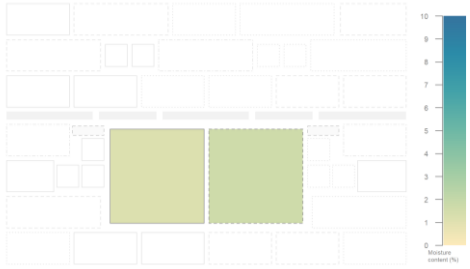

e) February 2020

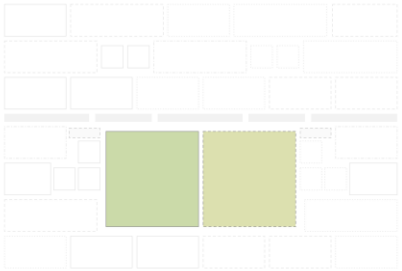

f) June 2020

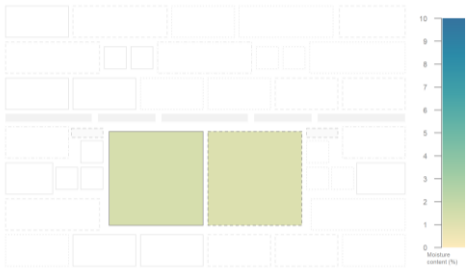

g) July 2020

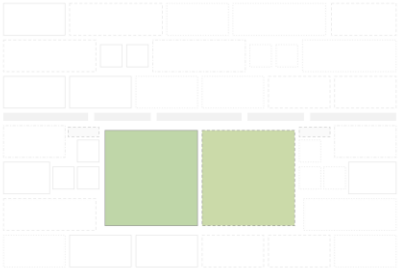

h) August 2020

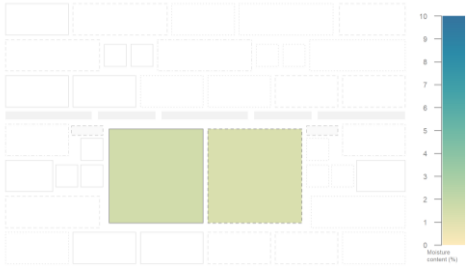

i) September 2020

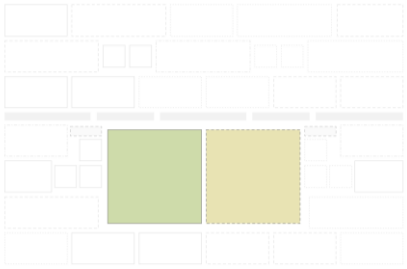

j) October 2020

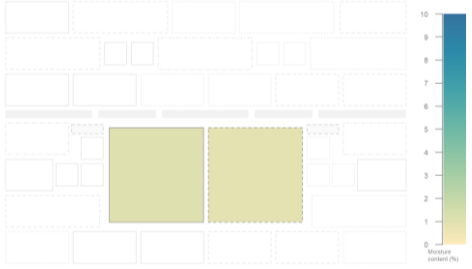

k) November 2020

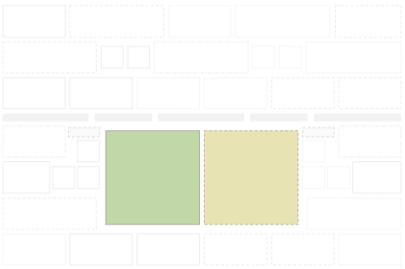

l) December 2020

Statistical Analysis for WC Blocks

Table 5.10 Single Factor ANOVA, WC subsets month-on-month, using an α value of 0.01

	F Stat	F Crit	P Value
WC1	16.637	2.438	0.000
WC2	6.464	2.438	0.000

Initially, assessment was made of each sample individually over time. Both WC1 and WC2 samples registered significant differences across the months of the trial, when their own performance was compared on a month-by-month basis. Each sample (which in this instance represents a total of nine readings per sample, per data collection point) was significantly different when comparing data over the full year of the trial (table 5.10).

For comparison to be made between consolidant application methods at this scale, a number of targeted two sample T tests has been carried out using data collected in months where certain weather conditions are recorded in order to focus the analysis on both extreme and average conditions. These are:

i) months of highest and lowest percentage relative humidity (November and June 2020 respectively)

ii) months of the highest and lowest rainfall (November 2019 and June 2020)

iii) the month where both are closest to mean (January 2020)

November datasets from 2019 and 2020 both recorded equal variance whereas January and June 2020 were unequal.

Table 5.11 P Value results for T Tests comparing WC1 and WC2 MOIST 350B results

α= 0.01	Nov 19	Jan 20	Jun 20	Nov 20
P Value	0.000	0.000	0.001	0.000

T tests were run on all pairings, shown in table 5.11. In all cases, the differences were statistically significant. This means that differences in the performance of consolidated stone are significant but are not linked to specific weather fluctuations. In contrast to the smaller samples in the wall, the application method appears to have an influence on the performance of the stone. As noted above however, comparison to other stone groups must be viewed with caution as these larger samples were not artificially weathered pre-treatment.

5.4.5 Control Samples (NF)

The next group to look at independently were the control samples contained in the structure. These included one WA sample (300x100x150 mm), two WB samples (200x100x150 mm), and two WD category samples, which are 150 mm in horizontal length, 100 mm high, and have a wall depth of 150 mm. The purpose of these samples is to allow for detection of drift in values as detected in any of the other sample groups contained in the structure, and to assess how stone in its natural condition reacts to the temperate climate of the south of England (at the Wytham test site).

Figure 5.15 Key to control sample placement

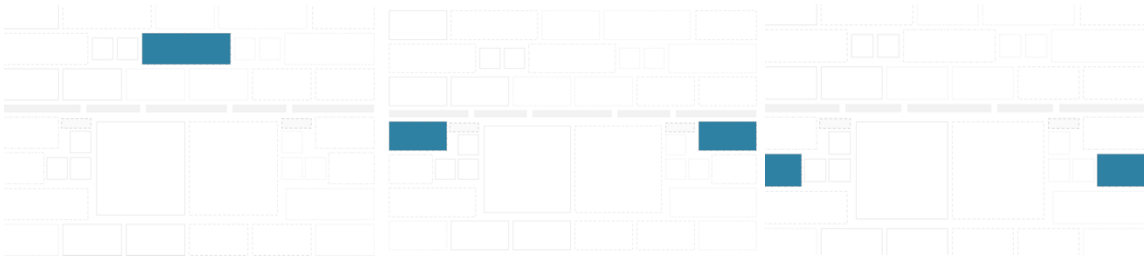

a) WA4 control sample b) WB4 control samples c) WD4 control samples

As with other groups in this trial, a combination of ANOVA and T Tests have been carried out to quantify the existence and extent of significant variability within the data. Firstly, the month-by-month analysis showed that the control samples were significantly affected by weather conditions across the full trial period.

Focusing on the extreme and average months, Table 5.12 shows that with the exception of the highest-lowest relative humidity pairings, all comparisons were significantly different

Table 5.12 T Test P Values for Control sample pairings

α=0.01	**Closest to mean (rainfall)**	**Closest to mean (%RH)**	**Highest/Lowest Rainfall**	**Highest/Lowest %RH**
P Value	0.000	0.000	0.000	0.011

These results are to be expected, the stone in its natural state will fluctuate in moisture levels in response to the weather they are exposed to. Further ANOVA failed to detect any significant variability across the different sizes in this category, meaning that mass or size of face exposed to direct rainfall is not the sole determinate of condition at this scale.

Figure 5.16 Size-delineated Groupings, No.3. Control Blocks

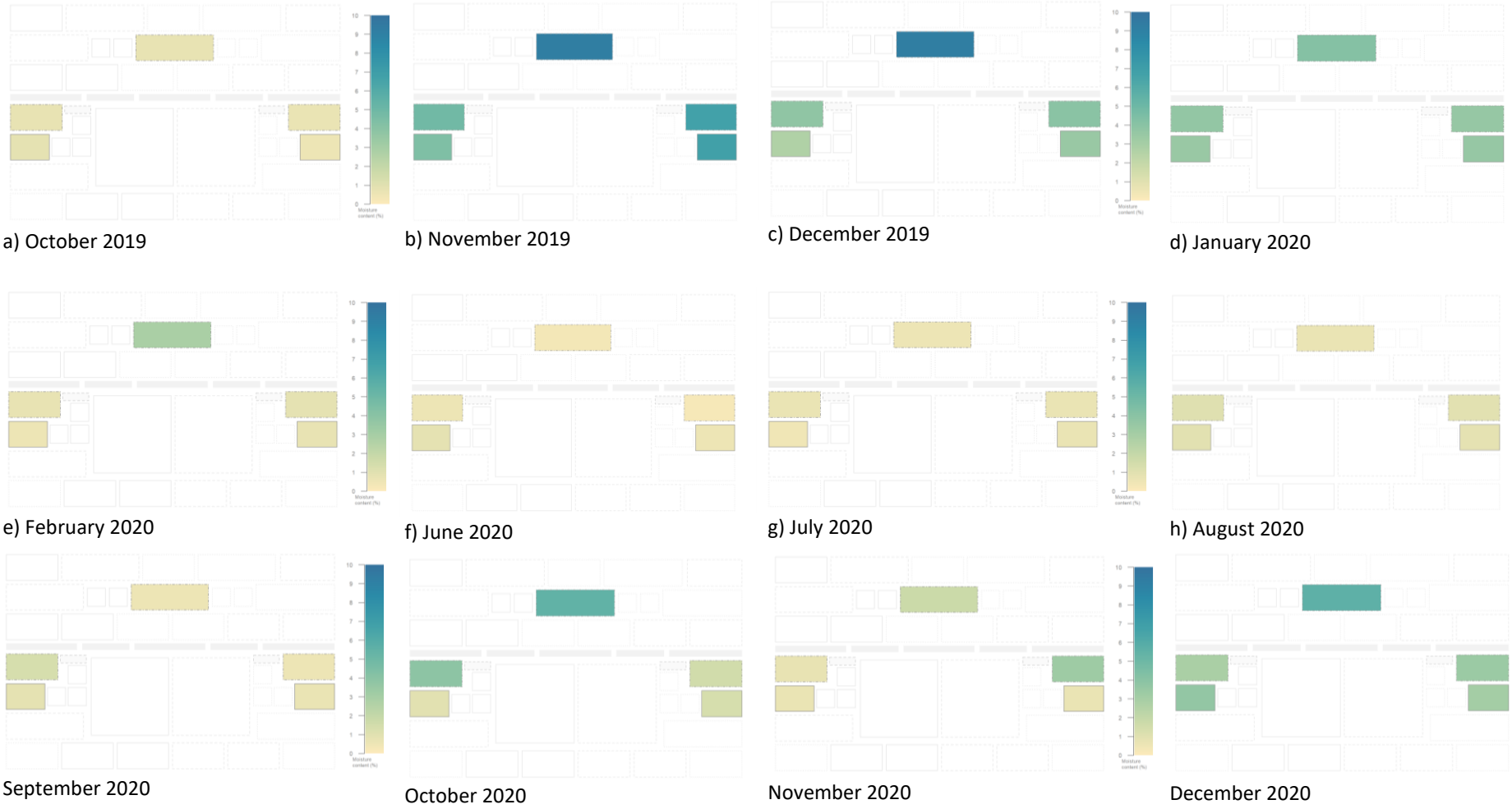

a) October 2019 b) November 2019 c) December 2019 d) January 2020

e) February 2020 f) June 2020 g) July 2020 h) August 2020

September 2020 October 2020 November 2020 December 2020

When looking at the colour plots there appears a difference between the behaviour of the WA control sample (located top, centre of wall) and those lower down in the wall. These are most obvious in December 2019 and 2020, and October 2020, during which periods the WA sample plotted a darker blue than the other control samples. Looking at the data, T tests run on the sample points from the WA control sample and those from the WB sample for the four months of significant weather variation as above (November 2019, and January, June and November 2020). No significant differences were measured in January, June, and November 2020, whereas the performance of the WA and WB samples was significantly different in November 2019 ($p = 0.009$)

Whilst sample numbers are low in this set of comparison, it does demonstrate that there are conditions in which the upper courses of the wall are influenced to a more extreme degree than the lower courses.

5.5 Discussion

There are a number of general trends that arise from the data in this experiment. The first observation to note is that in all categories where comparison is possible, both brush and capillary TEOS treated samples recorded lower percentage moisture? values across the complete range of weather conditions within the trial period, as one might expect from successfully consolidated stone. In the non-consolidated groups, the weathered only samples typically registered higher variability in response to weather conditions than both consolidated and natural stone, but not statistically significant different in the latter. Regarding the potential influence of consolidant application method only the WC blocks record statistically different values wherein brush and capillary absorption treated stones did behave in significantly different ways. In other groups there is no clear trend that could be used to differentiate the two methods, merely that both groups behave in markedly different ways to both the weathered only and natural stone sets.

With regards response to weather conditions rain falling within 48 hours of the data collection has more effect on the stone groups as a whole than fluctuations of relative humidity, the former more consistently associated with significant variability within the data. February 2020 represented an important example of this, wherein the relative humidity was one of the highest recorded, but an absence of rain meant that none of the samples tested registered a significant variation from paired months with lower humidity. There is also a threshold for rainfall under which changes in pore-bound moisture are either too brief (and therefore missed by sampling) or are not detected by the moisture meter, evidenced by the lack of universally significant result across samples and time.

For comparison between brush and capillary absorption of TEOS, the data does not demonstrate that the application method has a significant influence at smaller scale (WA and WB sizes) but that at larger scales (WC size) there are differences in the response to weather, especially rainfall. Caution must be taken when attributing these differences entirely to the mass of the samples however, as pre-treatment of samples differs between the WC blocks and the rest of the wall (these were not heat weathered due to their size). Furthermore, the relative position of the blocks must be taken into account, with WA and WB samples more exposed to direct rainfall in the outer areas of the wall, in contrast to the WC samples which were both set within the central mass of the structure. In order to satisfactorily address these caveats, it may be desirable to add samples analogous to the WC blocks to the outer area of the test wall and run further tests.

Turning to the Weathered Only samples, there was a mixed message within the results. In some instances there were significant differences to the other sample groups, but not uniformly in line with weather trends. These may point to the known variability within the Locharbriggs stone, or to nuances related to position within the structure. It may be possible to resolve any uncertainty here through further data collection linked directly to weather conditions (or by simulating conditions through application of water or low heat), rather than arbitrarily set on a monthly time lapse.

Natural (or quasi control) samples have provided a useful reference point for the other sample sets, both viewed in size-related groupings and as a condition set in their own right. As a sample set they effectively confirm the performance of TEOS treated stone by comparison, whilst demonstrating in a range of examples that the Weathered Only samples did not act in ways markedly different to natural stone in most- if not all- conditions. As a set, they effectively define the presence of consolidants in other sets through comparative testing, a definition that would only be possible using statistical analysis in their absence, and then only in certain conditions.

5.6 Conclusion

The results garnered from this trial have demonstrated that the Hf Sensor MOIST 350B moisture meter has the capability of detecting variability in the condition of stone in the field in a range of preconditions and climatic conditions. Using a gravimetric test to create a reference point for the values produced by the meter has added a degree of certainty to the recorded data and allowed for a level of interpretation not readily available from use of the meter alone.

By combining analysis of contemporaneous data sets each month with time series analysis of individual sample sets across the trial, it has been possible to track both performance of consolidants and reaction of stone (both natural and adapted) to environmental conditions. For these data, applied statistical tests allowed for the determination of significance between focused pairs of data (wet/dry; high/low %RH etc), and pairing the output of the MOIST350B with these tests produced easily replicable comparative values. Some imbalance in sample numbers made this analysis more complicated however, as different tests had to be run on sample groups with unequal replicates. Any extension to the trial could add sample sets to the wall to combat this in future, allowing for a unified statistical method to be applied. Despite these issues however, it has been demonstrated that the data collected by the MOIST350B can effectively detect not only the presence of consolidated stone where comparison to non-treated stone is possible but to assess its performance in a range of climatic conditions.

By definition, a DPhil experiment such as this is time constrained in such a way that natural breakdown of consolidants cannot be assessed in response to extended field conditions. Whilst an extended field trial would allow for the detection and analysis of end-of-use consolidant breakdown when it occurs, the data collected here has demonstrated that the concept of building model scale structures for short term (1-2 year) assessment has value. By extension, the design of the test wall trial as well as the pre-treatment steps used here have been proved sound. Throughout the duration of the trial, a range of valuable information on the performance of consolidants in the field have been collected, and it has been possible to determine the performance of stone simultaneously in a range of variables. Finally, the use of this test wall is not limited to this experiment. It remains extant on site at Wytham Woods and has been built in such a way that it can be utilised again either in its current form, or as the base for an extended test platform.

Chapter Six: The Pedatron Erosion Trial

6. Introduction

6.1 Aims and Objectives.

This experiment has two main objectives. The first is to improve understanding of how sandstone erosion develops in areas of high pedestrian footfall, with a view to informing conservation practice in a variety of heritage situations. The second objective of the experiment is to evaluate the capability of consolidant treatments to mitigate for pedestrian-derived erosion, by comparing changes between consolidated and unconsolidated surfaces within a sample floor surface.

In order to achieve these objectives, an experiment has been designed which employs a mechanical 'walking foot' (the SATRA Technologies 'Pedatron') to accelerate erosion on a composite floor surface of sandstone samples. Data was collected using a hand-held 3D laser scanner (the 'Creaform Handyscan'), which generated digital point clouds containing measurements in three dimensions allowing for change to be measured as the experiment progressed. In addition to this, surface roughness data has been collected using an INNOWEP TRACE-iT optical sensor to compliment the laser scans and allow for evaluation of data and collection methodologies. This experiment used a combination of laboratory-based and portable equipment to model on-site erosion on heritage sandstone, using Kenilworth Castle as a case study to provide context for the application of its findings.

6.1.1 Links to DPhil Project Framework

The experiment addresses objectives 3 and 4 of the DPhil research framework:

Objective 3. To investigate the use of simulated wear experiments for the assessment of consolidant performance on sandstone

Objective 4. To produce a 'Toolkit' of methods for the evaluation of consolidant performance on sandstone, arising from Objectives 1,2, and 3

6.1.2 Overview of Experimental Design

This experiment comprises a 'wear platform' designed and constructed to mimic a section of sandstone flooring, artificially eroded in tests which employed a mechanised prosthetic foot designed to test safety footwear. The test ran in two parts, each 100,000 steps in duration; and was facilitated in part by SATRA Technologies Ltd in Kettering, UK. The 'wear platform' was constructed by the author at the University of Oxford Geolabs facility, following field observations at Kenilworth Castle. The first 100,000 step test took place in December 2019 at the SATRA facility, followed by scanning, data processing, and preparations for a second 100,000-step test which took place in July 2020. The experiment used a combination of optical and laser time-of-flight sensors to map changing characteristics on the stone surface of the wear platform.

6.2. Methodology

6.2.1 Selection and Preparation of Stone for the Pedatron Experiment

As with other elements of this project, Locharbriggs Sandstone was used for this experiment. The preparation of this stone differs slightly from that for chapters five and six however, as the stone was pre-cut by the suppliers into a 'paving slab' of 350 mm² with a thickness of 40 mm roughly parallel with the bedding planes in the stone. As a result, this stone was not subject to the same batch control as the source material for the other trials in this project.

In preparation for this experiment the manufacturer-cut slab was further sub-divided into four equal 'tiles' by the author, each measuring 170 mm² (5mm was lost on each cut for saw blade width) using a water-cooled Norton Clipper CM 501 Rock Saw.

Following cutting, all four of the samples were subject to the heat weathering treatment developed for this project (refer to Chapter three for heat weathering methodology). This process has been developed to condition the stone for increased receptivity to consolidant application by decreasing the time taken to achieve capillary saturation of liquids (Grove 2017). Following heat weathering, two of the four samples (hereafter numbered 1 and 4) were consolidated using the capillary absorption technique. In line with other experiments in this project, the consolidant selected for this trial is tetraethyl orthosilicate (TEOS); an ethyl ester with the compound $Si(OC_2H_5)_4$. It is commonly used as a binder and surface consolidant on historic stone and is used widely under the commercial name "Wacker OH100" (distributed by ACS Ltd).

Consolidation was achieved by placing the sample sections on cylindrical glass rods in a bath of liquid TEOS consolidant, the level of which is maintained so that the base and lower 5 mm of the sides of the samples are constantly immersed in the liquid. The container was stored in laboratory conditions (23°C ±5°C, 55% RH ±5%) for the duration of the treatment and the samples were monitored to ensure liquid level was constant throughout. Mass readings were taken every 12 hours and full consolidation was judged to be achieved once mass became stable to ±1% over two consecutive readings. In both samples, this consolidated mass was achieved after 48 hours of soaking. Following removal from the consolidant bath the samples were sealed in airtight containers, again in laboratory conditions, for a period of 28 days during which time mass was monitored, neither of the samples lost any significant mass during this time.

6.2.2 Preparation of "Wear Platform" for the Pedatron Experiment

Following preparation of the four Locharbriggs sandstone samples, a plywood frame was prepared measuring 550 mm², with a border raised 35 mm clear of the base, to allow a bedding of mortar to support the samples from below as well as around the outside edge (see Figure 6.1). A sand and Portland cement mortar was prepared with a ratio of 4:1 for the bedding material.

The four samples were set symmetrically with a gap of approximately 10 mm separating them, aligned on the centre line of the frame. Bedding of 13 mm was inlaid across the base, onto which the tiles were placed, and a further border of mortar was made up to level with the top of the frame. Before setting, each tile was assigned a reference number, marked on both the tile and in the mortar. In addition to this, five reflective rectification points (secured to bolts) were fixed into place to assist post-scanning processing and alignment of images. Following this, the platform was stored indoors for a period of 14 days to allow for the mortar to fully set before being transported to the SATRA laboratory test site in Kettering, UK. After the first Pedatron test run, the sandstone samples had become loose and required resetting in fresh mortar before the second 100,000 step test was undertaken. For this second test, the bottom of the plywood frame was replaced with a thicker ply to reduce flexibility in the frame. The same cement-to-sand ratio was used during this resetting, and the tiles were measured to place them as close to their original pre-test position as possible. It is worth noting that the resetting of stone did not affect the alignment of scans as each tile was sub-sampled from the 3D scan prior to processing, centring the scans on the faces of the tiles themselves and meaning their absolute position within the frame was not needed as a reference point.

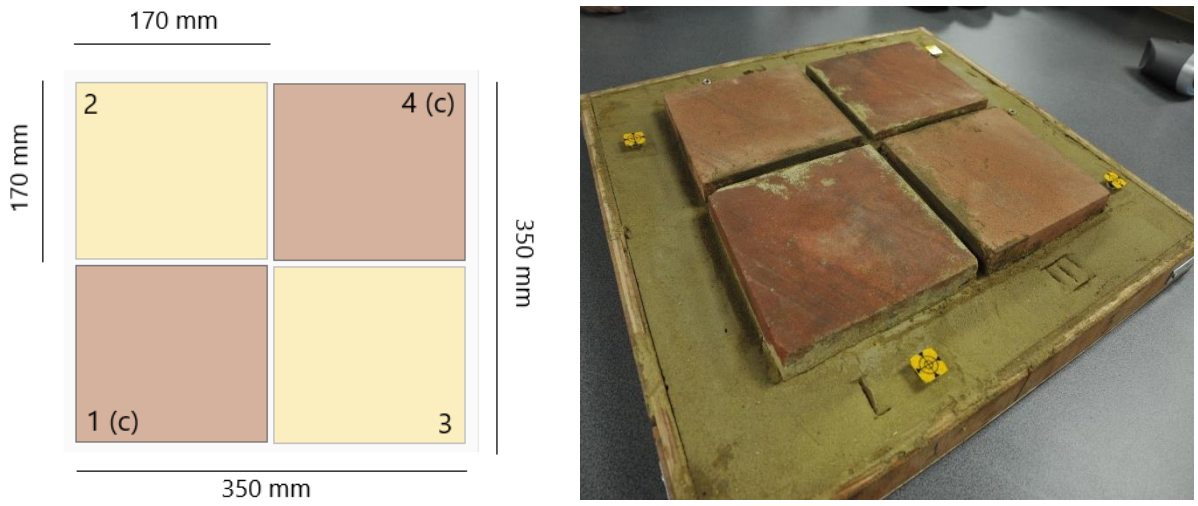

Figure 6.1 ***LEFT****: plan of experimental platform with dimensions. (c) denotes consolidated with teos.* ***RIGHT****: The prepared walking platform, samples 1 (closest to camera) and 4 (farthest corner) are treated with TEOS consolidant*

6.2.4 Pedatron Experimental Methodology

The Pedatron walking foot is a "biomechanical walking machine" (Smith 2019a; 3) designed and built by SATRA Technologies. Though novel to heritage conservation research, the device is recognised as standard testing equipment for both the floor covering and footwear industries (Smith 2019a; 3). It uses a pneumatically driven leg fitted with a prosthetic foot to simulate the walking pattern and gait of a 'typical' adult male (this specified as an individual weighing around 80kg). The placing, roll, and lift-off forces are pre-programmed to 1100 ±100N, 700 ±150N, and 1000 ±100N respectively to reflect these characteristics, and have been determined after extensive research by the manufacturer (Smith, D. pers. comm. 2019). In addition to the placement forces, the Pedatron applies a ball-of-the-foot twist of 15°, which replicates an average natural twist observed in human movement (ibid. 2019).

The Pedatron distributes this lateral twist in a pseudo-randomised progression across the surface, with the cumulative effect that over the course of any test run the contact area of the foot is evenly distributed, pivoting around a central point and creating a full circle on the base platform, commonly referred to as the 'doughnut' pattern.

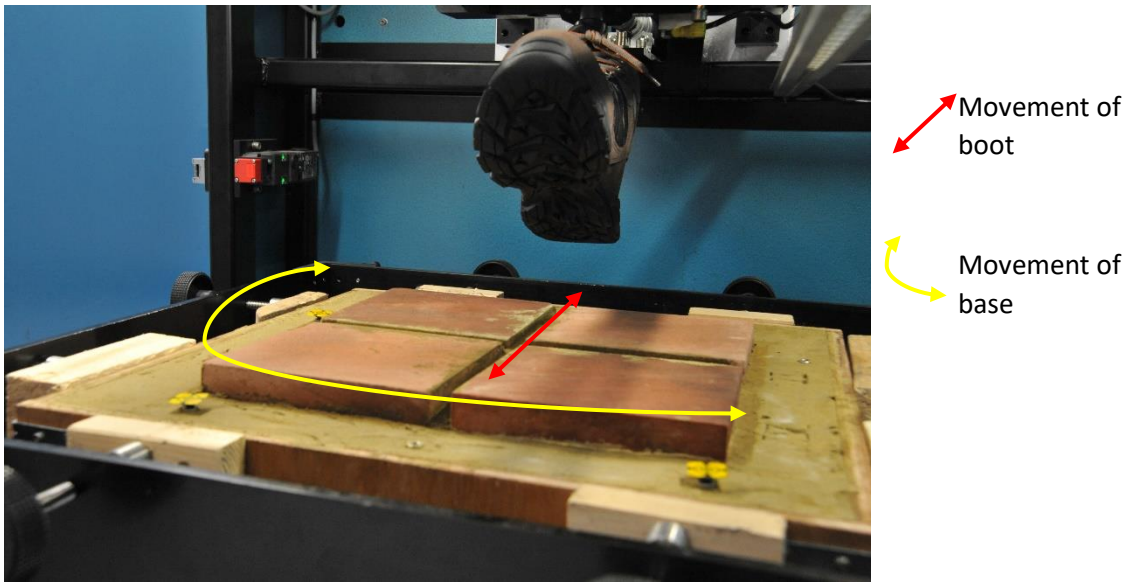

Figure 6.2 Pedatron with platform, denoting movement of boot and rotation of base to simulate foot twist. Note: extent of individual twist is 15, smaller than indicated by arrow. Image © SATRA

The Pedatron test ran in two stages, each for a duration of 100,000 steps, taken over a 48-hour period. Each quadrant (or individual tile) received 50,000 contact 'steps' during the tests. To place this in context it is useful to refer back to the case study site at Kenilworth Castle (Chapter two), which received a total of 114,972 visitors between 1st March 2019- and 29th February 2020 (R. Crites, pers. comm, 18 March 2020), and a mean number of visitors of 109,220 for the years 2012-2018 (Visit Britain, 2018). Across the 12 months of the year to March 2020 a mean of 9,581 visitors crossed the site per month (refer to Chapter two for further information). No formal data exists for average distance travelled or route walked around the site though observations taken by the author during the course of fieldwork and information gathered from site staff suggests a common circuit which is set out in Figure 6.3. In this scenario a journey around the main areas of the castle consists of a route between 900-1005 metres in length of which approximately 550 linear metres are across exposed historic stone surfaces. This being so, an approximate total of 123,020,040 steps fell across the site in 2019-20, which equates to 24,604 steps for each linear metre.

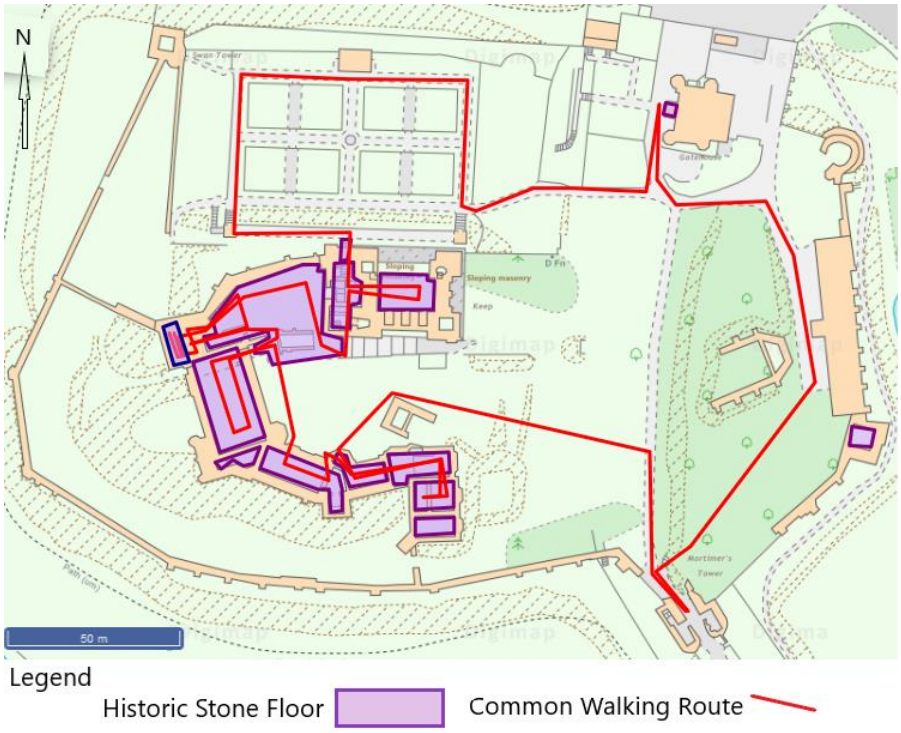

Figure 6.3 Kenilworth Castle site plan, including exposed stone flooring and common visitor route through site. Base map © Edina Digimap 2021

Each Pedatron test run therefore equates to approximately a year's total footfall in a given section of commonly walked stone floor, per sample tile. Furthermore, taking sample areas such as doorways and staircase returns as shown in Figure 6.4, where visitors will be changing direction within a confined space and therefore increasing sideways scrub on the ball of the foot, the Pedatron data represents a unique way of quantifying year-on-year wear.

Figure 6.4 Representative Exposed Stone Flooring At Kenilworth Castle. Image ©Author

During the test, the Pedatron foot completed each step-cycle within approximately 1.8 seconds, including the pseudo-randomised twist of the platform and foot. Conditions within the Pedatron operating chamber were maintained at a general ambient condition of approximately 18-23°C 50-60% RH throughout the test, and a small amount of water was manually applied to the surface of the samples at the start of both days of both tests using a pneumatic spray mister, to a visually uniform state. The purpose of this was to wash away dusty deposits building up on the surface from the broken-up mortar. The quantities of water were recorded by weight using a precision pan balance (SATRA instrument #3353) and are presented in Table 6.1, below.

Table 6.1 Water applied to surface of walking platform during Pedatron test

Step Number		Water (by mass) applied (g)
0 (start of first test)		13.4
40,000		27.6
	Total	41.g
0 (Start of second test)		11.6g
40,000		19.3g
	Total	30.9g

6.2.5 3D Scanning Equipment

For this experiment a Creaform Handyscan 700 handheld scanner was used to capture pre-and post-experiment renderings of the wear platform, creating a total three sets of point clouds. The Creaform scanner has an accuracy of 0.020 mm (Creaform 2017). In addition to this, the proprietary VX software was used to initially render all scans, prior to their being post-processed in the opensource CloudCompare software package. Initial scans were taken on-site at SATRA Technologies immediately prior- and post- test runs, to reduce the potential for unintended damage or changes to the blocks (for example damage caused in transit).

6.2.6 Pre- and Post- Experiment Measurement Methodology

This section sets out the preparatory steps taken prior to the running of the first Pedatron test. Each sandstone tile was assessed before and after the application of TEOS consolidant, for the purposes of confirming successful uptake of treatment. For this experiment, the stone has been assessed using Ultrasonic Pulse Wave Velocity and Colorimetry for the purposes of confirming consolidant uptake. The results of these tests are included in this section, separate to experimental results which are detailed in section 6.3.

Table 6.2 Summary of measurements and their timing

Method	Occurrence			
	Pre-test	Post-Consolidant	Pre-Pedatron	Post- Pedatron
Ultrasonic P Wave Velocity	X	X		
Colorimetry	X	X		
TRACE-iT Surface Roughness			X	X
3D Scanning			X	X

6.2.6.1 Ultrasonic Pulse Wave

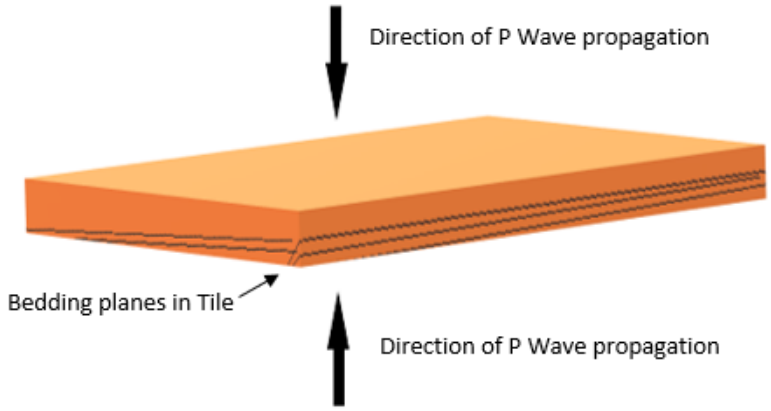

Figure 6.5 Diagram of Tile as laid within frame, showing bedding planes and direction of P Wave Propagation for pre-test assessment.

Pulse Wave Velocity measurement was carried out pre- and post- artificial heat weathering treatment, as a means of testing the effects of the process prior to treating the stone with Ethyl Silicate. Pulse Wave readings were taken using a Proceq Punditlab using flat faced transducers with a contact surface diameter of 30mm (Proceq part 325 40 141). Wave frequency is 150kHz, and calibration of the equipment was carried out prior to each recording using a 25.4 µs calibration rod (Proceq part 710 10 028). Measurements were taken 'top to bottom' of each tile as they are typically laid in practice, almost perpendicular to the strata in the stone (see Fig 6.5). Using this arrangement, the 40 mm distance between transducers is above the minimum threshold for effective wave

propagation and detection (>23 mm) (Proceq 2017a, 17). These measurements are taken in triplicate and a mean value generated for each. P Wave values were taken prior to the construction of the wear platform but owing to the adhesion of mortar to the underside of the tiles it is not possible to reliably repeat the measurements following Pedatron runs. It was also decided to leave the platform intact following the second test run to allow for the possibility of repeated experimental runs in the future.

Table 6.3 Mean P Wave Values Pre- and Post- Artificial Weathering. (c) denotes consolidated tiles

Tile Number	Pre-Weathering (Mean)	Post-Weathering (Mean)
1 (c)	2821	2286
2	2760	2260
3	2897	2391
4 (c)	2845	2348

Each of the four tiles was measured three times on each occasion for P Wave Velocity, and a final mean reading was generated from these (Table 6.4). Furthermore, in addition to these readings the two samples treated with TEOS consolidant were tested following application and curing time, to assess the establishment of the consolidant prior to the final construction of the platform (Table 6.4).

Table 6.4 Consolidated Tiles, Mean P Wave Values Pre- and Post- Consolidation

Tile Number	Pre-Consolidant (Mean)	Post-Consolidant (Mean)
1	2286	3110
4	2348	2941

As per Table 6.4, P Wave velocity increases by a significant amount when comparing means- 37% in the case of Tile 1, and 21% for Tile 4. For the purposes of evaluating consolidant uptake, these figures- compared against pre-consolidation and against Tiles 2 and 3 which have not been consolidated, are sufficient to confirm the treatment has become established.

6.2.6.2 Colorimetry

For this experiment, data was collected using a Konica Minolta CM700D portable Spectrophotometer with a 6mm diameter sampling aperture fitted and set to SAV sampling. In

addition, an aluminium mask was prepared with pre-drilled holes to allow set spaces on each tile to be repeatedly sampled for direct comparison.

To ensure comparability of results across each of the test stages, a template mask was cut with for use on all sandstone sections, with holes drilled equidistant from each other and at 45° to the central corner of the mask (and stone sections). These holes are placed to correspond with the three main zones of impact from the Pedatron test (see Figure 6.6).

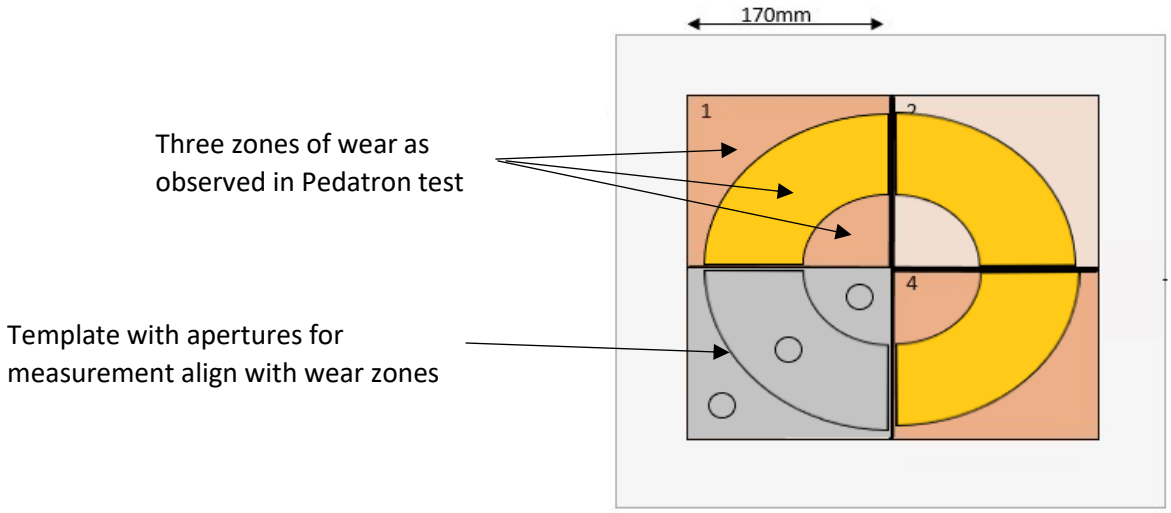

Figure 6.6 Explanation of colorimetry and Surface Roughness templates as fitted to platform for measurement

For each aperture at each point of recording, readings are taken in triplicate and a mean generated. These are tabulated according to position on tile; inner zone, midsole, and heel edge.

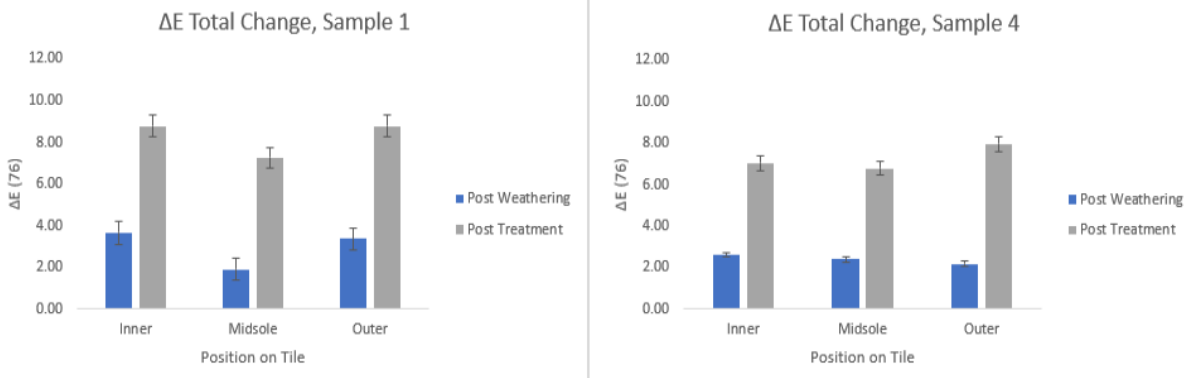

Figure 6.7 Colorimetry ΔE (total change) for each Tile and sub-section (including error bars), before and after consolidation (Samples 1 and 4 only)

Examination of the Colorimetry results summarised in Fig. 6.7 indicates a significant change following consolidation both of the treated samples (Tiles 1 and 4). Each area of the Tile is affected to a similar extent on the ΔE scale (between 6 and 9) by consolidant, and that this is largely uniform across the three tested zones of both tiles. By this metric it may be asserted that consolidation of both stones took place successfully prior to the first Pedatron Test.

6.2.6.3 Surface Roughness

In addition to laser scanning, surface roughness measurements were taken prior to and following each Pedatron test run using an INNOWEP TRACE-iT sensor. The TRACE-iT records surface profiles in three dimensions and renders the profile using the Rz metric at µm scale. The roughness profile itself is made up from the mean of five 'peak to valley' z-axis measurements within the optical measurement zone (a 5 x 5 mm sample area), constructing surface topography from 1500 measurements in each direction. For the purposes of this test, a masking template was used to focus readings in specific areas, as with Colorimetry (see Figure 6.6), and a single measurement was taken for each area. The instrument captures detail at a resolution of 1.2µm (INNOWEP 2017), and results are rendered within the native software as a graphical plot in both two and three dimensions, as well as exported numerically for further analysis.

6.2.6.4 3D Scanning and Rendering

Scanning of samples was carried out to the manufacturers specified methodology and point clouds were created with the native proprietary Creaform VX Software, before being output in the .obj file format for analysis in CloudCompare (v2.11) processing software.

The scan data collection process itself is iterative; with multiple passes of the samples being rendered in real time to allow for the identification of missed or complex areas. To aid with the

construction of accurate point clouds, adhesive targets supplied by the manufacturer are added to the border of the platform structure in an asymmetrical pattern. The targets themselves are circular black and white tags with a precise diameter, allowing the processing software to automatically recognise them as alignment markers and remove them from the point cloud (see Figure 6.8).

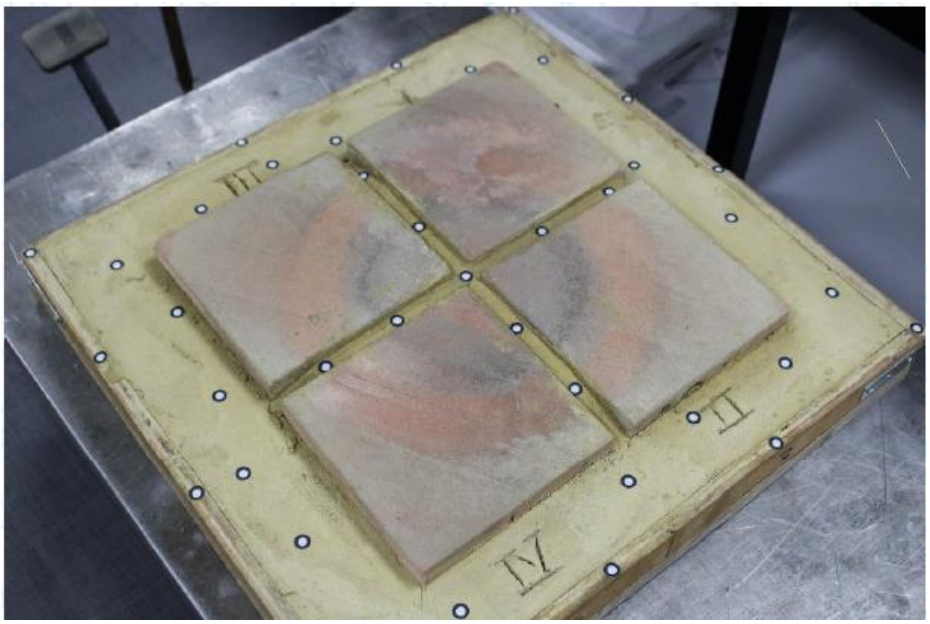

Figure 6.8 Test Platform with rectification points, image ©SATRA

Following scanning and initial point cloud construction, alignment of the paired point clouds is carried out in CloudCompare. Owing to the movement of the four sample tiles during the first test and the need for them to be re-set for the second trial, each full point cloud needed to be subdivided into four individual tile-only point clouds and then aligned using the upper surface of each tile as reference. This allows the sequential scans to be accurately aligned for change detection without the loosened mortar or position of the tile within the frame introducing erroneous error to the calculations change calculations.

Initial alignment is achieved through the identification of characteristic points that remain unchanged across the three Pedatron test runs. A minimum of eight points were selected across the upper edge of the tiles, grouped onto easily defined features such as deep gouges or chipped corners which allowed for accurate identification on subsequent scans. Once roughly aligned using

this technique, the scans were then put through an automated fine registration function which uses the Iterative Closest Point algorithm (hereafter 'ICP registration').

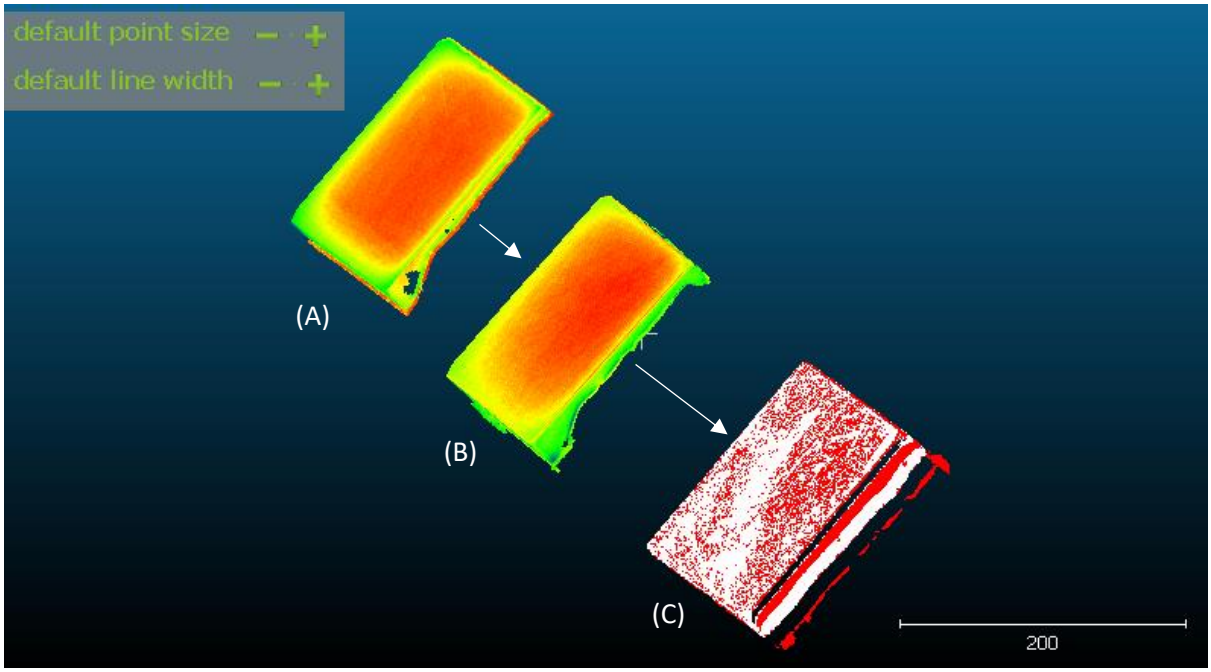

Figure 6.9 Alignment of individual tiles (sample 1 shown). Before first test (a) is closely aligned with the post-test tile (b) and the difference determination is represented as a colour scale representation (c)

Functionally, ICP registration sets one of the already roughly aligned point clouds as a reference (static) point, and then moves the second point cloud incrementally using a subset of matching 'core points' (50,000 randomly sampled points per cloud) as a target for the alignment. The process repeats for either a set maximum number of cycles, or until the root of the mean squared error value passes a set limit (typically a value of 1.0e-6). Following the process, a final RMSE value is assigned to the aligned cloud, which are summarised within the results section in §6.3.3.

Following the two-stage alignment process, the assessment of change for each individual tile was done after each of the two Pedatron tests. For this experiment, a technique called Multiscale Model to Model Cloud Comparison was used (hereafter shortened to M3C2), which was developed by Dimitri Lague, Nicolas Brodu, and Jérôme Leroux (Lague et al 2013). This process, which has been formalised into a plug-in function for CloudCompare, utilises an algorithm to automate distance calculation between selected core points within the paired clouds. It uses sub-selected neighbouring

points within a pre-defined cylindrical region of interest surrounding the core point to define which points relate to a core point, and then measure the distance of divergence (or change) from the predicted position of the sampled points. The M3C2 application has proven advantages over other common point cloud comparison approaches as it works directly on the point cloud data without the need for meshing of surfaces or the creation of 2D grids as reference frameworks (such as with the creation of Digital Elevation Models). In this way, potential for the introduction of unintended bias is reduced, in addition to increased simplicity and processing speeds (Lague *et al* 2013).

6.3 Results

6.3.1 Observations During the Pedatron Test

During the first test, the forces exerted by the Pedatron quickly began to affect the mortar setting of the walking platform. However, after some loosening the samples regained some stability in the now-loose bedding material and remained largely in place, moving only vertically within the outer setting. After some monitoring, it was decided that the movement would not compromise the data obtained from the test to a significant extent, and so the test was allowed to continue. The powdered mortar did create a noticeable layer of dust which accumulated across the surface (see Figure 6.10) which required careful cleaning with both vacuum and washing prior to post-test scanning.

Figure 6.10 Walking Platform immediately post- first test, pre-cleaning. The 'doughnut' effect is clearly visible as a circle spanning the four tiles. Also clear is the movement of the tiles within the frame. Image © SATRA

6.3.2 3D Scans and Visualisation

Following two 100,000-step tests, three full point clouds were generated by the Creaform Handyscan. Owing to the movement of the four sample tiles during the first test, and the need for them to be re-set for the second trial, the 'whole platform' renderings as generated in the initial scan needed to be subdivided into four individual point clouds which were centred on the upper surface of each tile. This step allowed the progressive scans to be accurately registered for areas of change to be measured.

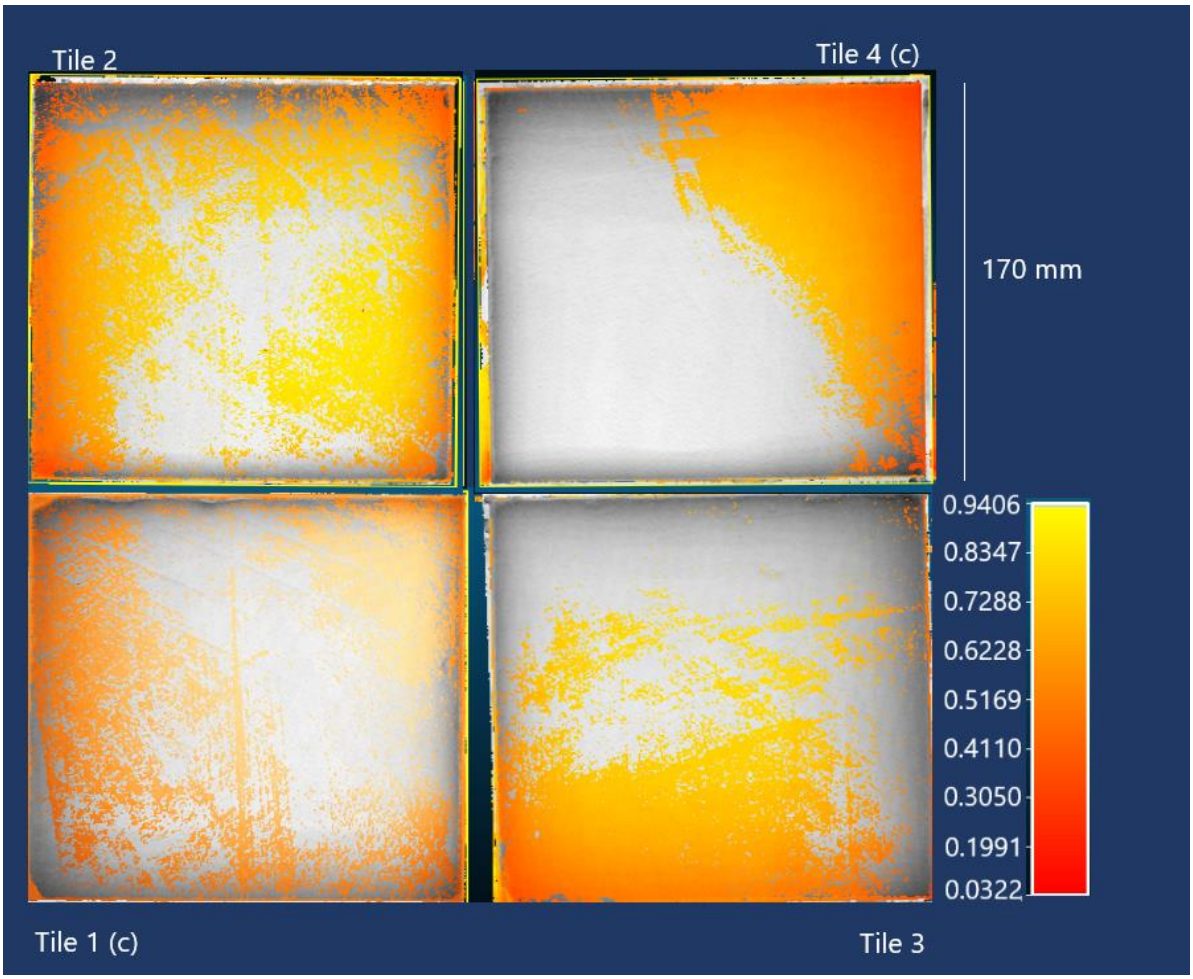

Figure 6.11 Difference models showing change after first Pedatron test, created using CloudCompare. Grey areas denote no significant alteration between two models. Scales are mm (c) denotes Consolidated tile.

Figure 6.11 plots the four tiles from the test platform as they are positioned in situ. The 'tiles' in this graphic represents an alignment of before-and-after point clouds from the first Pedatron trial, each corresponding tile being first manually aligned using common points, and then finely registered using the ICP (Iterative Closest Point) algorithm to an accuracy measured using the root mean square error (RSME) value at 0.250 ±0.05 mm. The platform as illustrated here pivots at the central intersection point of the four tiles during the Pedatron test. The colour scale of the plots 6.11 and 6.12 is graduated red- yellow, with shade becoming lighter (towards yellow) as the difference between the two aligned tiles increases; a change produced during the Pedatron test runs. Areas of the tiles with no detectable difference are shaded grey. The wear patterns demonstrate non-uniformity across the four tiles, though there is a diagonal grey area detectible in tiles one and two

(6.11) and three and four (6.12) which corresponds roughly to the circular progress of the midsole arch of the boot used by the Pedatron, where no contact is made between the sole and the platform. This is the cause of 'doughnut effect' as visible in Figure 6.10, and the area remains virtually unchanged and in fact saw an accumulation of loose material during both tests, owing to the void left by the arch of the boot. This material was removed from the platform before measurements were taken using a vacuum cleaner with a soft bristled brush head fitted.

In each of the four tiles in figure 6.11 it is clear to see how the heel contact of the boot is facilitating wear on the outer portion of each tile (i.e. within the outermost circle of wear identified in Figure 6.6 (§6.2.6.2). Interestingly though, the first contact point between heel and edge of tile does not appear to have facilitated any significant edge loss as one might expect. The consolidated tile number one registers slightly less wear in the outer heel strike areas than the unconsolidated tiles (two and three), although tile number four does show extensive overall wear in this outer zone, leading to an inconclusive interpretation of the effectiveness of TEOS consolidant in the mitigation of surface wear in this part of the trial.

After the first test run it was unclear to what extent the loosening of the tiles influenced the wear patterns of the tiles. The extent of tile movement during Pedatron operation was limited to a few millimetres vertically, and the rocking motion of the tiles under the boot was partially abated by redistributed loose mortar which settled after some time. The final position of the tiles was at most 8mm in any one corner at the end of the experiment, which though significant in terms of quantifying wear behaviour, is analogous of the movement of loose stone observed on-site at Kenilworth.

Figure 6.12 shows the four tiles following the second Pedatron run. The plots here denote the change between the tiles at the end of test 1 (as illustrated in Figure 6.11) and the second run of 100,000 steps.

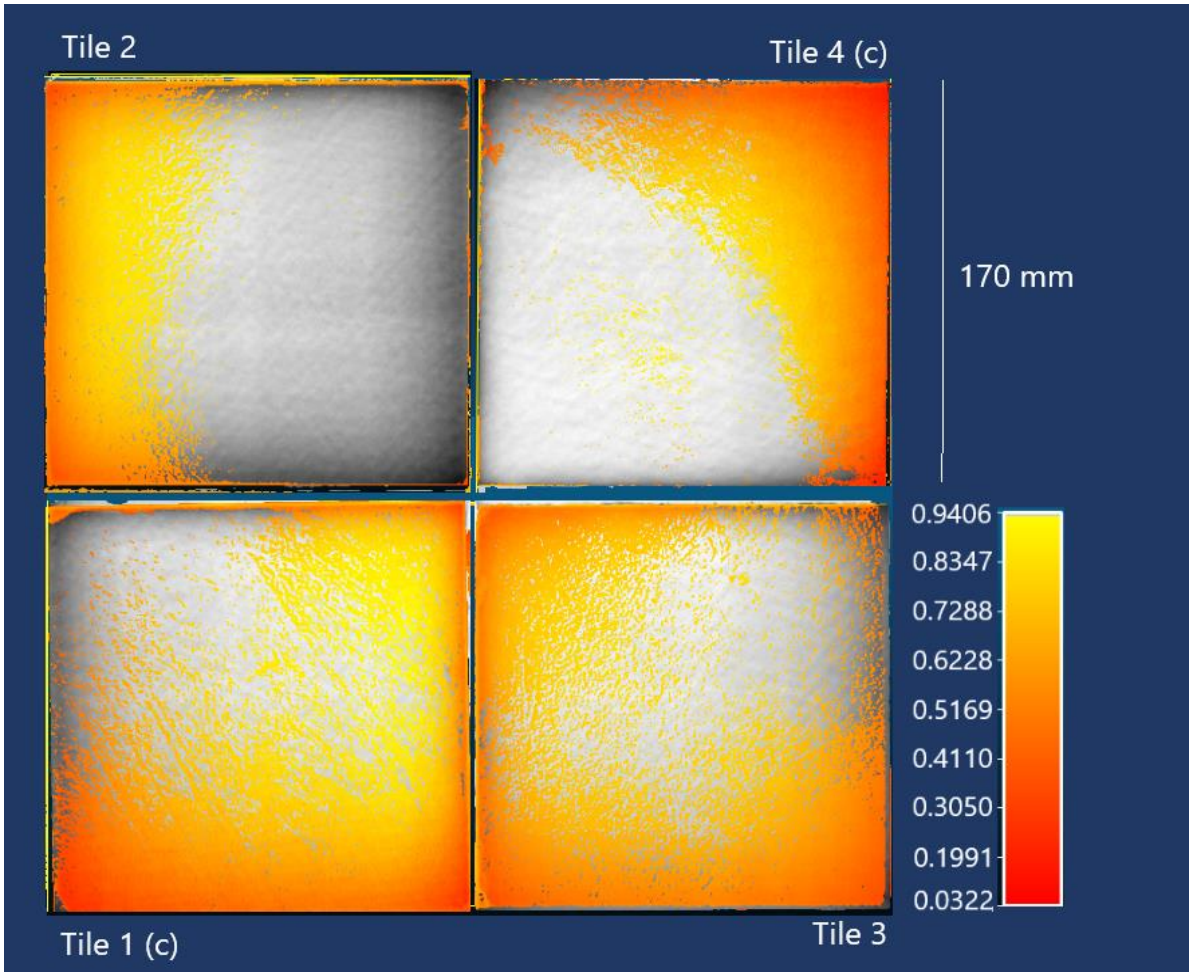

Figure 6.12 Difference models showing change after second Pedatron test, created using CloudCompare. Grey areas denote no significant alteration between two models. Scales are mm (c) denotes Consolidated tile

During this second run of the test, the tiles did not loosen as with the first experiment, owing to the increased thickness of the plywood base, so wear patterns from this test run can be seen to represent the direct influence of footwear on stable flooring. In general, there is an indication of the doughnut effect as seen in figure 6.10 though it is less prominent, with the exception of the consolidated Tile four where the path of the heel is defined by its inner edge. Again, neither consolidated tile (one and four) present an obvious deviation in wear extent or pattern that can readily be applied to their treatment.

Significant Change

In addition to the creation of plots which show observable difference, it is desirable apply a test of significance to the zones of change. In order to achieve this, the M3C2 cloud comparison tool has been used, which uses a significance threshold, set to 0.05% of the overall measurable difference across the tile. In the instance of this set of tests, this equates to 0.6 mm of the overall cut-off depth of 12 mm for the generation of all plots.

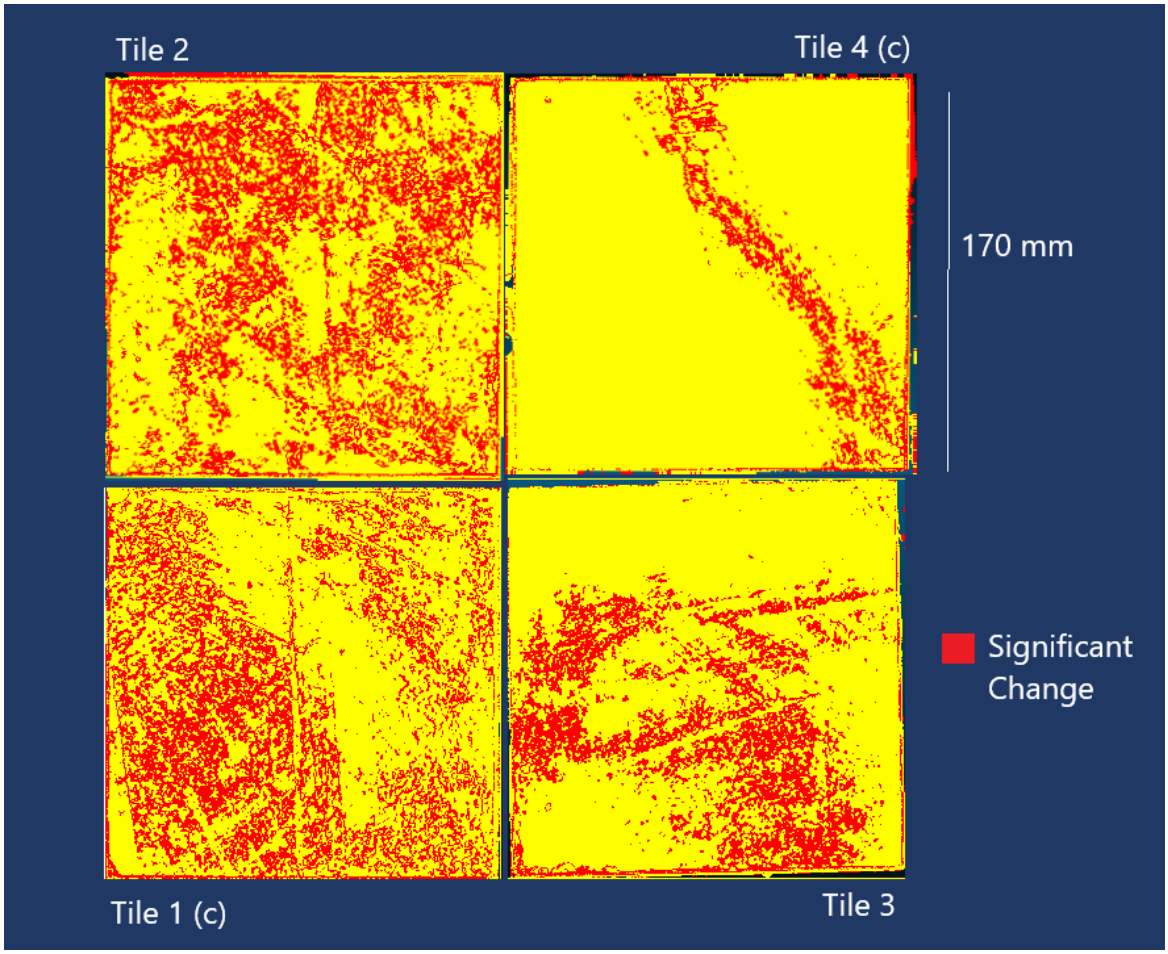

Figure 6.13 Significant change as determined by M3C2 algorithm, test 1. Red areas denote change in excess of a minimum threshold of 0.6 mm

Figure 6.13 shows the areas of significant change as per the 0.6 mm threshold for the first test. What is clear on this metric is that there is a clear distinction between the consolidated tile number four and the three other tiles. It should be reiterated that there is some movement in all of the tiles during this test, and this movement was not uniform across the platform. Regardless of this

however, figure 6.13 shows that all the tiles underwent significant change during the first test run, tiles one, two, and three to a considerable extent.

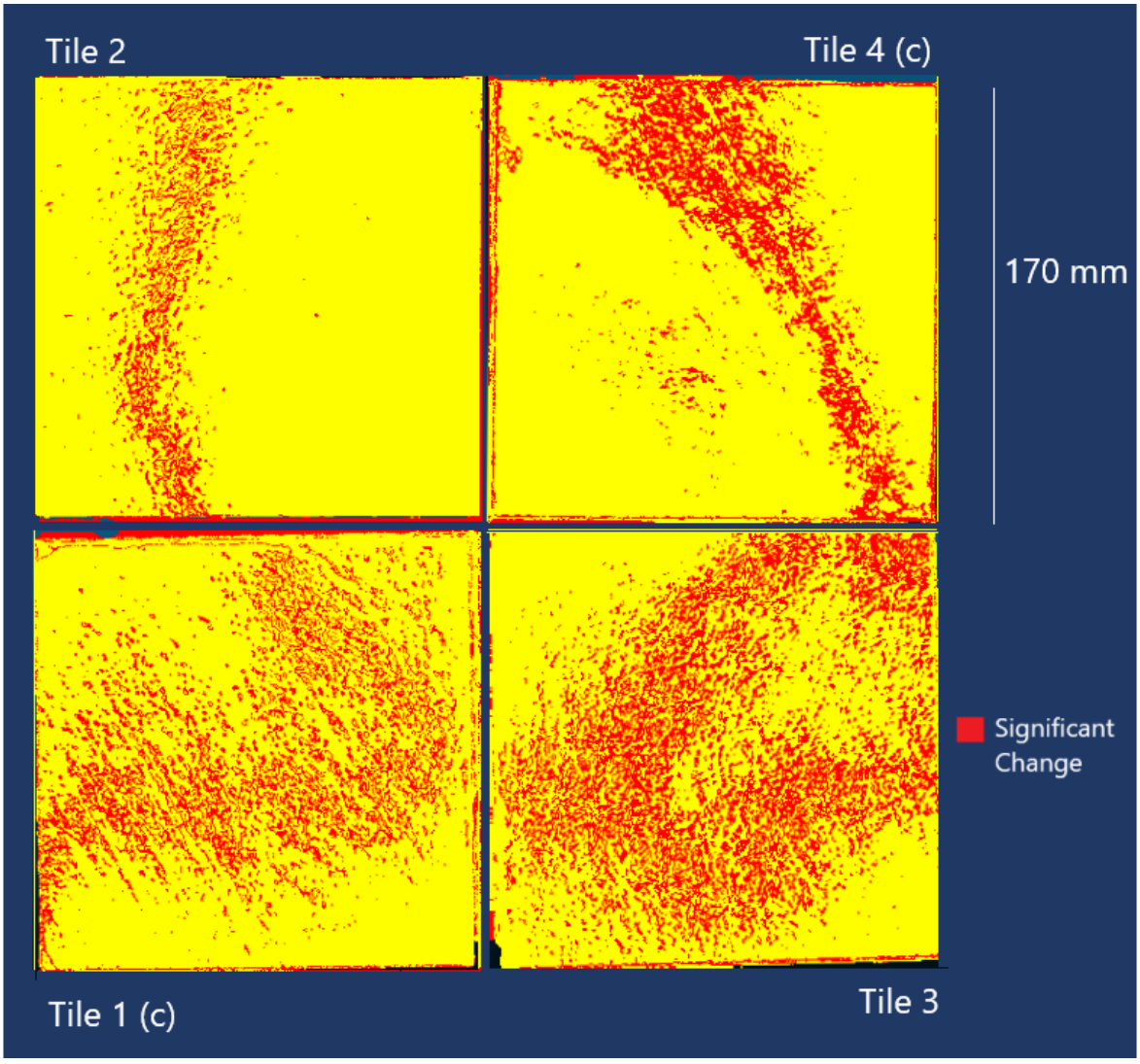

Figure 6.14 Significant change as determined by M3C2 algorithm, test 2. Red areas denote change in excess of a minimum threshold of 0.6 mm

Furthermore, figure 6.14 also plots differences in registered point clouds for tiles between test run one and two (steps 100,000 and 200,000) based on the same minimum 0.6 mm distance threshold. In tiles one and three the pattern of wear after the second test run is more uniform and does not have clear delimitation between the zones. Interestingly, in tiles two and four in figure 6.14 the only significant change appears to be propagated by the heel or front edge of the heel, creating a line

outside of the arch void area. There appears a clear distinction in how tiles one and three wore in comparison to tiles two and four in this second plot, with one and three wearing over a much more extensive area. This difference does not correspond to consolidant treatment, and as the tiles did not become loose in this second run the contrast cannot be attributed to movement under stress.

With regards accuracy of point cloud registration, a value of accuracy is placed on the paired point clouds known as the Root Mean Square Error (or RMS/ RMSE). This value must be below 1 for the paired clouds to be considered accurate, though when measuring distance between clouds which diverge in some capacity (i.e. when measuring change) the value can never be processed down to absolute zero. During alignment of all cloud pairings in this analysis, the RMSE value was calculated to 0.250 mm ±0.05 mm before generation of plots was undertaken.

6.3.2 Surface Roughness

In addition to laser scan modelling, surface roughness measurements were taken before and after both Pedatron tests using the INNOWEP TRACEiT sensor. These readings measure change at the resolution of microns (as opposed to sub-millimetre detail of the laser scanner used in the previous section), focussed on the three key zones of the stone surface as outlined in Figure 6.6: the inner 'toe strike' zone, midsole arch area, and outside edge/ heel strike zone. Table 6.5 summarises topographical roughness before and after the first Pedatron test expressed in µm, followed by the standard deviation as generated by the TRACEiT native software. Table 6.6 summarises the surface roughness values following the second Pedatron test run.

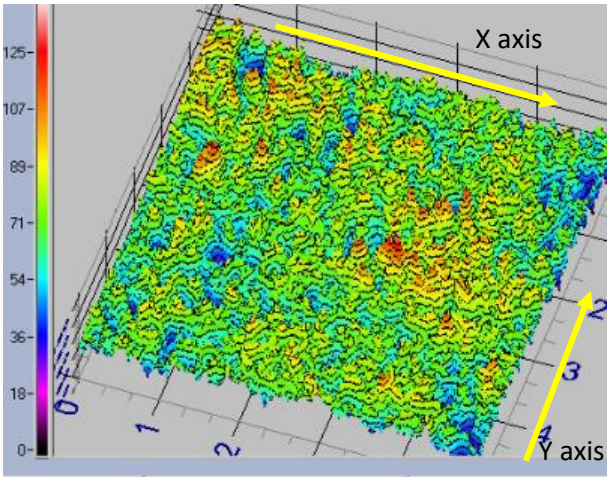

Figure 6.15 Graphical representation of surface hardness plot as generated by INNOWEP TRACEiT, showing axes of measurement. Scale within plot in mm, depth scale in µm. Image © Author

In all instances after the first Pedatron test run the surface roughness was reduced in both directions. There is no discernible characteristic trend in the changes on consolidated and unconsolidated stone in the first test run, and Rz value drop for these tiles spread from 1.66 µm (tile one, outer) to 9.11 (tile four, midsole), compared to a Rz drops of 1.9 µm (tile two midsole) to 10.86 (tile two inner) and 2.6 (tile three, midsole) to 10.66 (tile three, outer).

Table 6.5 Surface Roughness measurements (Rz) and standard deviation (SD), taken pre- and post- first Pedatron Test, in µm. Green background denotes drop in Rz value

	Tile 1 (c) Pre- First Test			Tile 1 (c) Post- First Test		
	Inner	**Mid**	**Outer**	**Inner**	**Mid**	**Outer**
X axis: Rz/ SD	39.17/6.17	36.35/3.53	37.46/4.44	31.89/3.54	31.35/2.97	35.80/4.02
Y axis: Rz/ SD	39.85/5.18	38.7/3.64	39.12/3.87	33.04/3.77	31.01/3.87	35.05/4.06
	Tile 2 Pre- First Test			**Tile 2 Post- First Test**		
	Inner	**Mid**	**Outer**	**Inner**	**Mid**	**Outer**
X axis: Rz/ SD	42.63/5.34	38.27/4.16	35.9/4.98	32.96/4.39	36.37/4.18	33.54/4.79
Y axis: Rz/ SD	44.35/5.09	39.95/4.22	37.17/4.77	33.49/3.96	35.86/4.55	33.17/4.2
	Tile 3 Pre- First Test			**Tile 3 Post- First Test**		
	Inner	**Mid**	**Outer**	**Inner**	**Mid**	**Outer**
X axis: Rz/ SD	36.3/3.59	37.22/4.29	43.03/5.33	28.14/3.39	34.62/3.57	30.34/3.54
Y axis: Rz/ SD	39.56/3.83	40.56/4.36	42.81/5.29	29.11/3.54	36.22/4.93	32.15/4.18
	Tile 4 (c) Pre- First Test			**Tile 4 (c) Post- First Test**		
	Inner	**Mid**	**Outer**	**Inner**	**Mid**	**Outer**
X axis: Rz/ SD	38.92/4.41	40.04/4.62	36.05/4.02	32.55/4.35	34.89/3.4	32.86/4.06
Y axis: Rz/ SD	39.93/4.91	44.2/4.99	37.98/4.44	34.67/3.94	35.09/4.02	32.24/3.72

In addition to the consolidant pre-treatment condition, there is no apparent trend resulting from the position of the boot falling on the platform during this test. The three 'zones' of wear as identified in figure 6.6 (§6.3.1) do not correlate to any typical change in roughness values despite the difference in force and scrub as propagated by the Pedatron in operation. The mean overall change for readings in consolidated tiles (tiles one and four) for test run one is 4.75 µm (x axis), 6.44 µm (y axis), 5.61 µm combined. For the two unconsolidated tiles (two and three), the mean drop for test one is across the x axis is 6.23 µm, and for the y axis it is 7.4 µm. The combined drop in Rz is 6.81 µm.

The second Pedatron test run presented a less uniform change in roughness value across the test platform. Following this run there was an increase in roughness in three instances. On tile two a very slight increase in roughness in the x axis, outer zone, which is complemented by further slight increases in the inner toe strike zone of tile three (both axes), and further by marginal increases in both the inner (x axis) and outer zones of tile four (both axes). Of these increases only tile three (inner zone, both axes) is of a magnitude exceeding one µm (1.79 and 1.59 µm), all others vary between 0.03 and 0.34 µm. Table 6.7 sets out these values in full.

Table 6.6 Surface Roughness measurements (Rz) and standard deviation (SD), taken pre- and post- second Pedatron Test, in µm. Green background denotes a decrease in Rz value, red an increase

	Tile 1 (c) Pre- Second Test			**Tile 1 (c) Post- Second Test**		
	Inner	**Mid**	**Outer**	**Inner**	**Mid**	**Outer**
X axis: Rz/ SD	31.89/3.54	31.35/2.97	35.80/4.02	30.12/3.59	30.52/3.58	32.59/3.78
Y axis: Rz/ SD	33.04/3.77	31.01/3.87	35.05/4.06	30.03/ 3.38	30.54/2.8	33.02/3.79
	Tile 2 Pre- Second Test			**Tile 2 Post- Second Test**		
	Inner	**Mid**	**Outer**	**Inner**	**Mid**	**Outer**
X axis: Rz/ SD	32.96/4.39	36.37/4.18	33.54/4.79	29.14/ 3.05	29.17/ 4.22	33.67/ 4.1
Y axis: Rz/ SD	33.49/3.96	35.86/4.55	33.17/4.2	29.63/ 3.25	28.44/ 3.45	32.85/ 3.77
	Tile 3 Pre- Second Test			**Tile 3 Post- Second Test**		
	Inner	**Mid**	**Outer**	**Inner**	**Mid**	**Outer**
X axis: Rz/ SD	28.14/3.39	34.62/3.57	30.34/3.54	29.89/ 3.81	33.59/ 3.6	29.88/ 3.27
Y axis: Rz/ SD	29.11/3.54	36.22/4.93	32.15/4.18	30.70/ 3.62	35.35/ 4.44	31.04/ 3.44
	Tile 4 (c) Pre- Second Test			**Tile 4 (c) Post- Second Test**		
	Inner	**Mid**	**Outer**	**Inner**	**Mid**	**Outer**
X axis: Rz/ SD	32.55/4.35	34.89/3.4	32.86/4.06	32.78/ 3.36	33.52/ 3.79	32.89/ 3.86
Y axis: Rz/ SD	34.67/3.94	35.09/4.02	32.24/3.72	34.58/ 3.58	32.57/ 3.55	32.58/ 3.53

Table 6.7 Difference in Surface Roughness (Rz) values for each measurement before and after the Pedatron tests (μm).

Changes between reference and post- first Pedatron test				
	Axis	**Inner**	**Mid**	**Outer**
Tile 1	X	-7.28	-5	-1.66
	Y	-6.81	-7.69	-4.07
Tile 2	X	-9.67	-1.9	-2.36
	Y	-10.86	-4.09	-4
Tile 3	X	-8.16	-2.6	-12.69
	Y	-10.45	-4.34	-10.66
Tile 4	X	-6.37	-5.15	-3.19
	Y	-5.26	-9.11	-5.74
Changes between post- first Pedatron and post- second Pedatron test				
	Axis	**Inner**	**Mid**	**Outer**
Tile 1	X	-1.77	-0.83	-1.34
	Y	-2.03	-7.42	-2.03
Tile 2	X	-3.82	-7.23	+0.13
	Y	-3.86	-7.42	-0.32
Tile 3	X	+1.75	-1.03	-0.46
	Y	+1.59	-0.87	-1.11
Tile 4	X	+0.23	-1.57	+0.03
	Y	-0.09	-2.52	+0.34

Changes are +/-ve as indicated. Red denotes an increase in roughness from previous data point.

6.3.3 Statistical Analysis

For this experiment, statistical analysis for the 3D scan data was carried out as part of the multiscale model-to-model scale comparison (M3C2) function. The threshold for significance in this process was predefined at 0.05 of total tile height (independent of the supporting frame). This translated to a real point displacement measurement of 0.6 mm, above which the point clouds were said to have changed significantly as a result of erosion from the Pedatron run. This change is plotted in figures 6.13 and 5.14, with the significantly altered areas displayed in red. It is possible in this process to set the significance level at other values, such as 0.01 as has been used in other experiments for this project, however, the root mean square error (RMSE) value generated from the fine alignment process must be taken into account. For the scans used in this experiment, the best fit RMSE values range from 0.11 to 0.32 mm, therefore a significance threshold set to less than one millimetre would introduce too great an opportunity for introduction of error to the plot.

For the surface roughness measurements, data was separated into three groups, based on the zone of wear on the tile, and these groups were subject to a pair of T tests (unequal variances) for differences before-and-after the first Pedatron test, and before-and-after the second Pedatron test. For these tests the α value was determined at 0.01 to reduce the opportunity for Type I error. Results of these tests are outlined in Table 6.8, and show that during the first Pedatron test run, there was significant change to all areas of the wear zone across the test platform, whereas in test run two, none of the zones recorded significant change by this metric.

Table 6.8 Results of T Tests for Surface Roughness change

	Inner Zone	Midsole Zone	Outer Zone
Pedatron Test 1	0.000	0.000	0.000
Pedatron Test 2	0.293	0.030	0.287

6.4 Discussion

In order to establish the success of pre-experimental consolidation, Pulse Wave velocity values were taken, which increased by 37% in the case of Tile 1, and 21% for Tile 4. These figures confirm that consolidant is present within the pore network of the stone at the time of construction of the platform prior to the Pedatron Test, and these values and changes are analogous to those collected for other trials in this project. Changes in colour recorded at this time further corroborate the presence of consolidant, through the darkening of tiles one and four after consolidation using the colorimetry ΔE metric.

For the experimental data collection of this trial however laser scanning and roughness measurements have been used to gain understanding of the effects of simulated footfall erosion resulting from the Pedatron test. Examining first the operation of the Pedatron, it is first necessary to evaluate the performance of the test platform during the trial runs. As is noted in §6.3.1 during the first test run, all four tiles quickly broke free of their mortar setting, and their subsequent

movement within the frame, though limited to vertical 'rocking', caused further breakdown of mortar mass, which was then deposited across the tiles as the run progressed. The movement of this dusty material was suppressed by the application of water at intervals for the rest of the test, but it must be concluded that there was some effect on the tiles themselves, either in relation to their roughness values through the deposition and 'walking in' of fine particles, or as a mitigation for direct erosion by acting as a medial layer.

Whilst this change in condition must be taken into account as an undesirable development which had the potential to cause some deviation from design in the performance of the experiment, the movement of the tiles in fact mirrored that which is seen in the field, as observations confirm. The results of the first test run not only remain valuable, but perhaps have some added variability which reflects in-situ wear. In seeking to limit this variability however, the platform was modified prior to the second test run, replacing the original plywood supporting base with a more substantial 12 mm thick structural ply. The tiles were replaced using the same ratio mortar mix as before and were measured for position to ensure they were re-set in close proximity to their original pre-test position. The improvements to the platform were successful in preventing the breaking out of the tiles in the second test. During the second run it was noted that there was a significant reduction in dust and loose material, such as to make the post experiment cleaning in preparation for scans a quick and straightforward process by comparison to the first.

Turning to the test results, the laser scans provided a range of valuable outputs, and of particular interest is the application of the M3C2 processing algorithm to improve accuracy of point cloud-to-cloud comparison. Comparing the M3C2 significance plots to the difference plots generated following fine registration of clouds the following elements are clear.

In both formats it is possible to detect the midsole arch void in post- test images, notably the outer edge, though it is most readily detectable following the first test run. For the first test run, tiles one (consolidated) and two registered the most extensive wear, distributed across the face of the tile

and not limited to one zone. In addition, there is clear wear on at least one outer edge of tiles one, two and three after the first test, propagated by the heel action of the boot. Also notable are tiles one and three which had the most extensive significant change occurring during the first test. In contrast, tile four has only a limited stripe of significant wear on both tests, corresponding to the area where the inner portion of the heel contacts the tile, leaving a clear line of wear, a trend also seen in tile two after test run two.

Following the second test run, tiles one and three display the most extensive significant wear. However, for this test there is less evidence of prominent wear to the tile edges as can be seen following test run one. This is possibly due to the setting pitch of the tiles, and the fact they remained in place throughout the test. Reference to Figure 6.16 shows the final position of tiles following first test (centre image), with their outer edges most prominent; a phenomenon that did not occur in the second test.

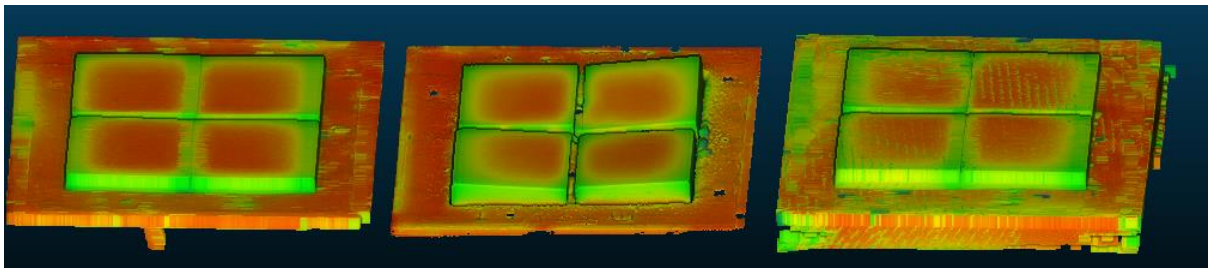

Figure 6.16 Oblique scans of the test platform at each stage of test. Left: before first test, Middle: after first test, Right: after second test. Note pitch of tiles in middle image following loosening

Applying the significant change function to the second test scans, tile three registers the most extensive change, in line with the difference plots. Tile two presents only a narrow line of significant change at the inner edge of the heel strike after the second test run, as with tile four after the first test. Tile four registers the smallest amount of change of all tiles in both tests.

Moving on to the surface roughness measurements taken with the INNOWEP TRACE-iT, each test run propagated change in the Rz value for all tiles, regardless of consolidant or position. Referring to table 6.5 shows that during the first test run there was significant change to all areas of the wear

zone across the test platform, whereas in test run two none of the zones passed the significance threshold of α0.01. This may well reflect a combination of elements such as the deposition of loose material from the broken-out mortar in the first test, and the significant reduction of this in the second trial. The second element that may have influenced this is that the first test may have removed all loose or proud material from the surface of the stone, with the result that the surface going into the second test was already consolidated by abrasion.

6.5 Conclusion

This experiment had two main objectives. The first was to improve understanding of how sandstone erosion develops in areas of high pedestrian footfall, with a view to informing conservation practice. The second objective was to evaluate the potential of consolidant treatments to mitigate footfall-driven erosion by comparing changes between consolidated and unconsolidated surfaces within a sample floor surface.

A novel element of this experiment was the use of the mechanical Pedatron machine, and thanks must be given to SATRA Technologies for working to facilitate access to their lab and equipment, especially during the COVID-19 lockdown. In all, the Pedatron performed its function exceptionally well; propagating the equivalent of two years' worth of visitor footfall in less than four days. This experiment would not have been possible within the timeframe of a DPhil without this mechanised simulation. Further to the concept testing steps of this experiment, further repetition of test runs would allow for the study of the development of this mechanical erosion, and with the addition of more incremental steps allowing for animation of scans, the pattern and nature of pedestrian erosion could be far better understood.

The experiment used two non-destructive and portable systems to generate datasets for analysis. The Creaform Handyscan 700 laser scanner, and the INNOWEP TRACE-iT optical surface roughness sensor. Regarding the Creaform scanner, the experiment effectively demonstrated the suitability of the process for the detection of sub-millimetre change in sandstone surfaces vulnerable to physical

erosion. The Handyscan and its native VX rendering software produced a range of useful instantaneous readings which allowed users to ensure that data collection had been successful and had no missing parts, a key consideration when planning on-site monitoring. Furthermore, the ability to export these models in a range of formats suitable for analysis in other software packages adds to its value as a technique. The combination of iterative closest point (ICP) and multiscale model-to-model scale comparison (M3C2) functions as available through the open source CloudCompare software suite provided a robust and verifiable means of quantifying change between the laser scan models and defining statistical thresholds for the significance of changes.

The use of the TRACE-iT surface roughness sensor added a second level of data, offering the potential to see deposition of material within the changing surface of the samples at a resolution not detected by the laser scanner. It is clear that without the TRACE-iT there would not have been any clear indication that the mortar material loosened during test run one had any bearing on the condition of the stone at the end of that test. Working with these two metrics allows for a high resolution and highly accurate visualisation to be created of the material to be studied.

The second stated aim of the experiment was to use these techniques to determine the presence and performance of consolidants on sandstone, in their capacity as a wear-resistant treatment for stone. In this instance, the laser scans were not able to detect any effect of consolidant on erosion. The results from the TRACE-iT were similar, there were differences recorded in the data between consolidated and non-consolidated tiles, although not passing the statistically significant threshold. Despite this, the instrument has demonstrated that it is capable of detecting change at this scale, and at the level of expected change based on the footfall. Overall, the concept of mimicking in-situ wear using mechanical simulation such as with the SATRA Technologies Pedatron has proved its use for heritage science research. A cost-effective and efficient way of facilitating long-term change in a short time, whose further application should be fully investigated. Finally, the two non-destructive techniques used here have proved themselves capable of operating on samples both within a

laboratory setting and potentially in the field. Neither of them needed a controlled environment to operate in, nor require stable infrastructure such as mains electricity or fixed workstations. The experiment can therefore be considered both informative and successful, in the context of the Sandstone Consolidants Project.

Chapter Seven: Discussion and Conclusions

7.1 Introduction

The discussion and conclusions is separated into two main sections; the discussion will look at the main aim and objectives of the project and discuss the extent to which the work carried out within this thesis has met each of them. Following this, the second, concluding section will form a final evaluation of the project overall, drawing conclusions as to the overall success of the project in meeting its aim.

The overall aim of this project was "**To improve the evaluation of consolidant performance on deteriorating sandstone through the combined use of laboratory and field experimentation".** This aim was achieved through addressing four main objectives, listed here:

Objective 1. To investigate the development of a novel methodology for the preparation and analysis of sandstone for consolidant assessment trials

Objective 2. To investigate the use of sample-based and structure-based experiments in field settings for the assessment of consolidant performance on sandstone

Objective 3. To investigate the use of simulated wear experiments for the assessment of consolidant performance on sandstone

Objective 4. To produce a 'Toolkit' of methods for the evaluation of consolidant performance on sandstone, arising from Objectives 1,2, and 3

Looking at each of these in turn, **Objective one** was met through laboratory preparation work as outlined in chapter three, covering sample preparation for elements of all experimental work undertaken. The heat weathering process as adapted from Franzoni *et al* (2013) and Grove (2017) provided a suitably conditioned stone substrate for the application of both TEOS and MTMOS consolidants used throughout. For the purposes of this project, trialling was focused on Locharbriggs sandstone, identified and chosen through its use on sandstone heritage sites such as the case study at Kenilworth (chapter two), and through advisory literature such as by Historic England (2017a). By using heat exclusively as the catalyst for change, and setting aside more immediately deleterious

weathering methods (such as salt weathering) owing to the complexity involved in controlling many of the processes of deterioration (Doehne 2002), the procedure can be readily applied to other lithotypes without the need for highly specialised facilities or testing equipment. The approach was successful as a preparation of freshly quarried stone for the acceptance of consolidants, evidenced by a reduction in P Wave Velocity of around 15% (see §4.3.2.3). Further to this, the effectiveness of both application and assessment (data collection) methods trialled in this part of the project are borne out in both the exposure rack and test wall method, notably P Wave Velocity, and Microwave Moisture measurement, evidenced by the use of comparative natural samples in each which allow for the quantification of change across sample preparation and size differentiation. The test wall trial (chapter five) further demonstrated the ability of microwave moisture meter technology to detect changes in performance relating to sample size, at least over a minimum size threshold (see §5.5). In addition to the steps set out within this thesis, and thanks to a grant of beamtime at the Harwell Science campus from the Science and Technologies Facilities Council, an experiment has been carried out using neutron beam technology to investigate consolidant distributions. As a result of the COVID-19 disruption, this could not be completed and included in this thesis, but will be developed and written up during an EPSRC Impact Accelerator Award Project "Bridging the gap: An online toolkit to help conservation professionals evaluate treatments for historic sandstone" (Project Ref: 0010550) that will lead on from this work.

Project **Objective two**, pertaining to the use of sample- and structure-based field trials in the assessment of consolidant performance, was addressed in experimental chapters four and five. Looking first at the exposure rack trial, results demonstrated that these sample-based field trials provide useful data on consolidant performance, especially when monitored using Pulse Wave Velocity. The parallel use of pre-treated, pre-weathered, and samples in a natural condition was key, as the comparative assessment of all groups provided contextual data for the behaviour of treated samples.

Some tweaking of the data collection timing would be required to maximise the usefulness of the data from this trial. Aligning rainfall events, extremes of hot and cold, and more data points of differential relative humidity with data collection could be better achieved through the introduction of flexibility in timing, though in the case of the exposure rack trial there were enough coincidences to provide the necessary data for interpretation. Taking mass first, whilst it was measured throughout, there was a lack of significant variability within the data to provide any useful metric of change. The arbitrary monthly-spaced data collection may be responsible for this, as data collection did not fall during the heavy rain events that may have resulted in significant liquid uptake in the samples. However, It could equally be argued that small samples such as the 70 mm^3 cubes used here simply are not large enough to take up sufficient liquid during a single rain event as experienced in a typical British year. Furthermore, P Wave provided the most immediately evident signs of change in the exposure rack trial. Of note were the early readings following consolidation and exposure, which denoted a significant increase in velocity related to the presence of consolidant (up to ~30% for TEOS and ~20% in MTMOS treated samples, §4.3.2.3). As the treatment progressed through its evaporation-hydrolysis process, the readings reduced as would be expected until stabilising around a mean more analogous to pre-treated samples. Colorimetry was useful in confirming the changes to surface condition following consolidation, but less effective in the measurement of all but the most extreme measures once in field conditions. Towards the conclusion of the exposure rack trial, some bio-colonisation was beginning to appear on some of the samples (particularly unconsolidated sets), a phenomenon which suggests that in an extended trial the technique would have become more informative. Also of note here is the combined value of using the three techniques in collaboration. Through reference to one another it has been possible to increase confidence in the data gathered from each, for example regarding the influence of moisture (using mass as a proxy) and P Wave Velocity in the rack trial, where the former is understood to influence the latter (Hu *et al* 2016). In addition, to this the importance of having detailed and reliable

meteorological data from the local environment has been key, without which it would have been extremely difficult to contextualise many of the data collected.

Moving on to the test wall trial, remaining with project **Objective two**, the increased complexity in its design allowed for a more diverse range of questions to be addressed within a single field trial. Comparison to the Brethane trial previously conducted at Kenilworth Castle (see p22 and p47-8) and other sandstone sites during the 1980s and 1990s allows for a demonstration of where these model scale field trials can play an important role in modern research. Whilst the sort of trials represented by the Brethane tests are not practically or ethically feasible in the UK today, test wall type trials offer a useful alternative in a range of ways. In the earlier type of trial, the removal of cores is common, and though none have been taken from the wall as part of this project, there is no constraint- practically, ethically, or legislatively in taking them from test structures, something that would not be possible on most heritage structures today due to legislative protections. Samples taken from a model scale structure could easily be used to form comparative studies with previous field trials such as the Brethane tests, where core samples up to a depth of 100mm were taken from the structure. In this regard, the wall provides the option to sample the façade up to an analogous depth (the test wall being 150 mm deep). The conditions faced by the wall, which can be orientated to mimic any given elevation on a heritage structure, can be manipulated to be directly analogous to those faced on an extant heritage asset, with natural weather conditions possible augmented- where required- with the application of simulated rainfall (as per Fusade *et al* 2019) or heat. In practice, it may always prove beyond the capability of artificially weathered samples, or structures built from them to directly replicate historic structures. Where possible, the use of historic materials taken from a sit*e* may overcome this (although ageing of any mortars used presents another set of issues), although as discovered during the MRes project which preceded this work, obtaining these samples is rarely straightforward, if possible at all and their exact weathering histories are often unknown. This being the case, there is value to further developing the artificial weathering processes

piloted here, to test methods which might work on other lithotypes and induce a wider variety of characteristic changes.

In addition to the comparison to previous trial types, there are a number of design features within this trial that provide an increased variability in data. Differentiated block sizes within the test structure are a good example of this; these elements allowed for direct comparison of mass as an influencing factor in consolidant uptake and performance, a factor which was effectively identified and confirmed through testing. In addition to the influence of size on consolidant performance, the wall allowed for the comparison of behaviour of unconsolidated stone for both artificially weathered and natural-state samples. These provided important insights into the effect of the heat weathering process on samples in relation to size, and the presence of variably sized natural state (control) samples allowed these inferences to be placed into context. Finally, the size of the test structure must be evaluated in relation to its complexity and the case study it seeks to simulate. There are several factors that must be considered when designing and constructing such test pieces; including cost, complexity of research design, safety, and longevity. Of the former, materials and expertise are a large potential drain on project finances. The materials for this modest test wall totalled almost £1000, and were it not that the author was able to carry out the sample cutting and subsequent construction of the wall this would have been significantly higher. In other situations there may not be the option of long-term accommodation of the structure without ground rent, and safety of the public must be taken into account if any structure is to be left in place at the conclusion of the test. Of the other considerations listed here, longevity and size of trial are important. One of the key findings from these trials is that one-year experiments are not sufficient for the assessment of consolidants in the round. The extension of this work into three-, five-, or ten-year research projects would enable a more in-depth analysis of the treatments over a full use-cycle.

One of the positive aspects of the dual field trial at Wytham was the ability to make cross-category comparisons between the exposure rack and test wall. Aside from block size variations, consolidant

application method and sample position within an exposed structure were both examined as part of the trial. Of these, application method yielded interesting data, wherein the size of sample was demonstrated to be a determinant factor in consolidant performance related to application method, with the largest sample size in the test wall returning lower moisture meter values when brush treated, in contrast to the smaller samples which performed better when treated by capillary action. For the test wall trial, the MOIST350B provided a quick and highly effective means of gathering information; especially when used in concert with the gravimetric calibration method and visualised using the purpose made *R* software script. These provide a robust and rapid reference source for examination of field data, and both methods will be made freely available for other researchers as part of the toolkit (**objective four)**. As with other elements of this DPhil project, the COVID disruption impacted this field trial. It had been planned that high frequency radar would be trialled as a second comparative data collection method, but due to restrictions on travel and training this was not possible within the timeframe. Overall, both sample- and structure- based field trials have demonstrated an effective means of collecting valuable information on both the behaviour of sandstone and on consolidants applied to it. The crossover element of this trial with the exposure rack is an important factor in the holistic design of the project, allowing for comparative testing of performance of samples between the two tests. Inclusion of samples such as the “F” category blocks into structure-based trials should not be limited to purpose-built test walls such as used here. In principle, these can be readily incorporated into a range of extant heritage structures for medium- to long- term trials, particularly where the historic fabric itself is protected.

Objective three is principally addressed through the Pedatron erosion trial. In this novel? experiment, the effects of 200,000 ‘heritage visitor’ steps were simulated in two short experimental trial runs on a replica floor surface. The experiment comprised three main assessment stages: first was the concept-testing of simulated wear trials for heritage surfaces such as (but not limited to) stone flooring. The second element of the experiment was the trialling of two portable, non-

destructive methods (3D scanning and optical surface roughness sensor); and the final part of the testing inspects free-to-use 'open source' comparison software for the analysis of scan data.

Taking these in turn, the design of the experiment was derived from observations on site at Kenilworth Castle (see §2.2.2), where an area of approximately 2328 m^2 of stone flooring is exposed to visitor footfall every year. On average, the castle welcomes over 100,000 visitors each year (Visit Britain 2018) representing a significant potential driver of change to historic surfaces. In order to develop a method for measuring change over a movable target area, the test platform was built to trial the use of portable scanning equipment, short- cutting the time required to measure change on the heritage asset itself. In facilitating wear over two short experimental runs, the Pedatron walking foot allowed for the creation of a directly applicable dataset without the need for an extended on-site data collection period. Further to this, by using replica tiles in a remote location, the requirement for complex legislative approval was removed, a not insignificant simplification for the management of the project. As with the experimental structure in the test wall trial, the wear platform used in the Pedatron experiment has proved a durable item and remains available for further test runs. At the conclusion of this DPhil project, two of the tiles within the platform are consolidant treated, whilst two are not. This allows for the future treatment of the untreated samples using an alternative consolidation method for further test runs, facilitating a broader level of information to be gathered from the same experimental pieces. To this end there are a number of possibilities available to the researcher. The Pedatron itself is open to adaptation; speed and pressure of footfall can be altered, as well as the type of footwear used. Indeed, simply running the test to a much higher step count would yield valuable insights, allowing a more direct comparison with wear patterns on-site at Kenilworth (or other venues) and adaptation of the method as required. Furthermore, the Pedatron itself is not the only mechanism for simulating this wear, there are other devices within the SATRA facility alone that would allow for an augmented level of simulation, including those for wheeled and pressure point erosion (mimicking wheelchair and trolley/cage use, and high heels or walking aids respectively).

Turning to instruments trialled during the experiment, the INNOWEP TRACE-iT optical surface roughness sensor, and the Creaform Handyscan portable 3D scanning system formed the basis for data collection. The latter instrument is commonly used in engineering and manufacturing testing, including quality control, but although other laser scanning systems have been utilised in conservation science, the self-contained, mobile Creaform instrument has little or no use-history in heritage science. Likewise, the TRACE-iT optical roughness sensor is underused in these type of erosion trials (although there are examples such as Sanmartin *et al* 2020); and this experiment was the first example of the two methods being used together to the author's knowledge. Both methods proved effective in the detection of change in surface conditions, and their portability and ease of use would make both appropriate for use in other trials such as the sample and structure based field trials within this project. With regards to the detection of consolidants and their effect on surface wear, changes to tile condition at both scales (sub-millimetre scanning, and micron resolution surface roughness) were registered successfully, showing minimal differences in performance between consolidated and unconsolidated tiles. The laser scan data detected significant change in all tiles at each scanning stage, and though there is variability between the extent and depth of wear between consolidated and non-consolidated tiles, no clear differences emerge. In addition to this, surface roughness values also showed change between test runs, though none of the values passed the threshold for statistical significance. What is clear from these test runs, is that both metrics offer an effective way of identifying change, and further application in repeated or analogous tests will bear this out.

The third and final experimental element of the trial was testing the use of the 'open source' software package CloudCompare to combine and examine 3D point clouds generated by the laser scanning, principally for the purpose of measuring change. This component of the trial pertains to making as many as possible people able to access and interpret datasets. Traditional CAD-CAM (Computer Aided Design- Computer Aided Manufacture) type software packages capable of handling these complex datasets can be prohibitively expensive, with industry standard AutoCAD costing

between £1986 and £3594 per annual subscription (prices correct for June 2021), and requiring extensive training and support, often including a need for specialist hardware. By comparison, CloudCompare is not only free-to-use, but supported by an extensive user community, peer reviewed papers outlining the analytical methods used within (e.g. Lague *et al* 2013, James *et al* 2017), and a range of free text and video tutorials. Hardware requirements for this processing are also no longer punitively expensive. Standard office specification PCs with 8GB of RAM and SSD storage are capable of handling these datasets, although it is highly desirable to have an upgraded graphics processing unit (for this project a 6GB graphics card was used to good effect). Distance measurement (between aligned point clouds) is carried out using an iterative combination of methods that are each appropriate for analysis at different scales, increasing in resolution with each successive step. In practice, the application of the M3C2 (Multiscale model-to-model cloud comparison) algorithm is straightforward, and the level of manipulation available through its application provides a range of outputs suitable to this kind of analysis. The option to apply a 0.05 significance value though calculation of total sample depth and distance between aligned clouds allows for an important statistical confidence to be applied, and offers a useful binary metric for the definition of wear. In conclusion, each of the three experimental elements of this trial has proven to be effective in facilitating and detecting change, offering a time efficient and robust means of mimicking on-site erosion to help inform conservation management.

Project **objective four**, the final element of the DPhil work contained herein, pertains to the creation of a 'toolkit' for the evaluation of consolidant performance. This encompasses the evaluation of all methods used, assessing both their capabilities and the ease in which each of them can be used by a range of potential operators including academics, researchers, and conservators. Taking elements of each of the three previous objectives, and work from chapters three to six in this thesis, the concept of the toolkit is introduced here, and will be further developed in an EPSRC Impact Acceleration Project that follows this DPhil thesis.

Table 7.1 The four toolkit compartments arising from the Sandstone Consolidant Project

Preparation	**Trialling**	**Measurement**	**Analysis**
Workflow			
-Stone selection -Heat Weathering -Sample size assessment -Consolidant application method	-Sample based Trials -Structure based trials -Simulated wear trials	-Water Uptake -Ultrasonic P Wave -Colorimetry -Microwave Moisture Meter -Portable 3D laser Scanning -Optical surface roughness sensor	-ANOVA and T tests for significance -Opensource software e.g. CloudCompare, "R"

Summarised in table 7.1, the 'toolkit' concept includes each operational step taken within this thesis in a decision-making process for further research. The toolkit itself represents a quick reference tool for sandstone research which shapes possible future projects by allowing researchers to see what worked for quartz rich sandstone such as Locharbriggs, and presents alternative formats for fieldwork which can draw on the design and execution of the three experiments contained herein. It is envisaged that this basic framework will be taken into the EPSRC IAA "Bridging the Gap" project, and will form the basis of a formalised decision making tool which amalgamates items from each area (as relating to the columns of Fig 7.1) into a 'holistic research design assistant' guiding the decision making process from the pairing of consolidant types with stone substrate, through pre-treatment and experimental design, to the selection of testing equipment and analysis-visualisation steps.

Column one of figure 7.1 relates to **objective one** as discussed earlier in this chapter. The heat weathering process has facilitated successful consolidation uptake by temporarily increasing porosity without causing irreversible damage to the substrate (as borne out in the P Wave results within 4.3.2.3). The use of differentiated sample sizes in relation to the test wall trial (**objective two**) provides an extra level of understanding for project designers looking for guidance on creation of

sample sets. Coupling this with results of the application method comparisons from the test wall further informs the design of future projects by again offering insight into how samples may behave based on size and method of consolidation.

Moving on to the second column, guidance is available from these items on the most appropriate setting for any future tests. Direction can be sought relating to the complexity of research design, and by the conditions that are to be replicated therein. Exposure rack type trials have been shown here to be useful in providing simple performance assessments for materials and treatments. For those projects seeking direct comparison with extant heritage structures, or those looking for studies of more complex multi-level relationships, the format of the structure-based and simulation-based trials of chapters five and six (**objectives two** and **three**) provide useful guides as to the value of both approaches. These can be adapted to a range of situations, placed near to extant assets or placed in controlled environments for simulated weathering, or abraded using a variety of mechanical aids.

Central to the creation of the toolkit is the testing and application of a suite of instruments, each with ease of use and reliability in mind for a range of users. The tools used for assessment of consolidant performance and stone behaviour are separated into two broad categories: internal condition and surface condition. For the former, direct measurement of sample performance has been carried out using open capillarity testing during sample preparation, and Ultrasonic P Wave and the Microwave Moisture Meter during trials. The P Wave assessment used in this trial is limited to direct measurement, which requires access to two opposite sides of a sample throughout testing, but in this capacity it showed that it was capable of producing reliable field data in a range of weather conditions and therefore is worthy of a place within the toolkit for stone of this type. Further trials may be added to the work here on the P Wave with transducers in an indirect array, with both transducers placed on the same face of the sample. This would allow for the technique to

be further used on larger, more complex structures such as extant buildings, where both faces may not be accessed for measurement.

In contrast to P Wave measurement, the MOIST350B moisture meter works with only a single sensor head and therefore can be used on more complex structures such as at the case study site at Kenilworth Castle. The ability to use different sensor heads for surface and deep moisture assessment (up to a depth of approximately 200 mm) makes this technique extremely useful, and tests carried out here to calibrate the values produced have shown that the output has a direct and quantifiable relationship with real moisture conditions in the stone. The MOIST350B is a contact-only instrument in contrast to the Punditlab P Wave sensor which uses a coupling gel to prevent wave attenuation, so it is more readily usable where heritage materials are to be directly tested. Moving to the surface condition measurement tools, the list includes assessment of colour (colorimetry), shape (3D laser scanning), and texture (surface roughness). These cover three of the most common mechanisms of sandstone deterioration in mineralogical change (including efflorescence and leaching), alveolisation, and surface breakdown (powdering, flaking, and delamination). All of the instruments trialled here have effectively demonstrated a capability of detecting change at a range of scales, and the results of each are easily verified using simple statistical tests.

The range of instruments gathered here all fall into the category of non-destructive testing, meaning their use can be sanctioned in the most sensitive of conservation situations, with the only caveat that the use of the Punditlab may require legislative approval owing to the coupling gel, which although water-based and non-corrosive leaves a small residue on the surface of the test area. These five instruments, covering internal and surface condition assessment to a range of depth and resolutions, provide a significant combination of tools for research on sandstone in a range of lab and field trials going forward. This toolkit concept is to be formalised following the completion of this DPhil project into a range of differentiated teaching and support materials for potential

researchers, during the EPSRC Impact Accelerator Award "Bridging the Gap" project, and will be further augmented by the addition of high resolution radar surveys of the test wall, and neutron tomography scanning of samples taken from the exposure trial, the latter thanks to a grant of beamtime at the Harwell Science campus from the Science and Technologies Facilities Council.

7.2 Conclusions

The overall aim of this project was "**To improve the evaluation of consolidant performance on deteriorating sandstone through the combined use of laboratory and field experimentation**". This is a broad aim, and variability in materials, histories and environmental situations make it difficult to extrapolate results to wider contexts. As noted in chapter 1, sandstone is a diverse and often complex natural building material and many different lithotypes could have been used for the research. Any project focused on historic stone must take into account the characteristics of the selected stone, and the implications of this for the wider applicability of the research arising from it, particularly where this represents a sample substrate that is unique. In this regard, the choice of Locharbriggs sandstone for this project represents a conscious move to design the work around a stone that is not only found in existing historic structures, but one that is still being quarried and used in both new buildings and repairs to a range of existing sandstone structures (including those not originally built from Locharbriggs) and that will become increasingly relevant for conservation architects and conservators as the 21st century progresses. That the stone is used not only in the UK, but also in Ireland and the United States only adds to its suitability as the basis for this research, included as it is in some of the world's most prominent monuments (the Statue of Liberty being a notable example). Coupling this with two of the most commonly applied Silane consolidants (TEOS and MTMOS) further widened the potential audience for this research, not least in the UK where consolidant application is still far from the norm in conservation practice.

Much of the previous research reviewed in the preparatory stages of this project (and summarised in §1.2) on consolidants and their performance focuses on a laboratory **or** field based experimental

approach, selecting a small number of instruments or methods to interrogate their samples throughout. The alternative approach adopted here which combined field and laboratory approaches, and deliberately selected a wide array of evaluation methods allowed for the assessment of a far wider range of instruments and methods, including some that did not make it into the final analysis (such as Equotip surface hardness testing and Grindosonic impulse excitation technique). The clear benefit of this combined approach has been the ability to test each method and instrument in a range of situations, and then where possible applying it in more than one experiment, thus demonstrating its flexibility in use, whilst simultaneously developing a range of novel applications for the visualisation and interpretation of data.

Underpinning the approach to this project is the concept of holism (as recognised in the thesis title), which posits that the whole is more than the sum of its parts. In essence, the holistic approach taken here brought together multiple approaches and methods to provide an 'in the round' evaluation of the performance of two consolidants on one type of sandstone of importance to Kenilworth Castle and other sites, which is flexible enough and robust enough to be adapted for use on other products, stone types and situations. A structured, unified approach has been developed which combines sample-based laboratory methods with structure-based field work, standard testing with novel methodologies, and well-understood experimental frameworks with entirely novel erosion trials. By extension, the EPSRC Impact Accelerator Project which follows this project will take this further, expanding and formalising the 'toolbox' into an open access resource that will provide practical guidance for a diverse audience including not only academic researchers but conservators and stakeholders in historic assets.

Overall, the narrative arc of this project, which began in literature review and moved through *in situ* observations and engagement with conservation managers before the formulation and successful execution of three experiments, each in turn increasing in complexity, demonstrates the value of field observation as a formative stage. That the combined results from both field trials and the

Pedatron experiment can be used to inform conservation practice at sites such as the case study at Kenilworth Castle is final proof of concept, providing the basis for an ongoing feedback loop for future trials of this nature.

8. Bibliography

Adams, A.E., MacKenzie, W.S., & Guildford, C., 1984, *Atlas of Sedimentary Rocks Under the Microscope*, The English Language Book Society/ Longman Scientific and Technical, Harlow, Essex

Adamson, C., McCabe, S., Warke, P.A., McAllister, D. and Smith, B.J., 2013. "The influence of aspect on the biological colonization of stone in Northern Ireland". *International Biodeterioration & Biodegradation*, *84*, pp.357-366

Allison, R.J. & Bristow, G.E., 1999 "The Effects of Fire on Rock Weathering: some further considerations of laboratory experimental simulation" *Earth Surface, Processes and Landforms*, Vol 24, Pp 707-13

André, M.F., Phalip, B., Voldoire, O., Vautier, F., Géraud, Y., Benbakkar, M., Constantin, C., Huber, F. and Morvan, G., 2011. Weathering of sandstone lotus petals at the Angkor site: a 1,000-year stone durability trial. *Environmental Earth Sciences*, *63*(7), pp.1723-1739

Andrew, C., Young, M., & Tonge, K., 1994, *Stone Cleaning- A Guide for Practitioners*, Historic Scotland and the Robert Gordon University, Edinburgh

Aoki, H. & Matsukura, Y. 2007, "A new technique for non-destructive field measurement of rock-surface strength: an application of the Equotip hardness tester to weathering studies", *Earth Surface Processes and Landforms*, Vol 32 Issue 12, Pp1759-1769

Arnold, L., Honeyborne, D., & Price, C. 1976, *Conservation of Natural Stone*, Chemistry and Industry, pp. 345-347

Artioli, G., 2010. *Scientific methods and cultural heritage: an introduction to the application of materials science to archaeometry and conservation science*. Oxford University Press.

Ashurst, J., and N. Ashurst. 1988. *Practical Building Conservation.* Vol. 1*, Stone Masonry*. English Heritage Technical Handbook. English Heritage, Swindon

Ashurst, N. 1994. *Cleaning Historic Buildings,* Donhead Publishing, London

Ashurst, J. 1998. "The cleaning and treatment of limestone by the lime method", In *Conservation of Building and Decorative Stone*, ed. J. Ashurst and F. G. Dimes, vol. 2, 169–76. Butterworth-Heinemann Series in Conservation and Museology. Butterworth-Heinemann, London

Ashurst, J. & Ashurst, N. 2005, *Practical Building Conservation, Volume 5; Wood, Glass and Resins*, English Heritage, Swindon

Ashurst, J. 2007. *Conservation of Ruins*. Butterworth-Heinemann Series in Conservation and Museology, Butterworth- Heinemann, London

Ashurst, J., and Dimes, F. (eds) 1998, *Conservation of Building and Decorative Stone*. Butterworth-Heinemann Series in Conservation and Museology, Butterworth-Heinemann, London

Assefa, S., McCann, C., and Sothcott, J., 2003 "Velocity of Compressional and Shear Waves in Limestones," in *Geophysical Prospecting*, Vol. 51, No. 1, pp. 1-13

AutoCAD 2021, "AutoDesk Products", Available at: https://www.autodesk.co.uk/products

Ban, M., Baragona, A., Ghaffari, E., Weber, J. and Rohatsch, A., 2016. "Artificial aging techniques on various lithotypes for testing of stone consolidants". In *Science and Art: A Future for Stone: Proceedings of the 13th International Congress on the Deterioration and Conservation of Stone* (Vol. 1, pp. 253-260)

Ban, M., De Kock, T., Ott, F., Barone, G., Rohatsch, A. and Raneri, S., 2019. "Neutron radiography study of laboratory ageing and treatment applications with stone consolidants" *Nanomaterials*, *9*(4), p.635

Baker, M. 2016*, "*Is there a reproducibility crisis?" *Nature* 533*,* 452–454*.*

Baraka-Lokmane, S., Main, I.G., Ngwenya, B.T. and Elphick, S.C., 2009, "Application of complementary methods for more robust characterization of sandstone cores" *Marine and Petroleum Geology*, *26*(1), pp.39-56.

Barberena-Fernández, A.M., Carmona-Quiroga, P.M. and Blanco-Varela, M.T., 2015. "Interaction of TEOS with cementitious materials: Chemical and physical effects". *Cement and Concrete Composites*, *55*, pp.145-152.

Benavente, D., de Jongh, M., Galiana-Merino, J.J., Pla, C., Martinez- Martinez, J., Lee, M., & Young, M. 2020, "Automatic Estimation of the P- and S- wave Onset Times in Weathered Sandstones by Salt Crystallisation" in Siegsmund, S. & Middendorf, B. (eds), 2020, *Monument Future: Decay and Conservation of Stone, Proceedings of the 14th International Congress on the Deterioration and Conservation of Stone, Volume I and II* Mitteldeutscher Verlag

Benjamin, D. & Sivilarkitekt, M.N.A.L., 2009. "Architectural Heritage: A Challenge to Sustainable Design Practices And An Opportunity For Learning From The Past" Smart and Sustainable Built Environments Conference, CIB W116. *Delft University of Technology*, *15*, p.19.

Best, W. 1860, "The state of the church and vicarage of Kenilworth in the diocese of Lichfield and Coventry and in the county of Warwick, from 1558 to 1716", *Warwickshire Antiquarian Magazine*, 2 61–2; Available at: Warwickshire County Record Office item: CR311/54

Bewley, R.H., Crutchley, S.P. and Shell, C.A., 2005. New light on an ancient landscape: lidar survey in the Stonehenge World Heritage Site. *Antiquity*, *79*(305).

Bergamonti, L., Bondioli, F., Alfieri, I., Alinovi, S., Lorenzi, A., Predieri, G. and Lottici, P.P., 2018. "Weathering resistance of PMMA/SiO2/ZrO2 hybrid coatings for sandstone conservation", *Polymer Degradation and Stability*, *147*, pp.274-283.

Bidner, T., Mirwald, P.W., Recheis, A. and Brüggerhoff, S., 2002. "Stone as sensor material for weathering", In *Understanding and Managing Stone Decay: Proceedings of the International Conference Stone Weathering and Atmospheric Pollution Network: SWAPNET 2001,* pp. 97-111

Bischoff, V., Englert, A., Nielsen, S. and Ravn, M., 2014. "Post-excavation documentation, reconstruction and experimental archaeology applied to clinker-built ship-finds from Scandinavia", *Archeologia Postmedievale* pp.21-29.

Bracci, S., Melo, M J., & Tiano, P., 2004. "Comparative study on durability of different treatments on sandstone after exposure in natural environment." In *I silicati nella conservazione: indagini, esperienze e valutazioni per il consolidamento dei manufatti storici. Congresso internazionale, 13-15 febbraio 2002: volume degli atti*, pp. 129-135.

Bradley, R., 2007, *The Prehistory of Britain and Ireland*, Cambridge University Press

Briffa, S.M., Sinagra, E. and Vella, D., 2012. "TEOS based consolidants for Maltese globigerina limestone: effect of hydroxyl conversion treatment", Available at: https://www.um.edu.mt/library/oar/handle/123456789/18235

Brimblecombe, P., 2004, "Damage to Cultural Heritage" in Saiz-Jimenez, C. (ed), Air Pollution & Cultural Heritage, A.A. Balkema/ Taylor & Francis, London Pp 87-90

British Geological Survey, 2020, BGS Lexicon of Named Rock Units: https://www.bgs.ac.uk/lexicon/lexicon.cfm?pub=HEY, accessed 10/07/20

British Geological Survey, 2021a, "Building Stone Database for Scotland": http://webservices.bgs.ac.uk/buildingstone/buildingstones/10014?q=Locharbriggs&mapType=recordMap&recordId=10014&recordType=buildingStone accessed 10/08/21

British Geological Survey, 2021b, "Building Stones of Edinburgh: Stratigraphy and Origin of Sandstones": http://earthwise.bgs.ac.uk/index.php/Building_stones_of_Edinburgh:_stratigraphy_and_origin_of_sandstones#Locharbriggs_Sandstone_Formation accessed 10/08/21

Brunskill, R.W., 1987*, Illustrated Handbook of Vernacular Architecture*, Faber & Faber, London

BSI, 2013, *BS7913:2013 Guide to the Conservation of Historic Buildings,* The British Standards Institution, BSI Standards Ltd, London

Butlin, R. N., Yates, T.J., and Martin, W. 1995, "Comparison of traditional and modern treatments for conserving stone" in Tabasso, M. (ed) *Methods of Evaluating Products for the Conservation of Porous Building Materials in Monuments*, ICCROM, Rome

Cappelletti, G. and Fermo, P., 2016. "Hydrophobic and superhydrophobic coatings for limestone and marble conservation", In *Smart Composite Coatings and Membranes*, pp. 421-452, Woodhead Publishing

Cardiano P., Ponterio, R.C., Sergi, S., Lo Schiavo, S., Piraino, P., 2005, "Epoxy-silica polymers as stone conservation materials" in *Polymer*, Issue 46, Pp 1857–1864

Chakrabarti, B., 1993 "An Assessment of Effects of Fire Damage to Stone in Building & Procedures for Restoration and Conservation of Stone in some Historic Stone Buildings" BRE Note N15/93, Pp 311-322

Chakrabarti, B., Yates, T. & Lowry, A., 1996, "Effects of Fire Damage on Natural Stonework in Buildings" *Construction & Building Materials*, Vol 10, No 7, Pp 539-44

Choquette, P.W. & Pray, L.C. 1970, "Geologic Nomenclature and Classification of Porosity in Sedimentary Carbonates". *AAPG Bulletin 54*

Ciliberto E., Condorelli, G.G., La delfa S., & Viscuso, E., 2008, "Nanoparticles of Sr(OH)2: synthesis in homogeneous phase at low temperature and application for cultural heritage artefacts" in Applied Physics A , Vol 92, Pp137–141

Clarke, B. L., & Ashurst, J. 1972. *Stone Preservation Experiments*. Watford: Building Research Establishment; London: Directorate of Ancient Monuments and Special Services

Clifton, J. 1980, *Stone Consolidating Materials; a Status Report 1118*, National Bureau of Standards

Clifton-Taylor, A., 1972. *The Pattern of English Building*, Faber and Faber, London

Coombes, M.A., Viles, H.A. & Zhang, H. 2018, "Thermal blanketing by ivy (*Hedera helix* L.) can protect building stone from damaging frosts", *Scientific Reports* 8

Conserv n.d. "The Lime Mortar Guide, in Collaboration with Leeds Beckett University". Available at: https://www.lime-mortars.co.uk/lime-mortar/guides/the-lime-mortar-guide

Creaform 2021 "HandyScan3D Black Series: The Truly Portable Metrology-Grade 3D Scanners", Available at: https://www.creaform3d.com/sites/default/files/assets/brochures/files/handyscan3d_brochure_en_hq_20210202_1.pdf

Crites, R., 2019, Personal Communication. Meeting between author and Rebecca Crites, Site Manager at Kenilworth Castle, 18th March 2020

Cumbrian Stone, ND, Locharbriggs Datasheet, Available at: https://cumbrianstone.co.uk/wp-content/uploads/2020/04/Locharbriggs-Datasheet.pdf

Danehey, C., Wheeler, G.S. and Su, S.C.H., 1992, June. The influence of quartz and calcite on the polymerization of methyltrimethoxysilane. In *Proceedings of the 7th International Congress on Deterioration and Conservation of Stone: held in Lisbon, Portugal, 15-18 June 1992* (pp. 1043-1052).

Daniele, V., and G. Taglieri. 2010. "Nanolime suspensions applied on natural lithotypes: The influence of concentration and residual water content on carbonatation process and on treatment effectiveness", in *Journal of Cultural Heritage* Vol 11, issue 1: Pp102–6.

De Ferri, L., Lottici, P.P., Lorenzi, A., Montenero, A. and Salvioli-Mariani, E., 2011. Study of silica nanoparticles–polysiloxane hydrophobic treatments for stone-based monument protection. *Journal of Cultural Heritage*, *12*(4), pp.356-363.

Dellepiane, M., Callieri, M., Corsini, M., Scopigno, R., 2011, *Using Digital 3D Models for Study and Restoration of Cultural Heritage Artefacts,* in *Stanco, F., Battiato, S., Gallo, G. (eds),* 2011*, Digital Imaging for Cultural Heritage Preservation,* CRC Press, Florida USA

DeWhite, E. 1975, "Soluble Nylon as Consolidation Agent for Stone", *Studies in Conservation*, Vol. 20, No. 1, Pp 33-34

Dillon, C., Bell, N., Fouseki, K., Laurenson, P., Thompson, A. and Strlič, M., 2014. "Mind the gap: rigour and relevance in collaborative heritage science research". *Heritage Science*, *2*(1), pp.1-22.

Doehne, E. 2002, "Salt weathering: a selective review" Geological Society, London, Special Publications, 205, 51-64, https://doi.org/10.1144/GSL.SP.2002.205.01.05

Domaslowski, W. 1969. "Consolidation of stone objects with epoxy resins", in *Monumentum* 4: 51–64. www.international.icomos.org/monumentum/vol4/vol4_3.pdf.

Dott, R., H., 1964, "Wacke, graywacke and matrix; what approach to immature sandstone classification?", *Journal of Sedimentary Research*; 34 (3), Pp625–632

Drdacky, M., Frankeova, D., & Slížková, Z. 2020, "Variations of Characteristics of Sandstone Subjected to Weathering and Conservation Interventions" in Siegsmund, S. & Middendorf, B. (eds) 2020, "Monument Future: Decay and Conservation of Stone, Proceedings of the 14th International Congress on the Deterioration and Conservation of Stone, Vol I and II, Mitteldeutscher Verlag Dutton, S. P., & Willis, B.J. 1998, "Comparison of outcrop and subsurface sandstone permeability distribution, Lower Cretaceous Fall River Formation, South Dakota and Wyoming" Journal of Sedimentary Research 68 (5): Pp890–900.

Egermann, R., Cook, D. and Anzani, A., 1991., "Investigation Into the Behaviour of Scale Model Brick Walls". *Brick and Block Masonry*, *1*, pp.628-635.

Eklund, J.A., Zhang, H., Viles, H.A. and Curteis, T., 2011, "Using handheld moisture meters on limestone: factors affecting performance and guidelines for best practice" *International Journal of Architectural Heritage*, 7(2): 207-224.

El-Gohary, M.A., 2013. Evaluation of treated and un-treated Nubia Sandstone using ultrasonic as a non-destructive technique. *Journal of archaeological science*, *40*(4), pp.2190-2195

Elhaddad, F., Carrascosa, L.A. and Mosquera, M.J., 2018. "Long-term effectiveness, under a coastal environment, of a novel conservation nanomaterial applied on sandstone from a Roman archaeological site". *Journal of Cultural Heritage*, *34*, pp.208-217.

EN (BS) 1341: 2012 **"**Slabs of natural stone for external paving. Requirements and test methods" British Standards Institution, London

EN (BS) 1925: 1999 "Natural stone test methods. Determination of water absorption coefficient by capillarity" British Standards Institution, London

EN (BS) 1926: 2006 "Natural stone test methods. Determination of uniaxial compressive strength", British Standards Institution, London

EN (BS) 1936:2006 "Natural stone test methods. Determination of real density and apparent density, and of total and open porosity", British Standards Institution, London

Evans, J.D. 1996, *Straightforward Statistics for the Behavioural Sciences*, Brooks/Cole Publishing, Pacific Grove. British Standards Institution

Fassina V. 1995, "New findings on past treatments carried out on stone and marble monuments' surfaces" in *The Science of the Total Environment*, Issue 167, Pp185-203

Fidler, J. (ed) 2002, *Stone: Stone Building Materials, Construction and Associated Component Systems. Their Decay and Treatment,* English Heritage Research Transactions 2. English Heritage, Swindon

Forster, A.M., 2010a. "Building conservation philosophy for masonry repair: part 1 "ethics"". *Structural Survey*.

Forster, A.M., 2010b. "Building conservation philosophy for masonry repair: part 2 "principles"". *Structural survey.*

Franzen, C. & Mirwald, P.W., 2004. "Moisture content of natural stone: static and dynamic equilibrium with atmospheric humidity". *Environmental Geology*, *46*(3-4), pp.391-401.

Franzoni, E. Graziani, G. Sassoni, E. 2015, "TEOS-based treatments for stone consolidation: acceleration of hydrolysis–condensation reactions by poulticing", *Journal of Sol-Gel Science and Technology*, Vol 74, Pp398–405

Franzoni, E., Sassoni, E., Scherer, G.W. and Naidu, S., 2013. Artificial weathering of stone by heating. *Journal of Cultural Heritage*, *14*(3), pp.e85-e93.

Freudenburg, N., Frühwirt, T., Kohl, K J., Kutz, M., Siedel, H., & Wichert, J. 2020 "Thermal Behaviour of Building Sandstone: Laboratory Heating Experiments vs Real Fire Exposure" in Siegsmund, S. & Middendorf, B. (eds) 2020, "Monument Future: Decay and Conservation of Stone, Proceedings of the 14th International Congress on the Deterioration and Conservation of Stone, Vol I and II, Mitteldeutscher Verlag

Fusade, L., Orr, S.A., Wood, C., O'Dowd, M. and Viles, H., 2019. Drying response of lime-mortar joints in granite masonry after an intense rainfall and after repointing. *Heritage Science*, *7*(1), pp.1-19.

Garrod, E. 2001, "Stone Consolidation; Halts Decay and Prolongs Life", in *The Building Conservation Directory 2001*, Cathedral Communications Ltd, Salisbury

Gaviglio, P., 1989, "Longitudinal Waves Propagation in a Limestone: The Relationship between Velocity and Density," *Rock Mechanics and Rock Engineering,* Vol. 22, No. 4, pp. 299-306

Gelest Inc, 2014, *Silane Coupling Agents; Connecting Across Boundaries*, Gelest, Pennsylvania, US. https://www.gelest.com/wp-content/uploads/Goods-PDF-brochures-couplingagents.pdf

Giorgi, R., L. Dei, and P. Baglioni. 2000. "A new method for consolidating wall paintings based on dispersions of lime in alcohol", in *Studies in Conservation* Vol 45 issue 3:154–61

Giorgi R., Ambrosi, M., Toccafondi, N., and Baglioni, P. 2010, "Nanoparticles for Cultural Heritage Conservation: Calcium and Barium Hydroxide Nanoparticles for Wall Painting Consolidation" in *Chemistry European Journal,* Vol 16, Pp9374 – 9382

Göller A., 2006, "Microwave scanning technology for material testing", in Proceedings of the 9th European Conference on NDT. DGZfP- Proceedings BB September 25–29 2006

Gomes, L., Bellon, O.R.P. & Silva, L., 2014. "3D reconstruction methods for digital preservation of cultural heritage: A survey". *Pattern Recognition Letters*, *50*, pp.3-14.

Goudie, A.S., Allison R.J. & MClaren, S.J., 1992, "The Relations Between Modulus of Elasticity and Temperature in the Context of the Experimental Simulation of Rock Weathering by Fire" *Earth Surface Processes and Landforms*, Vol 17, Pp 605-15

Griffith, M.C., Vaculik, J., Lam, N.T.K., Wilson, J. and Lumantarna, E., 2007. "Cyclic testing of unreinforced masonry walls in two-way bending", *Earthquake Engineering & Structural Dynamics*, *36*(6), pp.801-821.

Grossi, D., Lama, E.A.D., García Talegón, J., Iñigo, A.C., Iñigo, A.C. and Vicente Tavera, S., 2015. Evaluation of colorimetric changes in the Itaquera granite of the Ramos de Azevedo Monument, São Paulo, Brazil.

Grove, R., 2017, *Built on Sand, Predicting the Metrics of Weathered Sandstone in Heritage*, Master of Research Dissertation submitted August 2017, University College London

Gulotta, D., Wilhelm, K., Desarnaud, J., Otero, J., Grove, R., Leslie, A. and Viles, H., 2020. Integrated Strategy to Assess Conservation Treatments on Sandstone. *Studies in Conservation*, *65*(sup1), pp.P119-P123

Guidi, G., Beraldin, J. & Atzeni, C., 2004 "High-accuracy 3D modelling of cultural heritage: the digitizing of Donatello's "Maddalena"" in *IEEE Transactions on Image Processing*, 13; 3, Pp. 370-380

Hameed, F., Schillinger, B., Rohatsch, A., Zawisky, M. and Rauch, H., 2009. "Investigations of stone consolidants by neutron imaging", *Nuclear Instruments and Methods in Physics Research Section A: Accelerators, Spectrometers, Detectors and Associated Equipment*, *605*(1-2), pp.150-1

Hains, B.A., Horton, A. and Edmunds, F.H., 1987. *British Regional Geology: Central England (No. 10)* (3rd Edition), HMSO, London

Halsey, D.P., Dews, S.J., Mitchell, D.J. and Harris, F.C., 1995. Real time measurements of sandstone deterioration: a microcatchment study. *Building and Environment*, *30*(3), pp.411-417.

Hall, C. & Hoff, W.D., 2012, *Water transport in brick, stone and concrete 2nd Edition*, Taylor and Francis, London

Hansen, E., E. Doehne, J. Fidler, J. Larson, B. Martin, M. Matteini, C. Rodriguez-Navarro, E. Sebastian. Pardo, C. Price, A. de Tagle, J.-M. Teutonico, and N. R. Weiss. 2003, "A review of selected inorganic consolidants and protective treatments for porous calcareous materials" in *Reviews in Conservation* 4: Pp13-25

Hajpál, M. & Török Á. 2004, "Mineralogical and colour changes of quartz sandstones by heat", *Environmental Geology*, 46, Pp311–322

Henry, A. (ed), 2006, *Stone Conservation, Principles and Practice,* Donhead Publishing, Dorset

Hf Sensor, ND, "Process Moisture Measurement" Available at: http://www.hf-sensor.de/englisch/processmoisturemeasurementxe.html

Historic England, 2017a, *Strategic Stone Study: A Building Stone Atlas of Warwickshire*, Historic England, Swindon

Historic England 2017b, *Nanolime: A Practical Guide to its Use for Consolidating Weathered Limestone*, HEAG 151, Historic England, Swindon

Historic England 2021, "Long Meg and Her Daughters, List Entry1007866", Available at: https://historicengland.org.uk/listing/the-list/list-entry/1007866

Hochmańska, P., Mazela, B. and Krystofiak, T., 2014. Hydrophobicity and weathering resistance of wood treated with silane-modified protective systems. *Drewno: prace naukowe, doniesienia, komunikaty*, *57*.

Howe, E. 2007. *A Report on the Conservation of the Lichfield Angel*. Birmingham: Birmingham Museum & Galleries Collection Centre http://lichfield-angel.net/data/LichfieldAngel_Conservation_Howe.pdf

Hu, Y., Deng, H., Wang, W., Wang, Z., Zhang, X. and Assefa, E., 2016. "Influence of moisture content and stress cyclic loading amplitude on the dynamic characteristics of sandstone". *Electronic Journal of Geotechnical Engineering*, *21*(16), pp.5167-5182.

Huang, T.S. 1996, “Computer Vision, Evolution and Promise” in Vandoni, C.E. (ed) 1996, *Proceedings; Cern School of Computing,* European Organisation for Nuclear Research, Pp 21-25

Hutton Stone, ND, “Locharbriggs”, Available at: https://www.huttonstone.co.uk/portfolio/lochar-briggs/

ICOMOS 1965, *International Charter for the Conservation and Restoration of Monuments and Sites (The Venice Charter 1964)*, ICOMOS, Paris

ICOMOS 2003, *ICOMOS Charter- Principles for the Analysis, Conservation and Structural Restoration of Architectural Heritage*, ICOMOS, Paris

ICOMOS 2008, *Illustrated Glossary on Stone Deterioration Patterns*, ICOMOS, Paris

INNOWEP, 2017, “Test Report TRACEiT, mobile optical surface structure analysis” INNOWEP GMBH, Würzberg, Germany

INNOWEP, 2021, “TRACEiT 3D Mobile Optical Profilometer” Available at: https://www.innowep.com/traceit/

James, M.R., Robson, S. and Smith, M.W., 2017. “3-D uncertainty-based topographic change detection with structure-from-motion photogrammetry: precision maps for ground control and directly georeferenced surveys”, *Earth Surface Processes and Landforms*, *42*(12), pp.1769-1788.

Kahraman, S., and Yeken, T., 2008, “Determination of Physical Properties of Carbonate Rocks from P-wave Velocity,” Bulletin of Engineering Geology and the Environment, Vol. 67, No. 2, pp. 277-281

Kassab, M. A. & Weller, A., 2014, “Study on P Wave and S Wave Velocity in Dry and Wet Sandstone of the Tushka Region, Egypt”, *Egyptian Journal of Petroleum*, 24, Pp 1-11

Keay, A. N.D. “From Romantic Ruin to Historic Monument” available at: https://www.english-heritage.org.uk/visit/places/kenilworth-castle/history-and-stories/history

Kennedy, C. J., 2015, “The Role of Heritage Science in Conservation Philosophy and Practice”, The Historic Environment: Policy & Practice, 6:3, 214-228

King, E. 1988, “The Use of Resin (Polymer) Products in the Repair and Conservation of Buildings” in Ashurst, J. & Ashurst, N. 2005, *Practical Building Conservation, Volume 5, Wood, Glass and Resins*, English Heritage, Swindon

Konica Minolta ND, “*Precise Colour Communication Part III*”, Available at: https://www.konicaminolta.com/instruments/knowledge/color/part3/02.html

Lague, D., Brodu, N., & Leroux, J., 2013, “Accurate 3D comparison of complex topography with terrestrial laser scanner: application to the Rangitikei canyon (N-Z)” *ISPRS journal of photogrammetry and remote sensing*, *82*, pp.10-26

La Russa, M.F., Comite, V., Aly, N., Barca, D., Fermo, P., Rovella, N., Antonelli, F., Tesser, E., Aquino, M. and Ruffolo, S.A., 2018. “Black crusts on Venetian built heritage, investigation on the impact of pollution sources on their composition”. *The European Physical Journal Plus*, *133*(9), pp.1-9.

Leica 2016, “Leica ScanStation P30/P40 Because Every Detail Matters”, Available at: https://leica-geosystems.com/products/laser-scanners/scanners/leica-scanstation-p40--p30

Lehmann, J. 1970, “Damage by Accumulation of Soluble Salts in Stonework”, *in Conservation of New Stone and Wooden Objects* Proceedings of The International Institute for Conservation of Historic and Artistic Works, London

Licchelli M., Malagodi, M., Weththimuni, M., Zanchi, C., 2014, “Nanoparticles for conservation of bio-calcarenite stone” in *Applied Physics A,* Issue 114, Pp673–683

Liu, R., Han, X., Huang, X., Li, W. and Luo, H., 2013. Preparation of three-component TEOS-based composites for stone conservation by sol–gel process. *Journal of sol-gel science and technology*, *68*(1), pp.19-30.

Logan, J.M., 2004. “Laboratory and case studies of thermal cycling and stored strain on the stability of selected marbles”. *Environmental Geology*, *46*(3-4), pp.456-467.

López, F. J., Lerones, P. M., Llamas, J., Gómez-Garcia-Bermejo, J., & Zalama, E., 2018 “A Review of Heritage Building Information Modelling (H-BIM)” in *Multimodal Technologies and Interaction* 2;2,21

Lorusso, S., Natali, A. and Matteucci, C., 2007. Colorimetry applied to the field of cultural heritage: examples of study cases. *Conservation Science in Cultural Heritage*, *7*, pp.187-220.

Ludovico-Marques, M. and Chastre, C., 2014. Effect of consolidation treatments on mechanical behaviour of sandstone. *Construction and Building Materials*, *70*, pp.473-482

Martin, B., Mason, D., Teutonico, J.M. and Chapman, S., 2002. “Stone consolidants: Brethane report on an 18-year review of Brethane-treated sites”, in Fidler, J. (ed) *Stone: Stone Building Materials, Construction and Associated Component Systems. Their Decay and Treatment,* English Heritage Research Transactions 2. English Heritage, Swindon

McAllister, D., McCabe, S., Smith, B.J., Srinivasan, S. & Warke, P.A., 2013, “Low temperature conditions in building sandstone: the role of extreme events in temperate environments”, *European Journal of Environmental and Civil Engineering*, 17:2, 99-112

McCabe, S., Smith, B.J. & Warke, P.A., 2007a, “Preliminary Observations on the Impact of Complex Stress Histories on the Response of Sandstone to Salt Weathering: Laboratory Simulations of Process Combinations”, *Environmental Geology* Vol 52, Pp269-76

McCabe, S., Smith, B.J. & Warke, P.A., 2007b, “Sandstone Response to Salt Weathering Following Simulated Fire Damage: A Comparison of the Effects of Furnace Heathing and Fire” *Earth Surface Processes and Landforms* Vol 32 Pp1874-83

McKay, A. G. 1975, *Houses, Villas, and Palaces in the Roman World*, Thames and Hudson, London

Messali, F., Ravenshorst, G., Esposito, R., & Rots, J. 2017, “Large-scale testing program for the seismiccharacterization of Dutch masonry walls”, in *16th World Conference on Earthquake : Santiago, Chile*

Met Office, 2021, “UK Climate Averages, Coventry, West Midlands”, Available at: https://www.metoffice.gov.uk/research/climate/maps-and-data/uk-climate-averages/gcqfjn5xn

Mirowski, R. 1988. “A new method of impregnation of stone historical objects” in *Proceedings of the 6th International Congress on Deterioration and Conservation of Stone, 1988, Poland*

Molyneux, N. A. D. 2006, “Kenilworth Castle, Warwickshire: a complexity of designations” in *Conservation Bulletin* 52, Pp17-19, English Heritage, Swindon

Molina, E., Fiol, C. and Cultrone, G., 2018. “Assessment of the efficacy of ethyl silicate and dibasic ammonium phosphate consolidants in improving the durability of two building sandstones from Andalusia (Spain)”. *Environmental Earth Sciences*, *77*(8), pp.1-15

Morris, R.K. 2015, *Kenilworth Castle; English Heritage Guide*, English Heritage, Swindon

Mottershead, D., Gorbushina, A., Lucas, G. and Wright, J., 2003. “The influence of marine salts, aspect and microbes in the weathering of sandstone in two historic structures”, *Building and environment*, *38* (9-10), pp.1193-1204

Muir, C., 2006, “Chapter ten: Sandstone”, in Henry, A. (ed) 2006, *Stone Conservation, Principles and Practice*, Donhead Publishing, Dorset

Muir Wood, R. 1978, *On the Rocks, a Geology of Britain*, British Broadcasting Corporation, London

Mytum, H. & Meek, J., 2020, “Experimental archaeology and roundhouse excavated signatures: the investigation of two reconstructed Iron Age buildings at Castell Henllys, Wales” *Archaeological and Anthropological Sciences* 12, 78

NBSD (National Building Stone Database), 2015, “Locharbriggs”, Available at: https://ncptt.nps.gov/buildingstone/stone/locharbriggs

Nuzzo, R. 2015*, “*Fooling ourselves*”, Nature 526, 182–185*

Oak, N.D.https://oak.ucc.nau.edu/rh232/courses/EPS525/Handouts/Understanding%20the%20One-way%20ANOVA.pdf

Öberg, T., Karsznia, K., & Öberg, K., 1993, “Basic Gait Parameters: Reference Data for Normal Subjects 10-79 Years of Age” in *Journal of Rehabilitation Research* 30;2, Pp210-223
Odgers, D., 2014. *Stone in historic buildings–characterisation and performance.* Historic England, Swindon

Odgers, D., & Henry, A., 2012, *Stone- Practical Building Conservation*, Historic England, Swindon

Odgers, D., 2014. *Stone in historic buildings–characterisation and performance.* Historic England, Swindon

Oliver, A. B. 2002, “The variable performance of ethyl silicate: Consolidated stone at three National Parks”, *Association for Preservation Technology Bulletin* 33 Vol 2 Issue 3, Pp39-44

O’Kelly, M. J., 2004, *Newgrange: Archaeology, Art and Legend*, Thames & Hudson, London

Orr, S.A., Young, M., Stelfox, D., Curran, J. and Viles, H., 2018. “Wind-driven rain and future risk to built heritage in the United Kingdom: Novel metrics for characterising rain spells”. *Science of the Total Environment*, *640*, pp.1098-1111

Orr, S.A., Young, M., Stelfox, D., Leslie, A., Curran, J. and Viles, H., 2019. "An 'isolated diffusion' gravimetric calibration procedure for radar and microwave moisture measurement in porous building stone", *Journal of Applied Geophysics*, *163*, pp.1-12.

Otero, J., Charola, A. E., Grissom, C. A.; & Starinieri, V., 2017, "An overview of nanolime as a consolidation method for calcareous substrates" in *Ge-conservación*, 1 (11), Pp71-78

Over, L. M., Andres, C.J., Moore, B. K., Goodacre, C. J., & Munoz C.A., 1988, "Using a Colorimeter to Develop an Intrinsic Silicone Shade Guide for Facial Protheses", *Journal of Prosthodontics*, 7: 237-249

Pandey, S.C., Pollard, A.M., Viles, H.A., & Tellam, J.H. 2014, "Influence of ion exchange processes on salt transport and distribution in historic sandstone buildings", Applied Geochemistry, Vol 48, Pp 176-183

Parajuli, H.R., 2012, "Determination of mechanical properties of the Kathmandu World Heritage brick masonry buildings", In *The 15th World Conference on Earthquake Engineering, Lisbon, Portugal*.

Park, H.D. and Shin, G.H., 2009. "Geotechnical and geological properties of Mokattam limestones: Implications for conservation strategies for ancient Egyptian stone monuments". *Engineering geology*, *104*(3-4), pp.190-199

Price, C. 1975, "Stone Decay and Preservation", *Chemistry in Britain*, 11 (No. 9), Pp 350-353

Price, C.A. and Doehne, E., 2011. *Stone conservation: an overview of current research*. The Getty Conservation Institute, Los Angeles

Price, C., Ross, K., and White, G. 1988. A further appraisal of the "lime technique" for limestone consolidation, using a radioactive tracer. *Studies in Conservation* 33 (4): 178–86

Pummer, E. 2008. "Vacuum-circulation-process: Innovative stone conservation" in *Proceedings of the 11th International Congress on Deterioration and Conservation of Stone, 2008, Poland*

Proceq 2017a, *Punditlab Operating Instructions,* Proceq SA, Schwerzenbach. Available at: https://www.screeningeagle.com/Downloads/Pundit%20Lab_Operating%20Instructions_English_high.pdf

Proceq 2017b, *Equotip Operating Instructions,* Proceq SA, Schwerzenbach. Available at: https://www.proceq.com/uploads/tx_proceqproductcms/import_data/files/Equotip_550_Operating_Instructions_English_high.pdf

Proceq 2018a, *Pundit Ultrasonic Transducers Data Sheets*, Proceq UK, Bedford, UK

Proceq 2018b, *Determination of Poisson's Ration and the Modulus of Elasticity by measuring with P- and S-wave transducers,* Proceq UK, Bedford, UK

Rahmouni, A., Boulanouar, A., Boukalouch, M., Géraud, Y., Samaouali, A., Harnafi, M., and Sebbani, J., 2013, "Prediction of Porosity and Density of Calcarenite Rocks from P-Wave Velocity Measurements," *International Journal of Geosciences*, Vol. 4 No. 9, pp. 1292-1299

Raj B., Jayakumar, T. & Thavasimuthu, M., 2002, *Practical Non-Destructive Testing* (2nd Ed), Alpha science International, Pangbourne

Rao, N.V., Rajasekhar, M. and Rao, G.C., 2014. "Detrimental effect of air pollution, corrosion on building materials and historical structures". *American Journal of Engineering Research*, *3*(3), pp.359-364.

Rao, Q.H., Wang, Z., Xie, H.F. and Xie, Q., 2007. "Experimental study of mechanical properties of sandstone at high temperature", *Journal of Central South University of Technology*, *14*(1), pp.478-483.

Remondino, F., & El-Hakim, S. 2006, "Image Based 3D Modelling: A Review" in *The Photogrammetric Record*, 21:115, Wiley Online Library

Remzova, M.; Zouzelka, R.; Lukes, J.; Rathousky, J. 2019 "Potential of Advanced Consolidants for the Application on Sandstone". *Appl. Sci.*, *9*, 5252

Reynolds, L. 2020, Personal Communication between Author and Laura Reynolds, Senior Estates Manager, English Heritage, July 16th 2020

Richards, J., Viles, H., & Guo, Q., 2020. "The importance of wind as a driver of earthen heritage deterioration in dryland environments", Geomorphology, 369, pp. 107-363

Ruedrich, J., Kirchner, D., & Siegsmund, S., 2011, "Physical Weathering of Building Stones Induced by Freeze-thaw Action: a Laboratory O=Long Term Study", *Environmental Earth Sciences* 63, p1573-1586

Sabbioni, C., 2003, "Mechanisms of Air Pollution Damage to Stone" in Briblecombe, P. *The Effects of Air Pollution on the Built Environment: Air Pollution Reviews Vol 2*, Imperial College Press, London

Salazar-Hernández, C., Puy-Alquiza, M.J., Miranda-Avilés, R. *et al.* 2021, Comparative study of TEOS-consolidants for adobe building conservation. *J Sol-Gel Sci Technol* **97,** 685–696

Salzman, L. F. (ed) 1951, 'Parishes: Kenilworth', in *A History of the County of Warwick: Volume 6, Knightlow Hundred* Pp132-143, London
https://www.british-history.ac.uk/vch/warks/vol6/pp132-143

Sanmartín, P., Grove, R., Carballeira, R. and Viles, H., 2020. "Impact of colour on the bioreceptivity of granite to the green alga Apatococcus lobatus: Laboratory and field testing", *Science of The Total Environment*, *745*, p141-179.

Sansoni, G., Trebeschi, M., & Docchio, F. 2009, "State-of-the-Art and Applications of 3D Imaging Sensors in Industry, Cultural Heritage, Medicine, and Criminal Investigation" in *Sensors* 9; Pp 568-601

Sassoni, E., Franzoni, E., Pigino, B., Scherer, G.W. and Naidu, S., 2013. Consolidation of calcareous and siliceous sandstones by hydroxyapatite: comparison with a TEOS-based consolidant. *Journal of Cultural Heritage*, *14*(3), pp.e103-e108.

Sattler, L., & R. Snethlage. 1988, "Durability of stone consolidation treatments with silicic acid ester", in Marines, P. & Koukis, G.C. (eds) *The Engineering Geology of Ancient Works, Monuments and Historical Sites,* vol. 2, Pp953-56. A. A. Balkema, Rotterdam

Schaffer, R.J., 2016. *The weathering of natural building stones*. Routledge.

Scherer, G.W. and Wheeler, G.S., 2009. "Silicate consolidants for stone". In *Key Engineering Materials* (Vol. 391, pp. 1-25). Trans Tech Publications Ltd.

Schnabel, L., 1992, June. Evaluation of the barium hydroxide-urea consolidation method. In *Proceedings of the 7th International Congress on Deterioration and Conservation of Stone: held in Lisbon, Portugal, 15-18 June 1992* (pp. 1063-1072).

Scopigno, R., Cignoni, P., Pietroni, N., Callieri, M. and Dellepiane, M. 2017, "Digital Fabrication Techniques for Cultural Heritage: A Survey", *Computer Graphics Forum*, 36, Pp6-21

Scottish Places, 2021, https://www.scottish-places.info/towns/townfirst355.html
Sibley, D. F. 1978, "K-feldspar cement in the Jacobsville Sandstone" *Journal of Sedimentary Research* 48 (3): Pp983–985.

SILRES, 2014, Wacker OH100 Technical Data Sheet. Available at: https://www.brenntag.com/media/documents/bsi/product_data_sheets/material_science/wacker_silicone_resins/silres_bs_oh_100_pds.pdf

Simmon, R. 2013, "Elegant Figures, the Subtleties of Colour". Available at: https://earthobservatory.nasa.gov/blogs/elegantfigures/2013/08/05/subtleties-of-color-part-1-of-6/

Slížková Z. 2002 "Exposure trials of natural sensor materials for a use in future environmental monitoring of St. Vitus Cathedral in Prague (Czech Republic)" in Přikryl, R. & Viles, H. (eds) Understanding and Managing Stone Decay; Proceeding of the International Conference on Stone Weathering and Atmospheric Pollution Network (SWAPNET 2001), The Karolinum Press.

Slížková Z. and Frankeová, D. 2012, "Consolidation of Porous Limestone with Nanolime, Laboratory Study", 12th International Congress on the Deterioration and Conservation of Stone Columbia University, New York

Smith, D., 2019a, "Pedatron Testing to 100,000 Steps on Samples of Treated and Untreated Heritage Sandstone with 3D Scanning" Technical Report FWR0291165/1943, SATRA Ltd, Kettering, UK

Smith, D. 2019b, Personal Communication, Meeting between author and David Smith of SATRA Technologies of Kettering, November 18th, 2019

Stambolou, T., 1970, *Conservation of Stone*, pp. 119-124, in *Conservation of New Stone and Wooden Objects*, New York Conference, June 1970 -The International Institute for Conservation of Historic and Artistic Works, London

Stancliffe Stone, 2007, *Locharbriggs 36500_Swatches_01_16*, Available at: https://cms.esi.info/Media/documents/Stanc_Locharbriggs_ML.pdf

Stancliffe Stone, ND, *Locharbriggs Stone Data Sheet*, Available at: http://www.stancliffe.com/Content/ProductInformation/PDFs/StoneTypes/Stancliffe-Stone-Locharbriggs-Red-Sandstone.pdf

Stefani, C., Brunestaud, X., Janvier-Badosa, S., Beck, K., De Luca, L., & Al-Mukhtar, M. 2014, "Developing a toolkit for mapping and displaying stone alteration on a web-based documentation platform" in *Journal of Cultural Heritage* 15, Pp 1-9

Stone Specialist, 2004, "Locharbriggs for Manchester's New Courthouse", Available at: https://www.stonespecialist.com/news/locharbriggs-manchesters-new-courthouse

Stow, D. A. V. 2006, *Sedimentary Rocks in the Field, a Colour Guide,* Taylor and Francis, London

Tatton-Brown, T., 2001. "The quarrying and distribution of Reigate Stone in the Middle Ages", *Medieval Archaeology*, *45*(1), pp.189-20

Timberlake, S., 2007, "The use of experimental archaeology/archaeometallurgy for the understanding and reconstruction of Early Bronze Age mining and smelting technologies", *Metals and mines: Studies in archaeometallurgy*, pp.27-36.

Toghill, P., 2000, *The Geology of Britain, an Introduction*, Crowood Press, Marlborough

Toniolo L., Colombo C., Realini M., Peraio A., Positano M., 2001, "Evaluation of barium hydroxide treatment efficacy on a dolomitic marble". *Annali di Chimica Nov-Dec;91* (11-12): pp 813-821.

Torok, A. and Hajpál, M., 2005. "Effect of temperature changes on the mineralogy and physical properties of sandstones. A laboratory study". *International Journal for Restoration of Buildings and Monuments*, *11*(4)

Townend, S. 2007, "What have Reconstructed Roundhouses Ever Done for Us..?" *Proceedings of the Prehistoric Society, 73*, 97-111

Tucker, M.E., 2001. *Sedimentary petrology: an introduction to the origin of sedimentary rocks* 3rd ed., Oxford ; Malden, MA: Blackwell Science

Tümer, E. U. 2003, "Morphology and Deterioration of Sandstone", *Journal of Istanbul Kultur University,* pp71-82

Turkington, A.V., Martin, E., Viles, H.A. and Smith, B.J., 2003. "Surface change and decay of sandstone samples exposed to a polluted urban atmosphere over a six-year period: Belfast, Northern Ireland". *Building and Environment*, *38*(9-10), pp.1205-1216.

Vasconcelos, G., Lourenço, P. B., Alves, C. S. A., and Pamplona, J., 2007, "Prediction of the Mechanical Properties of Granites by Ultrasonic Pulse Velocity and Schmidt Hammer Hardness," Masonry Conference, Missouri, pp. 998-1009

Verwaal, W., & Mulder, A., 1993, "Estimating Rock Strength with the Equotip Hardness Tester" *International Journal of Rock Mechanics,* Vol 3, No 6, Pp659-663.

Vilbrandt, C., Pasko, G., Pasko, A., Fayolle, P.A., Vilbrandt, T., Goodwin, J.R., Goodwin, J.M., Kunii, T.L., "Cultural Heritage Preservation Using Constructive Shape Modelling", *Computer Graphics Forum*, 23, 1, Pp 25-41

Visit Britain, 2018, Annual Survey of Visits to Visitor Attractions: Latest results, Available at: https://www.visitbritain.org/annual-survey-visits-visitor-attractions-latest-results

Wacker 2014, "SILRES BS OH100 Product Guide", Available at: https://www.wacker.com/h/en-us/silanes-siloxanes-silicates/ethyl-silicates/silres-bs-oh-100/p/000008022

Walker B., McGregor C. & Little R. 1996, *Earth Structures and Construction in Scotland,* Historic Scotland Technical Advice Note 6, Edinburgh

Warnes, A. 1926, *Building Stones, Their Properties, Decay, and Preservation*, Ernest Benn Ltd, London

Wilhelm, K., Viles, H., & Burke, Ó. 2016, "Low impact surface hardness testing (Equotip) on porous surfaces; advances in methodology with implications for rock weathering and stone deterioration research" *Earth Surface Processes and Landforms*, Vol 41, Issue 8, Pp1027-1038

Wilhelm, K., Longman, J., Orr, S.A. and Viles, H., 2021. "Stone-built heritage as a proxy archive for long-term historical air quality: A study of weathering crusts on three generations of stone sculptures on Broad Street, Oxford", *Science of the Total Environment*, *759*, p.143916.

Wills, L J. 1970. "The Triassic succession in the central Midlands in its regional setting", *Quarterly Journal of the Geological Society of London,* Vol.126, Pp225-285.

Wheeler, G. 2005, *Alkoxysilanes and the Consolidation of Stone*, Getty Conservation Institute, Los Angeles

Wright, J.S., 2002. Geomorphology and stone conservation: sandstone decay in Stoke-on-Trent. *Structural Survey* Vol 20, No 2 pp 50-61

Yang, F., Zhang, B., Liu, Y., Wei, G, Zhang, H., Chen, W., Xu Z., 2011, "Biomimic conservation of weathered calcareous stones by apatite" *New Journal of Chemistry*, Vol 35, issue 4, Pp 887

Younan, S., & Treadaway, C. 2015 "Digital 3D Models of Heritage Artefacts: Towards A Digital Dreamspace" *Digital Applications in Archaeology and Cultural Heritage 2*, p240-247

Young, M.E., Urquhart, D.C.M. and Laing, R.A., 2003. "Maintenance and repair issues for stone cleaned sandstone and granite building façades", *Building and Environment*, *38*(9-10), pp.1125-1131

Young, M., Cordiner, P., & Murray, M., 2018, *Chemical Consolidants and Water Repellents for Sandstones in Scotland*, Historic Scotland, Edinburgh

Zhang, L., Mao, X. and Lu, A., 2009. "Experimental study on the mechanical properties of rocks at high temperature", *Science in China Series E: Technological Sciences*, *52*(3), pp.641-646.

Zhang, H., Liu, Q., Liu, T., Zhang, B., 2013, "The preservation damage of hydrophobic polymer coating materials in conservation of stone relics" Progress in Organic Coatings 76, pp1127-1134

Zlot, R., Bosse, M., Greenop, K., Jarzab, Z., Juckes, E., & Roberts, J., 2014, "Efficiently capturing large, complex cultural heritage sites with a handheld mobile 3D laser mapping system" in *Journal of Cultural Heritage*, 15; 6, Pp 670-678